

Green Chemistry

Cutting-edge research for a greener sustainable future

www.rsc.org/greenchem

Volume 9 | Number 5 | May 2007 | Pages 401–508



ISSN 1463-9262

RSC Publishing

Burrell *et al.*
The large scale synthesis of pure ionic liquids

Constable *et al.*
Key green chemistry research areas

Selva *et al.*
Chemoselective reactions of dimethyl carbonate

Ming-Lin and Hui-Zhen
Selective oxidation of benzyl alcohol to benzaldehydes



1463-9262(2007)9:5;1-7

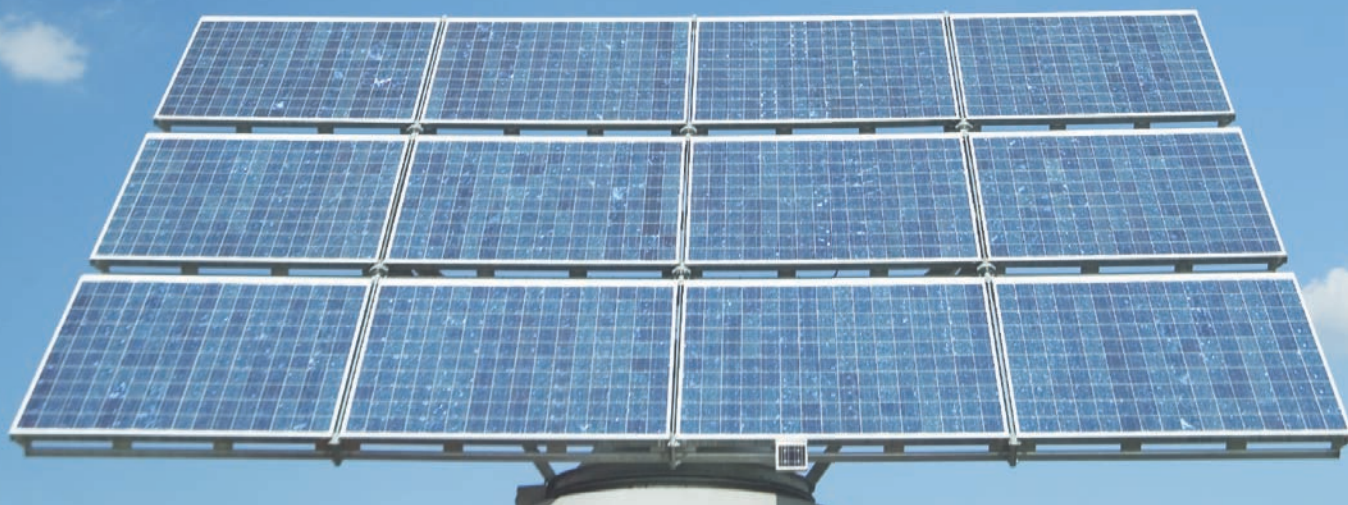
Alternative Fuel Technologies

A series of PCCP special issues guest edited by Joachim Maier (MPI Stuttgart), Dirk Guldi (Universität Erlangen-Nürnberg), and Adriano Zecchina (University of Torino)

Following on from the highly successful nano-themed issues, PCCP presents a series of themed issues on Alternative Fuel Technologies. Published in selected printed issues of PCCP in spring 2007 and collected online on a dedicated website, these issues feature the very latest research including:

- ▶ fuel cells
- ▶ electrochemical energy conversion
- ▶ supercapacitors and molecular materials
- ▶ hydrogen storage
- ▶ solar energy conversion
- ▶ biohydrogen

Sign up for RSS alerts to have the latest articles delivered directly to your desktop



RSC Publishing

www.rsc.org/pccp/altfuel

Registered Charity Number 207890

Green Chemistry

Cutting-edge research for a greener sustainable future

www.rsc.org/greenchem

RSC Publishing is a not-for-profit publisher and a division of the Royal Society of Chemistry. Any surplus made is used to support charitable activities aimed at advancing the chemical sciences. Full details are available from www.rsc.org

IN THIS ISSUE

ISSN 1463-9262 CODEN GRCHFJ 9(5) 401–508 (2007)



Cover

The large scale synthesis and purification of spectroscopic-grade, “water-white” ionic liquids is reported.

Image reproduced with permission of Anthony Burrell from *Green Chem.*, 2007, 9(5), 449.

CHEMICAL TECHNOLOGY

T33

Chemical Technology highlights the latest applications and technological aspects of research across the chemical sciences.

Chemical Technology

May 2007/Volume 4/Issue 5

www.rsc.org/chemicaltechnology

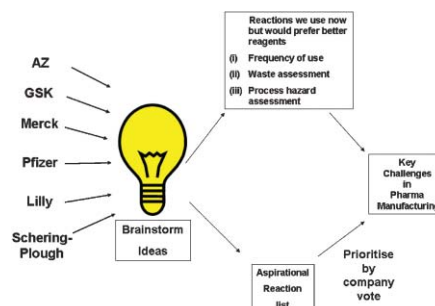
PERSPECTIVE

411

Key green chemistry research areas—a perspective from pharmaceutical manufacturers

David J. C. Constable, Peter J. Dunn,* John D. Hayler, Guy R. Humphrey, Johnnie L. Leazer, Jr., Russell J. Linderman, Kurt Lorenz, Julie Manley, Bruce A. Pearlman, Andrew Wells, Aleksey Zaks and Tony Y. Zhang

A consortium formed from pharmaceutical manufacturers and the ACS Green Chemistry Institute have agreed a list of 12 key green chemistry research areas from a pharmaceutical perspective.



EDITORIAL STAFF

Editor

Sarah Ruthven

Publishing assistant

Emma Hacking

Team leader, serials production

Stephen Wilkes

Technical editor

Edward Morgan

Administration coordinator

Sonya Spring

Editorial secretaries

Donna Fordham, Jill Segev, Julie Thompson

Publisher

Emma Wilson

Green Chemistry (print: ISSN 1463-9262; electronic: ISSN 1463-9270) is published 12 times a year by the Royal Society of Chemistry, Thomas Graham House, Science Park, Milton Road, Cambridge, UK CB4 0WF.

All orders, with cheques made payable to the Royal Society of Chemistry, should be sent to RSC Distribution Services, c/o Portland Customer Services, Commerce Way, Colchester, Essex, UK CO2 8HP. Tel +44 (0) 1206 226050; E-mail sales@rscdistribution.org

2007 Annual (print + electronic) subscription price: £902; US\$1705. 2007 Annual (electronic) subscription price: £812; US\$1534. Customers in Canada will be subject to a surcharge to cover GST. Customers in the EU subscribing to the electronic version only will be charged VAT.

If you take an institutional subscription to any RSC journal you are entitled to free, site-wide web access to that journal. You can arrange access via Internet Protocol (IP) address at www.rsc.org/ip. Customers should make payments by cheque in sterling payable on a UK clearing bank or in US dollars payable on a US clearing bank. Periodicals postage paid at Rahway, NJ, USA and at additional mailing offices. Airfreight and mailing in the USA by Mercury Airfreight International Ltd, 365 Blair Road, Avenel, NJ 07001, USA.

US Postmaster: send address changes to Green Chemistry, c/o Mercury Airfreight International Ltd, 365 Blair Road, Avenel, NJ 07001. All despatches outside the UK by Consolidated Airfreight.

PRINTED IN THE UK

Advertisement sales: Tel +44 (0) 1223 432246; Fax +44 (0) 1223 426017; E-mail advertising@rsc.org

Green Chemistry

Cutting-edge research for a greener sustainable future

www.rsc.org/greenchem

Green Chemistry focuses on cutting-edge research that attempts to reduce the environmental impact of the chemical enterprise by developing a technology base that is inherently non-toxic to living things and the environment.

EDITORIAL BOARD

Chair

Professor Martyn Poliakoff
Nottingham, UK

Scientific Editor

Professor Walter Leitner
RWTH-Aachen, Germany

Associate Editors

Professor C. J. Li
McGill University, Canada
Professor Kyoko Nozaki
Kyoto University, Japan

Members

Professor Paul Anastas
Yale University, USA
Professor Joan Brennecke
University of Notre Dame, USA
Professor Mike Green
Sasol, South Africa
Professor Buxing Han
Chinese Academy of Sciences,
China
Professor Roshan Jachuck
Clarkson University, USA

Dr Alexei Lapkin
Bath University, UK
Dr Janet Scott
Unilever, UK
Professor Tom Welton
Imperial College, UK

INTERNATIONAL ADVISORY EDITORIAL BOARD

James Clark, York, UK
Avelino Corma, Universidad
Politécnica de Valencia, Spain
Mark Harmer, DuPont Central
R&D, USA
Herbert Hugl, Lanxess Fine
Chemicals, Germany
Makato Misono, nite,
Japan
Colin Raston,
University of Western Australia,
Australia

Robin D. Rogers, Centre for Green
Manufacturing, USA
Kenneth Seddon, Queen's
University, Belfast, UK
Roger Sheldon, Delft University of
Technology, The Netherlands
Gary Sheldrake, Queen's
University, Belfast, UK
Pietro Tundo, Università ca
Foscari di Venezia, Italy

INFORMATION FOR AUTHORS

Full details of how to submit material for publication in Green Chemistry are given in the Instructions for Authors (available from <http://www.rsc.org/authors>). Submissions should be sent via ReSource: <http://www.rsc.org/resource>.

Authors may reproduce/republish portions of their published contribution without seeking permission from the RSC, provided that any such republication is accompanied by an acknowledgement in the form: (Original citation) – Reproduced by permission of the Royal Society of Chemistry.

© The Royal Society of Chemistry 2007. Apart from fair dealing for the purposes of research or private study for non-commercial purposes, or criticism or review, as permitted under the Copyright, Designs and Patents Act 1988 and the Copyright and Related Rights Regulations 2003, this publication may only be reproduced, stored or transmitted, in any form or by any means, with the prior permission in writing of the Publishers or in the case of reprographic reproduction in accordance with the terms of licences issued by the Copyright Licensing Agency in the UK. US copyright law is applicable to users in the USA.

The Royal Society of Chemistry takes reasonable care in the preparation of this publication but does not accept liability for the consequences of any errors or omissions.

☞ The paper used in this publication meets the requirements of ANSI/NISO Z39.48-1992 (Permanence of Paper).

Royal Society of Chemistry: Registered Charity No. 207890

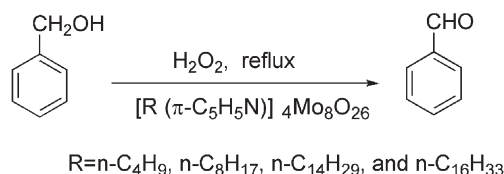
COMMUNICATIONS

421

Selective oxidation of benzyl alcohol to benzaldehyde with hydrogen peroxide over tetra-alkylpyridinium octamolybdate catalysts

Guo Ming-Lin* and Li Hui-Zhen

Some tetra-alkylpyridinium octamolybdate catalysts were used to perform 82.3%–94.8% benzyl alcohol conversion and 87.9%–96.7% benzaldehyde selectivity for selective oxidation of benzyl alcohol to benzaldehyde with 15% H_2O_2 at reflux temperature for a short period without any organic solvents.

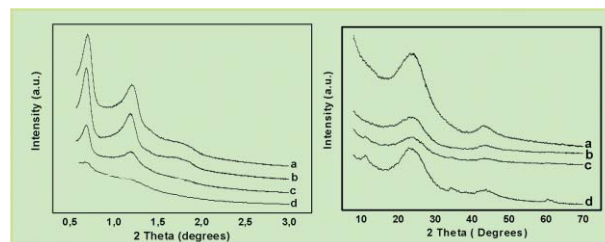


424

Synthesis and catalytic applications of CMK-LDH (layered double hydroxides) nanocomposite materials

Amit Dubey*

Nanosized LDH were synthesized inside mesopore carbon and were characterized and exploited for base catalysis in Knoevenagel and Claisen–Schmidt condensations.

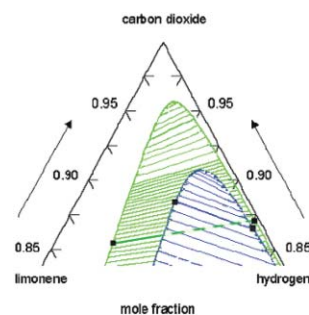


427

Phase equilibrium-driven selective hydrogenation of limonene in high-pressure carbon dioxide

Ewa Bogel-Łukasik, Isabel Fonseca, Rafał Bogel-Łukasik, Yuriy A. Tarasenko, Manuel Nunes da Ponte,* Alexandre Paiva and Gerd Brunner

Pressure-tuning of solubility in the hydrogenation of limonene in carbon dioxide was found in biphasic systems, close but below the critical conditions of the reaction mixture, where hydrogen solubility in the liquid is highly dependent on pressure.

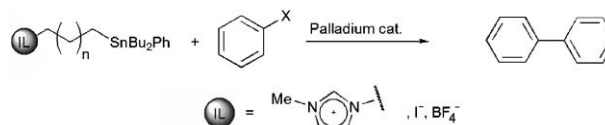


431

Ionic liquid supported tin reagents for Stille cross coupling reactions

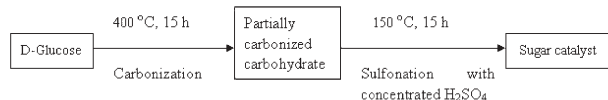
Jürgen Vitz,* Dinh Hung Mac and Stéphanie Legoupy*

New ionic liquid supported tin reagents were synthesized for use in Stille cross coupling reactions. With these reagents high yields at low reaction temperatures and the recycling of the tin compounds are possible.



COMMUNICATIONS

434

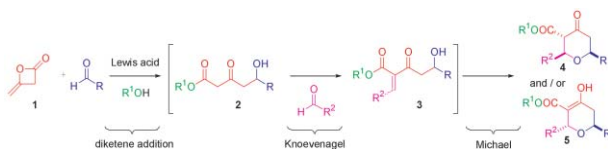


Preparation of a sugar catalyst and its use for highly efficient production of biodiesel

Min-Hua Zong,* Zhang-Qun Duan, Wen-Yong Lou, Thomas J. Smith* and Hong Wu

In this communication, a 'sugar catalyst' is prepared from D-glucose and its catalytic properties and structure are investigated in detail. This type of sugar catalyst is, for the first time, applied for the effective production of biodiesel from waste oils.

438



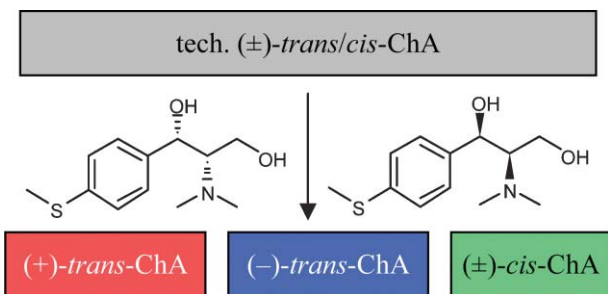
Combining pot, atom and step economy (PASE) in organic synthesis. Synthesis of tetrahydropyran-4-ones

Paul A. Clarke,* Soraia Santos and William H. C. Martin

Applications of principles 1, 2, 5 and 8 of the twelve principles of green chemistry to the synthesis of highly functionalised tetrahydropyran-4-ones has led to a significantly 'greener' synthesis of these molecules.

PAPERS

441

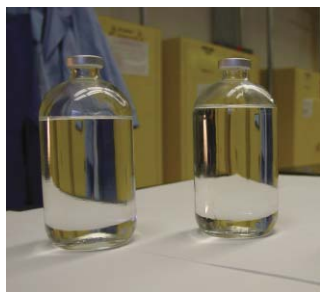


The same and not the same. Similarities and differences in the resolution of *trans*-chrysanthemic acid of industrial origin by the enantiomers of some *threo*-1-aryl-2-dimethylamino-1,3-propanediols

Goffredo Rosini,* Claudia Ayoub, Valerio Borzatta, Emanuela Marotta, Andrea Mazzanti and Paolo Righi

An effective and practical resolution of *trans*-chrysanthemic acid (ChA) from technical mixtures of stereoisomers of industrial origin has been achieved by using half an equivalent of MTDP enantiomers in a single solvent system, *i*-Pr₂O.

449



The large scale synthesis of pure imidazolium and pyrrolidinium ionic liquids

Anthony K. Burrell,* Rico E. Del Sesto, Sheila N. Baker, T. Mark McCleskey and Gary A. Baker

Ionic liquids are notoriously difficult to obtain as pure colourless materials. In many applications coloured, fluorescent or electrochemically active impurities are significant problems. Here we report a simple method for preparing large quantities of dry imidazolium and pyrrolidinium ionic liquids which are substantially free of impurities.

PAPERS

455

Gaining pH-control in water/carbon dioxide biphasic systems

Christoph Roosen, Marion Ansorge-Schumacher, Thomas Mang, Walter Leitner and Lasse Greiner*

Measurement and predictable control of pH in the green biphasic system carbon dioxide/water opens up its use in numerous applications.

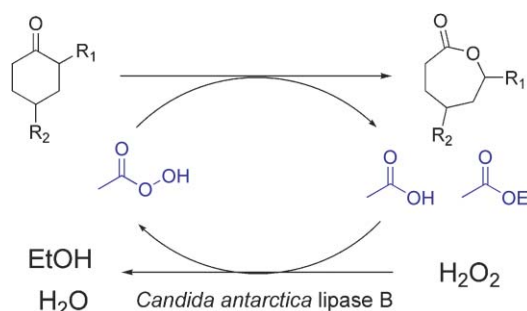


459

Baeyer–Villiger oxidation of substituted cyclohexanones via lipase-mediated perhydrolysis utilizing urea–hydrogen peroxide in ethyl acetate

María Yolanda Ríos, Enrique Salazar and Horacio F. Olivo*

Clean oxidation of various cyclohexanones to ϵ -caprolactones was demonstrated utilizing the Novozyme-435 mediated perhydrolysis of ethyl acetate and the urea–hydrogen peroxide complex.

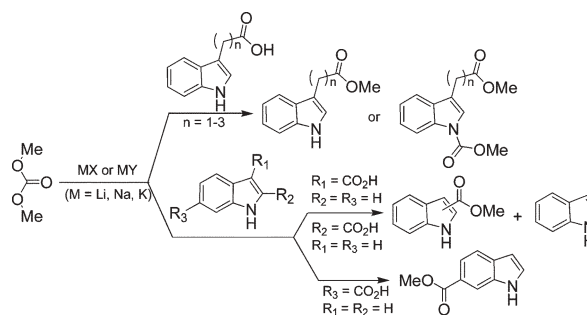


463

Chemoselective reactions of dimethyl carbonate catalysed by alkali metal exchanged faujasites: the case of indolyl carboxylic acids and indolyl-substituted alkyl carboxylic acids

Maurizio Selva,* Pietro Tundo, Davide Brunelli and Alvise Perosa

In the presence of recyclable solid catalysts (faujasite MY or MX), a genuine green procedure is described by using the non-toxic dimethyl carbonate (DMC) for highly chemoselective esterification and *N*-carboxymethylation reactions of indolyl-substituted carboxylic acids.

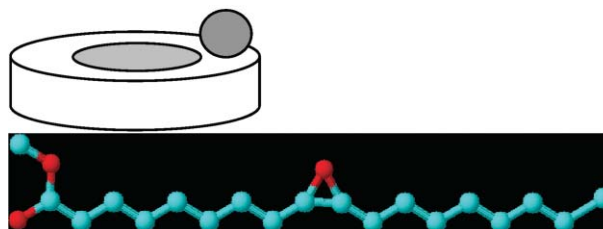


469

Oxidation, friction reducing, and low temperature properties of epoxy fatty acid methyl esters

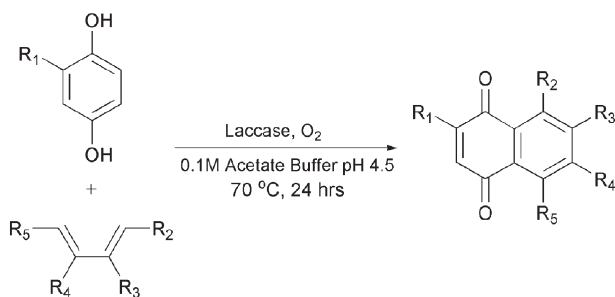
Brajendra K. Sharma, Kenneth M. Doll* and Sevim Z. Erhan

The suitability of epoxides, derived from oleochemicals, for use as lubrication fluids, was determined. Physical properties as well as oxidative stability were studied.



PAPERS

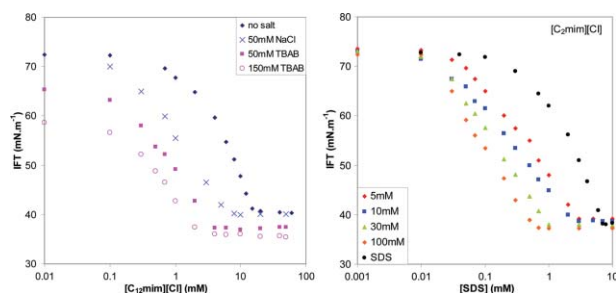
475

**One-pot synthesis of 1,4-naphthoquinones and related structures with laccase**

Suteera Witayakran and Arthur J. Ragauskas*

This study demonstrates the application of laccase to initiate aqueous based oxidative cascade reactions starting with 1,4-hydroquinones and dienes yielding 1,4-naphthoquinones.

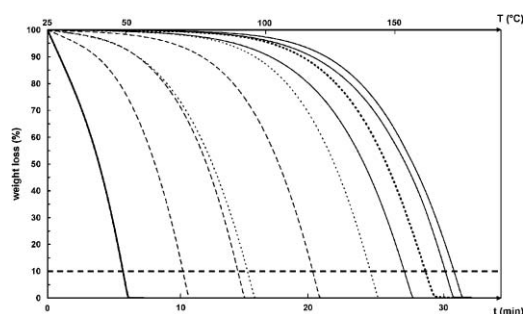
481

**Self-aggregation of ionic liquids: micelle formation in aqueous solution**

Marijana Blesic, Maria Helena Marques, Natalia V. Plechkova, Kenneth R. Seddon, Luis Paulo N. Rebelo* and António Lopes*

Interfacial tension, fluorescence, and 1H NMR were used to monitor the adsorption at the aqueous solution–air interface as well as the self-aggregation behaviour (critical micelle concentration, CMC) of room-temperature ionic liquids of the 1-alkyl-3-methylimidazolium family of cations.

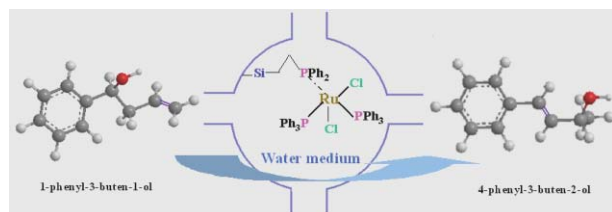
491

**Thermophysical and bionotox properties of solvo-surfactants based on ethylene oxide, propylene oxide and glycerol**

Sébastien Queste, Youlia Michina, Anny Dewilde, Roland Neueder, Werner Kunz and Jean-Marie Aubry*

TGA evaporation curves of a series of C_iE_j , C_iP_j and C_iGly_j . By increasing evaporation time: *n*-butyl acetate AcOBu (reference solvent), C_3P_1 , C_4P_1 , C_4E_1 , C_3P_2 , C_4E_2 , C_4Gly_1 , C_6E_2 , iC_5Gly_1 , C_5Gly_1 . Evaporation rates were calculated from the time corresponding to a loss of 90%, relatively to AcOBu.

500

**Water-medium isomerization of homoallylic alcohol over a Ru(II) organometallic complex immobilized on FDU-12 support**

Hexing Li,* Fang Zhang, Hong Yin, Ying Wan and Yunfeng Lu

A novel Ru–PPh₂–FDU-12 heterogeneous catalyst exhibited excellent activity, selectivity and durability in a water-medium homoallylic isomerization reaction, apparently owing to the high dispersion of Ru(II) active sites and the large 3D pore channels.

AUTHOR INDEX

- Anson-Schumacher, Marion, 455
 Aubry, Jean-Marie, 491
 Ayoub, Claudia, 441
 Baker, Gary A., 449
 Baker, Sheila N., 449
 Blesic, Marijana, 481
 Bogel-Lukasik, Ewa, 427
 Bogel-Lukasik, Rafał, 427
 Borzatta, Valerio, 441
 Brunelli, Davide, 463
 Brunner, Gerd, 427
 Burrell, Anthony K., 449
 Clarke, Paul A., 438
 Constable, David J. C., 411
 Del Sesto, Rico E., 449
 Dewilde, Anny, 491
 Doll, Kenneth M., 469
 Duan, Zhang-Qun, 434
 Dubey, Amit, 424
 Dunn, Peter J., 411
 Erhan, Sevim Z., 469
 Fonseca, Isabel, 427
 Greiner, Lasse, 455
 Hayler, John D., 411
 Hui-Zhen, Li, 421
 Humphrey, Guy R., 411
 Kunz, Werner, 491
 Leazer, Jr., Johnnie L., 411
 Legoupy, Stéphanie, 431
 Leitner, Walter, 455
 Li, Hexing, 500
 Linderman, Russell J., 411
 Lopes, António, 481
 Lorenz, Kurt, 411
 Lou, Wen-Yong, 434
 Lu, Yunfeng, 500
 Mac, Dinh Hung, 431
 Mang, Thomas, 455
 Manley, Julie, 411
 Marotta, Emanuela, 441
 Marques, Maria Helena, 481
 Martin, William H. C., 438
 Mazzanti, Andrea, 441
 McCleskey, T. Mark, 449
 Michina, Youlia, 491
 Ming-Lin, Guo, 421
 Neueder, Roland, 491
 Nunes da Ponte, Manuel, 427
 Olivo, Horacio F., 459
 Paiva, Alexandre, 427
 Pearlman, Bruce A., 411
 Perosa, Alvise, 463
 Plechkova, Natalia V., 481
 Queste, Sébastien, 491
 Ragauskas, Arthur J., 475
 Rebelo, Luis Paulo N., 481
 Righi, Paolo, 441
 Rios, Maria Yolanda, 459
 Roosen, Christoph, 455
 Rosini, Goffredo, 441
 Salazar, Enrique, 459
 Santos, Soraia, 438
 Seddon, Kenneth R., 481
 Selva, Maurizio, 463
 Sharma, Brajendra K., 469
 Smith, Thomas J., 434
 Tarasenko, Yuriy A., 427
 Tundo, Pietro, 463
 Vitz, Jürgen, 431
 Wan, Ying, 500
 Wells, Andrew, 411
 Witayakran, Suteera, 475
 Wu, Hong, 434
 Yin, Hong, 500
 Zaks, Aleksey, 411
 Zhang, Fang, 500
 Zhang, Tony Y., 411
 Zong, Min-Hua, 434

FREE E-MAIL ALERTS AND RSS FEEDS

Contents lists in advance of publication are available on the web *via* www.rsc.org/greenchem - or take advantage of our free e-mail alerting service (www.rsc.org/ej_alert) to receive notification each time a new list becomes available.



Try our RSS feeds for up-to-the-minute news of the latest research. By setting up RSS feeds, preferably using feed reader software, you can be alerted to the latest Advance Articles published on the RSC web site. Visit www.rsc.org/publishing/technology/rss.asp for details.

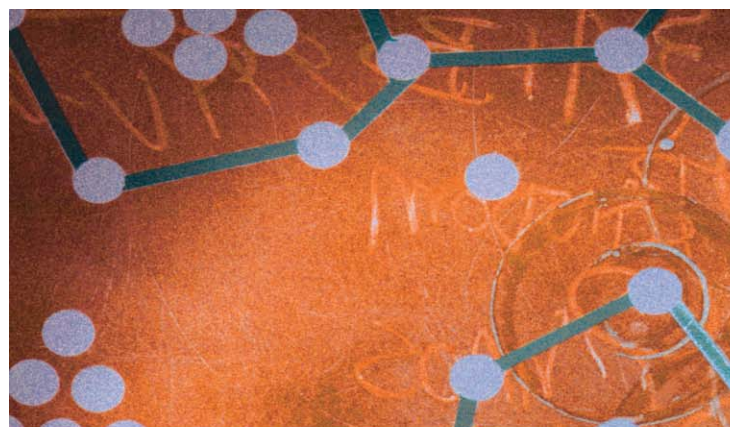
ADVANCE ARTICLES AND ELECTRONIC JOURNAL

Free site-wide access to Advance Articles and the electronic form of this journal is provided with a full-rate institutional subscription. See www.rsc.org/ejs for more information.

* Indicates the author for correspondence: see article for details.



Electronic supplementary information (ESI) is available *via* the online article (see <http://www.rsc.org/esi> for general information about ESI).



MARK YOUR CALENDAR

11th Annual Green Chemistry & Engineering Conference

» *From Small Steps to Giant Leaps —
Breakthrough Innovations for Sustainability*

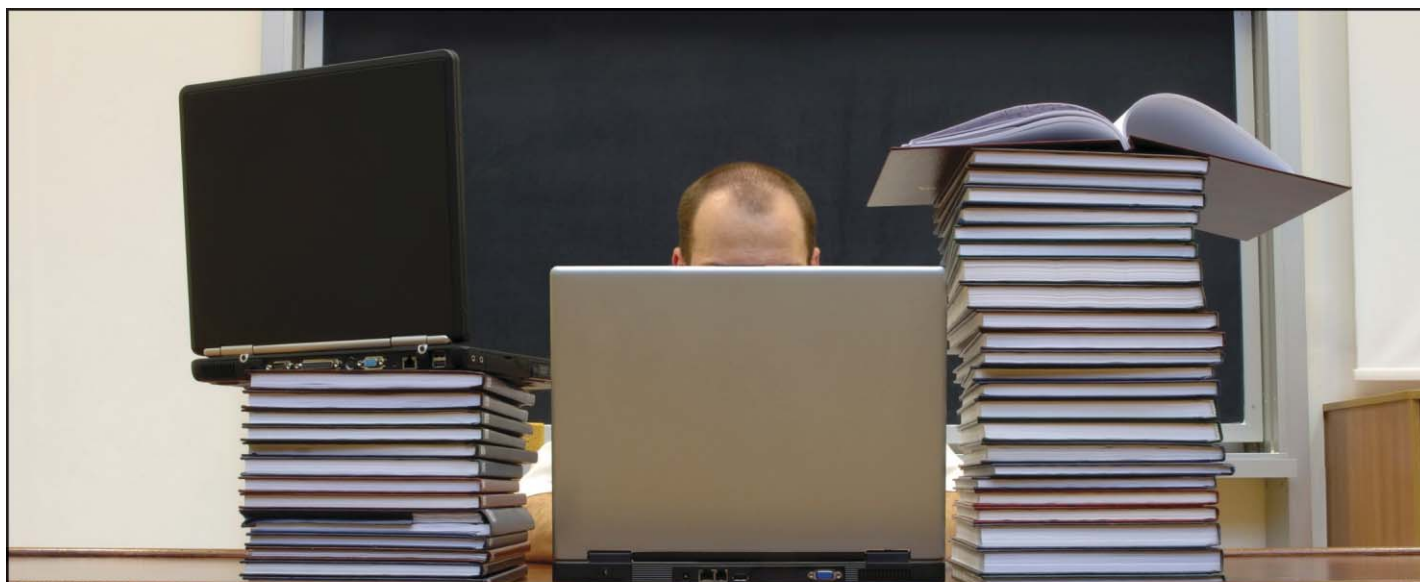
June 26–29, 2007

WASHINGTON, DC

www.GCandE.org



www.GCandE.org



There is an easier way to keep up with research in your field...

An integral part of managing your career as a scientist is staying on top of the news and developments in your field of research and related areas. A good knowledge of your industry is a key component to your success, but finding the time to keep up with the latest research news can pose the greatest challenge.

The solution? By signing up for e-alerts from one of our free news services, you can receive updates about newsworthy and significant research appearing in RSC journals in a quick and easily digestible monthly alert.

Free access. From each news item you can link directly to the source research paper, which is completely free to access and download for a limited period.

New tools to help you. In addition to research news, our news services also feature

- **Instant insights** – whirlwind tours of exciting research areas you should know about
- **Interviews** – leading scientists share their opinions

**Chemical
Technology**

www.rsc.org/chemicaltechnology

**Chemical
Science**

www.rsc.org/chemicalscience

**Chemical
Biology**

www.rsc.org/chembiology

10110633

RSCPublishing

www.rsc.org/ej_alert

Registered Charity Number 207890

Chemical Technology

Simplified electrolysis route to advanced batteries

Gentlemen, plug in your engines

The dream of environmentally friendly electric cars is a step closer to reality thanks to work by scientists in the UK and China.

The favourites for the power source in such cars are nickel metal hydride batteries, currently used to power MP3 players and laptop computers. However, until recently, the use of this type of battery for large-scale applications (like electric vehicles) has been hampered, not by a lack of resources, but by inadequate or expensive manufacturing technologies.

The traditional method for preparing these materials involves a multi-step high-energy input process, whose monetary and environmental cost may have outweighed any potential benefit. Now, George Chen from the University of Nottingham and Dihua Wang from Wuhan University have shown that the same materials can be made directly by a one-step electrolysis process from mixtures of the metal oxides.

'I am fascinated by the elegance



of this work, it shows that the electrochemical approach can be applied to the preparation of advanced battery materials from relatively inexpensive components,' said Viktor Balema, product manager in the materials science team of Sigma-Aldrich.

'The collaboration with Chinese

Large applications need large batteries

Reference

Y Zhu *et al.*, *Chem. Commun.*, 2007, DOI: 10.1039/b701770g

scientists is important as China has some of the best resources of the raw materials,' said George Chen. 'The next step in the research will be to get the chemical engineers involved to help transfer this process from a laboratory scale to an industrial process.'

Stephen Davey

In this issue

Nanodiamonds for HPLC

Physicochemical stability makes the gem perfect for columns

Sweet-toothed sensors

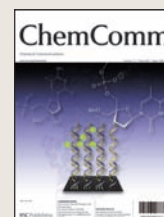
Blood sugar levels can be monitored with the naked eye

Interview: In a spin

Daniella Goldfarb talks to Colin Batchelor about her dreams for electron spin resonance

Instant insight: Nanocrystals as sensors

Rebecca Somers, Mounji Bawendi and Daniel Nocera explain how to make quantum dots both bright and sensitive



The latest applications and technological aspects of research across the chemical sciences

Application highlights

Improved dyes aid charge recombination

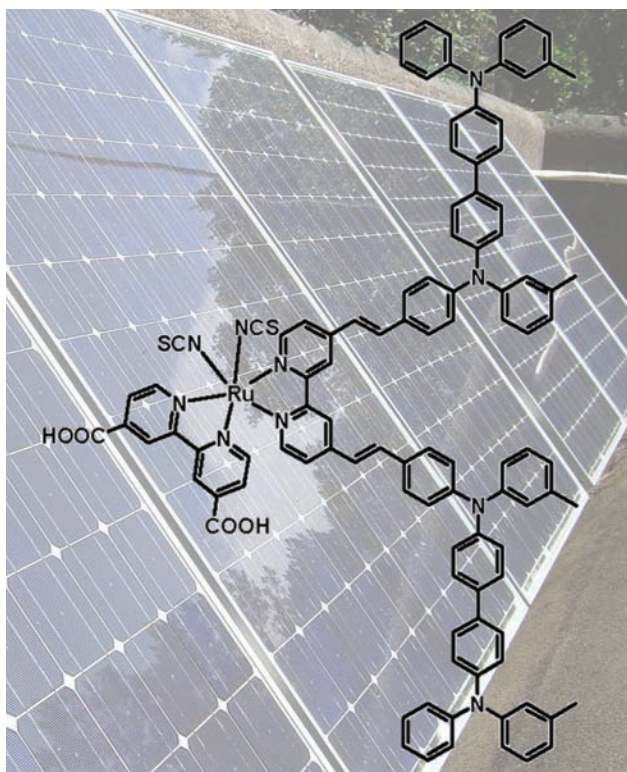
Super solar cells

Supramolecular dyes could boost efficiency in solar cells, say scientists from the UK.

Saif Haque, from Imperial College, London, found that supramolecular dyes gave a 25% improvement in performance as compared to conventional, non-supramolecular dyes.

Dye-sensitized solar cells typically consist of a dye-sensitized titania film and an organic semiconductor that transports positive 'holes'. The dye absorbs light and an excited electron is transferred from the dye to the conduction band of the titania. The dye then regains an electron from the semiconductor. The device performance depends on the efficiency of this charge recombination. Haque has found that supramolecular dyes improve the efficiency of solar cells by controlling the charge recombination between photo-injected electrons and the oxidised semiconductor.

'The field of supramolecular chemistry is well advanced but the application of such materials in solar cells to yield high efficiencies is yet to be realized,' explained



The supramolecular dye absorbs light and gives off an electron

Haque. 'A key issue holding this back is lack of quantitative structure-function relationships

that enable rational design of supramolecular electronic materials,' he said.

Haque thinks that this work may also prove useful for different applications. 'A key feature of the work is the achievement of long-lived charge separated states using supramolecular dye structures. Long-lived charge separation is also important for applications such as light driven hydrogen evolution from water, or new optical data storage devices,' he said.

Masao Kaneko, of Ibaraki University, Mito, Japan said that this strategy could lead to further advances. 'Dye-sensitized solar cells are attracting a great deal of attention as the next generation solar cell. The research group has had success in significantly reducing charge recombination losses. One could expect further improvement in conversion efficiency of dye-sensitized solar cells using this strategy.'

Rebecca Gillan

Reference

S Handa *et al.*, *Chem. Commun.*, 2007, DOI: 10.1039/b618700e

Sampled air is used as the carrier gas in rapid analysis

A portable way to measure smoke

Researchers in the US have developed portable equipment to measure tobacco smoke compounds in public areas.

Environmental tobacco smoke (ETS) is a complex mixture of compounds, so surrogate measures, or markers, are used to quantify exposure.

Edward Zellers and colleagues, from the University of Michigan, adapted a portable gas chromatograph (GC) to capture 2,5-dimethylfuran and 4-ethenylpyridine and separate them from the other main contaminants in ETS.

The equipment can perform



Markers give away the presence of smoke

a complete analysis every 15 minutes and ambient air is used as the GC carrier gas to avoid the need to transport gases to the test site.

Zellers' team collected and analysed air samples from a local bowling alley where smoking is permitted. They then used the results to generate a test atmosphere in the laboratory to test the portable equipment.

The tests confirmed that the portable instrument is capable of detecting the two markers at the levels typically found in environmental samples.

Joanna Stevens

Reference

Q Zhong *et al.*, *J. Environ. Monit.*, 2007, DOI: 10.1039/b700216e

Physical and chemical stability makes gems perfect for column packings

Nanodiamonds for HPLC

Diamonds show potential as column packings for high-performance liquid chromatography (HPLC).

Pavel Nesterenko and colleagues at Lomonosov Moscow State University, Russian Federation, have achieved efficient separations of mixtures of aromatic hydrocarbons using nano-sized diamonds as the stationary phase in HPLC.

An ongoing challenge in chromatography has been to improve the properties of the column packings to get better separation efficiency and selectivity. Many different materials have been tested as stationary phases but only a few fulfil both the mechanical and chemical stability requirements.

Diamonds are an ideal choice of material for column packings because they offer excellent stability, so they can be used at high temperatures and pressures in the



presence of strong alkalis, acids, and organic solvents. However, as Nesterenko explained, natural diamonds are too expensive and synthetic nanodiamonds, although they are cheap, have too small a particle size to be of use.

To solve the problems of cost and particle size, Nesterenko developed a sintering technology that enabled him to obtain nanodiamonds

Not just a girl's best friend

Reference

P N Nesterenko, O N Fedyanina and Y V Volgin, *Analyst*, 2007, DOI: 10.1039/b702272g

suitable for HPLC applications. He prepared polycrystalline porous diamond particles of micron size by sintering nanodiamonds at high pressures, up to 12,000 MPa, and temperatures of 1200°C.

Commenting on the sintered nanodiamonds, Paul Haddad of the Australian Centre for Research on Separation Science in Tasmania said 'These are an interesting new class of stationary phase because they show specific analyte interactions yet retain many important diamond properties, such as pH tolerance.'

Haddad predicts that the challenge with these materials will be to find ways to control the synthesis of suitable particles so that the chromatographic efficiency can be improved to levels similar to conventional packings, such as silica.

Janet Crombie

Blood sugar levels can be monitored with the naked eye

Sweet-toothed sensors

Medical researchers in the US have made a sensor device that can potentially be used to measure sugar levels in the blood. They hope it could help people suffering from diabetes and similar conditions to monitor their blood glucose levels.

Ching-Hsuan Tung and colleagues from Massachusetts General Hospital, Charlestown, based their system on an aqueous mix of a pH-sensitive dye and a boronic acid derivative.

The sensor depends on the change in the acid dissociation constant (pK_a) of the boronic acid when sugar molecules bind to it. This in effect raises the pH of the solution and causes a clear change in the colour of the dye. Almost uniquely, Tung's sensor operates in the near infrared range, where there is minimal background interference from biomolecules and blood.

'Despite the promising responses demonstrated by similar fluorescent probes in the past, their



development is a complex process and optical responses are not easily predictable,' said Tung. 'In addition, those fluorophores frequently require an organic co-solvent to increase solubility in aqueous media.'

The group extended their

Sugar molecules change the pK_a of the sensor

Reference

Y Kim *et al*, *Chem. Commun.*, 2007, DOI: 10.1039/b700741h

approach to produce 'test strips' that were suitable for semi-quantitative sugar detection using the naked eye. The sensor solution was spotted onto filter paper and then dried. The initial colour of each spot immediately changed from reddish-pink at neutral pH to blue as the pH increased following addition of sugars. 'We hope the inexpensive test strip will find use for health care in developing countries,' said Tung. 'Although not as accurate as the glucose-meters widely used in developed countries, they could provide critical information,' he asserted.

Duncan Graham of the Centre for Molecular Nanometrology at the University of Strathclyde commented: 'This work is interesting, and the team's approach is a significant advance on what's already out there. This offers promise, but there's a long way to go before it's an *in vivo* sensor.'

Michael Spencelayh

Microplate and biosensor integration reduces volumes for assays

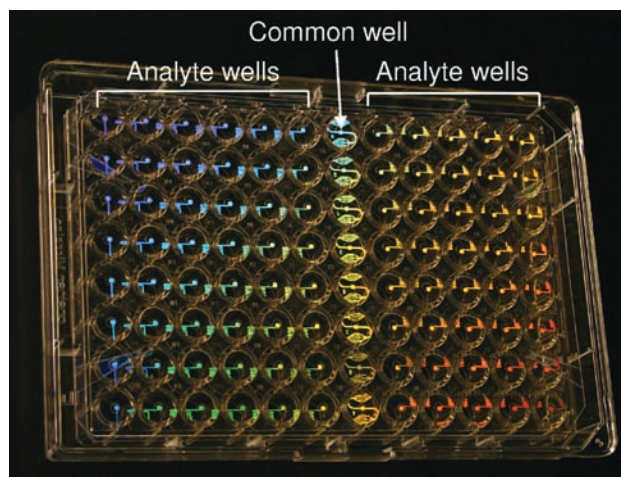
Shrinking screening for drugs

Scientists in the US have found a way to screen for potential drugs using just minuscule amounts of chemical reagents.

Brian Cunningham and Charles Choi at the University of Illinois at Urbana–Champaign have designed a 96-well microplate that reduces the volume of precious chemicals needed to perform a drug screening assay. The bottom surface is a network of fluid channels integrated with biosensors.

Microplates, flat plates with multiple wells used as tiny test tubes, are used in high-throughput screening (HTS). In HTS scientists screen though thousands of chemical compounds looking for an interaction with a target protein.

Detection of these biochemical interactions without the use of fluorescent labels is desirable as it can be tricky to add these labels in a reproducible way, and sometimes impossible to add at all. Optical



biosensors, like the photonic crystal ones used in this microplate, detect these interactions through the change in dielectric permittivity that occurs on the surface of the biosensor when molecules attach to it.

The common well adds or removes reagents

Reference
C J Choi and B T Cunningham,
Lab Chip, 2007, DOI: 10.1039/
b618554c

Integrating biosensors with microfluidic channels allows the scientist to reduce the quantity of chemicals they use. However, not many biosensors are capable of interfacing with a large number of microfluidic channels in parallel, especially when the biosensors and fluid channels are small, said Cunningham.

In each 12-well row within the microplate, the fluid channels form 11 analyte wells. They are gathered to a single detection region, where all 11 channels can be monitored at once. A central common well in each row serves as an access point for introduction or withdrawal of reagents for the flow channels.

Their plan, said Cunningham, is to increase the level of integration so that a single three by five inch photonic crystal surface can support around 2500 microfluidic channels and assays.

Sarah Corcoran

Slivers of silica doped with lanthanides emit white light

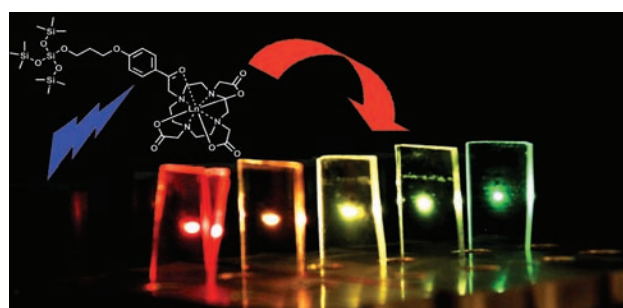
Light layers

A simple process for preparing light-emitting layers of silica with wide colour variation has been developed by Italian scientists.

The promise of preparing white light emitting materials for flat displays stimulated a team led by Gianluca Accorsi of National Research Council, Bologna, to develop luminescent hybrid layers. They combined the light emission properties of different lanthanide-based dyes with stable and optically transparent glassy films.

Lanthanide luminescence has major obstacles to overcome before it can realise its potential for many applications. The obstacles include low light absorption and losing luminescence intensity due to interactions between the long-lived lanthanide excited states and the hosting matrix.

Accorsi's team have overcome these hurdles by employing



acetophenone units to play the role of antennae and using a transparent silica layer as the host matrix, preventing excited state deactivation. Furthermore, these highly efficient lanthanide complexes are covalently linked to (rather than dispersed in) the matrix, allowing homogeneous loading of controlled distributions of the well-known red Eu(III) and green Tb(III) emitters.

Accorsi said that an advantage of

Acetophenone units act as antennae

Reference
L Armelao *et al*, *Chem. Commun.*, 2007, DOI: 10.1039/
b618554c

their synthetic strategy is that it is based on the 'statistical distribution of the different photoactive centres within the transparent film, and not on the tedious and time-consuming multistrata arrangement technique often used, as an example, in the fabrication of white-light emitting OLED devices'. He went on to forecast that 'The use of blue-greenish emitters could afford white-light emitting single layers obtained through the easily manageable synthesis of photoactive materials and simple fabrication processes.'

This view was echoed by Vincenzo Balzani, a specialist in photochemistry and nanotechnology at the University of Bologna, Italy, who believes that this 'most interesting result may open the way to construct colour tunable luminescent devices'.

Ian Gray

Instant insight

Nanocrystals as sensors

Rebecca Somers, Mounqi Bawendi and Daniel Nocera of MIT, US, explain how to solve a paradox: making quantum dots both bright and sensitive

Inorganic semiconductor nanocrystals (NCs), popularly known as quantum dots, have found application in biology mostly as optical imaging agents. Compared to conventional organic dyes, NCs exhibit broad absorption profiles, narrow tunable emission, photostability, and high quantum yields. Imaging applications exploit these optical qualities, and the NCs act as bright beacons of light that may be followed within the biological milieu. Although the synthesis of quantum dots dates back to the early 1990s, their application to biology rocketed with two significant advances in recent years. One is the development of core-shell structures formed by coating the original quantum dot with a thin layer of a higher band gap inorganic material. This 'overcoating' makes the NCs extremely bright and more robust by chemically and electronically shielding the cadmium selenide (CdSe) core from its surroundings. The other advance came in 1998, when two different methods to water-solubilize dots were published. The water solubility of core-shell dots enabled their ready application to the aqueous world of biology.

The foregoing advances present a paradox for the application of NCs beyond imaging and labeling. Now, current research is focused on making these small fluorescent dots sensitive, to be 'smart' and optically report on the chemical and biological environment that surround them. But here is the paradox: the properties of the NCs for imaging and labeling applications are achieved by making the NC impervious to its environment. How can NCs be sensitive to their environment if they are encased within the cocoon



Fluorescent quantum dots: beacons to follow in biological media

of a passivating overcoat?

The way out of this quandary is to design NCs that can participate in fluorescence resonant energy transfer (FRET). The binding of a second chromophore, which can resonantly accept energy from the NC excited state, introduces a new pathway for the flow of energy resulting from light absorbed by the NC. The efficiency of FRET between the NC donor and energy acceptors, which is highly dependent upon donor-acceptor distance and the spectral overlap between the donor emission and acceptor absorption, can be used to give specific information about the NC surroundings. In this way, chemically passivated quantum dots can report on their environment, thus turning NCs into sensors.

Information on nucleic acid processes such as telomerization, replication, hybridization and cleavage is usually obtained by modifying one strand with a NC and by conjugating the complementary strand with an energy acceptor dye. As the two strands begin to interact and intertwine, the distance

between the NC and the dye changes to modulate the efficiency of FRET.

Several different strategies are used to engender NC sensitivity to small molecules and ions. First, a receptor (such as an antibody fragment) with affinity for the target analyte can be tethered to the CdSe NC surface. The receptor is pre-loaded with a quencher dye, effectively turning off the emission of the NC. When the target is added, the quencher is displaced and the luminescence restored. A different strategy involves controlling the aggregation of differently sized (and hence differently colored) NCs in the presence of an analyte. If the analyte induces aggregation of NCs, an increase in FRET from the smaller to larger CdSe NCs will cause a redshift in the overall emission. Another emerging strategy relies on the energy transfer between NCs and permanently tethered, analyte-sensitive chromophores or fluorophores, which have been exemplified as pH sensors. In these sensors, a pH-sensitive spectral overlap between the NC and acceptor dyes affects the efficiency of energy transfer. This final strategy has the advantage of reversibility in the sensing mechanism, and in the case that the tethered dye is a fluorophore, a ratiometric signal from the NC and dye emission can be obtained, allowing for self-calibration.

While current research is expanding the repertoire of NC sensing to other analytes and other types of quantum dot NCs, the field of NC sensors has been established and is now a rapidly expanding one.

Read the full tutorial review 'CdSe nanocrystal based chem-/bio-sensors' in issue 4 of Chemical Society Reviews.

Reference

R C Somers, M G Bawendi and D G Nocera, *Chem. Soc. Rev.*, 2007, **36**, 579



IST Sample Preparation • Bioanalysis • Clinical • Environmental • Forensic • Agrochemical • Food • Doping Control

EVOLUTE™ ABN—easy and reliable

Minimize matrix effects, reduce ion suppression and concentrate analytes of interest for better quantitation

EVOLUTE™ ABN (Acid, Base, Neutral) is a water-wettable polymeric sorbent optimized for fast generic reversed phase SPE. The smaller (40Å) pore diameter prevents the retention of large molecular weight interferences providing cleaner extracts and higher analyte recoveries. Available in 96-well plate and column formats. Visit www.biotage.com to request a FREE sample.


Biotage
www.biotage.com

Interview

In a spin

Daniella Goldfarb talks to Colin Batchelor about her dreams for electron paramagnetic resonance

**Daniella Goldfarb**

Daniella Goldfarb is the Erich Klieger chair in chemical physics at the Weizmann Institute of Science, Rehovot, Israel. Her research interests in electron paramagnetic resonance range from metalloproteins to zeolites. She has been a member of the *Physical Chemistry Chemical Physics* editorial board since the start of 2007. Daniella Goldfarb was recently awarded the Bruker BioSpin Lectureship by the RSC's electron spin resonance group at their 40th annual international meeting.

What are you working on at the moment?

I concentrate on electron paramagnetic resonance (EPR) – the older and smaller brother of nuclear magnetic resonance. It deals with compounds that are paramagnetic, with one or more unpaired electron. We use it to learn about structure and dynamics in different systems, but we are involved in developing the spectroscopy and instrumentation. We not only use commercial instruments but we build our own spectrometers too, so we can do things that are out of the ordinary, but will hopefully turn into routine experiments.

What does EPR tell us that other methods can't?

Let's look at a metalloenzyme where the metal centre is paramagnetic. In this case NMR has difficulties because the lines of nuclei near the metal are usually very broad. X-Ray crystallography is great, but only if I have crystals. Even if I have crystals it tells me where the atoms are, but it doesn't tell me about the electronic structure, the oxidation state, charge distribution *etc.* In metalloenzymes these are very important because these really determine the activity of the site. Having the structure is the beginning, so you know where the atoms are and you can start working out what they do. For this you need spectroscopy. And for paramagnetic centres EPR is often the method of choice.

A lot of Israel's GDP goes on fundamental research – why do you think Israel does this?

We complain that it's not enough! When Israel was really young and the standard of living was much lower, more money was going into education and research than now, so although it looks a lot, it's going down. When times were really tough (economically) the government realized that the only resource that Israel has is its people, and you have to invest in education. Maybe our politicians don't understand that the successes we've had with Nobel Prizes in the past few years were based on work done years ago.

What started you on magnetic resonance problems?

After my B.Sc. I knew I would go into physical chemistry. I was looking for a PhD position and spoke to different people at several universities: you have to think about the advisor, though you know your general area of interest. I was lucky to talk to the one who 'fathered' the field of magnetic resonance in Israel, which has a long tradition. If you look at the number of people who do magnetic resonance in the Weizmann Institute you realize

the stature is relatively high for a small country. I started with NMR and once you're in the field of magnetic resonance it requires a lot of expertise, mastering both the theory and the experimental method. Once you achieve it, you don't move out so easily so I guess I'd always stay doing magnetic resonance, but I can apply it to new fields.

Are there any exciting new applications you'd like to follow up?

So far we've worked on metalloprotein systems in the resting state, characterizing the active site and aiming at relating its structure to what its function. What we'd like to do is follow the metal active site during a reaction, to quench the reaction and trap intermediates and unravel the reaction mechanism. I'd like to see a movie of the reaction – right now with standard freeze-quench instrumentation you have a resolution of 5 ms, which is enough for certain reactions. So, in principle, you can follow the time evolution of hyperfine coupling parameters and distances between paramagnetic centres. This will give a movie based on experimental results, not molecular dynamics simulations.

What's the big obstacle?

You just have to feel comfortable with the more advanced techniques. For conventional frequency EPR there is no problem. For high-field EPR the sample is in a very tiny capillary and to do this freeze-quench you have to rapidly freeze the reaction, then inject it into this tiny capillary. There is a group that has managed to do this and we'll find a way too. Another problem for biological samples is that the concentrations are low. EPR is still not as sensitive a technique as fluorescence. I believe that in a year or two we'll manage. Once the sample is frozen in the spectrometer it doesn't matter whether it's an intermediate or a stable state. This direction will keep us busy for the next ten years.

If you could work on a scientific problem in any field, what would it be?

I would like to stay in EPR spectroscopy, but apply it to nanostructures and single molecules. The problem is sensitivity right now. I'd like to go smaller, not to stay in the bulk, but to look at surfaces or single nanostructures. This is more of a dream than a new direction, but I'd like to look at a molecular machine at work. The problem is always resolution vs sensitivity; you have high sensitivity and low resolution or low sensitivity and high resolution.

Another successful ACS meeting

The RSC enjoyed a busy and exciting ACS spring meeting in Chicago. The RSC stand was so well attended that by the end of the four days books and puzzles had completely sold out and all of the promotional and informative material representing the breadth of our activities had been devoured by the conference delegates!

New products and innovations from the publishing division that were presented and demonstrated were very well received, and represented our commitment to providing publishing solutions to aid the communication and progress of the chemical sciences. New products introduced at the ACS meeting included:

Project Prospect, an innovative new project that makes the science in RSC journal articles really come alive, and the RSC **eBook Collection**, the



fully searchable archive giving access to over 700 RSC book publications. RSC Publishing also celebrated *New Journal of Chemistry*'s 30th and *Organic & Biomolecular Chemistry*'s 5th year of publication with a meet-the-editor session at the RSC stand. Delegates were invited to interact with each other and the editors of the two publications, Denise Parent and Vikki Allen, in an informal and friendly environment over coffee, cookies and cakes.

To complement the excellent exhibition we were delighted to be joined by so many friends and colleagues at a splendid RSC reception where the newly appointed publishing director, Robert Parker, discussed new and future endeavours of RSC Publishing. Year after year it is such a pleasure to see so many old and new friends supporting our activities and we look forward to strengthening those friendships at the next ACS meeting.

And finally...

The highly successful **Biomolecular Sciences Book Series** now includes seven titles that provide an authoritative insight to research at the chemistry–biology interface. Here are some of the great things people are saying about these topical books:

Sequence-specific DNA Binding Agents

'An excellent overview of the work being done'
ChemBioChem

Biophysical and Structural Aspects of Bioenergetics

'A beautifully produced research-level resource...'
Chemistry World

Structural Biology of Membrane Proteins

'...a snapshot of the state of the art'
ChemBioChem

Exploiting Chemical Diversity for Drug Discovery

'...is an excellent and astonishingly complete compilation on this broad and demanding topic for current practitioners'
Angewandte Chemie

Structure-Based Drug Discovery

'There are very few of us who will invent a drug, but by using the techniques described (in this book), you will shorten your own odds considerably'
Chemistry World

For more information visit
www.rsc.org/biomolecularscience

Bringing Biology in Focus

Scientists with an interest in specific topics at the chemistry–biology interface can easily find relevant research articles from across RSC journals, thanks to the launch of *Biology in Focus*. This new website will showcase a new subject area each quarter, beginning with 'Cancer and other disease states'. Future topics will include microarrays, metabolomics, quantitative proteomics, genomics and biomarkers.

Many scientists focus on the rapidly developing interface between chemistry and biology to achieve a better balance between research and real-world applications. Exciting new analytical and miniaturised tools are allowing better interrogation, improved measurement and increased understanding of biology and biological systems, which in turn are leading to major developments in these interfacial areas.

RSC journals *Molecular BioSystems*, *Lab on a Chip* and *The Analyst* have joined forces to encourage and promote this interdisciplinary collaboration and cooperation between the disciplines. The *Biology in Focus* website aims to increase knowledge by presenting material appearing in all three of these journals, with additional material from other RSC journals as appropriate.
www.rsc.org/biologyinfocus

Chemical Technology (ISSN: 1744-1560) is published monthly by the Royal Society of Chemistry, Thomas Graham House, Science Park, Milton Road, Cambridge UK CB4 0WF. It is distributed free with *Chemical Communications*, *Journal of Materials Chemistry*, *The Analyst*, *Lab on a Chip*, *Journal of Environmental Monitoring*, *Green Chemistry*, *CrystEngComm*, *Physical Chemistry Chemical Physics* and *Analytical Abstracts*. *Chemical Technology* can also be purchased separately. 2007 annual subscription rate: £199; US \$376. All orders accompanied by payment should be sent to Sales and Customer Services, RSC (address above). Tel +44 (0) 1223 432360, Fax +44 (0) 1223 426017 Email: sales@rsc.org

Editor: Neil Withers

Associate editors: Nicola Nugent, Celia Clarke

Essential Elements: Sarah Day, Valerie Simpson, Caroline Wain

Publishing assistant: Jackie Cockrill

Publisher: Graham McCann

Apart from fair dealing for the purposes of research or private study for non-commercial purposes, or criticism or review, as permitted under the Copyright, Designs and Patents Act 1988 and the copyright and Related Rights Regulations 2003, this publication may only be reproduced, stored or transmitted, in any form or by any means, with the prior permission of the Publisher or in the case of reprographic reproduction in accordance with the terms of licences issued by the Copyright Licensing Agency in the UK. US copyright law is applicable to users in the USA.

The Royal Society of Chemistry takes reasonable care in the preparation of this publication but does not accept liability for the consequences of any errors or omissions.

Royal Society of Chemistry: Registered Charity No. 207890.

RSC Publishing

©The Royal Society of Chemistry 2007

Key green chemistry research areas—a perspective from pharmaceutical manufacturers

David J. C. Constable,^a Peter J. Dunn,^{*b} John D. Hayler,^c Guy R. Humphrey,^d Johnnie L. Leazer, Jr.,^d Russell J. Linderman,^e Kurt Lorenz,^f Julie Manley,^g Bruce A. Pearlman,^h Andrew Wells,ⁱ Aleksey Zaks^h and Tony Y. Zhang^f

Received 7th March 2007, Accepted 26th March 2007

First published as an Advance Article on the web 17th April 2007

DOI: 10.1039/b703488c

In 2005, the ACS Green Chemistry Institute (GCI) and the global pharmaceutical corporations developed the ACS GCI Pharmaceutical Roundtable to encourage the integration of green chemistry and green engineering into the pharmaceutical industry. The Roundtable has developed a list of key research areas. The purpose of this perspective is to summarise how that list was agreed, provide an assessment of the current state of the art in those areas and to highlight areas for future improvement.

Introduction to the ACS Green Chemistry Institute Pharmaceutical Roundtable

In 2005, the American Chemical Society (ACS), Green Chemistry Institute (GCI)¹ and several leading global pharmaceutical corporations developed the ACS GCI Pharmaceutical Roundtable (ACS GCIPR, hereafter referred to as the Roundtable)² to encourage innovation while catalysing the integration of green chemistry and green engineering into the business of drug discovery, development and production. The pharmaceutical industry is devoted to inventing medicines that allow patients to live longer, healthier, and more productive lives. In addition these pharmaceutical companies are also committed to bringing key medicines to the patient with minimum impact on the environment.

The Roundtable's mission is to catalyse the implementation of green chemistry and green engineering in the global pharmaceutical industry. To achieve this mission, the Roundtable identified four strategic priorities.

1. Inform and influence the research agenda

To identify and to monitor new research opportunities for more efficient process development and production. To

influence the technical agendas of federal/international funding agencies by defining needs and advocating investment in specific areas of green chemistry and engineering innovation. To encourage external funding support for research in academic and government laboratories that will have direct value to the pharmaceutical industry.

2. Tools for innovation

To identify, design, and provide tools available to member companies to promote green chemistry and engineering innovation within the industry. To provide a centralised resource for accumulating alternatives, sharing tools, maintaining the toolbox, and minimising duplication of effort.

3. Education resource

To educate and influence today's and tomorrow's pharmaceutical leaders on the business value and scientific merit of applying green chemistry and engineering in the pharmaceutical industry.

4. Global collaboration

To provide green chemistry and engineering expertise to pharmaceutical corporations worldwide by utilising the GCI network of international affiliates and researchers and by sharing best practices among our members.

Membership to the Roundtable is open to all pharmaceutical research, development, and manufacturing companies. Members at the time of writing this paper were (in alphabetical order): AstraZeneca, Eli Lilly & Company, GlaxoSmithKline, Johnson & Johnson, Merck & Co., Inc., Pfizer, Inc., and Schering-Plough Corporation. Each company has a green chemistry program in various stages of development from infancy through more mature; however, the work of the Roundtable addresses the generally consistent underlying needs of all programs, thereby providing value to all members.

The activities of the Roundtable reflect the joint belief that the pursuit of green chemistry and green engineering is imperative

^aGlaxoSmithKline Pharmaceuticals, 1 Franklin Plaza, Philadelphia PA, 1 USA

^bPfizer Global Research and Development, Sandwich, Kent, UK CT13 9NJ

^cGlaxoSmithKline Pharmaceuticals, Old Powder Mills, nr Leigh, Tonbridge, UK

^dMerck Research Laboratories, Rahway, New Jersey, NJ 07065-0900, USA

^ePfizer Global Research and Development, Groton, Connecticut, CT-06340, USA

^fLilly Research Laboratories, Eli Lilly and Company, Indianapolis, 46285, USA

^gACS Green Chemistry Institute, 1155 Sixteenth Street, N.W. Washington DC, 20036, USA

^hSchering-Plough Research Institute, 1011 Morris Ave., Union, NJ, 07083, USA

ⁱAstraZeneca Global Process R&D Charnwood, Loughborough, Leicestershire, UK LE11 5RH

for a sustainable business and environment. Collaboration results in a strong organisation to prioritise research needs and to influence the technical research agendas of national/international funding agencies and to improve the cost effectiveness of investment in the design and implementation of green chemistry and engineering tools specific to the industry. The work presented in this paper reflects the collaborative efforts of member companies to identify key green chemistry research areas of need for the industry. With this information, we seek to influence research agendas and directly fund research through the ACS GCI Pharmaceutical Roundtable Research Grant Program, with the objective to provide our scientists with readily available, proven greener alternatives to current pharmaceutical process development methods.

Process for identifying and agreeing on the key green chemistry research areas

The process of identifying and agreeing on the key research areas is shown diagrammatically in Fig. 1. The process started with gathering ideas from all the companies *via* a brainstorming exercise, followed by a cross company debate and assessment of the research areas, then concluded by a voting exercise where each Roundtable company had an equal vote.

The output of the brainstorming exercise is shown below. The ideas were grouped into three categories: (i) reactions that pharmaceutical companies use, but would strongly prefer better and greener reagents, (ii) more aspirational reactions (*i.e.* reactions that companies would like to use, if they were available, as they offer potentially cleaner synthetic approaches to the current art) and (iii) ideas outside of the reaction theme (concerned with solvent use). We felt that all the ideas on the brainstorming list were good and worthy of research, but from a pragmatic point of view the ideas needed to be prioritised.

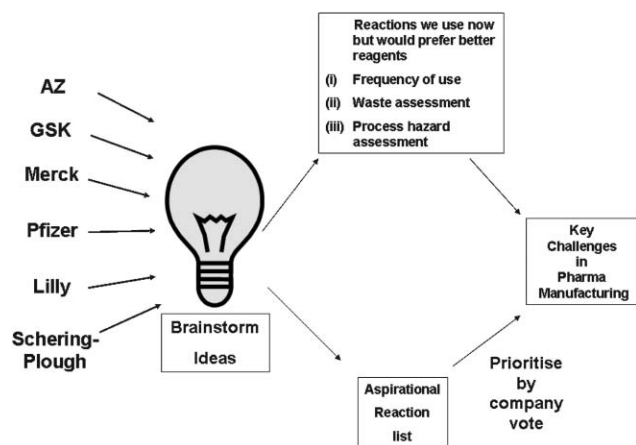


Fig. 1 The process for identifying and agreeing on the key research areas.

Brainstorm output on key research areas

Reactions currently used but better reagents preferred

Safer and more environmentally friendly Mitsunobu reactions

Reduction of amides avoiding LiAlH_4 or B_2H_6
 Bromination reactions
 Sulfonation reactions
 Amide formation avoiding poor atom economy reagents
 Nitration reactions
 Demethylation reactions
 Friedel–Crafts reactions on unactivated substrates
 Ester hydrolysis
 OH activation for nucleophilic substitution
 Epoxidation
 Wittig chemistry without (Ph_3PO)
 Radical chemistry without Bu_3SnH

More aspirational reactions

Asymmetric hydrocyanation
 Aldehyde or ketone + NH_3 + “X” to give a chiral amine
N-Centred chemistry avoiding azides, hydrazine *etc.*
 Asymmetric hydrolysis of nitriles
 Asymmetric hydrogenation of unfunctionalised olefins/enamines/imines
 Asymmetric hydroformylation
 C–H activation of aromatics (cross-coupling reactions avoiding the preparation of haloaromatics)
 C–H activation of alkyl groups
 New greener fluorination methods
 Oxygen nucleophiles with high reactivity
 Green sources of electrophilic nitrogen
 Asymmetric hydroamination of olefins
 Organocatalysis
 $\text{ROH} + \text{ArCl}$ to give ROAr

Solvent themes

Solvent-less reactor cleaning
 Replacements for polar aprotic solvents, NMP, DMAc, DMF *etc.*
 Alternatives to chlorinated solvents

For the reactions which companies currently use but better alternatives are needed, we decided to use a three point assessment. We looked at how often the reactions were used in making pharmaceutical products, taking advantage of a survey recently published by three of the Roundtable member companies.³ Another key component was to consider how much waste each reaction generated, and a GSK database was used to give a qualitative assessment. The third part of the assessment concerned process safety, for which data from the Pfizer database of reaction assessments (Toxtherm) was used to make the judgment. In addition, literature data and data on reported explosion hazards was taken into consideration. For example Barton and Nolan report⁴ that after polymerisation, the second and third most common causes of explosions are nitration and sulfonation reactions.

The voting process

Each company consulted its green chemistry teams and some of its most senior scientists in chemical development before coming to a company vote. All companies agreed that the

Table 1 Reactions companies use now but would strongly prefer better reagents

Research Area	Number of Roundtable companies voting for this research area as a priority area
Amide formation avoiding poor atom economy reagents	6 votes
OH activation for nucleophilic substitution	5 votes
Reduction of a mides without hydride reagents	4 votes
Oxidation/Epoxidation methods without the use of chlorinated solvents	4 votes
Safer and more environmentally friendly Mitsunobu reactions	3 votes
Friedel–Crafts reaction on unactivated systems	2 votes
Nitrations	2 votes

solvent-less reactor cleaning and replacements for polar aprotic solvents were critical and hence made the final list. Next, each company identified the top five areas within the two reaction categories.

A summary of the voting is shown in Tables 1 and 2.

One of the key messages was that there was a lot of commonality in the company votes. For example all 6 companies voted for amide formation,⁵ reflecting the high level of use (9.1%)⁶ and the poor atom efficiency of many current methods. All companies voted for cross couplings without preparation of haloaromatics, showing the high use of Suzuki⁷ and related reactions and a concern for the high level of waste that these palladium cross coupling reactions generate.

Hence the final list of the 12 key green chemistry research areas is the following: amide formation, OH activation, amide reduction, oxidations/epoxidation methods without the use of chlorinated solvents, safer and more environmentally friendly Mitsunobu reactions, C–H activation of aromatics, chiral amine synthesis, asymmetric hydrogenation, greener fluorination methods, *N*-centred chemistry, greener alternatives to polar aprotic solvents and solvent-less reactor cleaning. Each one of these key research areas is discussed in more detail.

(i) Amide formation avoiding poor atom economy reagents

An analysis of drug candidates prepared by three leading pharmaceutical companies found that amide bond formation was utilised in the synthesis of 84 (65%) of the 128 candidates surveyed.³ Forty four percent were based on acid chloride intermediate, a relatively environmentally benign approach where, for example if thionyl chloride is employed to make the acid chloride, the by-products, SO₂ and HCl, can be removed by scrubbing through a basic solution. About 36% of the 84 amide bond forming reactions were carried out by means of a coupling reagent such as *N*-ethyl-*N'*-(3-dimethylaminopropyl)carbodiimide hydrochloride [EDCI·HCl, catalysed by

HOBt (the triazole is a high energy molecule and potential explosive)], 1-propylphosphonic acid cyclic anhydride or *N,N'*-carbonyldiimidazole (CDI). These methods are less “atom economical” in that they generate greater quantities of waste as measured by their mass intensity factor (MI), (defined as the ratio of a total mass in a process divided by mass of product in kg).⁸ Commercial examples of amide formation using CDI include sildenafil⁹ and sunitinib,¹⁰ however this method still generates by-products with a combined molecular weight of 180 to accomplish a dehydration reaction, ten times more mass than if water itself were the only by-product.

Amide bond formation using enzymatic catalysis eliminates some of the issues associated poor atom economy as well as the potential hazards associated with non-aqueous chemical based approaches. Hydrolysis of nitriles catalyzed by nitrile hydrolases and lipase-catalysed amidation of carboxylic acids and esters with ammonia leading to the formation of primary amides are clean, safe and efficient.¹¹ For example, in a process practiced by Mitsubishi Rayon Corporation, both the %conversion of acrylonitrile and the %yield of acrylamide reach 99% under standard operating conditions of 0–5 °C, pH 7.5–8.5.¹² Likewise, enzyme-catalysed amide bond formation catalysed by peptidases and acylases eliminates the use of highly reactive coupling reagents and minimises the need for protection/deprotection steps, thus improving the MI significantly.¹³ Moreover, mild reaction conditions and the excellent stereo- and regioselectivity of enzymes precludes racemisation and guarantees structural fidelity of the product. Despite significant progress in biocatalytic amide synthesis and some commercial success, the narrow substrate specificity of the currently available enzymes severely limits their practical use. The development of new molecular biology tools has enabled the expansion of the numerous functional properties of biocatalysts, and is expected to increase their commercial utility in the next 3–5 years.

Table 2 More aspirational reactions

Research Area	Number of Roundtable companies voting for this research area as a priority area
C–H activation of aromatics (cross coupling reactions avoiding the preparation of haloaromatics)	6 votes
Aldehyde or ketone + NH ₃ + “X” to give chiral amine	4 votes
Asymmetric hydrogenation of unfunctionalised olefins/enamines/imines	4 votes
New greener fluorination methods	4 votes
<i>N</i> -Centred chemistry avoiding azides, hydrazine etc	3 votes
Asymmetric hydramination	2 votes
Green sources of electrophilic nitrogen (not TsN ₃ , nitroso, or diimide)	2 votes
Asymmetric hydrocyanation	2 votes

In summary, amide bond formations are one of the most common transformations carried out in pharmaceutical synthesis. Their efficiency, however, is hampered by widespread use of reagents with poor atom economy. Therefore, development of reagents with lower MI-factors or, ideally, catalytic methods, such as the exciting use of boric acid to catalyse amide formation,¹⁴ would favourably impact the environmental profile of many processes.

(ii) Alcohol activation for nucleophilic substitution

The substitution of activated alcohols is a frequently used approach for the preparation of active pharmaceutical ingredients (APIs). In a recent survey, 2% of transformations comprised conversions of alcohols to halides or sulfonate esters (invariably for further use), and 64% of all nitrogen substitution reactions were alkylations.³ Direct nucleophilic substitution of an alcohol is attractive as it should yield water as the by-product, however, hydroxide is a poor leaving group usually requiring activation. Direct substitution of some allylic, benzylic and tertiary alcohols may be achieved *via* an S_N1 reaction but this approach typically requires excess Brønsted or stoichiometric amounts of Lewis acids and does not afford control over stereochemistry. Secondary alcohols can be substituted with good stereospecificity using a Mitsunobu protocol, the issues of which are discussed below. Activation is wasteful as it requires additional processing and the activating group, once displaced, also has to be separated from the product and the resulting waste must be disposed. The consequences of activation are illustrated by the synthesis of the dopamine agonist ropinirole **1** (Scheme 1).¹⁵ The toluenesulfonate (**2**, R = OTs) is displaced with dipropylamine affording ropinirole in 85% yield. Whilst affording a significant improvement over an earlier route, where displacement of bromide (**3**, R = Br) gave ropinirole in 57% yield due to competing elimination, the net conversion of alcohol (**4**, R = OH) is achieved in 74% yield. The preparation of **2** from **4** had a mass intensity of 25 kg kg⁻¹.¹⁵

There are encouraging recent advances in this area. Catalytic activation of allylic and benzylic alcohols has been demonstrated using indium(III) chloride for displacement with acetylenic, allylic or propargylic silanes,¹⁶ and activation by 4-toluenesulfonic acid, including polymer bound acid, allows for displacement of the alcohol with a range of carbon, nitrogen, oxygen and sulfur nucleophiles.¹⁷ A wider range of alcohols, including primary and secondary, have been substituted with amines by *in situ* oxidation and reduction

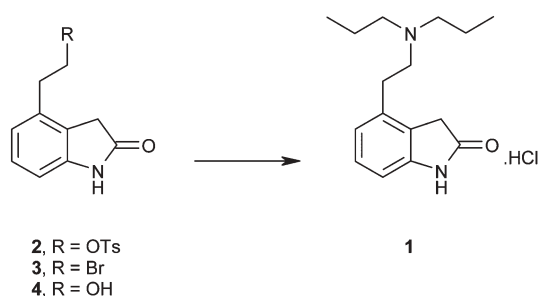
catalysed by iridium complexes.¹⁸ This approach has been extended to the preparation of carbon–carbon bonds, for example using a ruthenium catalyst.¹⁹ The challenge of achieving a method of activation for secondary alcohols that maintains control over the stereochemistry of the reaction remains.

(iii) Reduction of amides without hydride reagents

Essentially all medicines and current drug candidates contain at least one basic nitrogen atom. A common approach to the synthesis of amines is to reduce the corresponding amide with a hydride reagent such as LiAlH₄, DIBAL, RedAl, B₂H₆, Et₃SiH, or polymethylhydroxysilane (PMHS). The reaction survey³ reported that reduction of amides to amines was used in only 0.6% of chemical transformations; this number would surely be higher if safer methods for use on scale were available. The survey indicated that the number of amide reductions was equally split between diborane and hydride reagents. Lithium aluminium hydride, having a molecular weight of 38 and four hydrides per molecule, has the highest hydride density and is frequently used, even though it co-generates an inorganic by-product (lithium aluminum hydroxide) which is difficult to separate from the product. The workup procedure recommended by one bulk supplier (Chemetall) is to precipitate and filter the aluminum hydroxide salts. However, slow filtrations and product loss through occlusion or adsorption are typical problems that can be encountered. Options for disposal of the cake include dissolving in water and sending to a waste water treatment plant or drying the cake and sending to a chemical waste dump that accepts solids.²⁰ Both options have an environmental impact. Therefore, a generally applicable, safe, environmentally benign and economically viable method for the reduction of amides to amines would have an appreciable benefit to numerous processes.

Hydrogen gas is the ideal reductant because the only by-product is water. Thus, much research has been directed towards discovery of a transition metal catalyst selective for hydrogenation of amides. However, even with the best catalysts, both high temperature (~150 °C) and pressure (>100 bar) are required. These conditions involve expensive high pressure hydrogenation equipment not typically available in a common pharmaceutical manufacturing plant. The harsh conditions also preclude the use of these catalysts with substrates that contain other reducible or thermally labile functional groups. Recent research has led to the discovery of catalysts that are effective at lower temperature and pressure, giving encouragement that the goal of finding a selective, low pressure/temperature catalyst is realistic.²¹

Another approach would be to use a biotransformation to reduce the amide. It is notable that a number of bacteria and fungi reduce carboxylic acids to aldehydes or ketones.²² The usual fate of amides in biological pathways is hydrolysis. However, an anaerobic bacteria, *Clostridium sporogenes*, has been reported to reduce benzamide to benzylamine.²³ A key challenge in this technology area is gaining a detailed understanding of these complex enzyme-catalysed processes that require ATP/NADPH co-factor recycling, and getting the



Scheme 1 The synthesis of ropinirole **1**.

enzymes cloned and produced on a large scale in suitable expression systems.

The acylation/reduction strategy for *N*-alkylation avoids the need to handle alkylating agents and would be more widely used if a safer, more atom economical or preferably catalytic method for amide reduction were developed. The solution to this problem could be either chemical or biochemical.

(iv) Oxidation/epoxidation methods without the use of chlorinated solvents

The pharmaceutical industry performs more reduction reactions than oxidation reactions. The reaction survey³ shows that oxidations covered 3.9% of reactions whereas reductions were used in 14% of transformations. Oxidation reactions encompass transformations that either remove hydrogen from the molecule (for example, alcohol to aldehyde), or insert an oxygen into a C–C (Baeyer–Villiger, epoxidation) or C–H bond (aldehyde to acid).²⁴ By definition an oxidant is involved, and hence the reactions are generally of high energy in nature. While much progress has been made on the development of greener oxidation reagents (Ru^{II}/BuO₂H, TEMPO/NaOCl, Pd-catalysed aerobic oxidations), and the use of stoichiometric high valent metals (Mn, Os, Cr) have virtually been eliminated from pharmaceutical processes, several deficiencies among existing methods need to be addressed or supplanted with greener technologies. First, a great majority of oxidation reactions are conducted in inert, nonflammable chlorinated solvents. Second, catalysts containing heavy metals must be removed or recycled for toxicological, environmental or economic reasons. Third, transportation and storage of organic peracids, commonly used for epoxidation, incur significant business costs. Last, there is much to be desired in the choice of available oxidants. Molecular oxygen or air is the ideal oxidant; however, aerating flammable solvents is a significant safety concern that can only be fully addressed if the reaction can be conducted efficiently in water. Hydrogen peroxide is the second best choice with respect to atom economy, but utilisation, efficiency and narrow range of scope limit its application. Sodium hypochlorite is one of the most economical oxidants. However, it usually comes in the form of dilute aqueous solutions, which leads to the generation of large volumes of aqueous waste from the process. Several alternatives to Cl⁺, most prominently TCIA (trichloroisocyanuric acid), offer distinct advantages.²⁵ Yet, the preferred reaction medium still remains a chlorinated solvent. Developers of new reactions should bear in mind that any useful and widely adopted new reaction should offer certain advantages over existing methods. New reactions should target green reagents and solvents, safer and milder conditions, or improved selectivity. One unmet need for green oxidation is allylic oxidation. The insertion of oxygen into a C–H bond adjacent to a double bond can only be reliably achieved using a stoichiometric amount of SeO₂.

Biocatalysis is much further advanced in the area of oxidation than in reduction.²⁶ A classic example of the power of bio-oxidation is in the field of steroid synthesis. Without the development of highly regio- and enantioselective monooxygenase reactions, many potent steroidal medications would not

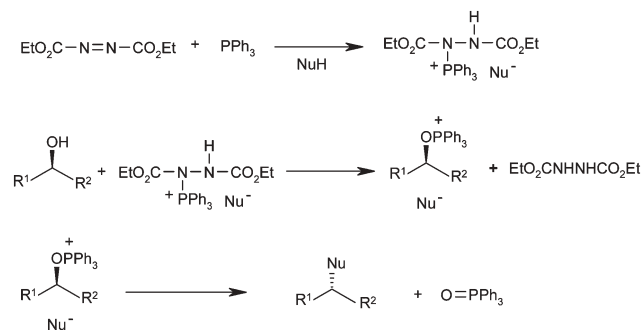
be available on scale at an economic price. However many challenges remain to be solved in this potentially highly valuable field.

The oxidation of methyl groups to produce certain functionalised aromatics and heteroaromatics has been scaled-up into production, but is by no means yet a universal solution. Some advances are being made into the understanding of how to scale-up reactions using redox enzymes thought to be too unstable to ever use—chloroperoxidase and Baeyer–Villiger monooxygenase being good examples.²⁷ Other exciting areas are the growth in the study of air oxidations catalysed by laccases with or without organic co-catalysts²⁸ and the use of peroxides and lipases to prepare epoxides.²⁹ It is interesting to note the serendipitous discovery of ‘ozonolysis-like reactions’ by several oxidising enzymes.³⁰ Could this be further developed into a useful technology to use in organic synthesis?

(v) A “greener” Mitsunobu reaction

The “redox” condensation reaction of alcohols with compounds having an active hydrogen (NuH), mediated by triphenylphosphine and dialkyl azodicarboxylates, has become known as the Mitsunobu reaction (Scheme 2) in recognition of his pioneering research during the 1960’s and 1970’s.³¹ This transformation has become a powerful and widely used reaction for organic chemists over the past 40 years due to several key attributes, which include: (1) chiral secondary alcohols are displaced with inversion with high stereospecificity; (2) extraordinary scope, including nucleophiles derived from oxygen, nitrogen, sulfur, and carbon, and a wide variety of alcohols; (3) compatibility with a broad range of functional groups; and (4) ease of operation, with most protocols requiring only simple addition of reagents to a flask and operating temperatures generally near room temperature.

The primary shortcoming of the Mitsunobu reaction is the use of stoichiometric quantities of the azodicarboxylate and triphenylphosphine, which overall function to eliminate water from this condensation reaction. Thus, waste products totaling more than 450 in molecular weight are generated to remove water, a highly atom-inefficient process. In addition, removal of these by-products requires additional processing, such as chromatography, to purify the product, producing additional waste. As well as the environmental considerations, diethyl azodicarboxylate is a high energy molecule and the Pfizer data base reports a decomposition energy of 1000 J g^{−1}. For these



Scheme 2 The Mitsunobu reaction.

reasons, commercial application of the Mitsunobu reaction has been very limited, and the reaction survey³² reports that only 0.2% of chemical transformations are Mitsunobu reactions.

Some research has been directed toward reducing the high environmental impact of the Mitsunobu reaction. Most of the work to date has focused on the use of polymer-bound triphenylphosphine.³³ The polymer bound reagent simplifies purification, allows for recycling and multiple use of the resin after reactivation, and minimises solvent usage. Use of both polymeric triphenylphosphine and polymeric azodicarboxylate equivalents was recently described by Toy and co-workers.³⁴ These polymer-bound reagents simplify product isolation, but recycling still requires cumbersome protocols and harsh reagents.

An alternate approach, that is also greener, is the use of the reagent cyanomethylenetriethylphosphorane, which combines both redox partners in a single reagent. The by-products of this reagent include acetonitrile and trimethylphosphine oxide, which are improvements over the original Mitsunobu reagents.³⁵

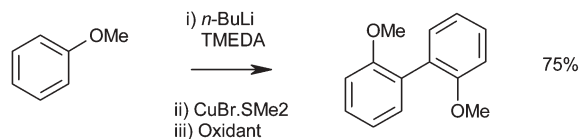
The ideal Mitsunobu reaction would be catalytic in nature, with the stoichiometric oxidant and reductant generating innocuous by-products. A first approach to this goal has been recently published by Toy and co-workers.³⁶ In their work, iodosobenzene diacetate is used as the stoichiometric oxidant, which produces the environmentally less burdensome by-products, acetic acid and iodobenzene, instead of the hydrazide. Triphenylphosphine is still employed (2 equiv.), so considerable research is still required to devise a reaction that is catalytic in both reagents.

The Mitsunobu reaction has become a powerful and popular transformation in the organic chemistry laboratory. Further research towards making this transformation green is required to realise its full potential in commercial applications.

(vi) C–H activation of aromatics

Aromatic groups are by far the most essential pharmacophores for medicinal chemistry and drug development. A cursory review of recent phase III and marketed pharmaceuticals reveals that more than 75% of them contain at least one aryl or heteroaryl group. A great number of the aryl groups, especially phenyls, are incorporated into the API preassembled. No aromatic ring synthesis was exercised in the process and virtually all of them are procured from basic or specialty chemical sources. Recent advances in metal-catalysed cross-coupling reactions have greatly facilitated the versatility of incorporating aryls for medicinal chemistry. However, most of these reactions rely on the availability of aryl bromides or iodides. Direct activation of aryl hydrogen (converting Ar–H into Ar–Ar) will be of great potential.

Directed metallation has gained popularity for its versatility at introducing electrophiles onto the aryl ring. A recent example of biaryl formation *via* an organocuprate oxidation without a preceding metal halogen exchange from an aryl halide is shown in Scheme 3. This directed lithiation avoids the separate preparation or purchase of an aryl halide, however, a prerequisite is the presence of a directing group at the *ortho* position.³⁷



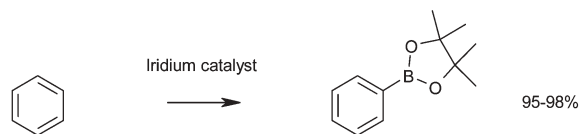
Scheme 3 C–H activation by directed metalation.

An unmet need for green chemistry is direct C–H activation using catalytic methods. An example is the iridium-catalysed C–H activation of aromatics (Scheme 4).³⁸ This chemistry provides the desired arylboronic acid directly from the C–H activation without the use of the aryl halide. The subsequent Pd-catalysed reaction with a second activated aryl group *via* known methods (for example aryl halides in a Suzuki–Miyaura coupling) provides efficient access to biaryls. However, new reactions that enable chemists to form a bond between aryl groups without having to go through any aryl halide (ArX) would be highly useful. An encouraging sign is that there has been a surge of exciting results in this area in the last few years.³⁹

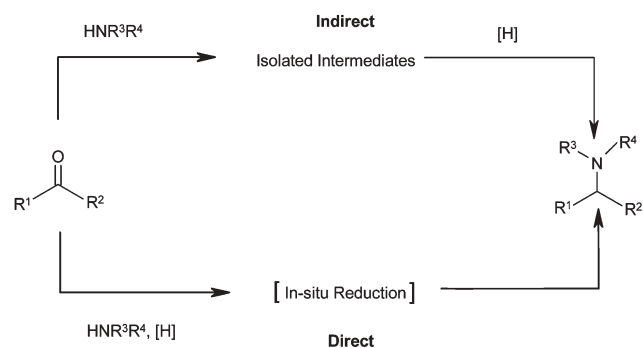
(vii) Asymmetric synthesis of amines from prochiral ketones

Over the past few decades researchers in academia and industry have explored the synthesis of α -chiral aliphatic amines from prochiral ketones. However, reports of general methods in high enantiomeric excess are rare.⁴⁰ In most cases, indirect reductive amination methods are used. These are generally limited to specific cases such as enamine hydrogenation,⁴¹ enantioselective alkylmetal addition to aliphatic aldimines,⁴² enantioselective transfer hydrogenation of ketimine derivatives,⁴³ diastereoselective addition to chiral imines,⁴⁴ or diastereoselective reduction of chiral methylbenzyl ketimine derivatives.⁴⁵

The direct reductive amination of ketones has been shown to be a very efficient methodology for the synthesis of racemic amines (Scheme 5). Development of asymmetric versions of



Scheme 4 Iridium catalysed C–H activation of aromatics.



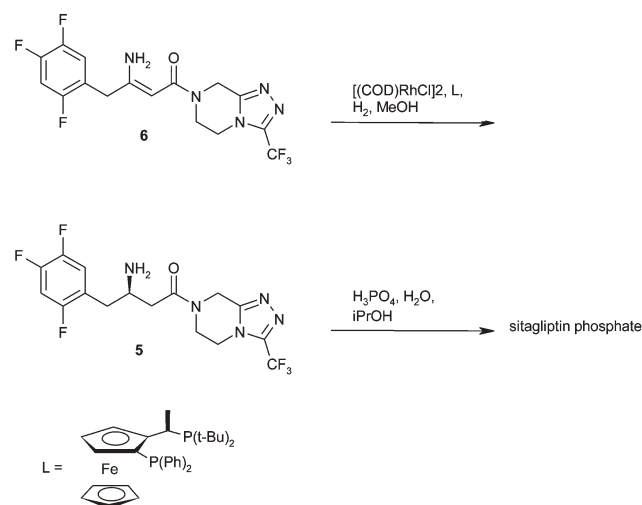
Scheme 5 Asymmetric synthesis of amines from prochiral ketones.

this reaction, on the other hand, have been difficult to realise.⁴⁶ A general methodology for the direct synthesis of α -chiral aliphatic amines from prochiral ketones would be an extremely valuable addition to the chemical transformation toolbox. Apart from the elimination of extra steps to prepare and isolate the imine substrates, the direct reductive amination of ketones could have major advantages in terms of overall efficiency and environmental impact.

(viii) Asymmetric hydrogenation of unfunctionalised olefins/enamines/imines

The reaction survey³ found that the predominant strategy for the introduction of chirality was through classical chemical resolutions as opposed to introductions through biotransformation or transition metal or organometallic catalytic means. Asymmetric hydrogenation provides an elegant methodology for the introduction of chirality, meeting many of the goals of green chemistry and is finding increasing application in API synthesis.⁴⁷ The efficiency of this approach is elegantly exemplified by the Merck second generation synthesis of sitagliptin **5** (Scheme 6), where an unprecedented final stage asymmetric hydrogenation of the unprotected enamide **6**⁴¹ resulted in an increase in overall yield of almost 50% and produced 100 kg less waste per kg sitagliptin⁴⁸ when compared with the first generation approach.⁴⁹

There are challenging areas remaining within the field, for example, the hydrogenation of enamides and related substrates in the synthesis of amino acids has numerous examples⁵⁰ but few examples exist for unsubstituted enamines⁴¹ and imines. Some classes of alkene offer additional challenges.⁵¹ For the pharmaceutical industry, the limited time for synthetic route identification is an issue and access to catalyst and ligand diversity is required to ensure the application of this approach.⁵² Some pharmaceutical companies have synthesised their own ligands and have found very effective catalysts.⁵³ The majority of academic asymmetric hydrogenation approaches are based on homogeneous catalysis to overcome issues of activation and mass transfer. For pharmaceutical use, efficient catalyst and ligand recovery, and eliminating heavy



Scheme 6 The synthesis of sitagliptin.

metal contamination of the API are significant requirements for the industry. These controls are often easier to achieve with heterogeneous methodology where there are less examples.⁵⁰ The demonstration of organocatalytic hydride transfer offers the possibility of future access to metal free asymmetric hydrogenations.⁵⁴

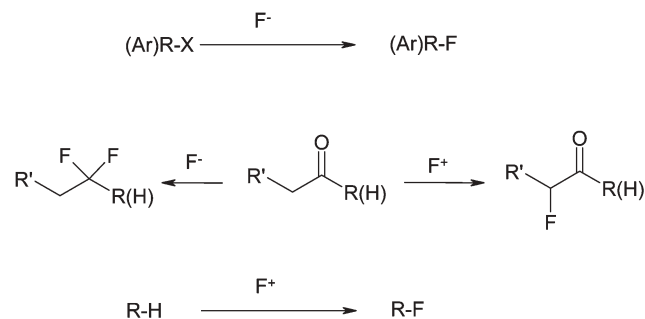
(ix) New greener fluorination methods

Owing to its unique stereoelectronic properties, fluorine has increasingly been used to block metabolism sites or to modulate electronic properties of the drug candidate without introducing steric bulk. Fluorine containing molecules account for 10% and 14% of launched pharmaceuticals and drug candidates currently in phase III clinical trials, respectively. The possibilities for fluorine incorporation only seem limited by the chemistry of forming the F–C bond. Unfortunately, there are only a handful of methods for introducing fluorine into target compounds—most of them involving harsh reaction conditions and the use of corrosive and hazardous reagents. As a result, chemists rely heavily on purchased starting materials with fluorine already incorporated, limiting their ability to explore all structure–activity relationship (SAR) spaces. Three categories for fluorination are commonly used (Scheme 7):

1. Fluorine exchange with a leaving group (Cl, Br, I, OH, OSO₂R, *etc.*) using either HF, or its alkali/ammonium salt.
2. Deoxyfluorination: converting either an aldehyde or ketone into a gemdifluoromethylene ($R_1R_2C=O \rightarrow R_1R_2CF_2$), or an alcohol into an aliphatic fluoride ($R_1R_2CHOH \rightarrow R_1R_2CHF$). For this purpose DAST has long ago replaced the notorious SF₄, and in recent years a more stable and user-friendly version (Deoxo-FluorTM) has emerged.⁵⁵
3. Direct fluorination from an electrophilic (F⁺) source (*e.g.* SelectfluorTM).⁵⁵ This usually requires a carbon nucleophile, such as the enolate of an aldehyde, ester or amide.

Fluorination is a very active area of research and new reagents are appearing all the time, for example 2,2-difluoro-1,3-dimethylimidazoline (DFI) which exchanges a fluorine for a hydroxyl group.⁵⁶

Unmet needs in the realm of incorporating fluorine into drug molecules include catalysts for increasing the nucleophilicity of F[–], milder conditions for conducting fluorine exchange reactions ($ArCl \rightarrow ArF$), and safer and more economical sources of electrophilic fluorine.



Scheme 7 Common methods to introduce fluorine.

(x) *N*-Centered chemistry avoiding azides, hydrazine, etc

The “hydroxyl to amine” transformation is important in pharmaceutical synthesis. Sodium azide is frequently used to effect the “hydroxyl to amine” transformation. It is popular in organic chemistry because it reliably affords high yields of products with predictable stereochemistry (enforced by the S_N2 mechanism) under relatively mild conditions. The “rule of six” states that six carbons (or other atoms of about the same size) per energetic functional group (azide or diazo or nitro) provides sufficient dilution to make a compound relatively safe.⁵⁷ However all Roundtable companies would consider organic azides intrinsically hazardous and would usually subject them to extensive safety testing using reaction calorimetry and adiabatic calorimetry techniques before considering scale-up of such chemistry. The preparation of amines requires treatment of a halide or sulfonate with aqueous sodium azide, a hazardous process due to the formation of heavy metal azides which are contact explosives. Sodium azide is a staple in every medicinal chemist’s shelf of reagents: for example Sharpless’ “click chemistry”⁵⁷ relies on alkyl azides, synthesis of beta lactams is based on azidoacetyl chloride, and that of 1,2,3-triazoles and tetrazoles is based on sodium azide. Tetrazoles, standard isosteres for carboxylic acids commonly used in medicinal chemistry are synthesised by cycloaddition of tri-*n*-butyltin azide to nitriles. Thus, there is a critical need in the industry to develop a technique for the safe handling of azides or more preferably chemistry which does not involve azides. The principal concern in azide chemistry is the risk of formation of heavy metal azide salts which are shock sensitive. The cadmium plated screws typically used to repair glass connectors in modern production plant equipment, and waste water pipes made of lead in older plants, present particularly high risk by potentially forming highly explosive cadmium or lead azides.⁵⁸ These realities make the handling of sodium azide in the plant environment hazardous. To address these issues, compounds like AZT are made in dedicated facilities which are designed and maintained at significant expense to handle azide compounds safely. Pyrazoles are generally made from hydrazine or a substituted hydrazine, examples such as sildenafil and celebrex are made from a substituted hydrazines, which require special handling and/or specialised facilities.

Considering the complexity of handling azides, many process units opt to use substitute reagents. Ironically, these substitute reagents generally have much higher MI-factors than azide or hydrazine. For example, the classical Gabriel synthesis involves displacing the leaving group with a bulky potassium phthalimide,⁵⁹ and then removing the phthalic acid group under harsh conditions.⁶⁰ Even though a number of equivalents of the Gabriel synthesis have been developed,⁶¹ they all require an activating, protecting, or blocking group, resulting in processes with elevated MI-factors. Nitrogen nucleophiles with lower MI-factors are also known, but they are generally insufficiently nucleophilic and tend to undergo polyalkylation (e.g., ammonia).⁶² Moreover, the inability to displace a sulfonate on a carbohydrate pyranose ring with clean inversion of configuration (without competing elimination) limits their synthetic utility.

Interestingly, even though azide is highly nucleophilic, sodium azide is not always the most effective reagent. For example, in the case of diacetone glucose tosylate, sodium azide gives no reaction, while ammonia and hydrazine displace the tosylate with inversion of configuration.⁶³ It is postulated that azide fails to displace tosylate because it is charged, and expulsion of a charged anionic leaving group into a non-polar environment is disfavored. Ammonia and hydrazine are more effective because the leaving group is not expelled as a charged anion, but rather as an ammonium salt into the non-polar environment. Therefore, even though the new azide-alternatives are unlikely to replace azide’s standing as the most nucleophilic nitrogen anion, their use in non-traditional media might address environmental and safety issues associated with the use of azide and its current replacements.

(xi) Replacements for dipolar aprotic solvents

This is a class of solvents of tremendous utility to chemists given their ability to solubilise a large number of chemicals and their support or promotion of a variety of chemistries through their polarity. However, solvents such as *N*-methylpyrrolidin-2-one (NMP), *N,N*-dimethylformamide (DMF) and *N,N*-dimethylacetamide (DMAc) have been found to have human reproductive risks and are therefore becoming targets of increasing regulatory constraint. They have also always been problematic from an environmental perspective because reaction work-ups usually involve large quantities of water, and the preferred disposal method for mixed aqueous/organic wastes has generally been incineration. Mixed aqueous/organic wastes of this type generally require additional fuel to incinerate, and have the added burden of NO_x formation. Given the high biological oxygen demand/chemical oxygen demand and nitrogen loadings these types of wastes have if they are discharged to a waste water treatment plant, there is reluctance to discharge to biological treatment, especially plants with tight NH_3 limits. Separation of the solvent from mixed aqueous waste streams is difficult in the batch chemical context, generally capital and energy intensive, and therefore not usually undertaken.

Therefore, given the utility of these solvents from a chemical perspective but the environmental and health risks they pose, suitable replacements of lower risk and less impact are required.

(xii) Solvent-less reactor cleaning

Organic solvents account for 75–80% of the waste associated with the synthesis of APIs. In addition to serving as media for reactions and separations, solvents are routinely used to clean reaction vessels following a campaign. Strict limits on cleanliness (typically 10–20 ppm) are followed by most pharmaceutical companies. In pilot plant operation, the volume of solvent used for cleaning is generally 2–3 times greater than the amount of solvent used in the reaction itself. Cleaning solvents are generally relatively green (e.g. methanol and acetone) and are sometimes recovered for subsequent reuse.⁶⁴ In the best case scenario, waste solvent is recycled; however distillation is frequently required, making the process energy and time intensive. Solvent waste disposal adds cost to

API production. Eliminating cleaning solvent would therefore decrease the environmental footprint of most pharmaceutical processes significantly.⁶⁵

Cleaning using solvent rinse and boil-out are generally inefficient. Frequently, the contaminants to be removed are structurally dissimilar from the product, and may have vastly different solubility properties from the desired product. For this reason, other cleaning systems have been evaluated. Aqueous hydrogen peroxide was found to be a suitable cleaning agent for the dissolution of certain organic residues.⁶⁶ Recent work utilising high-pressure water jet technology to clean reactors has proven beneficial.⁶⁷ The relationship between jet properties (e.g. temperature, pressure, composition, and impingement conditions) and cleaning efficiency has been defined. Development of efficient detergents acceptable for API equipment and research toward making vessel cleaning solvent less in commercial setting will have a major impact on reducing the environmental impact of pharmaceutical processes, while ensuring the integrity and quality of pharmaceutical products.

Conclusions

The Roundtable first announced the key research areas at the 10th Annual Green Chemistry and Engineering Conference in Washington (June 2006).⁶⁸ At the meeting the Roundtable announced that it would be launching a grant program for research in the 12 key research areas. A call for research proposals was made in November 2006 and the response from the academic community was outstanding, with 32 research proposals received within 1 month. The announcement of the award was made in December 2006.⁶⁹ The Roundtable sees the research grant program as an ongoing commitment.⁷⁰

It should be noted that great progress has been made over the last few years. For example, 20 years ago the industry was still using stoichiometric oxidations with chromium(VI) reagents whereas today bleach based oxidations catalysed by nitroxyl radicals are commonplace. There has also been a huge growth of large scale use of asymmetric reactions over the same time period. The idea of identifying and supporting research in the key research areas was to continue and to accelerate that improvement.

Of course chemistry changes quickly and almost certainly it will be necessary to refine and update the key research areas at some point in the future.

Acknowledgements

We thank many colleagues from our chemical process research and development functions who provided input to the voting process, evaluated proposals or provided useful discussions or management support. In addition we thank Paul Anastas, Ben Anderson and Berkeley Cue from the Roundtable for their strong encouragement and support.

References

- 1 www.greenchemistryinstitute.org.
- 2 www.chemistry.org/greenchemistryinstitute/pharma_roundtable.html.
- 3 J. S. Carey, D. Laffan, C. Thomson and M. T. Williams, *Org. Biomol. Chem.*, 2006, **4**, 2337–2347. See also: R. W. Dugger, J. A. Ragan and D. H. B. Ripin, *Org. Process Res. Dev.*, 2005, **9**, 253–258.
- 4 P. F. Nolan and J. A. Barton, *J. Hazard. Mater.*, 1987, **14**, 233–239.
- 5 The ACS GCIPR membership has been expanding, and at the time this sub-group of the ACS GCIPR started Johnson and Johnson were not members hence only six companies contributed to the voting exercise. However Johnson and Johnson contributed to the review of the research proposals which came later and we thank Michael Justus from Johnson and Johnson.
- 6 This figure of 9.1% is made up of 8.1% *N*-acylation reactions given in Table 8 of ref. 3 and 1% of nitrogen protection reactions.
- 7 N. Miyaoura, K. Yamada and A. Suzuki, *Tetrahedron Lett.*, 1979, **20**, 3437–3440. For a recent paper see: T. E. Barder, S. D. Walker, J. R. Martinelli and S. L. Buchwald, *J. Am. Chem. Soc.*, 2005, **127**, 4685–4696 and references therein.
- 8 R. A. Sheldon, *Chemtech*, 1994, 38–47.
- 9 (a) D. J. Dale, P. J. Dunn, C. Golightly, M. L. Hughes, P. C. Levett, A. K. Pearce, P. M. Searle, G. Ward and A. S. Wood, *Org. Process Res. Dev.*, 2000, **4**, 17–22; (b) P. J. Dunn, S. Galvin and K. Hettenbach, *Green Chem.*, 2004, **6**, 43–48.
- 10 R. Vaidyanathan, V. G. Kalthod, D. P. Ngo, J. M. Manley and S. P. Lapekas, *J. Org. Chem.*, 2004, **69**, 2565–2568.
- 11 M.-X. Wang, *Top. Catal.*, 2005, **35**(1–2), 117–130.
- 12 H. Yamada, *Chimia*, 1993, **47**, 5–10.
- 13 D. Kumar and T. C. Bhalla, *Appl. Microbiol. Biotechnol.*, 2005, **68**(6), 726–736.
- 14 (a) J. E. Anderson, R. Davis, R. N. Fitzgerald and J. M. Haberman, *Synth. Commun.*, 2006, **36**, 2129–2133; (b) P. Tang, *Org. Synth.*, 2005, **81**, 262.
- 15 (a) J. D. Hayler, S. L. B. Howie, R. G. Giles, A. Negus, P. W. Oxley, T. C. Walsgrove and M. Whiter, *Org. Process Res. Dev.*, 1998, **2**, 3–9; (b) J. D. Hayler, S. L. B. Howie, R. G. Giles, A. Negus, P. W. Oxley, T. C. Walsgrove, S. E. Walsh, R. E. Dagger, J. M. Fortunak and A. Mastocola, *J. Heterocycl. Chem.*, 1995, **32**, 875–882.
- 16 M. Yasuda, T. Saito, M. Ueba and A. Baba, *Angew. Chem., Int. Ed.*, 2004, **43**, 1414–1416.
- 17 R. Sanz, A. Martinez, D. Miguel, J. M. Alvarez-Gutierrez and F. Rodriguez, *Adv. Synth. Catal.*, 2006, **348**, 1841–1845.
- 18 (a) K. Fujita, Z. Li, N. Ozeki and R. Yamaguchi, *Tetrahedron Lett.*, 2003, **44**, 2687–2690; (b) G. Cami-Kobeci, P. A. Slatford, M. K. Whittlesey and J. M. J. Williams, *Bioorg. Med. Chem. Lett.*, 2005, **15**, 535–537.
- 19 M. G. Edwards, R. F. R. Jazsar, B. M. Paine, D. J. Shermer, M. K. Whittlesey, J. M. J. Williams and D. D. Edney, *Chem. Commun.*, 2004, 90–91.
- 20 Chemetall brochures, *Lithium Aluminum Hydride... strong, concentrated and economical*, Oct. 2000, pp. 18–19.
- 21 A. A. Smith, P. Dani, P. D. Higginson and A. J. Pettman, *World Pat.*, WO2005/066112 A1, 2005.
- 22 (a) A. Hage, H. E. Schoemaker and J. A. Field, *Appl. Microbiol. Biotechnol.*, 1999, **52**, 834–838; (b) A. He, T. Li, L. Daniels, I. Fotheringham and J. P. N. Rosazza, *Appl. Environ. Microbiol.*, 2004, **70**, 1874–1881.
- 23 O. Dipeolu, J. Gardiner and G. Stephens, *Biotechnol. Lett.*, 2005, **27**, 1803–1807.
- 24 (a) M. Hudlicky, *Oxidations in Organic Chemistry*. American Chemical Society, Washington, DC, 1990; (b) I. E. Marko, *Oxidations*, Oxford University Press, Oxford, UK, 1998.
- 25 L. De Luca, G. Giacomelli and A. Porcheddu, *Org. Lett.*, 2001, **3**, 3041–3043.
- 26 (a) F. Xu, *Ind. Biotechnol.*, 2005, **1**, 38–50; (b) S. G. Burton, *Tibtech*, 2003, **21**, 543–549.
- 27 K. M. Manoj and L. P. Hager, *Recent Res. Dev. Org. Chem.*, 2002, **6**, 393–405.
- 28 A. Wells, M. Teria and T. Eve, *Biochem. Soc. Trans.*, 2006, **34**, 304–308.
- 29 E. G. Ankudey, H. F. Olivo and T. L. Peebles, *Green Chem.*, 2006, **12**, 923–923.
- 30 (a) C.-L. Chen, A. Potthast, T. Rosenau, J. S. Gratzl, A. G. Kirkman, D. Nagai and T. Miyakoshi, *J. Mol. Catal. B: Enzym.*, 2000, **8**, 213–219; (b) H. Mang, J. Gross, M. Lara,

- C. Goessler, H. E. Schoemaker, G. M. Guebitz and W. Kroutil, *Angew. Chem., Int. Ed.*, 2006, **45**, 5201–5203.
- 31 Reviews: (a) O. Mitsunobu, *Synthesis*, 1981, 1–28; (b) D. L. Hughes, *Org. React.*, 1992, **42**, 335–656; (c) D. L. Hughes, *Org. Prep. Proced. Int.*, 1996, **28**, 127–164.
- 32 Ref 3. Note the published reaction survey does not detail the % use of the Mitsunobu reaction, however this information was available from the GSK/AZ/Pfizer spreadsheet that lies behind the publication.
- 33 (a) R. A. Amos, R. W. Emblidge and N. Havens, *J. Org. Chem.*, 1983, **48**, 3598–3600; (b) A. R. Tunoori, D. Dutta and G. I. Georg, *Tetrahedron Lett.*, 1998, **39**, 8751–8754; (c) K. D. Janda, P. Wentworth and A. M. Vandersteen, *Chem. Commun.*, 1997, 759–760.
- 34 A. M. Harned, H. S. He, P. H. Toy, D. L. Flynn and P. R. Hanson, *J. Am. Chem. Soc.*, 2005, **127**, 52–53.
- 35 (a) T. Tsunoda, M. Nagaku, C. Nagaino, Y. Kawamura, F. Ozaki, H. Hioki and S. Ito, *Tetrahedron Lett.*, 1995, **36**, 2531–2534; (b) T. Tsunoda, C. Nagino, M. Oguri and S. Ito, *Tetrahedron Lett.*, 1996, **37**, 2459–2462.
- 36 T. Y. S. But and P. H. Toy, *J. Am. Chem. Soc.*, 2006, **128**, 9636–9637.
- 37 (a) D. S. Surry, D. J. Fox, S. J. F. Macdonald and D. R. Spring, *Chem. Commun.*, 2005, 2589–2590 and references therein; (b) V. Snieckus, *Chem. Rev.*, 1990, **90**, 879.
- 38 (a) J.-Y. Cho, M. K. Tse, D. Holmes, R. E. Maleczka and M. R. Smith, *Science*, 2002, **295**, 305–308 and references therein; (b) T. Ishiyama, J. Takagi, K. Ishida and N. Miyaara, *J. Am. Chem. Soc.*, 2002, **124**, 390–391.
- 39 (a) D. Sames ACS Symposium Series 2004, **885**, 155–168; (b) D. Kalyani, A. R. Dick, W. Q. Anani and M. S. Sanford, *Tetrahedron*, 2006, **62**, 11483–11498.
- 40 T. C. Nugent, V. N. Wakchaure, A. K. Ghosh and R. R. Mohanty, *Org. Lett.*, 2005, **7**, 4967–4970 and references therein.
- 41 (a) N. Ikemoto, D. M. Tellers, S. D. Dreher, J. Liu, A. Huang, N. R. Rivera, E. Njolito, Y. Hsiao, J. C. McWilliams, J. M. Williams, J. D. Armstrong III, Y. Sun, D. J. Mathre, E. J. J. Grabowski and R. D. Tillyer, *J. Am. Chem. Soc.*, 2004, **126**, 3048–3049; (b) Y. Hsiao, N. R. Rivera, T. Rosner, S. W. Krska, E. Njolito, F. Wang, Y. Sun, J. D. Armstrong, III, E. J. J. Grabowski, R. D. Tillyer, F. Spindler and C. Malan, *J. Am. Chem. Soc.*, 2004, **126**, 9918–9919.
- 42 For recent references see: L. C. Akullian, J. R. Porter, J. F. Traverse, M. L. Snapper and A. H. Hoveyda, *Adv. Synth. Catal.*, 2005, **347**, 417–425.
- 43 (a) J. Blacker and J. Martin, Scale-up Studies in Asymmetric Transfer Hydrogenation, in *Asymmetric Catalysis on Industrial Scale Challenges, Approaches and Solutions*, ed. H.-U. Blaser and E. Schmidt, Wiley-VCH, 2004, 201–216; (b) Q. Yang, G. Shang, W. Gao, J. Deng and X. Zheng, *Angew. Chem., Int. Ed.*, 2006, **45**, 3832–3835; (c) Y.-Q. Wang and Y.-G. Zhou, *Synlett*, 2006, 1189–1192; (d) A. Ros, A. Magriz, H. Dietrich, M. Ford, R. Fernandez and J. Lassaletta, *Adv. Synth. Catal.*, 2005, **347**, 1917–1920; (e) I. R. Storer, D. E. Carrera, Y. Ni and D. W. C. MacMillan, *J. Am. Chem. Soc.*, 2006, **128**, 84–86.
- 44 J. A. Ellman, *Pure Appl. Chem.*, 2003, **75**, 39.
- 45 L. Storace, L. Anzalone, P. N. Confalone, W. P. Davis, J. M. Fortunak, M. Giangordano, J. J. Haley, Jr., K. Kamholz, H.-Y. Li, P. Ma, W. A. Nugent, R. L. Parsons, Jr., P. J. Sheeran, C. E. Silverman, R. E. Waltermire and C. C. Wood, *Org. Process Res. Dev.*, 2002, **6**, 54–63.
- 46 V. I. Tararov and A. Borner, *Synlett*, 2005, **2**, 203–211.
- 47 V. Farina, J. T. Reeves, C. H. Senanayake and J. J. Song, *Chem. Rev.*, 2006, **106**, 2734–2793. See also *Asymmetric Catalysis on Industrial Scale Challenges, Approaches and Solutions*, ed. H.-U. Blaser and E. Schmidt, Wiley-VCH, Weinheim, 2004.
- 48 <http://www.epa.gov/greenchemistry/pubs/pgcc/winners/gspa06.html>.
- 49 K. B. Hansen, J. Balsells, S. Dreher, Y. Hsiao, M. Kubryk, M. Palucki, N. Rivera, D. Steinhuebel, J. D. Armstrong III, D. Askin and E. J. J. Grabowski, *Org. Process Res. Dev.*, 2005, **9**, 634–639.
- 50 M. Studer, H.-U. Blaser and C. Exner, *Adv. Synth. Catal.*, 2003, **345**, 45–65.
- 51 X. Cui and K. Burgess, *Chem. Rev.*, 2005, **105**, 3272–3296.
- 52 I. C. Lennon and C. J. Pilkington, *Synthesis*, 2003, 1639–1642.
- 53 G. Hoge, H.-P. Wu, W. S. Kissel, D. A. Plum, D. J. Greene and J. Bao, *J. Am. Chem. Soc.*, 2004, **126**, 5966–5967.
- 54 H. Adolfsson, *Angew. Chem., Int. Ed.*, 2005, **44**, 3340–3342.
- 55 Deoxo-Fluor™ (a) R. P. Singh and J. M. Shreeve, *Synthesis*, 2002, 2561–2578; (b) R. P. Singh and J. M. Shreeve, *Acc. Chem. Res.*, 2004, **37**, 31–44; (c) Selectfluor™ P. T. Nyffeler, S. G. Duron, M. D. Burkart, S. V. Vincent and C.-H. Wong, *Angew. Chem., Int. Ed.*, 2005, **44**, 192–212.
- 56 H. Hayashi, H. Sonoda, K. Fukumura and T. Nagata, *Chem. Commun.*, 2002, 1618–1619. For an excellent review on new fluorination methods see: A. M. Thayer, *Chem. Eng. News*, 2006, **84**(23), 15–24.
- 57 H. C. Kolb, M. G. Finn and K. B. Sharpless, *Angew. Chem., Int. Ed.*, 2001, **40**, 2004–2021.
- 58 K. Thewalt, *Chim. Oggi*, 1993, **11**, 17.
- 59 M. S. Gibson and R. W. Bradshaw, *Angew. Chem., Int. Ed. Engl.*, 1968, **7**, 919–930.
- 60 A. Zwierzak and S. Pilochoowska, *Synthesis*, 1982, 922–924.
- 61 U. Ragnarsson and L. Grehn, *Acc. Chem. Res.*, 1991, **24**, 285–289.
- 62 T. Mukaiyama, T. Tsuji and Y. Watanabe, *Chem. Lett.*, 1978, 1057–1060.
- 63 *The Carbohydrates*, ed. W. Pigman and D. Horton, Academic Press, New York, vol. 1A, 2nd edn, 1972.
- 64 Green Chemistry Institute Pharmaceutical Round Table Meeting, Feb 2, 2006, Philadelphia, PA, USA.
- 65 K. Mulholland and J. Dyer, *Pollution Prevention: Methodology, Technologies and Practices*, American Institute of Chemical Engineers, New York, 1999, 147–156.
- 66 F. R. Brant and F. S. Cannon, Aqueous-Based Cleaning with Hydrogen Peroxide, *J. Environ. Sci. Health, Part A: Environ. Sci. Eng. Toxic Hazard. Subst. Control*, 1996, **31**(9), 2409–2434.
- 67 P. Meng, E. S. Geskin, M. C. Leu and Tismenetskiy, Waterjet In-Situ Reactor Cleaning, *Proceedings at the 13th International Conference on Jetting Technology*, BHR Group Conference Series Publications, 1996, vol. 21, 347–358.
- 68 P. J. Dunn, *Key Green Chemistry Research areas: A perspective from pharmaceutical manufacturers*, Abstract 184, 10th Annual Green Chemistry and Engineering conference. Slides are available on the Roundtable web site. See also, *Chem. Eng. News*, 2006, **84**(30), 36.
- 69 The winner of the 2007 Research Grant was Dr Jainlang Xiao, University of Liverpool, (UK).
- 70 For details on how to enter the 2008 Research Grant see: www.chemistry.org/greenchemistryinstitute/pharma_roundtable.html.

Selective oxidation of benzyl alcohol to benzaldehyde with hydrogen peroxide over tetra-alkylpyridinium octamolybdate catalysts

Guo Ming-Lin* and Li Hui-Zhen

Received 12th January 2007, Accepted 2nd February 2007

First published as an Advance Article on the web 12th February 2007

DOI: 10.1039/b700534b

Some tetra-alkylpyridinium octamolybdate catalysts were found to be recyclable and efficient for selective oxidation of benzyl alcohol with aqueous hydrogen peroxide as oxidant under simple reaction conditions. Organic solvent-free direct selective oxidation of benzyl alcohol to benzaldehyde with aqueous 15% hydrogen peroxide was performed at reflux temperature for a short period with 82.3%–94.8% benzyl alcohol conversion and 87.9%–96.7% benzaldehyde selectivity.

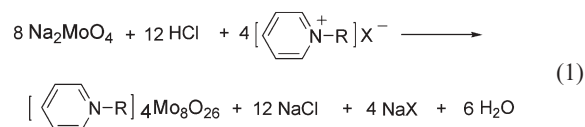
Introduction

Traditionally, oxidation of benzyl alcohol to benzaldehyde is performed with stoichiometric amounts of chromium (VI) reagents. These oxidants are not only relatively expensive, but also they generate copious amounts of heavy-metal waste. Moreover, the reaction is often performed in environmentally undesirable solvents, typically chlorinated hydrocarbons. Aqueous hydrogen peroxide is a highly attractive oxidant because it is a cheap, mild and an environmentally benign reagent with a high content of 'active' oxygen, and water is the only by-product. Thus, in recent years, the use of hydrogen peroxide as oxidant has attracted considerable attention.^{1–9} Many catalytic methods are currently available for the liquid-phase oxidation of alcohols with hydrogen peroxide. Among these, it has long been known that tungsten and molybdenum compounds are efficient catalysts for oxidation by hydrogen peroxide.^{3–9} Recently, we developed a novel and simple method for the preparation of tetra-alkylpyridinium octamolybdate, and found that it was efficient for selective oxidation of benzyl alcohol. Here, we disclose the no-solvent oxidation with aqueous hydrogen peroxide under entirely halide-free conditions. That is, some tetra-alkylpyridinium octamolybdate are used as selective catalysts for oxidation of benzyl alcohol to benzaldehyde with aqueous 15% hydrogen peroxide without any organic solvents.

Results and discussion

In this work, we first developed and prepared tetra-*n*-butylpyridinium octamolybdate according to the following eqn (1) in the presence of excess *n*-butylpyridinium bromide *via* a simple method instead of hydrothermal synthesis.

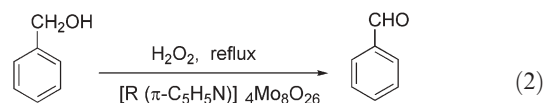
A mixture of 40 ml aqueous solution of dihydrate sodium molybdate (12.0 g, 0.05 mol) and 12% dilute hydrogen chloride



(19.0 ml, 0.076 mol) was added dropwise into a solution of *n*-butylpyridinium bromide (20.0 g, 0.093 mol) in 100 ml of distilled water under stirring at 70 °C. A white precipitate was immediately formed. After continuously stirring for 20 min, the resulting product was filtered, washed with water and dried at room temperature to produce the catalyst tetra-*n*-butylpyridinium octamolybdate (PyC4) in 85% yield.

A single crystal of catalyst PyC4 was separated from the above filtrate by slowly evaporating over a period of 1 d at 40 °C and structurally determined by single X-ray diffraction.[†] Just as we expected, the resulting complex from the above method was indeed tetra-*n*-butylpyridinium octamolybdate. Its octamolybdate anion lies about an inversion centre and is structurally a β -isomer (see Fig. 1). The structure of the β -isomer of the octamolybdate anion, as described previously,¹⁰ is constructed from an array of eight edge-shared MoO_6 octahedra. The Mo–O bond lengths can be grouped into four sets: Mo–O(t) 1.687 (4)–1.707 (4) Å, Mo–O(μ 2) 1.747 (4)–2.289 (4) Å, Mo–O(μ 3) 1.947 (4)–2.345 (4) Å, Mo–O(μ 5) 2.145 (3)–2.476 (3) Å.

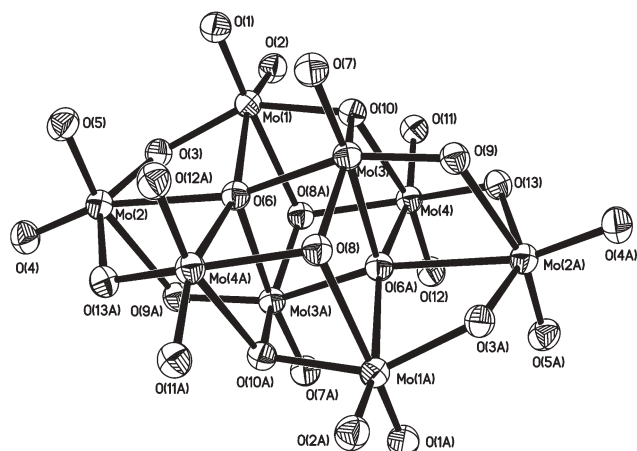
Although many complexes¹¹ which possess an octamolybdate structure have been synthesized, up to now examples of the use of tetra-alkylpyridinium octamolybdate as catalysts are rare for the oxidation of alcohol with hydrogen peroxide. In this work, direct selective oxidation of benzyl alcohol to benzaldehyde with 15% hydrogen peroxide was performed over tetra-alkylpyridinium octamolybdate catalysts with excellent benzyl alcohol conversion and benzaldehyde selectivity under the conditions of stirring, heating and refluxing for a short period (see eqn (2) and Table 1).



Where R = *n*-C₄H₉, *n*-C₈H₁₇, *n*-C₁₄H₂₉, and *n*-C₁₆H₃₃

The experimental results (Table 1) indicated that tetra-alkylpyridinium octamolybdate was an efficient catalyst for oxygen transfer from hydrogen peroxide to the substrate. When a mixture (Entry 1) of benzyl alcohol (10.8 g, 0.1 mol), 15% H_2O_2 (25.0 g, 0.12 mol), and PyC4 catalyst (0.5 g) was vigorously stirred in air at reflux temperature for 1.7 h, H_2O_2 was utilized efficiently and benzaldehyde was produced with 90.5% selectivity [as determined by gas chromatographic (GC) analysis].¹² When the amount of H_2O_2 was decreased (Entries 2 and 3), the reaction time declined

School of Materials and Chemical Engineering and Tianjin Key Lab of Fiber Modification & Functional Fiber, Tianjin Polytechnic University, Tianjin, 300160, China. E-mail: guomlin@yahoo.com



Selected geometric parameters (Å):

Mo(1)—O(2)	1.698 (4)	Mo(1)—O(1)	1.700 (4)
Mo(2)—O(4)	1.691 (4)	Mo(2)—O(5)	1.702 (4)
Mo(4)—O(12)	1.707 (4)	Mo(4)—O(11)	1.703 (4)
Mo(3)—O(7)	1.687 (4)		
Mo(1)—O(3)	1.897 (4)	Mo(2)—O(3)	1.918 (4)
Mo(2)—O(13A)	1.929 (4)	Mo(3)—O(9)	1.747 (4)
Mo(4)—O(13)	1.883 (4)	Mo(2)—O(9A)	2.289 (4)
Mo(3)—O(10)	1.947 (4)	Mo(1)—O(10)	2.000 (4)
Mo(3)—O(8)	1.950 (4)	Mo(1)—O(8A)	2.340 (4)
Mo(4)—O(8A)	2.005 (4)	Mo(4)—O(10)	2.345 (4)
Mo(3)—O(6)	2.145 (3)	Mo(2)—O(6)	2.476 (3)
Mo(1)—O(6)	2.347 (4)	Mo(3)—O(6A)	2.348 (4)
Mo(4)—O(6A)	2.300 (4)		

Symmetry codes: (A) $-x+2, -y+2, -z$.**Fig. 1** The structure of the β -[Mo₈O₂₆]⁴⁻ anion, showing 20% probability displacement ellipsoids.

(the corresponding time was 1.0 h, and 0.5 h, respectively) and benzaldehyde selectivity increased (the corresponding selectivity was 91.8%, and 94.6%, respectively). The catalysts of PyC8, PyC14, and PyC16 (Entries 5 to 7) were also efficient. The rate of the corresponding reaction was higher. As for 1.0 to 1.2 mol of H₂O₂ per 1 mol of benzyl alcohol, the results show that this catalyst system had a high efficiency and high selectivity for

oxidation of benzyl alcohol to benzaldehyde, and it did not induce the unproductive decomposition of H₂O₂ to any great extent and enables the economic use of the oxidant.

It was observed that benzoic acid was produced as a by-product by the oxidation of benzyl alcohol. It failed when we attempted to directly convert benzyl alcohol to benzoic acid. After a mixture of benzyl alcohol (10.8 g, 0.1 mol), 15% H₂O₂ (45.5 g, 0.20 mol), and PyC4 catalyst (0.8 g) was vigorously stirred in air at reflux temperature for 6.5 h (Entry 9), the H₂O₂ was used up, only a small amount of benzoic acid was separated in 20.5% yield, and benzaldehyde was still produced as the main product. A similar case was also evident in the oxidation procedure of cyclohexanol to cyclohexanone. When a mixture of cyclohexanol (10.8 g, 0.1 mol), 15% H₂O₂ (25.0 g, 0.11 mol), and PyC4 catalyst (0.8 g) was vigorously stirred in air at reflux, after 20 min, H₂O₂ was used up. Only 22.5% cyclohexanone¹² was produced. The results indicated that the use of tetra-*n*-butylpyridinium octamolybdate (PyC4) as catalyst was less active for oxidation of benzyl alcohol to benzoic acid and oxidation of cyclohexanol to cyclohexanone.

In this system, tetra-alkylpyridinium octamolybdate catalysts exhibited high activity and selectivity for oxidation of benzyl alcohol to benzaldehyde. During the reaction process, the catalyst dissolved in the organic substrate and product, and transferred from the solid phase to liquid phase under the action of hydrogen peroxide. The color of the reaction mixture changed from yellow to orange, after H₂O₂ was used up, and it then changed to blue. Added addition of 40 ml of water, the crude product was distilled off. The catalyst, which had precipitated in a small amount of the remaining aqueous phase, could be recovered in 85% yield (by weight) and could be easily recycled. In the second run (Entries 4 and 8) only the benzyl alcohol and H₂O₂ were added. The catalyst that was left in the flask from the previous run dissolved in the mixture again when it was stirred at reflux temperature. The phenomena and operation were the same as first run. The results indicated that in the second run benzaldehyde selectivity and the benzyl alcohol conversion were comparable with the fresh catalyst.

Conclusion

Some tetra-alkylpyridinium octamolybdate catalysts were found to be recyclable and efficient for selective oxidation of benzyl alcohol to benzaldehyde with 15% H₂O₂ at reflux temperature for a short period with 82.3%–94.8% benzyl alcohol conversion and 87.9%–96.7% benzaldehyde selectivity. The preparation of these catalysts

Table 1 Oxidation of benzyl alcohol to benzaldehyde by hydrogen peroxide over tetra-alkylpyridinium octamolybdate catalysts^a

Entry	Catalyst	Amount of catalyst/g	C ₆ H ₅ CH ₂ OH/H ₂ O ₂ molar ratio	Reaction time/h	Conversion (%)	Selectivity (%)
1	PyC4	0.5	1 : 1.2	1.7	93.6	90.5
2		0.8	1 : 1.1	1.0	86.4	91.8
3		0.8	1 : 1.0	0.5	82.3	94.6
4		Recycle ^b	1 : 1.0	0.6	83.9	93.3
5	PyC8	0.5	1 : 1.1	0.6	90.5	89.4
6	PyC14	0.5	1 : 1.0	0.4	85.5	96.7
7	PyC16	0.5	1 : 1.1	0.6	92.7	89.5
8	PyC16	Recycle ^c	1 : 1.1	1.0	94.8	87.9
9	PyC4	0.8	1 : 2.0	6.5	99.5	76.5
10	PyC4	0.8	1 ^d :1.1	0.4	22.6	99.6

^a Reaction conditions: 10.8 g (0.1 mol) of benzyl alcohol, aqueous 15% hydrogen peroxide, reflux. ^b The catalyst of entry 3 was recycled. ^c The catalyst of entry 7 was recycled. ^d Here, the alcohol is cyclohexanol. The catalysts of PyC4, PyC6, PyC14 and PyC16 are [n-C₄H₉(π-C₅H₅N)]₄Mo₈O₂₆, [n-C₈H₁₇(π-C₅H₅N)]₄Mo₈O₂₆, [n-C₁₄H₂₉(π-C₅H₅N)]₄Mo₈O₂₆, and [n-C₁₆H₃₃(π-C₅H₅N)]₄Mo₈O₂₆, respectively.

is simple, the recovery and utilization of used catalyst is easy, and the reaction time is shorter than the those reported in Sato *et al.*⁶ and Shi and Wei.⁸ These are beneficial for benzaldehyde production in industry. This solvent- and halide-free oxidation of benzyl alcohol is clean, safe, and reproducible, with conditions that are not corrosive. No operational problems are foreseen for a large-scale version of this green process. The experimental procedure is also suitable for performing in an academic teaching laboratory. An opportunity is provided to those teachers planning to use the experiment in their teaching laboratory setting.

Acknowledgements

We thank the Institute of Tianjin Education for financial support (Project No. 20040603) and Tianjin Polytechnic University for student creative financial support.

Notes and references

† Crystal data: $[\text{n-C}_4\text{H}_9(\pi\text{-C}_5\text{H}_5\text{N})]_4\text{Mo}_8\text{O}_{26}$, $M = 1728.37$, monoclinic, $P2_1/n$, $a = 11.6255(13)$ Å, $b = 15.2552(17)$ Å, $c = 15.2882(18)$ Å,

$\beta = 92.341(2)^\circ$, $V = 2709.1(5)$ Å³, $Z = 2$, $D_c = 2.119$ Mg m⁻³, $\mu(\text{Mo-K}\alpha) = 1.87$ mm⁻¹, $T = 294(2)$ K, block, colorless, 15109 measured reflections, 5514 independent reflections, $R_{\text{int}} = 0.027$, $R[F^2 > 2\sigma(F^2)] = 0.045$, $wR(F^2) = 0.132$. CCDC reference number 632456. For crystallographic data in CIF or other electronic format see DOI: 10.1039/b700534b.

- 1 P. K. Tandon, R. Baboo, A. K. Singh and Gayatri, *Appl. Organomet. Chem.*, 2006, **20**, 20.
- 2 C. Li, P. Zheng, J. Li, H. Zhang, Y. Cui, Q. Shao, X. Li, J. Zhang, P. Zhao and Y. Xu, *Angew. Chem., Int. Ed.*, 2003, **42**, 5063.
- 3 D. Sloboda-Rozner, P. Witte, P. L. Alsters and R. Neumann, *Adv. Synth. Catal.*, 2004, **346**, 339.
- 4 M. L. Guo, *Green Chem.*, 2004, **6**, 271.
- 5 M. L. Guo, *Acta Chim. Sin.*, 2004, **62**(19), 1956.
- 6 K. Sato, J. Takagi, M. Aoki and R. Noyori, *Tetrahedron Lett.*, 1998, **39**, 7549.
- 7 Z. H. Weng, J. Y. Wang and X. G. Jian, *Chin. Chem. Lett.*, 2006, **17**(6), 848.
- 8 X. Y. Shi and J. F. Wei, *J. Mol. Catal. A: Chem.*, 2005, **229**, 13.
- 9 I. V. Kozhevnikov, *Chem. Rev.*, 1998, **99**, 171.
- 10 W. J. Kroenke, J. P. Fackler Junior and A. M. Mazany, *Inorg. Chem.*, 1983, **22**, 2412.
- 11 D. G. Xiao, H. Y. An, E. B. Wang and L. Xu, *J. Mol. Struct.*, 2005, **738**, 217.
- 12 Agilent 6890N GC, HP-5 column, 0.25 mm by 30 m.

Synthesis and catalytic applications of CMK-LDH (layered double hydroxides) nanocomposite materials†

Amit Dubey*

Received 10th November 2006, Accepted 29th January 2007

First published as an Advance Article on the web 8th February 2007

DOI: 10.1039/b616482j

Nanosized layered double hydroxides (LDH) were synthesized inside the mesoporous carbon (CMK-1) known as CMK-LDH nanocomposites by simple impregnation and precipitation techniques. The catalytic activity of these nanocomposites for Claisen–Schmidt condensation reactions showed remarkably high activity and selectivity for the desired product under environmentally friendly conditions.

Introduction

Nanostructured materials are receiving tremendous attention due to their remarkable properties compared to bulk materials. Following the discovery of ordered mesoporous carbon synthesized using various mesoporous silica constructed with three dimensional (3-D) pore connectivity,^{1,5–7} considerable attention has been devoted to fabricate new carbon nano-architectures for potential applications.^{1–4} However, the pore diameter control of the mesoporous carbons is relatively more difficult due to the lack of an effective method to control the pore wall thickness of the silica templates and is limited typically to less than 5 nm. The small pore diameter would prevent these mesoporous carbons for advanced applications. Large pores will be necessary to permit the facile diffusion and reaction of large molecules to form a large variety of nano-structures in the large pores of mesoporous carbon. In their search for nanostructured materials, Jacobsen and coworkers synthesized nanosized ZSM-5 with a broad crystal size distribution *via* confined space synthesis using carbon black as the templates.⁸ More recently, the synthesis of mesoporous ZSM-5 monolith and mesoporous zeolites crystals by using carbon aerogel⁹ and colloid imprinted carbon¹⁰ have also been reported. However, to the best of the literature knowledge, there is no report on the synthesis of nanosized hydrotalcites, otherwise referred to as layered double hydroxide (LDH) supported on mesoporous carbon framework for catalytic applications. Hydrotalcites (HTs) are receiving considerable attention due to their advantageous applications in adsorptions, ion-exchange and catalysis *etc.*¹¹ Structurally, HTs can be perceived as having a similar structure to Brucite, Mg(OH)₂, wherein the partial substitution of Mg²⁺ with Al³⁺ occurs and the excess positive charge generated in the sheets is compensated by the presence of interlayer anions and water molecules. It is well known in HT literature that fresh hydrotalcites

(without calcinations) are less active for base catalysis than their calcined and rehydrated forms. Having knowledge of the different structural properties of nanomaterials compared to bulk materials, the present investigation deals with the synthesis of MgAl-hydrotalcites supported on large-pore mesoporous carbon (CMK-L) and comparison with the bulk hydrotalcites for base catalysis in Knoevenagel and Claisen–Schmidt condensation reactions for the production of chalcones. The use of various basic solids, such as K₂CO₃, barium hydroxides, alumina, MgO, natural phosphates modified with sodium nitrate and alkali metal exchanged zeolites, sepiolites, organic resins, magnesium–aluminum mixed oxides derived from hydrotalcites, their calcined and hydrated forms and more recently aluminophosphates oxinitrides (ALPON), cover a wide range of base strength but calcined and rehydrated hydrotalcites proved to be the most effective catalysts for this reaction.¹²

Experimental

The large-pore mesoporous carbon designated as CMK-1 was synthesized by the method reported earlier.⁵ The synthesis procedure to incorporate hydrotalcites involves the impregnation of a metal precursor solution into the CMK-1 followed by co-precipitation with NaOH/Na₂CO₃ solution after drying the impregnated solution. For 10 wt% loading, to 1 g of CMK-1, 1.475 ml solution of 0.75 M Mg(NO₃)₂·6H₂O and 0.25 M Al(NO₃)₃·9H₂O (keeping the Mg/Al atomic composition of 3 in all the samples) were impregnated at room temperature and dried at 100 °C for 4 h. After drying, the resultant mixture is co-precipitated with 2.36 ml solution of 0.1 M NaOH/Na₂CO₃ at room temperature with stirring for 12 h. The so obtained solution was filtered, washed with excess hot distilled water and dried at 110 °C for 6 h. The carbon composites were black in color and named as *x*MgAl/CMK, where *x* denotes the wt% age loading of hydrotalcites. The effective loading of the hydrotalcites in CMK-1 is 10, 5 and 2 wt%. The elemental composition and Mg/Al ratio determined from the EDAX correlated well with the theoretical values.

Results and discussions

The powder X-ray diffraction (PXRD) pattern of the MgAl/CMK composites at the low angle region (Fig. 1 left) showed the reduction of the (110) peak compared to pure CMK-1 with increase in the loading up to 5 wt% and the mesostructure completely disappeared with further increase in loading up to 10 wt%. The decrease in the XRD intensity infers the formation of hydrotalcites inside the pores of carbon. XRD patterns at the wide

Chemistry Group, Birla Institute of Technology and Science–Pilani, Rajasthan, India 333031. E-mail: amitdubey@bits-pilani.ac.in; amitdubey75@yahoo.com

† Electronic supplementary information (ESI) available: PXRD pattern of MgAl-hydrotalcite and its calcined form (mixed oxide) at 600 °C. See DOI: 10.1039/b616482j

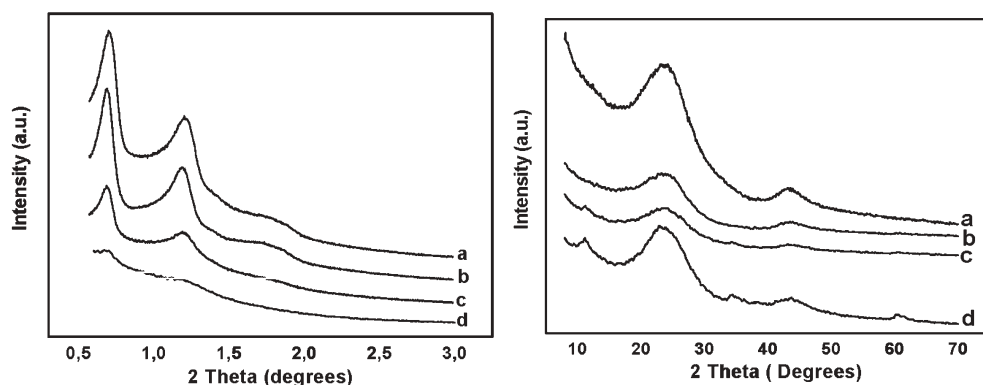


Fig. 1 PXRD pattern of (a) CMK-1, (b) 2% MgAl/CMK-1, (c) 5% MgAl/CMK-1, (d) 10% MgAl/CMK-1 at low (left) and wide (right) angle.

angle region (Fig. 1 right) showed the presence of a pure hydrotalcite phase assuming the 3R symmetry¹³ of the CMK-1, 2% MgAl/CMK and 5% MgAl/CMK; however, the peaks are broad compared to the pure MgAl hydrotalcite, inferring the formation of hydrotalcites with reduced particle size inside the pores of carbon. The broad peaks around ($2\theta = 23$ and 42°) are due to CMK-1. The N_2 adsorption isotherm^{5,7} showed the presence of a type IV adsorption isotherm (Fig. 2) with a sharp capillary condensation at relative pressure around 0.7. The shape of the isotherms changes with the increase in the loading and the mesostructural order disappeared for 10% MgAl/CMK. This may be due to the excess strain generated inside the carbon framework during the formation of hydrotalcite particles. The surface area, pore diameter and total pore volume of the CMK-MgAl composite were reduced compared to CMK-1 indicating the formation of hydrotalcites inside the pores of CMK-1 (Table 1). TEM results indicated the uniform distribution of metal ions but

because of the background generated from carbon we were not able to see the clear image of hydrotalcite particles inside the pores of mesoporous carbon. The catalysts thus obtained were tested for Knoevenagel condensation and the information obtained was extended to a Claisen–Schmidt condensation reaction between benzaldehyde and 2-hydroxyacetophenone (Scheme 1) at 393 K without solvent. The product analysis was done using gas chromatography by taking the authentic samples after considering their response factors. The results obtained were quite interesting with almost 85–90% conversion of the products with 95% selectivity of flavon as compared to 50% conversion with 70% selectivity of the flavon for the bulk catalyst. No conversion was noted for CMK-1 samples, clearly indicating that the observed activity is only due to the presence of hydrotalcites (Fig. 3).

The catalytic activity was further compared with activated carbon and physically mixed sample for 5% composition. However, no difference in the activity was observed for pure MgAl, activated carbon and physically mixed catalysts (not shown). This high activity and selectivity of CMK/MgAl catalysts may be due to the reduced particle size and better dispersion of the hydrotalcite particles on mesoporous carbon. The catalytic activity of these fresh (as-synthesized without any further treatment) catalysts can be compared with some of the calcined and rehydrated hydrotalcites.¹² In order to see the effect of calcination temperature on the progress of the reaction, both 5% loaded and bulk catalysts were calcined at 873 K in an inert atmosphere. It was observed that the reaction was completed within 3 h (90%) for MgAl/CMK catalyst compared to 9 h (85%) for the mixed oxides obtained from the bulk catalyst. This is due to the different nature of the mixed oxides formed in the bulk and carbon derived calcined hydrotalcites.

In order to see the reusability of the catalysts, the catalysts were washed thoroughly with acetone, centrifuged, dried and again

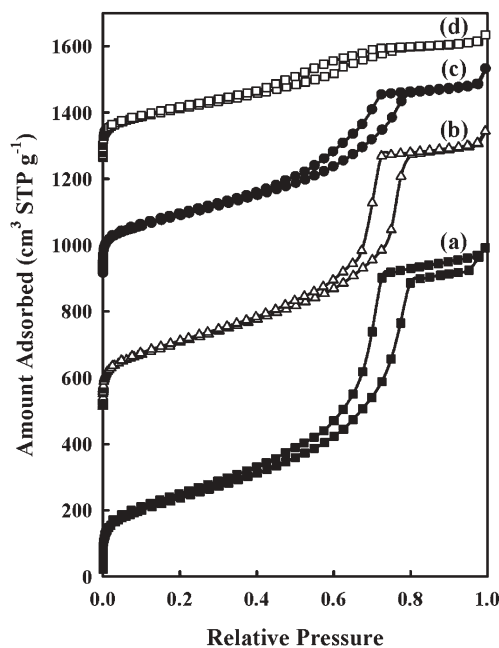
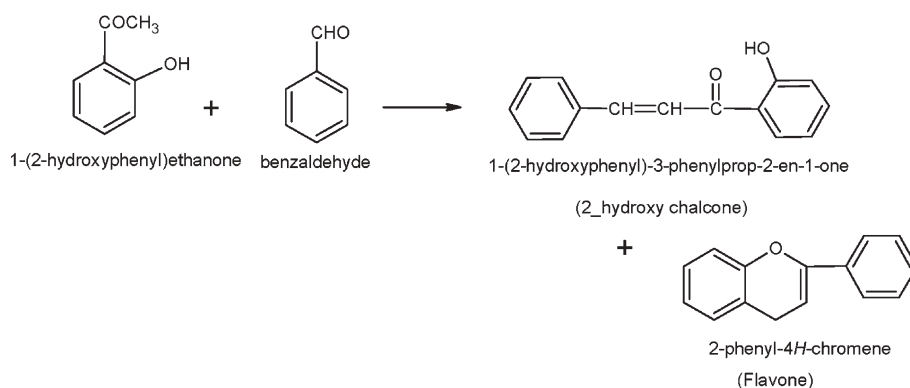


Fig. 2 N_2 adsorption–desorption isotherm of (a) CMK-1, (b) 2% MgAl/CMK-1, (c) 5% MgAl/CMK-1, (d) 10% MgAl/CMK-1.

Table 1 Structural parameters of CMK-I and MgAl/CMK-I

Sample	d/nm	a/nm	$S_{BET}/m^2\ g^{-1}$	$V_t/cm^3\ g^{-1}$	w_{BJH}/nm
CMK-I-L	12.2	17.3	854	1.43	9.4
2% MgAl/CMK	12.2	17.3	751	1.23	9.0
5% MgAl/CMK	12.1	17.1	690	0.89	8.8
10% MgAl/CMK	12.3	17.4	581	0.56	5.7



Scheme 1

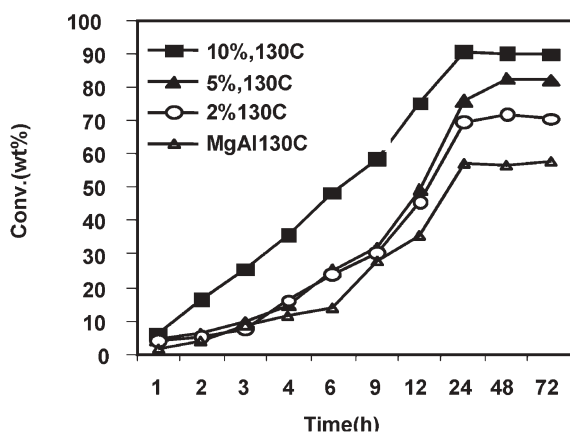


Fig. 3 Variation of conversion of 2-hydroxychalcone with time over MgAl/CMK-1 composites. Reaction conditions: Benzaldehyde—1 g, 2-hydroxyacetophenone—1 g, catalyst wt—50 mg, time—24 h, without solvent, temp.—393 K.

subjected to a fresh reaction (see ESI†). In all the cases, almost the same conversion and selectivity of *trans*-chalcone was observed for three cycles indicating the promising use of carbon-hydrotalcite composites for advanced applications.

Conclusions

In summary, we have synthesized nanosized hydrotalcites inside the pores of CMK-1 and tested for the Claisen–Schmidt reaction. Further efforts to explore the possibility to incorporate different bivalent and trivalent metal ions into this large pore carbon are currently underway. The catalytic activity and selectivity results of these nanocomposites may pave the way for more improved and high performance applications.

Acknowledgements

The authors thank the Birla Institute of Technology and Science–Pilani for providing necessary help and support for this work.

References

- R. Ryoo, S. H. Joo and S. Jun, *J. Phys. Chem. B*, 1999, **103**, 7743.
- C. R. Bansal, J. B. Donnet and F. Stoeckli, *Active Carbon*, Marcel Dekker, New York, 1988.
- H. Marsh, E. A. Heintz and F. Rodeiguez-Reinoso, *Introduction to Carbon Technology*, University of Alicante, 1997.
- H. C. Foley, *Microporous Mater.*, 1995, **4**, 407.
- S. Jun, S. H. Joo, R. Ryoo, M. Kruk, M. Jaroniec, Z. Liu, T. Ohsuna and O. Terasaki, *J. Am. Chem. Soc.*, 2002, **122**, 10712.
- S. H. Joo, S. J. Choi, I. W. Oh, J. H. Kwak, Z. Liu, O. Terasaki and R. Ryoo, *Nature*, 2001, **412**, 169.
- J.-S. Lee, S. H. Joo and R. Ryoo, *J. Am. Chem. Soc.*, 2002, **124**, 1156.
- (a) I. Schmidt, C. Madsen and C. J. H. Jacobsen, *Inorg. Chem.*, 2000, **39**, 2279; (b) I. Schmidt, A. Boisen, E. Gustavsson, K. Stahl, S. Pehrson, S. Dahl, A. Carlsson and C. J. H. Jacobsen, *Chem. Mater.*, 2001, **13**, 4416.
- A. Boisen, I. Schmidt, A. Carlsson, S. Dahl, M. Brorson and C. J. H. Jacobsen, *Chem. Commun.*, 2003, 958.
- Y. Tao, H. Kanoh and J. Kaneko, *Am. Chem. Soc.*, 2003, **125**, 6044; Y. Tao, H. Kanoh and J. Kaneko, *J. Phys. Chem. B*, 2003, **107**, 10974.
- (a) F. Trifiro and A. Vaccari, in *Comprehensive Supramolecular Chemistry*, ed. J. L. Atwood, J. E. Davies, D. D. MacNicol, F. Lehn, G. Alberti and T. Bein, Pergamon Press, F. Vogtle, Oxford, 1996, vol. 7, p. 251; (b) D. Tichit and A. Vaccari, *Appl. Clay Sci.*, 1998, **13**, 311; (c) V. Rives and M. A. Ulibarri, *Coord. Chem. Rev.*, 1999, **181**, 67; (d) A. de Roy, C. Forano, K. El Malki and J.-P. Besse, in *Synthesis of Microporous Materials*, ed. M. L. Occelli and H. E. Robson, Van Nostrand Reinhold, New York, 1992, vol. 2, p. 108; (e) S. Kannan and C. S. Swamy, *Catal. Today*, 1999, **53**, 725; (f) H. F. W. Taylor, *Mineral. Mag.*, 1973, **39**, 377.
- (a) W. Rochus and N. Kickuth, *German pat.*, 1,095,832, 1957; (b) S. Sathyanarayana and A. G. Krishnamurty, *Curr. Sci.*, 1988, **57**, 1114; (c) A. Aguilera, A. Alcantara, J. M. Marinas and J. V. Sinisterra, *Can. J. Chem.*, 1987, **65**, 1165; (d) A. Fuentes, J. M. Marinas and J. V. Sinisterra, *Tetrahedron Lett.*, 1987, **28**, 4541; (e) R. S. Varma, G. W. Kabalka, L. T. Evans and R. M. Pagni, *Synth. Commun.*, 1985, **15**, 279; (f) M. T. Drexler and M. D. Amiridis, *Catal. Lett.*, 2002, **79**, 175; (g) M. J. Climent, A. Corma, S. Iborra and J. Primo, *J. Catal.*, 1995, **151**, 60; A. Corma, V. Fornés, R. M. Martín-Aranda and F. Rey, *J. Catal.*, 1992, **134**, 58; A. Corma, V. Fornés and F. Rey, *J. Catal.*, 1994, **148**, 205; (h) A. Guida, M. H. Lhouty, D. Tichit, F. Figueras and P. Geneste, *Appl. Catal. A*, 1997, **164**, 251; (i) (1) S. Sebt, A. Solhy, R. Tahir, S. Boulaajaj, J. A. Mayoral, J. M. Fraile, A. Kossir and H. Oumimoun, *Tetrahedron Lett.*, 2001, **42**, 795(2) S. Sebt, A. Solhy, R. Tahir, S. Abdelatif, S. Boulaajaj, J. A. Mayoral, J. I. García, J. M. Fraile, A. Kossir and V. Oumimoun, *J. Catal.*, 2003, **213**, 1; (j) D. J. Macquarrie, R. Nazih and S. Sebt, *Green Chem.*, 2002, **4**, 56; (k) A. Corma, V. Fornés, R. M. Martín-Aranda, H. García and J. Primo, *Appl. Catal.*, 1990, **59**, 237; (l) A. Corma and R. M. Martín-Aranda, *J. Catal.*, 1991, **130**, 130; (m) K. Tanabe, in *Catalysis by Acids and Bases*, ed. B. Imelik, *et al.*, Elsevier, Amsterdam, 1985, p. 1. (n). (2).

Phase equilibrium-driven selective hydrogenation of limonene in high-pressure carbon dioxide†

Ewa Bogel-Lukasik,^a Isabel Fonseca,^a Rafał Bogel-Lukasik,^a Yuriy A. Tarasenko,^{‡a} Manuel Nunes da Ponte,^{*a} Alexandre Paiva^b and Gerd Brunner^b

Received 24th November 2006, Accepted 1st February 2007

First published as an Advance Article on the web 8th February 2007

DOI: 10.1039/b617187g

Pressure-tuning of selectivity in the hydrogenation of limonene in carbon dioxide was found in biphasic systems, close but below the critical conditions of the reaction mixture, where hydrogen solubility in the liquid is highly dependent on pressure. The subtle effects of pressure on the two-phase region in CO₂ + H₂ + a liquid reagent mixtures are essential factors in determining hydrogenation rates and selectivities in high-pressure carbon dioxide.

Reactions in supercritical fluids are an established field of research.¹ One of the advantages often mentioned for their use as solvents is in reactions involving gases, when all reactants can be brought into one phase. Supercritical fluids are gases, and they mix completely with other gases, like hydrogen. In these cases, the access of the gaseous reactant to the catalyst is not limited by mass transfer resistance across a phase boundary. Härröd *et al.*,² for instance, developed extremely fast and selective hydrogenation processes of fatty acid methyl esters in supercritical propane.

There are, however, examples where fast hydrogenations can be performed in biphasic mixtures containing high pressure carbon dioxide, like in many of the processes described by Hitzler *et al.*³ In previous publications from our laboratory, Chouchi *et al.*⁴ and Milewska *et al.*⁵ compared hydrogenation rates of (liquid) α -pinene in biphasic conditions, at lower CO₂ pressure, with rates in supercritical mixtures, at higher CO₂ pressure. This was a direct comparison for the same reactive system, where small differences in pressure induced a change in the number of phases. Their results have shown that hydrogenation in biphasic conditions can, in certain conditions, actually be as fast, or even faster, than in one supercritical phase.

In order to gain a better understanding of the factors that explain these results, and in particular the influence of vapour–liquid equilibrium, we proceeded to study the hydrogenation of limonene. Limonene or 1-methyl-4-isopropenyl-1-cyclohexene (1 in scheme 1) has two C=C double bonds, one in the cyclohexene ring and an external one. Hydrogenation of limonene, unlike pinene, can therefore yield different products. It can either be complete, producing a mixture of *cis*- and *trans*-*p*-menthane (4 and 5 in the

scheme), or partial, generating in principle the intermediates 2 and 3 (although previous studies, at low pressure, by Grau *et al.*⁶ and Shimazu *et al.*,⁷ have actually reported the preferential hydrogenation of the external double bond, to yield *p*-meth-1-ene).

On the other hand, phase equilibrium of limonene + CO₂ is very well documented.⁸ The critical pressure of the mixture is conveniently below 10 MPa at moderate temperatures, allowing an easy switching from two phases to a homogeneous one-phase fluid.

The hydrogenation of limonene was carried out at 50 °C and 4 MPa hydrogen pressure, to which carbon dioxide was added up to either 12.5 MPa or 16 MPa. In the first case, the reaction mixture was biphasic and in the second, monophasic. 0.4 g of a platinum catalyst in a SKN^{9a} carbon support was used.

The core of the apparatus used in this work was a 50 cm³ sapphire-windowed cell (VC), which allowed direct visual observation of the number of phases, as described in detail by Milewska *et al.*⁵ and is shown in Fig. 1.

The bottom of the cell was connected, *via* a circulation pump (CP), to a tubular reactor (TR) that enclosed a catalyst bed. The cell contents were vigorously stirred, in order to promote phase equilibrium, and continuously withdrawn from the bottom of the view cell, circulated through the catalyst bed, and sent back to the upper entrance of the cell. The flow-rates of circulation were very low. The main purpose was to keep the composition of the feed minimally disturbed by the reaction products entering the top of the cell. Samples have been taken at regular intervals through a system of two valves with a sampling loop (S), at the top of the tubular reactor. 1 ml of limonene was used in each experiment, which resulted in a large excess of hydrogen in the overall volume of the cell.

Hydrogenation of limonene at 16 MPa total pressure and one phase, supercritical conditions is fast, as shown in Fig. 2.

The intermediate product *p*-menth-1-ene, corresponding to the hydrogenation of only one C=C double bond, is detected at the outlet of the catalytic bed during the first 5 min. After that period, a stationary state is attained where only a 50–50 mixture of isomers of the completely hydrogenated product, *p*-menthane, is produced.

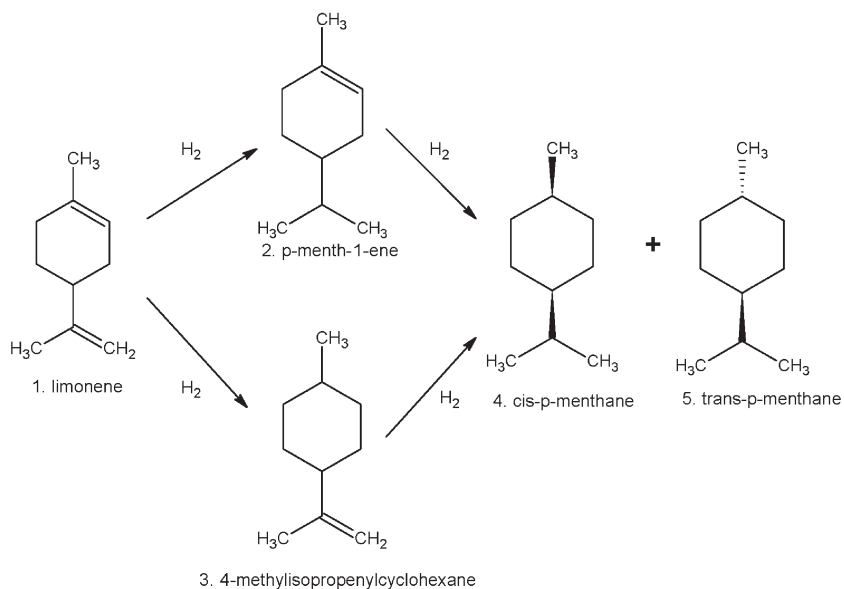
At 12.5 MPa total pressure, where a biphasic (vapour–liquid) system can be seen in the cell, the results of hydrogenation are completely different, as shown in Fig. 3.

The initial rate of disappearance of limonene is slower than for the reaction in supercritical conditions, but much faster than for biphasic (gas–liquid) reactions carried out in hydrogen + limonene mixtures without carbon dioxide.⁶ In quasi-stationary conditions, after 20 min, the main product is the mono-hydrogenated

^aREQUIMTE/CQFB, Departamento de Química, Faculdade de Ciências e Tecnologia, Universidade Nova de Lisboa, 2829-516 Caparica, Portugal. E-mail: mnp@dq.fct.unl.pt; Fax: +351 212948385

^bInstitute of Thermal and Separation Processes, Technische Universität Hamburg-Harburg, Eißendorfer Straße 38, 21073 Hamburg, Germany
† Electronic supplementary information (ESI) available: A detailed experimental section. See DOI: 10.1039/b617187g

‡ Permanent address: Institute of Sorption and Problems of Endoecology, 13 General Naumov Str., Kiev, Ukraine.



Scheme 1 Hydrogenation of limonene.

p-menth-1-ene (70 mol%), while the yield of fully hydrogenated *p*-menthane is kept at about 20 mol% (10 mol% for each isomer). Limonene is not completely converted, and remains at 10 mol% in the final product mixture.

As the stream of reactants is withdrawn from the bottom of the visual cell, it should be mostly the liquid phase to be circulated through the catalyst bed. The relatively fast initial consumption of limonene indicates that hydrogen should be dissolved in this phase in the right amounts to hydrogenate 90 mol% of the internal double bonds of limonene and 20 mol% of the external ones, producing 70 mol% *p*-menth-1-ene + 20 mol% *p*-menthane, and leaving 10 mol% limonene unreacted. The results strongly suggest that the hydrogen/limonene molar ratio should be very close to 1.1

in the liquid phase (in equilibrium with the vapour phase) in the visual cell, before it is pumped through the catalyst.

As there are no phase equilibrium results for CO₂ + limonene + H₂ mixtures available in the literature, we performed VLE^{9b} measurements at 50 °C and in the pressure range of interest for this work. The phase equilibrium measurements were made by an analytical method using a visual high-pressure cell with variable volume.¹⁰

Mixtures of initial hydrogen to limonene molar ratio of approximately 10 were studied at 11 MPa and at 13 MPa. At 11 MPa, a composition in mole fraction of (0.515 CO₂ + 0.380 limonene + 0.105 H₂) was measured for the liquid in equilibrium with a vapour of (0.512 CO₂ + 0.488 H₂), with traces of limonene, at the 0.0001 level. At 13 MPa, the equilibrium was established

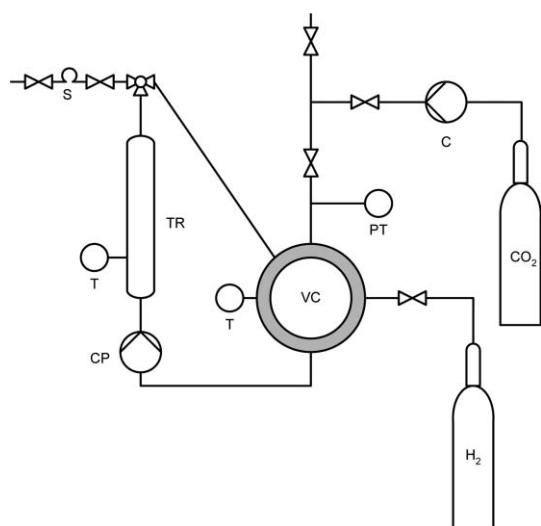


Fig. 1 Schematic diagram of the apparatus for hydrogenation at high pressure: (C) CO₂ compressor, (TR) tubular reactor, (VC) view cell, (S) sampling loop, (CP) circulation pump, (PT) pressure transducer, (T) temperature controller.

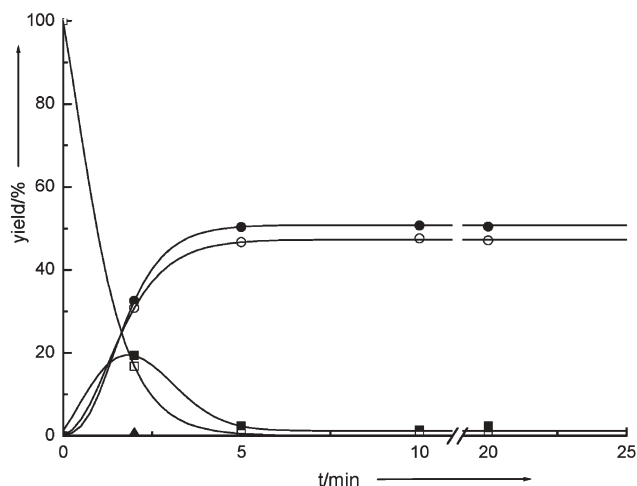


Fig. 2 Mol percentages of (●) *trans*-*p*-menthane; (○) *cis*-*p*-menthane; (■) *p*-menth-1-ene; (□) limonene; (▲) α -terpinene, products of limonene's hydrogenation on 1 wt% Pt SKN in single-phase at 50 °C, 4 MPa H₂, 16 MPa total pressure vs. time.

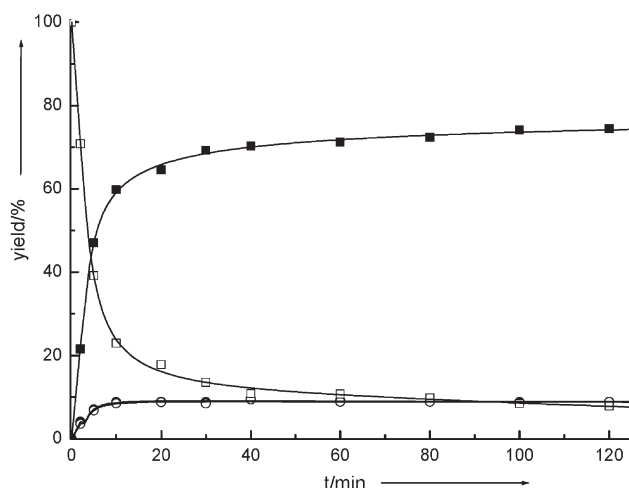


Fig. 3 Mol percentages of (●) *trans-p*-menthane; (○) *cis-p*-menthane; (■) *p*-menth-1-ene; (□) limonene, products of limonene's hydrogenation on 1 wt% Pt SKN in biphasic (liquid + gas) system at 50 °C, 4 MPa H₂, 12.5 MPa total pressure vs. time.

between a liquid (0.530 CO₂ + 0.305 limonene + 0.155 H₂) and a vapour (0.505 CO₂ + 0.002 limonene + 0.493 H₂).

In the method used, sampling from phases in the vicinity of the critical region is a difficult task. Due to the similarity of density between the phases and to its sensitivity to pressure changes, even small pressure drops on sampling can generate large perturbations in the phases in equilibrium, such as local condensation and vapourisation. A strategy was therefore adopted where measurements were performed away from the critical composition and the experimental data so obtained were used to fit the parameters of the Peng–Robinson equation of state,¹¹ using the Mathias–Klotz–Prausnitz¹² mixing rule.

The correlations parameters are presented in the ESI. A detailed calculation of phase equilibrium of the reactive system was carried out using the program package PE.¹³

Fig. 4 shows the region of CO₂-rich mixtures of the triangular phase equilibrium diagram for the ternary mixture. This is the area

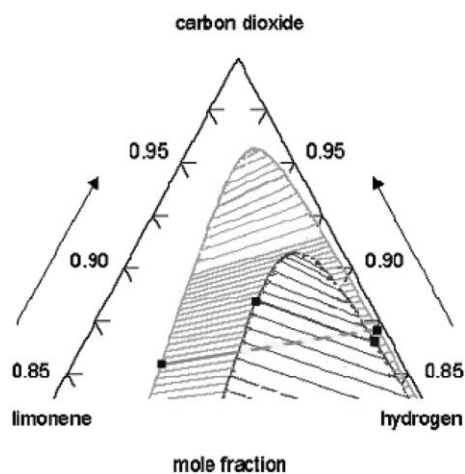


Fig. 4 Correlation of the calculated *p*–*x*–*y* data with the Peng–Robinson equation of state and the Mathias–Klotz–Prausnitz mixing rule. VLE diagram limited for mole fraction of CO₂ higher than 0.80.

of composition corresponding to the reaction mixtures used in the above-presented kinetic studies. Pictured in dark grey are the tie-lines for the isobar at 12.5 MPa, the pressure corresponding to the biphasic reaction illustrated in Fig. 3. The overall composition (in mole fraction) of the liquid + vapour mixture in the visual cell was calculated as 0.874 CO₂ + 0.010 limonene + 0.116 H₂. Inserting this value in the graph, the corresponding tie-line gives 0.889 CO₂ + 0.045 limonene + 0.066 H₂ for the liquid and 0.874 CO₂ + 0.007 limonene + 0.120 H₂ for the vapour. The important parameter for hydrogenation is the H₂ to limonene ratio, which changes from 18.5 in the vapour phase to 1.5 in the liquid. If the uncertainties associated with the use of the Peng–Robinson equation in the vicinity of the critical region are taken into consideration, this last value is remarkably similar to the 1.1 value inferred from the kinetic data. It is also remarkable that both calculations give more hydrogen than limonene in the liquid phase at 12.5 MPa.

In Fig. 4, liquid–vapour equilibrium is also plotted at the slightly lower pressure of 11 MPa, and shown in light grey. The two-phase region is wider than at the higher pressure, and the slope of the tie-lines is markedly different. If the same mixture of reactants was used at this pressure, the corresponding tie-line is drawn in light grey. The hydrogen/limonene ratio in the liquid phase is now only 0.4. This means that a small change in pressure has a really dramatic effect on the reactant ratio.

One of the most claimed advantages of supercritical fluids as solvents is their tunability, that is, the use of their high compressibility to change the products of the reaction by varying pressure. However, as stated by Licence *et al.*,¹⁴ although tunability of reactions is perhaps the most appealing aspect of supercritical fluids, there are surprisingly few examples where it has been achieved in practice. Poliakoff and collaborators,³ in their comprehensive study of flow reactor hydrogenations in carbon dioxide, remarked that the important reaction parameters were temperature and H₂ concentration. Changes in solvent pressure were not important, except when, in their own words, it “was close to or below the critical pressure of the fluid”.

The diagram of Fig. 4 gives an explanation of why this is so. In fact, it is in the conditions depicted in Fig. 4, where carbon dioxide in large excess is the solvent and the system is relatively close to the critical line of the mixture, but is still biphasic, that the partition of the solutes limonene and hydrogen between the liquid and the vapour is highly sensitive to pressure. Reaction selectivity is therefore really pressure-tunable only in a biphasic system where phase equilibrium ratios determine the composition of the liquid phase in contact with the catalyst. On the other hand, when pressure is sufficiently high for the system to be in a single phase, the composition of the mixture is fixed, and “tunability” is mostly lost.

In conclusion, the subtle effects of pressure on the two-phase region in CO₂ + H₂ + a liquid reagent mixtures are essential factors in determining hydrogenation rates and selectivities in high-pressure carbon dioxide.

Acknowledgements

This work was supported by the European Commission in the frame of Marie Curie Research Training Network SUPERGREENCHEM (EC Contract No.: MRTN-CT-2004-504005).

Notes and references

- 1 E. J. Beckman, *J. Supercrit. Fluids*, 2004, **28**, 121–191; R. Noyori, *Supercritical Fluids*, *Chem. Rev.*, 1999, **992**, 353–354; *Chemical Synthesis in Supercritical Fluids*, ed. P. G. Jessop and W. Leitner, Wiley-VCH, Weinheim, 1999.
- 2 M. Härröd, S. van den Hark, M.-B. Macher and P. Möller, in *High Pressure Process Technology: Fundamentals and Applications*, ed. A. Bertucco and G. Vetter, Elsevier, Amsterdam, 2001, p. 496.
- 3 G. Hitzler, F. R. Smail, S. K. Ross and M. Poliakov, *Org. Proc. Res. Dev.*, 1998, **2**, 137–146.
- 4 D. Chouchi, D. Gourguillon, M. Courel, J. Vital and M. Nunes da Ponte, *Ind. Eng. Chem. Res.*, 2001, **40**, 2551–2554.
- 5 A. Milewska, A. M. Banet Osuna, I. M. Fonseca and M. Nunes da Ponte, *Green Chem.*, 2005, **7**, 726–732.
- 6 R. J. Grau, P. D. Zgolicz, C. Gutierrez and H. A. Taher, *J. Mol. Catal. A: Chem.*, 1999, **148**, 203–214.
- 7 S. Shimazu, N. Baba, N. Ichikuni and T. Uematsu, *J. Mol. Catal. A: Chem.*, 2002, **182–183**, 343–350.
- 8 J. Fonseca, P. C. Simões and M. Nunes da Ponte, *J. Supercrit. Fluids*, 2003, **25**, 7–17; H. A. Matos, M. A. Costa, E. G. De Azevedo, P. C. Simões and M. Nunes da Ponte, *J. Supercrit. Fluids*, 1994, **7**, 101–106; M. Budich, PhD Thesis, Technische Universität Hamburg, Harburg, 1999.
- 9 (a) SKN – type of synthetic carbon sorbent; (b) VLE –vapour liquid equilibria.
- 10 J. Stoldt and G. Brunner, *Proceedings of the Third International Symposium on Supercritical Fluids*, Strasbourg, 1994.
- 11 D. Y. Peng and D. B. Robinson, *Ind. Eng. Chem. Fundam.*, 1976, **15**, 59–64.
- 12 P. M. Mathias, H. C. Klotz and J. M. Prausnitz, *Fluid Phase Equilib.*, 1991, **67**, 31–44.
- 13 O. Pföhl, S. Petkov and G. Brunner, PE V2.9.9a—Software for Phase Equilibria Calculations, Technische Universität Hamburg-Harburg, Hamburg, 1998.
- 14 P. Licence, W. K. Gray, M. Sokolova and M. Poliakov, *J. Am. Chem. Soc.*, 2005, **127**, 293–298.



STOP!

searching...

Save valuable time searching for that elusive piece of vital chemical information.

Let us do it for you at the Library and Information Centre of the RSC.

We are your chemical information support, providing:

- Chemical enquiry helpdesk
- Remote access chemical information resources
- Speedy response
- Expert chemical information specialist staff

Tap into the foremost source of chemical knowledge in Europe and send your enquiries to

library@rsc.org

RSCPublishing

www.rsc.org/library

12120515

Ionic liquid supported tin reagents for Stille cross coupling reactions†

Jürgen Vitz,* Dinh Hung Mac and Stéphanie Legoupy*

Received 7th November 2006, Accepted 2nd February 2007

First published as an Advance Article on the web 12th February 2007

DOI: 10.1039/b616218e

New ionic liquid supported tin reagents were synthesized for use in Stille cross coupling reactions at low reaction temperatures and with the possibility for recycling the tin compounds.

Stille cross coupling reactions have been well established methods for C–C coupling reactions for years.¹ However, organic tin chemistry presents disadvantages such as pollution of products by tin salts and difficulties of separation. Efforts to overcome these problems have been undertaken for the last few years, leading for example to the use of solid phase synthetic methods or fluorous phases.² With the aim at developing nontoxic methodologies, room temperature ionic liquids (RTILs) were found to be very useful as solvents for a wide range of organic and transition-metal catalyzed reactions.³ Indeed, ionic liquids were used in Stille type reactions with aryl bromides and aryl iodides,⁴ Suzuki cross coupling reactions,⁵ or Grignard reactions.⁶ In addition, task specific ionic liquids (TSILs) have emerged and one of their principal applications refer to supported synthesis. For example, they were used to support iodobenzoate compounds for Suzuki cross coupling reactions or to support a ruthenium carbene complex for use as a catalyst in ring closing olefin metathesis,⁷ and as a soluble support for synthesis on small organic molecules.⁸

We proposed to extend the potentialities of TSILs by supporting tin reagents on ionic liquids in Stille cross coupling reactions. For our cross coupling experiments two components were necessary, the ionic liquids as solvents and the tin supported ionic liquids. Therefore some simple imidazolium based ionic liquids were synthesized starting from 1-methylimidazole (**1**) only by mixing them with the halogeno alkanes (Table 1).^{3a-d,9} No solvent was necessary and the crude products were purified by extraction with diethyl ether, toluene, or ethyl acetate to remove traces of starting materials. The ionic liquids were obtained in very good yields in high purities. Afterwards, the halogeno anions were exchanged by the tetrafluoroborate anion. Whereas it was found that for [BMIM]Br water is the best solvent,¹⁰ other exchange reactions must be carried out in acetone^{3c,11,12} or dichloromethane.¹³ The completeness can be checked by adding a silver nitrate solution to a solution of the ionic liquid in water.¹⁰

Furthermore, it is possible to synthesize the ionic liquids starting from imidazoles **4** (Table 2). This procedure was the method of choice especially for long side chains or the 2-substituted starting materials. Table 2 gives an overview of the different products **5**

Laboratoire de Synthèse Organique, UCO2M, UMR CNRS 6011, Université du Maine, Avenue Olivier Messiaen, 72085 Le Mans cedex 9, France. E-mail: jurgen.vitz@univ-lemans.fr; stephanie.legoupy@univ-lemans.fr; Fax: +33 243 833902; Tel: +33 243 833340

† Electronic supplementary information (ESI) available: Experimental procedures and characterization data for ionic liquids and Stille products. See DOI: 10.1039/b616218e

Table 1 Synthesis of ionic liquids starting from 1-methylimidazole (**1**)

Reaction scheme showing the synthesis of ionic liquids from 1-methylimidazole (1) and R¹-X, followed by reaction with NaBF₄ to yield products 2 and 3.

R ¹ -X	X ⁻	Yield	X ⁻	Yield		
4-Bromo-1-butene	2a	Br ⁻	97%	3a	BF ₄ ⁻	99%
1,3-Dibromopropane	2b	—	^a	—	—	—
1,4-Dibromobutane	2c	—	^a	—	—	—
1-Bromo-3-chloropropane	2d	Br ⁻	98%	—	—	—

^a Double substitution products.

^a Double substitution products.

synthesized. Afterwards, only stirring with methyl iodine delivers the desired ionic liquids with an iodine anion.

To prepare ionic liquid supported tin reagents, we first planned to use a hydrostannylation of a terminal double bond present on the ionic liquid. To avoid interactions with the imidazole part of the molecule and the anchor group an alkyl side chain should be used as a “spacer” between both functionalities. Therefore, 4-bromo-1-butene was chosen to synthesize **2a** (Table 1). The necessary stannanes (*n*-Bu)₃SnH and (*n*-Bu)₂SnPhH for the hydrostannylation step were prepared by known literature procedures.¹⁴ For the hydrostannylation reactions, a standard procedure using AIBN was used.¹⁴ Unfortunately all reactions to couple the tin hydride species to the double bond of **2a** were unsuccessful. Starting materials were equally recovered using Pd(OH)₂ as the catalyst.^{15,16} In addition, the hydrostannylation step was fruitless with the “non-ionic liquid” starting material **5a** (Table 2). The imidazole starting materials were recovered as well as tin degradation products.

Table 2 Synthesis of the ionic liquid precursors starting from imidazoles **4**

Reaction scheme showing the synthesis of ionic liquid precursors **5** from imidazoles **4**. Imidazole **4** (with substituent R^1) reacts with NaH , THF , and then $\text{R}^2\text{-X}$ to form the ionic liquid precursor **5** (with substituents R^1 and R^2).

Entry	R^1	$\text{R}^2\text{-X}$	P	R^2	Yield ^a	
7	4a	H	4-Bromo-1-butene	5a	$(\text{CH}_2)_2\text{CH}=\text{CH}_2$	50%
8	4a	H	$\text{Br}(\text{CH}_2)_3\text{Cl}$	5b	$(\text{CH}_2)_3\text{Cl}$	82%
9	4a	H	$\text{Br}(\text{CH}_2)_6\text{Cl}$	5c	$(\text{CH}_2)_6\text{Cl}$	96%
11	4b	Me	$\text{Br}(\text{CH}_2)_3\text{Cl}$	5d	$(\text{CH}_2)_3\text{Cl}$	73%
12	4c	Ph	$\text{Br}(\text{CH}_2)_3\text{Cl}$	5e	$(\text{CH}_2)_3\text{Cl}$	65%

^a Isolated yields.

^a Isolated yields.

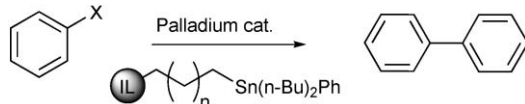
As a solution, a substitution reaction of a halogen atom in the side chain by stannyl lithium should replace the hydrostannylation step. Therefore the first targets were the 1-(3-bromo-propane)- and 1-(4-bromo-butane)-3-methylimidazolium ionic liquids **2b** and **2c**. Unfortunately, no selective reaction between both reaction partners 1-methylimidazole (**1**) and the dibromo compounds could be achieved; the NMR-spectra showed symmetrical products. A reaction under low reaction temperature and low concentration of the reaction partners by use of a high amount of solvent was also unsuccessful.

By reaction with 1-bromo-3-chloropropane, 1-methylimidazole (**1**) could be converted to the ionic liquid **2d**. No double substitution was observed and the product was obtained in high yield (Table 1).¹⁷ Unfortunately, the following substitution reaction by tributyltin lithium with ionic liquid **2d** did not occur. With the “non-ionic liquid” product **5b**,¹⁸ synthesized from imidazole **4a** and 1-bromo-3-chloropropane (Table 2), the substitution was possible and provided the tin compound **6a** in 54% yield after column chromatography. The subsequent transformation to the ionic liquid **7a** was achieved in 99% yield (Table 3).

Since this reaction sequence offers access to various tin coupled ionic liquids, we prepared—starting from imidazole (**4a**), 2-methylimidazole (**4b**), or 2-phenylimidazole (**4c**)—ionic liquid supported tin reagents for a later use in Stille cross coupling reactions (Tables 2 and 3). Whereas the products **6a** and **6c** could be purified by column chromatography to obtain the pure products in 54% and 73% yield, all other separations failed at the first step of the reaction sequence caused by similar polarities of products and starting materials. After conversion to the ionic liquids, it was possible to purify the products **7b**, and **7d–e** by extraction. Overall yields between 32% and 44% were obtained. In two cases the anions were exchanged with BF_4^- to afford **8b** and **8d** in good yields.

Initial Stille cross coupling reactions were unsuccessful (Table 4). Although copper is often mentioned as a cocatalyst for palladium catalyzed cross coupling reactions,^{6,19,20} we found that with our ionic liquid tin compounds **7b–c**, **8b**, **8d** side reactions are favored, one of them is the formation of $\text{Ph}_2\text{Sn}(n\text{-Bu})_2$ in relatively high

Table 4 Stille reactions with ionic liquid supported tin reagents



E	IL	Anion	X	Condition ^a	Solution	T	Time	Yield ^b	Ph_2SnBu_2
1	8b	BF_4^-	Br	i	I	80 °C	16 h	32%	57%
2	8b	BF_4^-	Br	ii	I	80 °C	16 h	—	15%
3	7c	I^-	I	iii	—	80 °C	40 h	52%	27%
4	8d	BF_4^-	I	iii	—	80 °C	16 h	—	43%
5	7c	I^-	I	iv	—	35 °C	40 h	99%	7%
6	7b	I^-	I	v	—	35 °C	160 h	98%	—
7	7c	I^-	I	v	—	35 °C	112 h	98%	—
8	7c	I^-	I	v	II	35 °C	160 h	87%	—
9	7c	I^-	I	vi	—	35 °C	160 h	93%	—
10	7c	I^-	I	v	—	35 °C	184 h	72%	—

^a Conditions: (i) 5 mol% $\text{Pd}_2\text{Cl}_2(\text{PhCN})_2$, 10 mol% CuI , 10 mol% AsPh_3 ; (ii) 5 mol% $\text{Pd}(\text{PPh}_3)_4$, 10 mol% CuI , 10 mol% AsPh_3 ; (iii) 5 mol% $\text{Pd}(\text{PPh}_3)_4$, 10 mol% CuI ; (iv) 5 mol% $\text{Pd}(\text{PPh}_3)_2\text{Cl}_2$, 10 mol% CuI ; (v) 5 mol% $\text{Pd}_2\text{dba}_3\cdot\text{CHCl}_3$; (vi) 5 mol% $\text{Pd}(\text{dba})_2$.

^b Conversion as determined by GC. ^c Recycled tin compound; (I) [BMIM] BF_4 , (II) [BMIM] PF_6 .

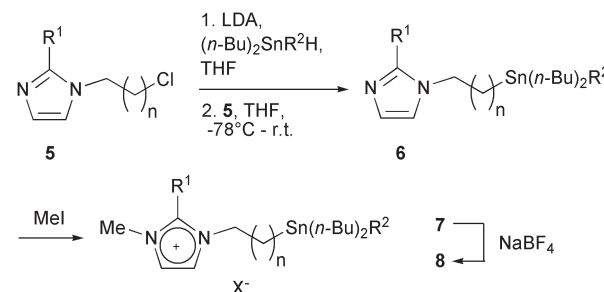
yields up to 57% (entries 1–5). In addition, high temperatures were necessary to perform the catalytic reactions (entries 1–4). At low reaction temperatures only a slow conversion was observed but also a formation of $\text{Ph}_2\text{Sn}(n\text{-Bu})_2$ (entry 5). In comparison, no reaction took place when using $\text{Pd}(\text{PPh}_3)_4$ without copper iodide.

Fortunately, we found that the $\text{Pd}_2\text{dba}_3\cdot\text{CHCl}_3$ and $\text{Pd}(\text{dba})_2$ catalysts are able to provide good yields of the desired product. Low reaction temperatures were sufficient without adding copper salts or ligands (Table 4, entries 6–10).^{3e,21} A first reaction with tin compound **7b** and the catalyst $\text{Pd}_2\text{dba}_3\cdot\text{CHCl}_3$ showed a conversion of 98% (entry 6). At 35 °C without additional organic solvents, this coupling procedure shows no formation of side products like $\text{Ph}_2\text{Sn}(n\text{-Bu})_2$. Under the same conditions the cross coupling reaction with compound **7c** showed a conversion of 98% after 112 h (entry 7). By using [BMIM] PF_6 as co-solvent the reaction rate is reduced, a conversion of 87% was estimated after prolonged reaction time (entry 8). The catalyst $\text{Pd}(\text{dba})_2$ showed a reduced activity in the cross coupling reaction with a conversion of 93% (entry 9) in contrast to 98% with $\text{Pd}_2\text{dba}_3\cdot\text{CHCl}_3$ (entry 7).

Furthermore, it is possible to recycle and to reuse the system tin compound/palladium catalyst at the end of the reaction. Products and remaining starting materials and/or side products are extracted by non-ionic liquid miscible organic solvents like pentane, while the ionic liquid phase still contains the palladium catalyst and the halogenotin supported ionic liquid **9**. Simply adding PhLi to a solution of compound **9** in THF regenerates the Stille starting material **7** (Scheme 1). This was carried out in the case of compound **9c** ($\text{X} = \text{I}$) to recover product **7c**. Because the palladium catalyst was not separated, the product was directly used for a subsequent cross coupling reaction (entry 10, Table 4). However the activity is reduced with respect to the original product **7c**, a conversion of 72% was observed after 184 h.

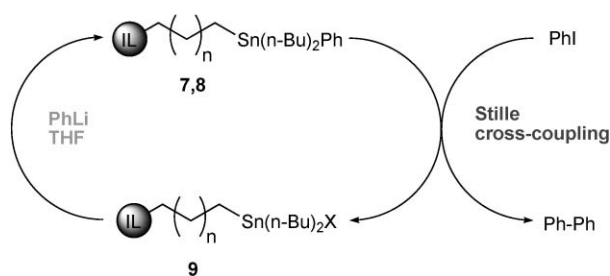
In summary, new ionic liquid supported tin reagents were synthesized and successfully used in Stille cross coupling reactions. With these reagents high yields at low reaction temperatures and the recycling of the tin compounds are possible. The best results were achieved with the $\text{Pd}_2\text{dba}_3\cdot\text{CHCl}_3$ catalyst, which does not

Table 3 Ionic liquid supported tin reagents



R^1	n	P	R^2	Yield	X^-	Yield	X^-	Yield
5b	H	2	6a $n\text{-Bu}$	54% ^a	7a I^-	99%	—	—
5b	H	2	6b Ph	nd	7b I^-	44% ^b	8b BF_4^-	99%
5c	H	5	6c Ph	73% ^a	7c I^-	99% ^a	—	—
5d	Me	2	6d Ph	nd	7d I^-	32% ^b	8d BF_4^-	74%
5e	Ph	2	6e Ph	nd	7e I^-	44% ^b	—	—

^a After purification. ^b Two steps, purification.



Scheme 1 Recycling the tin compounds.

require additional additives or ligands. This reduces costs and simplifies the work-up procedure.

With these advantages, the experimental investigations will be continued in our laboratory focused on the recycling of the tin compounds and the separation of lithium iodide, but also to extend this catalytic system to other substrates. These results will be reported in due course.

Acknowledgements

We thank the Région des Pays de la Loire for financial support; J. Vitz also thanks the Région des Pays de la Loire for his research fellowship. We thank P. Gangnery at the University of Le Mans and Prof. P. Guenot and F. Lambert at CRMPO Rennes for conducting the mass spectra. In addition, we thank Professor F. Huet, Dr G. Dujardin and Dr A.-S. Castanet for their discussions and advice.

Notes and references

- (a) P. Espinet and A. M. Echavarren, *Angew. Chem., Int. Ed. Engl.*, 2004, **43**, 4704; (b) K. Lee, W. P. Gallagher, E. A. Toskey, W. Chong and R. E. Maleczka, Jr., *J. Organomet. Chem.*, 2006, **691**, 1462; (c) C. Chiappe, D. Pieraccini, D. Zhao, Z. Fei and P. J. Dyson, *Adv. Synth. Catal.*, 2006, **348**, 68; (d) J.-H. Li, Y. Liang, D.-P. Wang, W.-J. Liu, Y.-X. Xie and D.-L. Yin, *J. Org. Chem.*, 2005, **70**, 2832; (e) V. Calo, A. Nacci, A. Monopoli and F. Montingelli, *J. Org. Chem.*, 2005, **70**, 6040; (f) J. C. Garcia-Martinez, R. Lezutekong and R. M. Crooks, *J. Am. Chem. Soc.*, 2005, **127**, 5097; (g) W. Su, S. Urgaonkar, P. A. McLaughlin and J. G. Verkade, *J. Am. Chem. Soc.*, 2004, **126**, 16433.
- (a) G. Dumartin, G. Ruel, J. Kharboul, B. Delmond, M.-F. Connil, B. Jousseau and M. Pereyre, *Synlett*, 1994, 952; (b) J. Cossy, C. Rasamison and D. G. Pardo, *J. Org. Chem.*, 2001, **66**, 7195; (c) J.-F. Chretien, F. Zammattio, E. Le Grogne, M. Paris, B. Cahing, G. Montavan and J.-P. Quintard, *J. Org. Chem.*, 2005, **70**, 2870; (d) M. Gerlach, F. Jördens, H. Kuhn and W. P. J. Neumann, *J. Org. Chem.*, 1991, **56**, 5971; (e) X. Zhu, B. E. Blough and F. I. Carroll, *Tetrahedron Lett.*, 2000, **41**, 9219; (f) E. J. Enholm and J. P. Schulte, *Org. Lett.*, 1999, **1**, 1275; (g) K. Olofsson, S.-Y. Kim, M. Larhed, D. P. Curran and A. Halberg, *J. Org. Chem.*, 1999, **64**, 4539; (h) G. F. Santori, A. G. Moglioni, V. Vetere, G. Y. M. Iglesias, M. L. Casella and O. A. Ferretti, *Appl. Catal. A: General*, 2004, **269**, 215.
- (a) T. Welton, *Chem. Rev.*, 1999, **99**, 2071; (b) P. Wasserscheid and W. Keim, *Angew. Chem., Int. Ed. Engl.*, 2000, **39**, 3772; (c) N. Jain, A. Kumar, S. Chauhan and S. M. S. Chauhan, *Tetrahedron*, 2005, **61**, 1015; (d) J. Dupont, R. F. de Souza and P. A. Z. Suarez, *Chem. Rev.*, 2002, **102**, 3667; (e) C. Chiappe, G. Imperato, E. Napolitano and D. Pieraccini, *Green Chem.*, 2004, **8**, 33; (f) M. C. Law, K.-Y. Wong and T. H. Chan, *Green Chem.*, 2004, **6**, 241; (g) C. M. Gordon and C. Ritchie, *Green Chem.*, 2002, **4**, 124; (h) X.-L. Zhao, L. Liu, Y.-J. Chen and D. Wang, *Tetrahedron*, 2006, **62**, 7113.
- (a) S. T. Handy and X. Zhang, *Org. Lett.*, 2001, **3**, 233; (b) J.-H. Li, B.-X. Tang, L.-M. Tao, Y.-X. Xie, Y. Liang and M.-B. Zhang, *J. Org. Chem.*, 2006, **70**, 7488.
- F. McLachlan, C. J. Mathews, P. J. Smith and T. Welton, *Organometallics*, 2003, **22**, 5350.
- A. L. Casado and P. Espinet, *Organometallics*, 2003, **22**, 1305.
- (a) W. Miao and T. H. Chan, *Org. Lett.*, 2003, **5**, 5003; (b) N. Audic, H. Clavier, M. Mauduit and J.-C. Guillemin, *J. Am. Chem. Soc.*, 2003, **125**, 9248.
- J. Fraga-Dubreuil and J. P. Bazureau, *Tetrahedron Lett.*, 2001, **42**, 6097.
- D. Zhang, J. Chen, Y. Liang and H. Zhou, *Synth. Commun.*, 2005, **35**, 521.
- X. Creary and E. D. Willis, *Org. Synth.*, 2005, **82**, 166.
- N. Jain, A. Kumar and S. M. S. Chauhan, *Tetrahedron Lett.*, 2005, **46**, 2599.
- Y. Génisson, N. Lauth-de Viguerie, C. André, M. Baltas and L. Gorrichon, *Tetrahedron Asym.*, 2005, **16**, 1017.
- L. Cammarata, S. G. Kazarian, P. A. Salter and T. Welton, *Phys. Chem. Chem. Phys.*, 2001, **3**, 5192.
- A. Chemin, H. Deleuze and B. Maillard, *J. Appl. Polym. Sci.*, 2000, **79**, 1297.
- D. Stien and S. Gastaldi, *J. Org. Chem.*, 2004, **69**, 4464.
- M. Lautens, N. D. Smith and D. Ostrovsky, *J. Org. Chem.*, 1997, **62**, 8970.
- D₂O as solvent onto position 2 of the imidazole ring system as well as the hydrogen atoms of the side chain without adding base or heating, see: S. T. Handy and M. Okello, *J. Org. Chem.*, 2005, **70**, 1915.
- Product **5b** is only stable in solution.
- V. Farina, S. Kapadia, B. Krishnan, C. Wang and L. S. Liebeskind, *J. Org. Chem.*, 1994, **59**, 5905.
- S. P. H. Mee, V. Lee and J. E. Baldwin, *Chemistry*, 2005, **11**, 3294.
- A. Herve, A. L. Rodriguez and E. Fouquet, *J. Org. Chem.*, 2005, **70**, 1953.

Preparation of a sugar catalyst and its use for highly efficient production of biodiesel†

Min-Hua Zong,^{*a} Zhang-Qun Duan,^a Wen-Yong Lou,^a Thomas J. Smith^{*b} and Hong Wu^a

Received 24th October 2006, Accepted 8th February 2007

First published as an Advance Article on the web 19th February 2007

DOI: 10.1039/b615447f

Novel solid acid catalysts for esterification have recently been described that are made by incomplete carbonization of carbohydrates followed by sulfonation. Herein, such a 'sugar catalyst' is prepared from D-glucose and its catalytic properties and structure are investigated in detail. This type of sugar catalyst is, for the first time, applied for the effective production of biodiesel from waste oils. Our results indicate that sugar catalysts are highly effective, minimally polluting and re-usable catalysts that are highly suited to the production of biodiesel from waste oils with a high acid value.

The price of fossil diesel has soared in recent years and the available reserves of this important fuel will eventually be exhausted if large-scale use continues. Biodiesel is a renewable alternative to fossil diesel that is composed of monoalkyl esters of fatty acids. Waste oils, which are available cheaply, are an attractive starting material that can help in improving the economical feasibility of biodiesel. However, they are challenging due to the presence of considerable amounts of free fatty acids (FFAs), which interfere with the transesterification process and must first be converted into their corresponding esters through esterification. Reported catalysts for the production of biodiesel have included homogeneous strong bases¹ such as alkali metal hydroxides and alkoxides, homogeneous acids^{1c,2} such as H₂SO₄ and enzymes such as lipases.³ However, alkaline catalysts are generally corrosive to equipment and also react with FFAs to form unwanted soap by-products that require expensive separation.^{1b} Homogeneous acid catalysts are difficult to recycle and operate at high temperatures, and also give rise to serious environmental and corrosion problems.^{2f} Although the lipases are generally effective and non-polluting, they are usually expensive and there are problems associated with both FFAs and short chain alcohols (such as methanol and ethanol), which denature the lipase to some extent as well as substantially decreasing the operational stability of the enzyme. In addition, glycerol, which is one of the products of the reaction, is easily absorbed onto the surface of the lipase and has a serious negative effect on the enzyme.⁴ Therefore, the development of solid acid catalysts, which have recently gained much attention in view of their ease of separation and lack of corrosion or toxicity problems, is a desirable goal.^{2f,5,6}

Unfortunately, the inorganic-oxide solid acids such as zeolite and niobic acid have low densities of effective acid sites and readily lose their activities under harsh conditions.^{7,8} Although strong acidic ion-exchange resins such as amberlyst and nafion have abundant sulfonic acid groups (–SO₃H) that function as strong acid sites, these resins are expensive and their catalytic activities are still much lower than that of sulfuric acid. In addition, such resins show low operational stability and their catalytic activity is lost after a few cycles of re-use.^{6,9,10} Sulfated zirconia, on the other hand, is an efficient solid acid catalyst,^{9,11} but is expensive because zirconium is a rare and costly metal. Besides, high temperatures are required both for the calcination which is necessary for preparation of sulfated zirconia and for reactivation of the catalyst.

Only recently have carbon-based solid acid catalysts been reported as promising catalysts for esterification reactions. Such a catalyst can be cheaply produced by incomplete carbonization of sulfopolycyclic aromatic hydrocarbons (such as sulfonate derivatives produced by reaction of naphthalene and anthracene with H₂SO₄)¹² or sulfonation of incompletely carbonized D-glucose.¹³ Unfortunately, the former is a soft material and its aromatic molecules are leached out during liquid-phase reactions above 100 °C or when higher fatty acids are used as reactants, thus resulting in a rapid deactivation of the catalyst. However, sugar-derived solid acid catalysts, known as sugar catalysts, are physically robust and there is no leaching of SO₃H groups during use and so these catalysts exhibit a high and stable activity during the esterification reactions. In this paper, we describe the preparation of a solid acid catalyst from D-glucose (Fig. S1 in the ESI†), and use the resulting sugar catalyst for efficient production of biodiesel from higher fatty acids and especially waste oils with a high acid value. The physical and chemical properties of the D-glucose-derived catalyst are also characterized.

D-Glucose powder (10 g) was heated for 15 h at 400 °C under N₂ flow to produce an incomplete carbonization. The resulting material was then ground to a powder and heated in 100 mL of concentrated H₂SO₄ at 150 °C under N₂ flow for 15 h. The mixture was diluted with distilled water and the black precipitate was collected by filtration and washed repeatedly with hot distilled water (>80 °C) until impurities such as sulfate ions were no longer detected in the wash water.¹³ The resulting black solids (*i.e.* the sugar catalyst) were dried at 60 °C *in vacuo* and were subsequently evaluated for the catalytic activity in biodiesel production as described below.

High-grade biodiesel can be produced by esterification of oleic acid, one of the constituent fatty acids of the triglycerides of vegetable oils, with short chain aliphatic alcohols (methanol or ethanol). In order to rationally evaluate the activity of sugar

^aLaboratory of Applied Biocatalysis, South China University of Technology, Guangzhou, 510640, China. E-mail: btmhzong@scut.edu.cn; Fax: +86 20-2223-6669; Tel: +86 20-8711-1452

^bBiomedical Research Centre, Sheffield Hallam University, Owen Building, Howard Street, Sheffield, UK S1 1WB. E-mail: t.j.smith@shu.ac.uk

† Electronic supplementary information (ESI) available: Experimental section. See DOI: 10.1039/b615447f

catalyst in this reaction, a comparative study was made between the D-glucose-derived sugar catalyst and three typical solid acid catalysts (sulfated zirconia, amberlyst-15 and niobic acid). The reaction used was the esterification of oleic acid (10 mmol) with methanol (100 mmol) at 80 °C. As can be seen in Fig. 1, the sugar catalyst showed a much higher esterification activity than either sulfated zirconia ($67 \mu\text{mol min}^{-1}$ vs. $21 \mu\text{mol min}^{-1}$) or amberlyst-15 ($67 \mu\text{mol min}^{-1}$ vs. $7 \mu\text{mol min}^{-1}$), and gave a markedly enhanced yield of methyl oleate after 5 h (95% vs. 85% or 15%). Niobic acid, which is a solid acid catalyst, manifested no significant catalytic activity ($<1.5 \mu\text{mol min}^{-1}$) towards the esterification of oleic acid with methanol. Surprisingly, the solid acid catalyst sulfated zirconia exhibited much lower esterification activity than the sugar catalyst although the former has a substantially larger BET surface area ($214 \pm 0.08 \text{ m}^2 \text{ g}^{-1}$) than the latter ($4.13 \pm 0.03 \text{ m}^2 \text{ g}^{-1}$), which suggests that the surface of the greater part of the micropores in sulfated zirconia do not participate in the esterification reaction. The main reason for the unexpected result might be that the acid sites of sulfated zirconia were fewer than those of the sugar catalyst prepared from D-glucose, which is the subject of ongoing investigation in our laboratory. In order to compare the sugar catalyst with a homogeneous acid catalyst, the esterification of oleic acid with methanol was also conducted using concentrated H_2SO_4 as the catalyst. In spite of its slightly higher esterification activity than the sugar catalyst ($78 \mu\text{mol min}^{-1}$ vs. $67 \mu\text{mol min}^{-1}$), the concentrated H_2SO_4 as a liquid acid catalyst cannot be readily recycled, and it presents a threat to the environment and the operator's health, especially when it is employed on a large scale. Although H_2SO_4 is used during the preparation of the sugar catalyst, the catalyst itself is relatively non-toxic and can be re-used many times. It therefore represents a greener solution to biodiesel production than concentrated H_2SO_4 .

The esterifications of other higher fatty acids such as palmitic acid and stearic acid with methanol were also successfully conducted with the D-glucose-derived sugar catalyst. As depicted in Fig. 2, the yield of fatty acid methyl ester clearly increased with increasing reaction time up to 5 h, and subsequently showed no significant improvement. After 5 h, the yield of the methyl ester

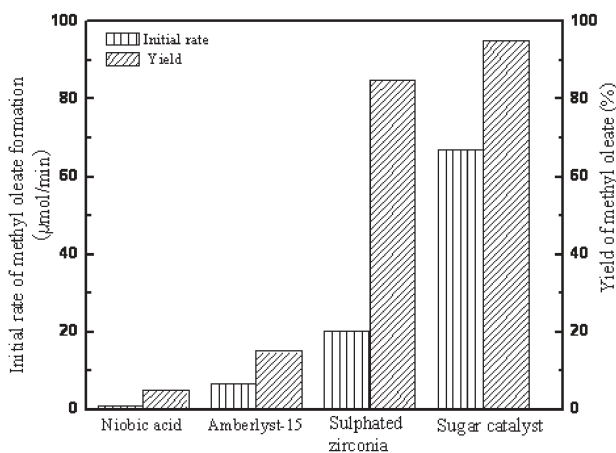


Fig. 1 Initial rate of methyl oleate formation and the yield during esterification of oleic acid by the D-glucose-derived sugar catalyst and other catalysts. Reaction condition: 10 mmol oleic acid; 100 mmol methanol; 0.14 g catalyst; 80 °C; reflux system.

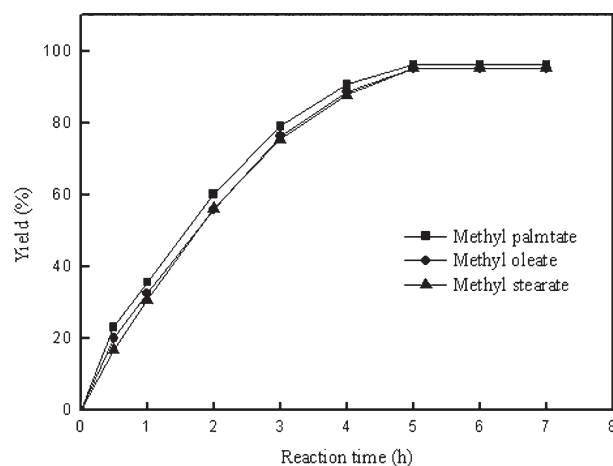


Fig. 2 Esterification of higher fatty acids with methanol catalyzed by the D-glucose-derived sugar catalyst. Reaction condition: 10 mmol palmitic acid, oleic acid or stearic acid; 100 mmol methanol; 0.14 g sugar catalyst; 80 °C; reflux system.

product was high ($\geq 95\%$) for the sugar catalyst-catalyzed esterification of all three higher fatty acids (Fig. 2). Palmitic acid gave slightly faster initial rate of esterification than oleic acid and stearic acid. Among the three fatty acids tested, the initial rate of the esterification decreased slightly with increasing the carbon-chain length of the fatty acids, possibly resulting from the steric hindrance effect of the carbon chains.

Presently one bottleneck for biodiesel production is the high cost of the feedstock. Therefore, the production of biodiesel directly from vegetable oils and greases is obviously uncompetitive. The introduction of waste oils for biodiesel production is, in contrast, very competitive and promising.¹⁶ The D-glucose-derived sugar catalyst was therefore also tested for the production of biodiesel from waste oils with a high acid value (27.8% FFAs). Such high acid-value oils are unsuitable for conversion to biodiesel with alkaline catalysts because the FFAs form unwanted soap byproducts in the presence of alkali. Enzyme catalyzed conversion of such materials is not favourable either, owing to denaturation of the enzymes under acidic conditions. Fig. 3 illustrates the profiles of biodiesel production from waste oils with a high acid value catalyzed by the three typical solid acid catalysts (sulfated zirconia, amberlyst-15 and niobic acid) and the sugar catalyst prepared during this study. A remarkable enhancement in the reactivity and the yield was observed with sugar catalyst as compared with the other solid acid catalysts examined. The D-glucose-derived catalyst afforded a high yield of above 90%.

For evaluation of the operational stability of the sugar catalyst, the catalyst was recovered for further reaction by filtration, extensive washing with *t*-butanol (until no trace of reaction solution was left from the previous esterification), and drying *in vacuo*. It was found that the sugar catalyst still retained a remarkably high proportion (93%) of its original catalytic activity in the methyl oleate formation reaction, even after more than fifty cycles of successive re-use. Thus the sugar catalyst had excellent operational stability.

The physical and chemical properties of the D-glucose-derived sugar catalyst were also investigated. As can be seen in Fig. 4, the X-ray diffraction (XRD) pattern of the sugar catalyst exhibited a

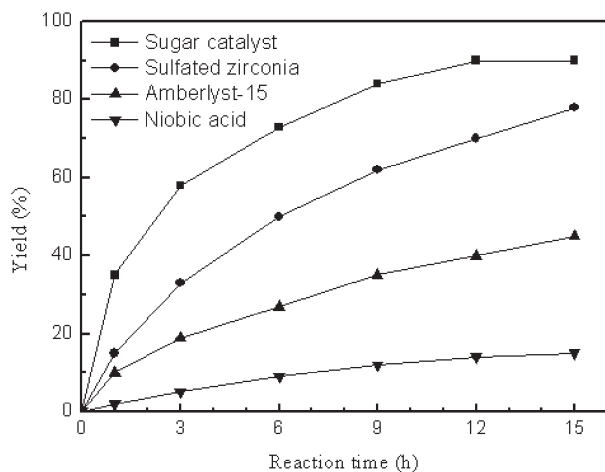


Fig. 3 Profiles of the production of biodiesel from waste oils with a high acid value by the D-glucose-derived sugar catalyst and other solid acid catalysts. Reaction condition: 5.0 g waste oil (27.8% FFAs); 5.54 g methanol; 0.5 g catalyst; 80 °C; reflux system.

broad diffraction peak ($2\theta = 10\text{--}30^\circ$) and a weak diffraction peak ($2\theta = 35\text{--}50^\circ$), which can typically be attributed to amorphous carbon.¹⁴ This indicates that the sugar catalyst had an amorphous structure, which may be important in the catalyst's activity during esterification reactions. In contrast, catalysts prepared by sulfonation of familiar carbon materials such as graphite, carbon black, graphitized carbon fibre, activated carbon and glassy carbon, displayed no catalytic activity in the esterification reaction.¹⁵

Fig. 5 depicts the FT-IR spectra of the sugar catalyst before and after sulfonation. The strong peak at around 1712 cm^{-1} and the weak peak at around 1207 cm^{-1} could be typically assigned to the stretching modes of SO_3H groups which are the "active sites" of the sugar catalyst. The FT-IR spectra clearly demonstrate that the sugar catalyst after sulfonation contains SO_3H groups. In addition, the higher the SO_3H group content in the material, the higher its catalytic activity. Elemental analysis (EA) of the sugar catalyst showed that the sulfur content was 4.7% (by mass) and that the catalyst had the elemental composition of $\text{CH}_{1.14}\text{S}_{0.03}\text{O}_{0.39}$. All sulfur atoms in sulfonated sugar catalysts have previously been

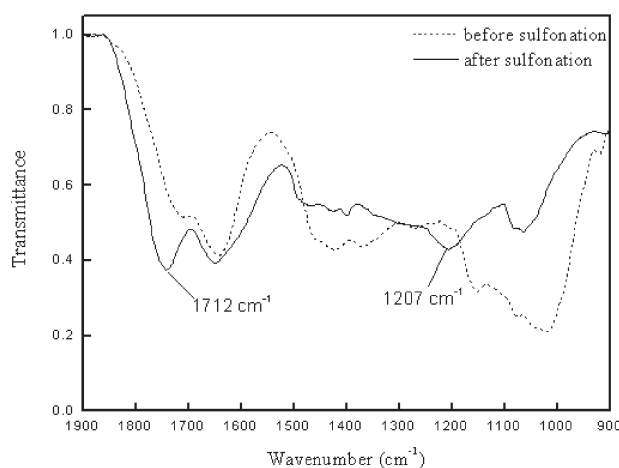


Fig. 5 Comparison of FT-IR spectra of sugar catalyst prepared from D-glucose before and after sulfonation.

shown to be present as SO_3H groups.¹⁵ Thus, the mass content of SO_3H groups was calculated to be about 11.9% based on the sulfur content, and the acid site concentration of the sugar catalyst was calculated to be around 1.5 mmol g^{-1} according to the SO_3H group content. Analysis by means of ultraviolet-visible diffuse reflectance spectroscopy (UV-vis DRS; Fig. S2 in the ESI†) indicated that the acid strength (pK_a) of the sugar catalyst was in the range of -11 to -8 , which is comparable to that of concentrated H_2SO_4 .

Additional information about the sugar catalyst was provided by scanning electron microscopy (SEM) and Brunauer–Emmett–Teller (BET) analysis. As is evident from the SEM image in Fig. S3 (ESI†), the particles of the sugar catalyst reached micrometre dimensions and did not significantly aggregate. The large surface area of the sugar catalyst almost certainly contributes to its catalytic activity. The BET surface area of the sugar catalyst prepared under the conditions described in the ESI† was found to be $4.13 \pm 0.03\text{ m}^2\text{ g}^{-1}$ based on calculations from adsorption isotherms using the standard BET equation, and was much larger than that of other sugar catalysts prepared under different carbonization temperatures and times, as well as with different duration and temperature of sulfonation (data not shown).

The thermal stability of the sugar catalyst was examined by thermogravimetric analysis (TGA) under a flow of air at a heating rate of 10 °C min^{-1} . As shown in Fig. 6, the sugar catalyst before sulfonation displayed a slight weight loss (about 3%) over a temperature range of $25\text{--}380\text{ °C}$, possibly due to the loss of a small amount of water in the H_2SO_4 -untreated catalyst. The catalyst after sulfonation exhibited a marginal weight loss over the temperature range of $25\text{--}275\text{ °C}$, but showed a rapid weight loss between 275 and 325 °C . The sample weight remained almost constant from 325 to 380 °C . The H_2SO_4 -treated sugar catalyst underwent a total weight loss of about 15%, which equals the total content of SO_3H groups (around 11.9%) and water (around 3%). These results clearly indicate that the rapid weight loss of the sugar catalyst upon heating can be attributed to the thermal decomposition of the SO_3H groups that are the active sites of the catalyst, which was confirmed by elemental analysis of the catalyst after heating (data not shown). This conclusion is further supported by

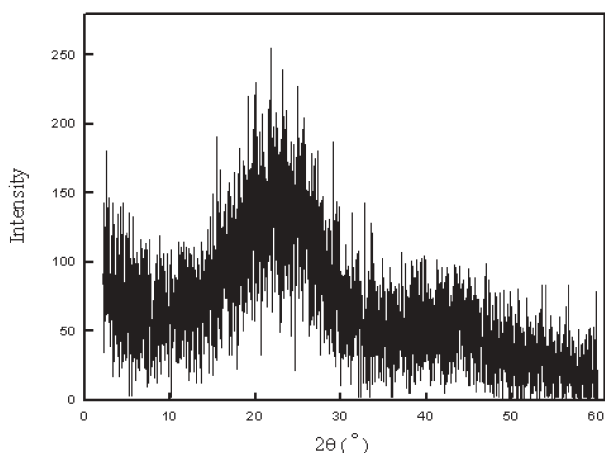


Fig. 4 XRD pattern of sugar catalyst prepared from D-glucose.

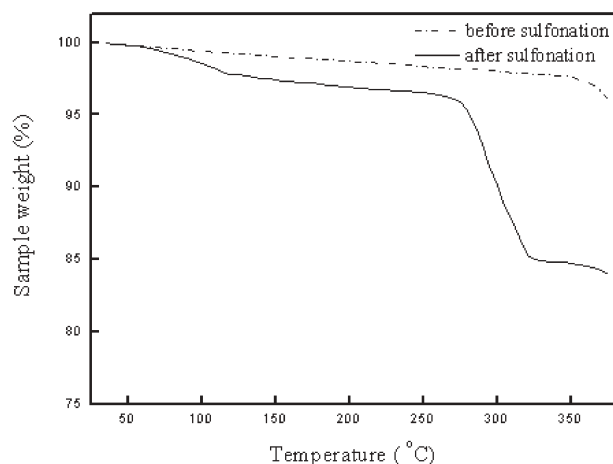


Fig. 6 TGA of sugar catalyst prepared from D-glucose before and after sulfonation.

the observation that the sugar catalyst exhibited no significant esterification activity after being incubated at 275–325 °C for 1 h. Nonetheless, the sugar catalyst that we prepared worked excellently at a temperature as high as 275 °C, while the previously reported H₂SO₄-treated carbon nanotube worked only below 230 °C.¹⁷ In addition, the H₂SO₄-treated carbon nanotube manifested no esterification activity towards higher fatty acids such as oleic acid, palmitic acid and stearic acid, but the sugar catalyst exhibited high esterification activity towards these compounds (Fig. 2). These results clearly indicate that the sugar catalyst is superior to the H₂SO₄-treated carbon nanotube with respect to thermal stability and esterification activity towards long-chain fatty acids.

In summary, our results support the conclusions that sugar catalysts have much higher catalytic activity than other solid acid catalysts and as such are very promising to replace sulfuric acid and other catalysts as a green catalyst for efficient production of biodiesel from higher fatty acids and especially waste oils with a high acid value. In addition, it is possible that environmentally benign, recyclable sugar catalysts may find wide applications in reactions where concentrated H₂SO₄ or other acids are currently used as catalysts.

Notes and references

- (a) R. Sridharan and I. M. Mathai, *J. Sci. Ind. Res.*, 1974, **33**, 178; (b) B. Freedman, E. H. Pryde and T. L. Mounts, *J. Am. Oil Chem. Soc.*, 1984, **61**, 1638; (c) B. Freedman, R. Q. Butterfield and E. H. Pryde, *J. 11 Am. Oil Chem. Soc.*, 1986, **63**, 1375; (d) U. Schuchardt, R. Sercheli and R. M. Vargas, *J. Braz. Chem. Soc.*, 1998, **9**, 199; (e) H. Fukuda, A. Kondo and H. Noda, *J. Biosci. Bioeng.*, 2001, **92**, 405; (f) Van Gerpen, *Fuel Process. Technol.*, 2005, **86**, 1097; (g) A. J. Kinney and T. E. Clemente, *Fuel Process. Technol.*, 2005, **86**, 1137.

- (a) M. J. Nye, T. W. Williamson, S. Deshpande, J. H. Schrader, W. H. Snively, T. P. Yurkewich and C. L. French, *J. Am. Oil Chem. Soc.*, 1983, **60**, 1598; (b) K. Liu, *J. Am. Oil Chem. Soc.*, 1994, **71**, 1179; (c) M. Canakci and J. Van. Gerpen, *Trans. ASAE*, 1999, **42**, 1203; (d) M. Canakci and J. Van. Gerpen, *Trans. ASAE*, 2001, **44**, 1429; (e) M. Canakci and J. Van. Gerpen, *Trans. ASAE*, 2003, **46**, 945; (f) E. Lotero, Y. Liu, D. E. Lopez, A. Suwannakaran, D. A. Bruce and J. G. Goodwin, *Ind. Eng. Chem. Res.*, 2005, **44**, 5353.
- (a) L. A. Nelson, T. A. Fogia and W. N. Marmer, *J. Am. Oil Chem. Soc.*, 1996, **73**, 1191; (b) B. Selmi and D. Thomas, *J. Am. Oil Chem. Soc.*, 1998, **75**, 691.
- (a) Y. Shimada, Y. Watanabe, T. Samukawa, A. Sugihara, H. Noda, H. Fukuda and Y. Tominaga, *J. Am. Oil Chem. Soc.*, 1999, **76**, 789; (b) V. Dossat, D. Combes and A. Marty, *Enzyme Microb. Technol.*, 1999, **25**, 194; (c) M. Kaieda, T. Samukawa, T. Matsumoto, K. Ban, A. Kondo, Y. Shimada, H. Noda, F. Nomoto, K. Ohtsuka, E. Izumoto and H. Fukuda, *J. Biosci. Bioeng.*, 1999, **88**, 627; (d) Y. Watanabe, Y. Shimada, A. Sugihara, H. Noda, H. Fukuda and Y. Tominaga, *J. Am. Oil Chem. Soc.*, 2000, **77**, 355; (e) G. Steinke, R. Kirchhoff and K. D. Mukherjee, *J. Am. Oil Chem. Soc.*, 2000, **77**, 361; (f) M. Iso, B. X. Chen, M. Eguchi, T. Kudo and S. Shrestha, *J. Mol. Catal. B: Enzym.*, 2001, **16**, 53; (g) O. Kose, M. Tuter and H. A. Aksoy, *Bioresour. Technol.*, 2002, **83**, 125.
- J. H. Clark, *Acc. Chem. Res.*, 2002, **35**, 791.
- T. Okuhara, *Chem. Rev.*, 2002, **102**, 3641.
- W. M. Van Rhijn, D. E. De Vos, B. F. Sels, W. D. Bossaert and P. A. Jacobs, *Chem. Commun.*, 1998, 317.
- M. A. Harmer, W. E. Farneth and Q. Sun, *Adv. Mater.*, 1998, **10**, 1255.
- A. A. Kiss, A. C. Dimian and G. Rothenberg, *Adv. Synth. Catal.*, 2006, **348**, 75.
- M. A. Harmer and Q. Sun, *Appl. Catal., A*, 2001, **221**, 45.
- G. D. Yadav and J. J. Nair, *Microporous Mesoporous Mater.*, 1999, **33**, 1.
- M. Hara, T. Yoshida, A. Takagaki, T. Takata, J. N. Kondo, S. Hayashi and K. Domen, *Angew. Chem., Int. Ed.*, 2004, **43**, 2955.
- M. Toda, A. Takagaki, M. Okamura, J. N. Kondo, S. Hayashi, K. Domen and M. Hara, *Nature*, 2005, **438**, 178.
- N. Tsubouchi, C. B. Xu and Y. Ohtsuka, *Energy Fuels*, 2003, **17**, 1119.
- M. Okamura, A. Takagaki, M. Toda, J. N. Kondo, K. Domen, T. Tatsumi, M. Hara and S. Hayashi, *Chem. Mater.*, 2006, **18**, 3039.
- (a) R. Alcantara, J. Amores, L. Canoira, E. Fidalgo, M. J. Franco and A. Navarro, *Biomass Bioenergy*, 2000, **18**, 515; (b) A. V. Tomasevic and S. S. Siler-Marinkovic, *Fuel Process. Technol.*, 2003, **81**, 1; (c) Y. Watanabe, P. Pinsirodom, T. Nagao, T. Kobayashi, Y. Nishida, Y. Takagi and Y. Shimada, *J. Am. Oil Chem. Soc.*, 2005, **82**, 825; (d) H. Wu, M. H. Zong and W. Y. Lou, *Chin. J. Catal.*, 2005, **25**, 903; (e) Z. F. Chen, H. Wu and M. H. Zong, *Chin. J. Catal.*, 2006, **27**, 146.
- F. Peng, L. Zhang, H. G. Wang, P. Lv and H. Yu, *Carbon*, 2005, **43**, 2405.

Combining pot, atom and step economy (PASE) in organic synthesis. Synthesis of tetrahydropyran-4-ones†

Paul A. Clarke,^{*a} Soraia Santos^a and William H. C. Martin^b

Received 29th January 2007, Accepted 15th February 2007

First published as an Advance Article on the web 27th February 2007

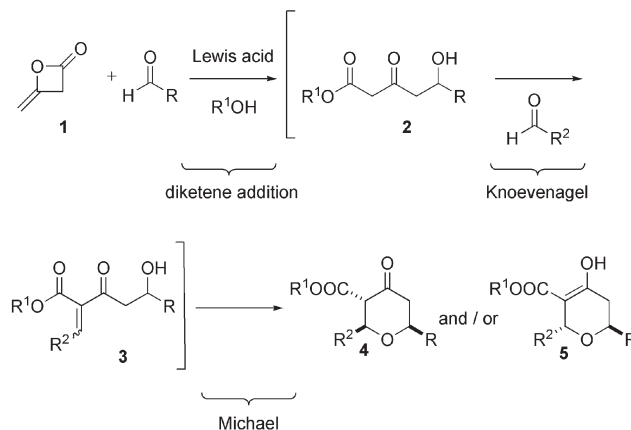
DOI: 10.1039/b700923b

The combination of pot, atom and step economy (PASE) in the synthesis of organic molecules of medium complexity can lead to a significant 'greening' of a synthetic route. This is demonstrated by the synthesis of highly substituted tetrahydropyran-4-ones and is quantified by a series of recognised metrics, which demonstrate the efficiency of combining PASE over conventional synthetic strategies.

For several years synthetic chemists have been familiar with the concept of step economy,¹ which is the drive to increase the brevity and efficiency of a synthesis by a reduction in the number of synthetic steps. Traditionally, this has manifested itself in the attempt to limit the use of protecting group manipulations. A step economic synthesis has the potential to reduce the number and amount of reagents employed by reducing the number of synthetic steps. This should also lead to an increase in chemical yield of the desired product. Trost has introduced synthetic chemists to the idea of atom economy,² which is the concept that every atom of each reagent being used is included in the desired product of the reaction. While this concept does address the issue of waste in the form of reaction by-products, it does not address the fundamental problem of how to eliminate the solvent and the waste generated by any work-up or product isolation and purification procedure. These factors are addressed by the concept of pot economy, which is the drive to complete as many sequential synthetic transformations in the same reaction vessel without the need for work-up and product isolation between successive synthetic steps. The ultimate aim would be to complete an entire multi-step, multi-reaction synthesis in a single pot. A pot economic synthesis would, therefore, reduce dramatically the amount of solvents used in the synthesis, solvents used in work-up and product isolation, solvents used in product purification, silica gel or related substances used in chromatographic purification, contaminated aqueous waste generated from cleaning equipment and glassware, etc. While individually each of these strategies have the potential to 'green' organic synthesis, a more significant reduction in waste (and cost) could be achieved by combining all three of these concepts to produce a pot, atom and step economic (PASE) synthetic route. A PASE synthesis has the potential to (i) reduce the number and amount of reagents employed by reducing the number of synthetic

steps, (ii) reduce the waste inherent in the generation of reaction by-products and (iii) to reduce the solvent and associated waste caused by many work-up and product isolation procedures along the synthetic route. Indeed, process chemists in industry have been striving for such sustainable routes to desired molecules for several years, on the basis of cost. Interestingly, this commercial drive for increased efficiency (and lower costs) by adoption of PASE synthesis embodies principles 1, 2, 5 and 8 of the twelve principles of green chemistry.³

However, it is a fact that even though process chemists in industry are seeking to adopt more sustainable synthetic routes, organic chemists in academia have been very slow to embrace these ideas. After discussions with process chemists, we were interested by the possibility of applying these ideas to our own work. The area which was highlighted by these discussions was our syntheses of highly substituted tetrahydropyran-4-ones (THPs), as these are present in a vast number of biologically and pharmaceutically important molecules. We have had prior experience in the construction of THP rings and THP containing natural products.⁴ However, in this previous work we were not concerned with issues of sustainability and a reduction of the environmental impact. For example, we regularly used two equivalents of *bis*-silylenol ethers in our syntheses. This obviously led to the generation of 4 equivalents of silanol waste and the need to separate this from the product. In order to circumvent this we developed an alternative strategy for the synthesis of THP units, still incorporating our original ideas, but now taking account of the principles of pot, atom and step economy as exemplified in the principles of green chemistry.



Scheme 1 PASE Synthesis of THP rings.

^aDepartment of Chemistry, University of York, Heslington, York, UK YO10 5DD. E-mail: pac507@york.ac.uk; Fax: +44 1904 432516; Tel: +44 1904 432614

^bSchool of Chemistry, University of Nottingham, University Park, Nottingham, UK NG7 2RD

† Electronic supplementary information (ESI) available: Full experimental procedures, spectroscopic data and HPLC data. See DOI: 10.1039/b700923b

Our new 'greener' strategy is outlined in Scheme 1. In practice, for PASE to be realised it was important that the three individual reactions, Lewis acid promoted addition of diketene to an aldehyde,⁵ Knoevenagel condensation and intramolecular Michael reaction, all follow on from each other in one pot—thus achieving pot and step economy. Atom economy is achieved as all of the atoms of the reagents (with the exception of one equiv. of H₂O and the Lewis acid catalyst) are all included in the desired THP product.

In our initial investigations, we chose to use TiCl₄ as the Lewis acid as it had been shown to promote both the addition of diketene to aldehydes,⁵ as well as the Knoevenagel and Michael reactions.⁴ As this initial reaction (**1** → **2**) would generate the acyl chloride of the δ -hydroxy- β -ketoester, we opted to add an alcohol (MeOH) to the reaction mixture in order to form the ester and also introduce another potential site of diversity. We rationalised that after promoting the addition of diketene to the first aldehyde, the Lewis acid would be capable of promoting the Knoevenagel reaction of a second, different, aldehyde to the α -position of the β -ketoester, followed by an intramolecular Michael reaction. To our delight, when the above sequence of events was carried out, THP products were formed as a mixture of 2,6-*cis* (**4**) and 2,6-*trans* (**5**) diastereomers in good to excellent yields (Table 1).

We were somewhat disappointed by the low diastereoselectivity of the reaction. Previous experience in THP synthesis *via* an intramolecular oxy-Michael reaction had taught us that the isomerisation of the double bond was very facile, and that the Michael reaction was reversible and under thermodynamic control when TiCl₄ was employed as a Lewis acid.⁴ Unfortunately, a number of other Lewis acids investigated failed to promote the reaction at all. We therefore decided to buffer the second stage of the reaction in an attempt to prevent the Lewis acid catalysed retro-Michael reaction. The buffer of choice was found to be pyridine, which suppressed the retro-Michael reaction and led

Table 1 Formation of THP rings: PASE synthesis method A General method for the PASE synthesis of THPs **4a–i** and **5a–i**. Method A. To a stirred solution of diketene (0.1 ml, 1.30 mmol) and aldehyde (0.72 mmol) in CH₂Cl₂ (2 ml) at –78 °C, was added TiCl₄ (80 μ l, 0.72 mmol). After 5 min, dry methanol (117 μ l, 2.88 mmol) was added to the dark red mixture. The reaction was stirred for 30 min at –30 to –20 °C before it was again cooled to –78 °C, when the second aldehyde (0.87 mmol) was added. The reaction mixture was warmed back to –20 °C and stirred at this temperature for 16 h. After dilution with ether, the mixture was washed with a 20% (w/v) aqueous solution of citric acid (3 \times 30 ml), brine (2 \times 40 ml), dried (MgSO₄) and concentrated *in vacuo*. Purification by flash chromatography (Petrol–EtOAc–Pyridine: 200 : 1 : 2 to 100 : 4 : 2) gave the tetrahydropyran products. Full experimental procedures, spectroscopic data and HPLC data are included in the ESI.

Compound	R	R ²	Ratio (4 : 5) ^a	Yield ^b (%)
a	Ph	<i>i</i> Pr	1.5 : 1	87
b	<i>i</i> Pr	Pr	2.1 : 1	72
c	<i>i</i> Pr	Ph	0.6 : 1	70
d	Cyhex	Ph	0.6 : 1	73
e	Ph	Ph	1 : 1	79
f	Ph	<i>p</i> -MeOC ₆ H ₄	1 : 1	78
g	C ₈ H ₁₇	Ph	1 : 1	96
h	Pr	CH ₂ OBn	4.2 : 1	58
i	<i>i</i> Pr	(CH ₂) ₂ CH=CH ₂	1.2 : 1	77

^a As determined by 400 MHz ¹H NMR of the crude reaction mixture. ^b After flash column chromatography.

Table 2 Formation of THP rings: PASE synthesis: method B

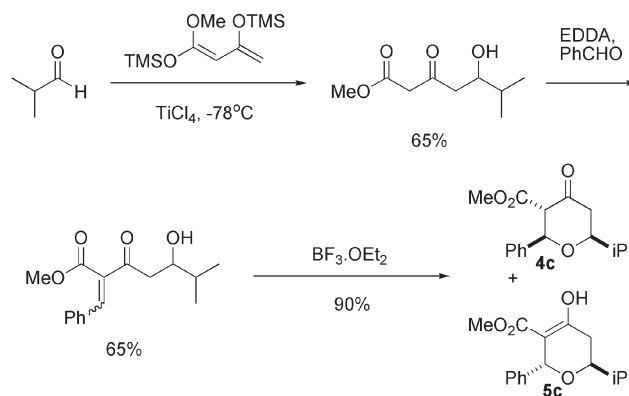
Compound	R	R ^{2a}	Ratio (4 : 5) ^b	Yield ^c (%)
a	Ph	<i>i</i> Pr	5.7 : 1	81
b	<i>i</i> Pr	Pr	4.7 : 1	81
c	<i>i</i> Pr	Ph	2 : 1	84
d	Cyhex	Ph	1.6 : 1	83
e	Ph	Ph	1.7 : 1	89
f	Ph	<i>p</i> -MeOC ₆ H ₄	3 : 1	39
g	C ₈ H ₁₇	Ph	1.5 : 1	47
h	Pr	CH ₂ OBn	4.8 : 1	76 ^d
i	<i>i</i> Pr	(CH ₂) ₂ CH=CH ₂	4.2 : 1	83

^a Pyridine (1 eq.) added at the introduction of the second aldehyde.

^b As determined by 400 MHz ¹H NMR of the crude reaction mixture. ^c After flash column chromatography. ^d 2.4 eq. of benzyloxyacetaldehyde used.

predominantly to the formation of the 2,6-*cis* diastereomer **4** (Table 2).

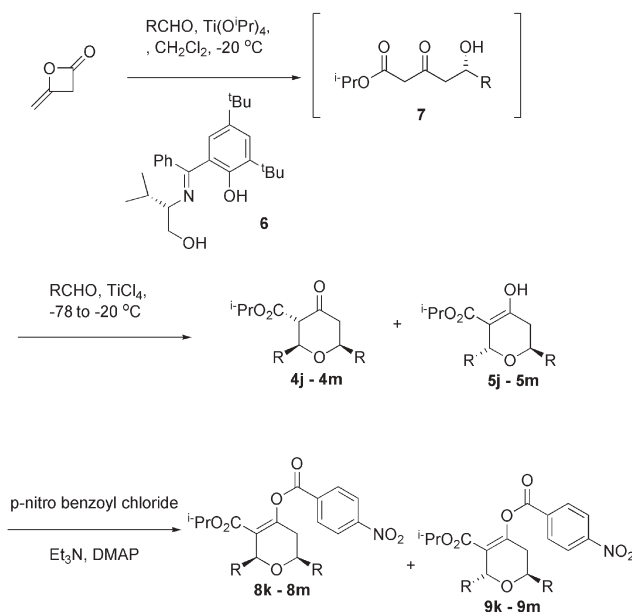
In order to assess the increased efficiency of our new PASE synthesis of these THPs over their traditional stepwise synthesis, we conducted a stepwise synthesis of **4c/5c** according to Scheme 2, and compared two sets of recognised and relevant metrics,⁶ namely the mass intensity⁷ and the atom economy² of the traditional route to the PASE route. These data are shown in Table 3. The mass intensity (MI) is defined as the total mass used/mass of product (kg kg^{–1}) and the atom economy is defined as (FW product/FW of all reagents used) \times 100%. The mass intensity of the traditional route is therefore calculated to be 1.0790 kg/2.45 \times 10^{–4} kg = 4404 kg kg^{–1}, while the traditional synthesis is 29% atom economic. While the mass intensity of the PASE route is only 0.38 kg/4.17 \times 10^{–4} kg = 911 kg kg^{–1}, and the atom economy has



Scheme 2 A traditional synthesis of THP rings **4c/5c**.

Table 3 Comparison of traditional vs. PASE synthesis

Metric	Traditional	PASE
Steps	3	2
Pots	3	1
Yield (%)	38	70
Reaction solvent/mL	54	6
Work-up solvent/mL	260	70
Aqueous/mL	280	80
Drying agent/g	6	3.9
Silica gel/g	19	15
Chromatography solvent/mL	450	315
Reagents/mmol	19.2	19.8



Scheme 3 Asymmetric PASE synthesis of THP rings.

risen significantly to 90%. This clearly shows that combining pot, atom and step economy in general academic organic synthesis can lead to a reduced environmental impact and increased efficiency of a synthesis.

However, one area of waste which has yet to be addressed is that of enantiomeric waste. An increasing number of potential drug candidates are now required as single enantiomers, and the use of a racemic synthesis, no matter how pot, atom and step economic, inevitably leads to 50% of the final product mass being an unwanted by-product, and therefore classified as waste. It is possible to envisage solving this problem with the development of a catalytic asymmetric reaction. Our preliminary studies in this area focused on adapting the $\text{Ti}(\text{O}^i\text{Pr})_4$ promoted asymmetric addition of diketene to aldehydes developed by Oguni and Hayashi.⁸

As we had previously demonstrated that the chiral centre installed in the aldol reaction is configurationally stable under cyclisation conditions,⁴ we were confident that if we could form the aldol adducts in enantioenriched form then we would be able to form THPs with at least that level of enantioselectivity. A set of aldehydes were submitted to the conditions reported by Hayashi in the presence of enantiopure Schiff's base **6**. Before the addition of the second aldehyde, an aliquot was removed to determine the % e.e. of the adduct. The remainder of the reaction mixture was treated with a further equivalent of aldehyde and TiCl_4 at -78°C and allowed to cyclise to form the THP products (Scheme 3, Table 4).

As conditions could not be found to assay the % e.e. of **4k–m** and **5k–m** directly due to the lack of chromophores, these pyrans had to be converted into the corresponding enol *p*-nitrobenzoates **8k–m** and **9k–m**. As can be seen from Table 4, the % e.e. of the products ranged from moderate (**9l**) through to excellent (**4j** and **5j**), and there is no appreciable erosion of the enantioselectivity in the Lewis acid promoted Knoevenagel–Michael reaction.

Table 4 Asymmetric PASE synthesis of THP rings

Compound	R	% e.e. (7) ^a	Ratio (4 : 5) ^b	% e.e. pyran ^c
j	Ph	82	1 : 2	92 (4j) ^{a,d} >95 (5j) ^d
k	Pr	62	1 : 1	59 (9k) ^e
l	Cyhex	n/d ^f	1 : 0.4	47 (9l) ^e
m	<i>i</i> Pr	59	1 : 0.3	59 (9m) ^e

^a Determined by 400 MHz ^1H NMR doped with chiral shift reagent (see ESI for full details). ^b As determined by 400 MHz ^1H NMR of the crude reaction mixture. ^c Determined by HPLC analysis on CHIRACEL OD–H column (see ESI for full details). ^d These pyrans were crystalline and the difference in % e.e. between them and **7j** is attributed to enrichment of the major enantiomer during crystallisation. ^e % e.e. of the diastereomers **8k–8m** could not be assessed by either 400 MHz ^1H NMR doped with chiral shift reagent or HPLC analysis. Precedent suggests (ref. 4) that the % e.e. of these diastereomers is the same as that of **9k–9m**. ^f Could not be determined by 400 MHz ^1H NMR doped with chiral shift reagents.

In conclusion, we have successfully applied the principles of green chemistry, specifically those of pot, atom and step economy to redesign a synthetic route to highly substituted THPs. The increased sustainability of this route has been quantified by the use of metrics such as mass intensity and atom economy, and it was shown to be significantly 'greener' than our original synthetic route. In addition to this, we have applied these same principles to develop an asymmetric variation of our pot, atom and step economic synthesis of THPs, which formed the desired products in moderate to excellent % e.e. Work is now underway at increasing the environmental benefits of this approach even further and applying these ideas to the synthesis of other molecular families.

We thank the EPSRC for funding under the Greener Chemistry Initiative (EP/C523970/1), the EPSRC Mass Spec. Service, Swansea for accurate mass determinations and Prof. Martyn Poliakoff (Nottingham) and Dr David Lathbury (AZ) for useful discussions.

Notes and references

- (a) P. A. Wender, F. C. Bi, G. G. Gamber, F. Gosselin, R. D. Hubbard, M. J. C. Scanio, R. Sun, T. J. Williams and L. Zhang, *Pure Appl. Chem.*, 2002, **74**, 25; (b) P. A. Wender, S. T. Handy and D. L. Wright, *Chem. Ind. (London)*, 1997, 765; (c) P. A. Wender and B. L. Miller, *Organic Synthesis: Theory and Applications*, ed. T. Hudlicky, JAI, Greenwich, 1993, vol. 2, pp 27–66.
- (a) B. M. Trost, *Science*, 1991, **254**, 1471; (b) B. M. Trost, *Angew. Chem., Int. Ed. Engl.*, 1995, **34**, 259.
- P. T. Anastas and J. C. Warner, *Green Chemistry – Theory and Practice*, Oxford University Press, Oxford, 1998.
- (a) P. A. Clarke, W. H. C. Martin, J. M. Hargreaves, C. Wilson and A. J. Blake, *Chem. Commun.*, 2005, 1061; (b) P. A. Clarke, W. H. C. Martin, J. M. Hargreaves, C. Wilson and A. J. Blake, *Org. Biomol. Chem.*, 2005, **3**, 3551; (c) P. A. Clarke and W. H. C. Martin, *Tetrahedron Lett.*, 2004, **45**, 9061.
- T. Izawa and T. Mukaiyama, *Chem. Lett.*, 1975, 161.
- A. D. Curzons, D. J. C. Constable, D. N. Mortimer and V. L. Cunningham, *Green Chem.*, 2001, **3**, 1.
- (a) R. A. Sheldon, *Chem. Ind. (London)*, 1992, 903; (b) R. A. Sheldon, *Chem. Ind. (London)*, 1997, 12.
- (a) M. Hiyashi, T. Inouse and N. Oguni, *J. Chem. Soc., Chem. Commun.*, 1994, 341; (b) M. Hayashi, T. Inouse, Y. Miyamoto and N. Oguni, *Tetrahedron*, 1994, **50**, 4385; (c) M. Hiyashi, K. Tanaka and N. Oguni, *Tetrahedron: Asymmetry*, 1995, **6**, 2833; (d) M. Hayashi, N. Nakamura and K. Yamashita, *Tetrahedron*, 2004, **60**, 6777.

The same and not the same. Similarities and differences in the resolution of *trans*-chrysanthemic acid of industrial origin by the enantiomers of some *threo*-1-aryl-2-dimethylamino-1,3-propanediols†

Goffredo Rosini,^{*a} Claudia Ayoub,^b Valerio Borzatta,^b Emanuela Marotta,^a Andrea Mazzanti^a and Paolo Righi^a

Received 30th October 2006, Accepted 5th January 2007

First published as an Advance Article on the web 25th January 2007

DOI: 10.1039/b615785h

The enantiomers of *threo*-dimethylamino-1-[4-(methylthio)phenyl]propane-1,3-diol (MTDP) were found to be effective resolving agents for *trans*-chrysanthemic acid (*trans*-ChA) on an industrial scale. (1*S*,2*S*)-(+)-MTDP and (1*R*,2*R*)-(–)-MTDP were revealed to be “blind” towards the enantiomers of *cis*-ChA. They work well on racemic and/or scalemic *trans/cis* mixtures of industrial production and are used in a stoichiometric amount with respect to the enantiomer of *trans*-ChA to be collected. Isopropyl ether is the solvent of choice, and it does not need the presence of co-solvents such as methanol to promote nucleation and crystal growth of the *n* salts as previously reported for *threo*-dimethylamino-1-[4-(nitro)phenyl]propane-1,3-diol (DMAD) enantiomers. X-ray crystal structures of the *n* salts of *trans*-ChA and MTDP revealed the peculiar features of two pseudopolymorphs. MTDP enantiomers are low cost, non-toxic, safe, and easily available from important precursors of thiamphenicol through a single straightforward reaction. After the resolution, they can be recovered almost quantitatively and reused without any loss of their chiral integrity. Similarities and differences of these resolving agents for *trans*-ChA with respect the behaviour of the enantiomers of DMAD and of the enantiomers of the parent compound, 1-phenyl-2-dimethylamino-1,3-propane-diol (DMPP), are shown in a comparative analysis of their performances.

Introduction

Due to the high economic value of pyrethroid insecticides,¹ the last thirty years have seen important industrial and academic works devoted to the synthesis of both *trans*- and *cis*-2,2-dimethyl-3-(2-methylprop-2-enyl)cyclopropane carboxylic acid (chrysanthemic acid, ChA), Fig. 1.

They are important starting materials for the preparation of a multitude of natural and synthetic pyrethroid insecticides, widely used in crop protection and in the public health sector for the control of many kinds of undesired insects, mites and spiders. Among the main features of these compounds are the low mammalian toxicity, the biodegradability and the high activities.

Nowadays several firms prepare many hundred tonnes of racemic chrysanthemic acid by an efficient copper catalysed carbene insertion reaction² of the ethyl diazoacetate on 2,5-dimethyl-2,4-hexadiene, producing³ esters of racemic mixtures of *trans*- and *cis*-chrysanthemic acid in ratios ranging from 65 : 35 to 9 : 1. Notwithstanding the use of toxic and hazardous ethyl diazoacetate, this process allows a great atom economy.

A safer, but more expensive process,⁴ has been developed more recently. This approach favoured the production of the more stable *trans*-ChA esters affording mixtures with a *trans/cis* ratio higher than 95%. Saponification and acidic treatment provide the desired mixtures of acids ready to be used in the preparation of racemic pyrethroids. More recent developments of the field have led to a new generation of synthetic pyrethroids with greater insecticidal activity, including (*S*)-bioallethrin, permethrin, and deltamethrin, and enantiopure *trans*- and *cis*-chrysanthemic acids are needed for their syntheses.

The catalytic asymmetric synthesis through a one-step process⁵ would be the most practical and elegant way for the

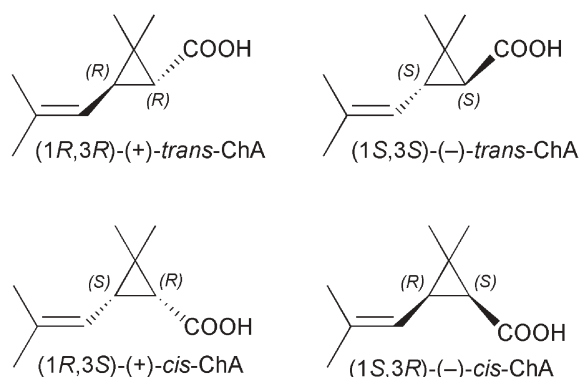
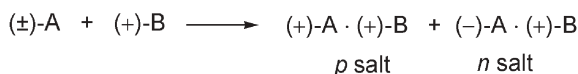


Fig. 1 Stereoisomers of chrysanthemic acid.

^aDipartimento di Chimica Organica “A. Mangini”, Alma Mater Studiorum – Università di Bologna, Viale del Risorgimento 4, Bologna, 40136, Italy. E-mail: goffredo.rosini@unibo.it; Fax: +39 051 20 93654; Tel: +39 051 20 93640

^bEndura SpA, Viale Pietramellara 5, Bologna, 40131, Italy

† Electronic supplementary information (ESI) available: Characterisation data of the salts and crystallographic data. See DOI: 10.1039/b615785h



Scheme 1 Resolution of a racemic acid (A) with an enantiopure base (B).

preparation of *trans* and *cis* chrysanthemic acid. Until now, an efficient, practical and selective asymmetric catalyst for the cyclopropane ring formation of (+)-*trans*-ChA on industrial scale has not emerged; scalemic mixtures of both diastereomers are obtained with important limits (expensive catalysts, low reaction temperature, high dilution, bulky and chiral alcohols for diazoacetate ester, low TONs, *etc.*). Frequently, to increase diastereo- and enantiomeric purity, further purification is needed.⁶ Though the progress in the field of asymmetric synthesis⁷ during the last two decades is indubitable and impressive,⁸ the optical resolution⁹ of racemic acids and bases *via* formation¹⁰ of diastereomeric *p* and *n* salts¹¹ (Scheme 1), and their separation by crystallization, is still the preferred route in the preparation of a vast majority of highly enantiomeric pure compounds required for the manufacture of pharmaceuticals and agrochemicals.

This methodology is the preferred option particularly when, as in the case of chrysanthemic acid, the undesired stereoisomer, may be recycled. It is also important to mention that during the “bench to market” route of a product, time is the most important factor at the *discovery stage*, and at the *early development stage*, whereas at *full development stage* and, with more emphasis, at the *production stage*, cost is a major concern and scale up feasibility is an absolute requisite. Among the reasons for the preference for the “separation of diastereoisomeric *n* and *p* salts” is that the crystallization techniques, at the industrial scale, are more economical and scalable than any other method and, in general, no complex and expensive equipment is necessary.

From the outset the aim of our work was to develop a practical and efficient procedure to prepare both the enantiomers of *trans*-ChA with a high degree of enantiomeric purity and free of the *cis*-isomers, starting from racemic ChA mixtures of industrial origin (ChA is currently sold in three different *trans/cis* ratios: 65/35, 80/20 and 92/8). Moreover, having in mind an industrial application of the procedure, our main concern was the development of a process according to the principles of *green chemistry*.¹² Therefore, we needed an easily available, low cost, non-toxic and safe resolving agent able to effect a sharp chiral discrimination among the enantiomers of the *trans*-ChA. A further, often understated, requirement was that, in order to simplify recycling and reuse, the process should work in a single solvent system.¹³

We undertook a study by using a variety of *threo*-2-dimethylamino-1-aryl-1,3-propanediols (Fig. 2) and several solvents. Here we report the main results of our efforts.

Results and discussion

Until now, the most efficient process¹⁴ to resolve *trans*-ChA is the one developed by Roussel-Uclaf,^{1d} that makes use of (1*R*,2*R*)-(–)-DMAD, a derivative of the base of chloramphenicol. When used with in a *i*-Pr₂O/MeOH mixed solvent

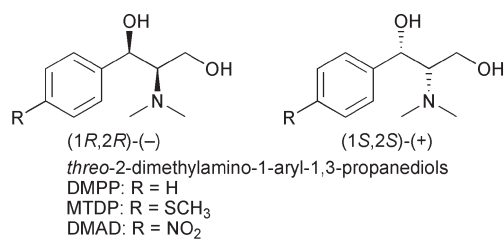


Fig. 2 Enantiomers of 2-dimethylamino-1-aryl-1,3-propanediols.

system, this base effects a clean precipitation of the *n* salt of (1*R*,3*R*)-(+)-*trans*-ChA, the natural enantiomer. Fogassy¹⁵ and co-workers found that in this resolution process, methanol is incorporated into the crystals of the less soluble *n* salt, in a non-stoichiometric amount and postulated that its role was to promote nucleation and crystal growth.

Recently, we have disclosed¹⁶ that DMPP enantiomers (Fig. 2) form *p*₁*n*₁ salts¹⁷ with *trans*-ChA. This peculiarity was exploited for the first time to effect: (a) the diastereomeric separation of racemic *trans*-ChA from racemic *cis*-isomer, and (b) the recovery of the excess enantiomer from scalemic mixtures of *trans*-ChA (Fig. 3). In both these separations the *p*₁*n*₁ salt acts as a “sequesterant” of racemic *trans*-ChA. Both these separations work in *i*-Pr₂O and require the minimum amount of DMPP, that is just that stoichiometric to the *trans*-ChA racemate contained in the starting mixture.

*p*₁*n*₁ Salts, by sequestering racemates, may turn out to be important and cheap tools to furnish enantiomerically pure substances when other methods fail. However, as efficient and practical these protocols may be, they are not the best answer to the call for a better methodology in resolving the enantiomers of *trans*-ChA working with racemic mixtures containing both the *trans* and the *cis* isomers.

This main goal was achieved by using the enantiomers of *threo*-dimethylamino-1-[4-(methylthio)phenyl]propane-1,3-diol¹⁸ (MTDPP, Fig. 2) as resolving agents, working in *i*-Pr₂O alone as solvent, and with the stoichiometric amount of the base, that is 0.5 equivalents with respect to the racemic *trans*-ChA observed in the mixture by GC analyses. The early experiments (Fig. 4) were carried out using racemic *trans*-ChA obtained from 80 : 20 *trans/cis* mixtures and freed from the *cis*-isomer through the procedure recently reported.¹⁶

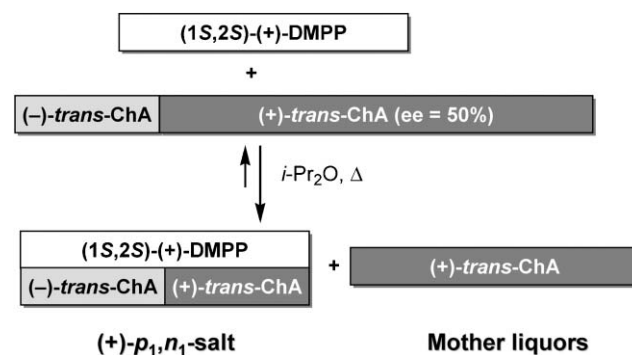


Fig. 3 Recovery of the excess enantiomer from an enantiomerically enriched mixture of *trans*-ChA through *p*₁*n*₁ salt formation.

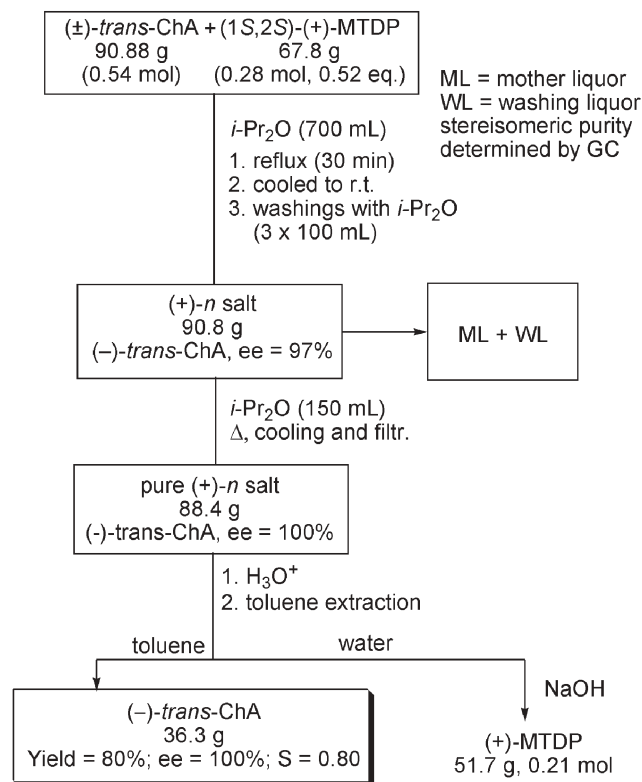


Fig. 4 Resolution of (±)-trans-chrysanthemic acid: the recovery of (–)-trans-ChA.

Mixing of racemic *trans*-ChA with half an equivalent of (1*S*,2*S*)-(+)-MTDP in refluxing *i*-Pr₂O produced the precipitation of the (+)-*n* salt (mp 138–140 °C; [α]_D +10.7). Upon acidic treatment and extraction, these solids furnished (–)-*trans*-ChA (yield = 80.0%; ee = 97%) with a good *S* parameter¹⁹ (*S* = 0.77). If needed, stereoisomeric purity of this *n* salt can be further improved by digestion in refluxing *i*-Pr₂O. The recovery of (1*S*,2*S*)-(+)-MTDP was accomplished by treating acidic waters with 10% aq. NaOH solution. Almost all the base precipitated as a white solid that was easily recovered by filtration. If needed, extraction with toluene allows a quantitative recovery of the base.

Combined mother and washing liquors were directly treated according to the procedure depicted in Fig. 5 to obtain scalemic (+)-*trans*-ChA (ee = 73%). Alkali addition to the aqueous layer allowed the recovery of a residual amount of (1*S*,2*S*)-(+)-MTDP.

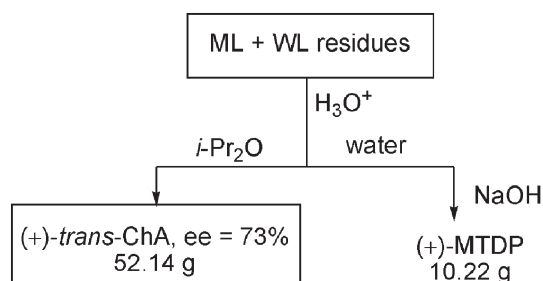


Fig. 5 The recovery of enriched (+)-*trans*-ChA.

The dextrorotating ChA enantiomer can now be recovered through two alternative routes: (a) sequestering the 27% of racemate through formation of the *p*₁,*n*₁ salt¹⁶ with (1*S*,2*S*)-(+)-DMPP (see Fig. 3), thus freeing the 73% excess (+)-*trans*-ChA; or (b) by recovering all the residual 86.5% of the (+)-*trans*-ChA present in the scalemic mixture with ee = 73%, through the formation of (–)-*n* salt by reaction with (1*R*,2*R*)-(–)-MTDP. Fig. 6 summarizes the results obtained with this latter approach that gave (+)-*trans*-ChA (yield = 90.7%; ee = 98%; *S* = 0.89).

Of course, on the base of yield and resolving efficiency (*S*) considerations, the order of use of MTDP enantiomers can be inverted at will, thus allowing the recovery of (+)-*trans*-ChA in the first stage of the resolution process (Fig. 3) and of (–)-*trans*-ChA in the second stage (Fig. 6).

(–)-*trans*-ChA can be recycled through well known radical induced racemization processes.²⁰ These reactions produce racemic mixtures with the thermodynamically more stable *trans*-ChA largely predominant (9 : 1). Another important utilization of (–)-*trans*-ChA is its conversion into (1*R*,3*S*)-*cis*-ChA through rather complicated transformations.^{1d}

Finally, we faced the main target of our work: the resolution of (+)-*trans*-ChA contained in a racemic *trans/cis*-ChA mixtures of industrial origin, without prior separation of the *cis* isomers. The racemic mixture with composition *trans/cis* = 80 : 20 was chosen as the more representative of the industrial production. We found that (1*R*,2*R*)-(–)-MTDP effects a sharp resolution even on this mixture (Fig. 7), and it is so efficient that it can be used just stoichiometrically to the ChA enantiomer being resolved. Thus for a racemic 80:20 *trans/cis* mixture, only 0.4 molar equivalents of (–)-MTDP can be used to achieve a nearly quantitative recovery of (+)-*trans*-ChA.

The first precipitate of *n* salt furnishes (+)-*trans*-ChA with ee = 94%. The stereoisomeric purity of this *n* salt can be further improved by refluxing it in *i*-Pr₂O. Ethereal mother liquors are rich in (–)-*trans*-ChA and contain all racemic *cis*-ChA.

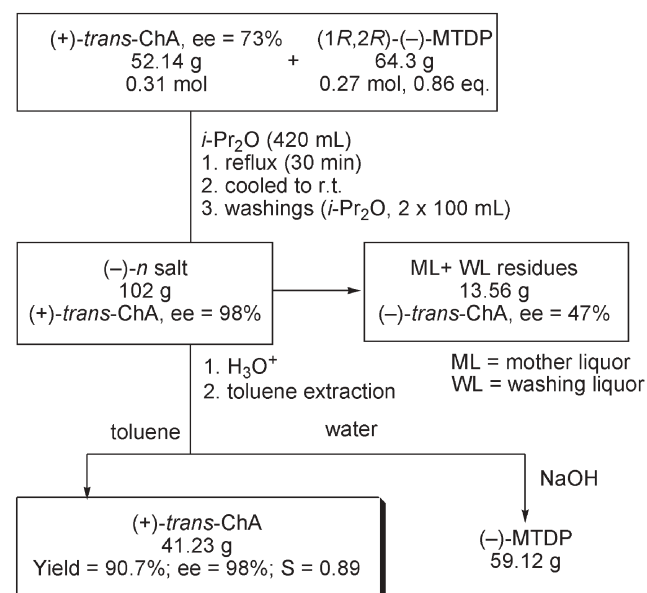


Fig. 6 The treatment of the scalemic mixture to complete the resolution of *trans*-ChA obtaining (+)-*trans* ChA.

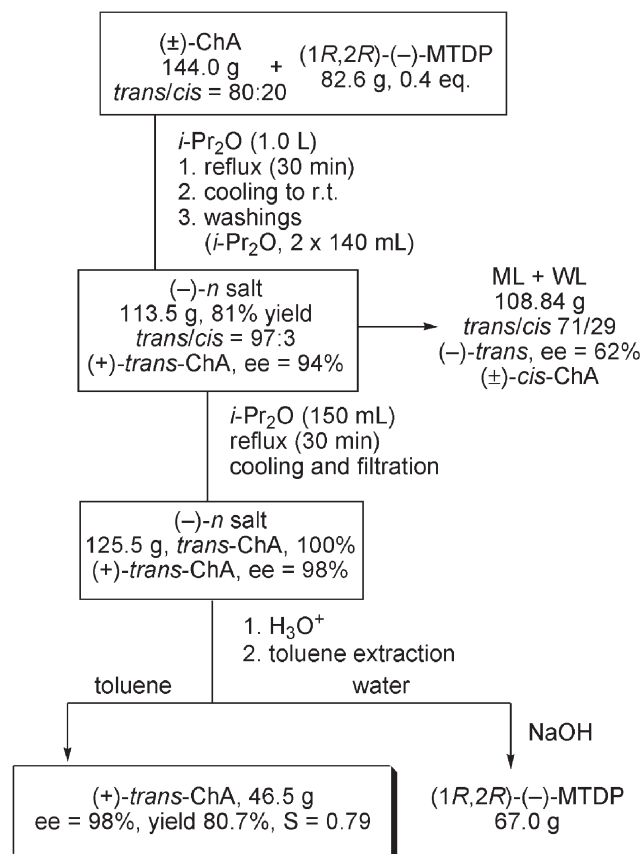


Fig. 7 Resolution of *trans*-ChA from a *trans/cis* mixture (80 : 20) of industrial origin.

Chrysanthemic acid recovered from this mother liquors can then be treated as such with the other enantiomer of the base, (1*S*,2*S*)-(+)-MTDP, in a molar equivalent amount with respect to the (-)-*trans*-ChA present in that mixture. Precipitation of (+)-*n* salt leaves in solution all the racemic *cis* isomer.

Therefore, working with an industrial mixture of racemic chrysanthemic acid (*trans/cis* = 80 : 20) and exploiting the combination of the enantiomers of MTDP as resolving agents and *i*-Pr₂O as solvent, we have performed the resolution of both the enantiomers of *trans*-ChA²¹ and their purification from racemic *cis* isomer, all at once. In every case the base used was recovered enantiomerically pure and in almost quantitative yield by precipitation that follows the alkaline treatment of the aqueous mother liquors, or, quantitatively, through extraction with toluene.

The protocol we have developed works well on the hundred gram scale and is amenable to a possible industrialization.

The efficacy of the resolution of *trans*-ChA with enantiomerically pure MTDP as resolving agent draws its origin from the low solubility of the *n* salts in *i*-Pr₂O (430 mg per 100 mL at 15 °C) and on the sharp chiral discrimination that the enantiomers of this base display in the reaction with the enantiomer of *trans*-ChA with the opposite sign of rotation. While the (+)-*n* salt obtained from (-)-*trans*-ChA and (1*S*,2*S*)-(+)-MTDP is a white solid, mp 138–140 °C, that immediately precipitates from *i*-Pr₂O and is filtered with facility, the (-)-*p* salt, prepared separately from (-)-*trans*-ChA and

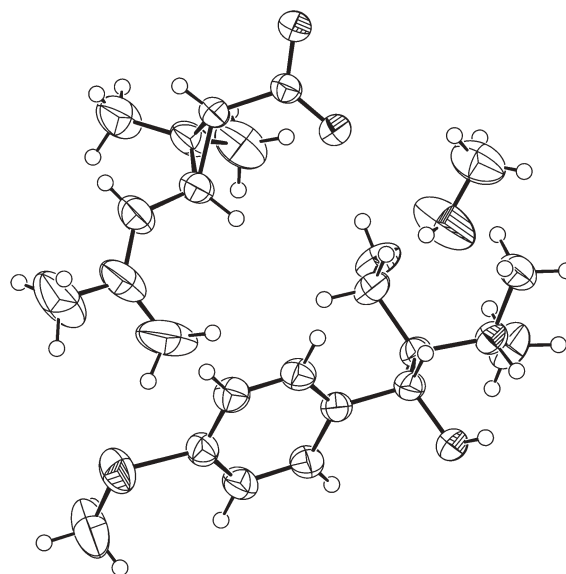


Fig. 8 ORTEP representation^{22,23} of the methanol solvated salt.

(1*R*,2*R*)-(-)-MTDP in *i*-Pr₂O, shows a higher solubility. After partial evaporation of the solvent, it separates as a gelatine and is filtered with great difficulty. This gelatinous, semi-solid compound incorporates the solvent that can be removed only by evaporation under reduced pressure to give a solid ($[\alpha]_D -34.1$) melting at 77–78 °C. This kind of material can represent a main hurdle, especially when thinking about possible industrial applications. However, the extreme efficiency of MTDP bases as resolving agents overcomes this potential problem. In fact, when MTDP is used just stoichiometrically to the ChA enantiomer being resolved, it specifically forms the *n* salt only, and not even a small amount of the gelatinous *p* salt was ever detected.

Structure and pseudopolymorphism of *n* salts of *trans*-ChA and MTDP

The crystals of the *n* salt obtained in *i*-Pr₂O were much too small for single crystal X-ray diffraction analysis. Nice crystals of the *n* salt could be obtained by crystallization from methanol. ¹H and ¹³C NMR analysis revealed that this compound is a three-component system containing *trans*-ChA, MTDP, and methanol in a 1 : 1 : 1 ratio. X-ray diffraction analysis of this salt (orthorhombic) revealed the solvated structure depicted in Fig. 8.‡

However, when either ethanol or isopropanol is used to crystallize the *n* salt, beautiful prismatic crystals free of any solvent were collected. The absence of the solvent, at first observed by NMR, was later confirmed by the X-ray diffraction analyses performed on single crystals of these unsolvated forms (monoclinic, Fig. 9).‡

The presence or absence of any molecule of crystallization alcohol thus results in relevant changes in the crystalline structure of these two pseudopolymorphic structures.

‡ CCDC reference numbers 626016 and 626017. For crystallographic data in CIF or other electronic format see DOI: 10.1039/b615785h

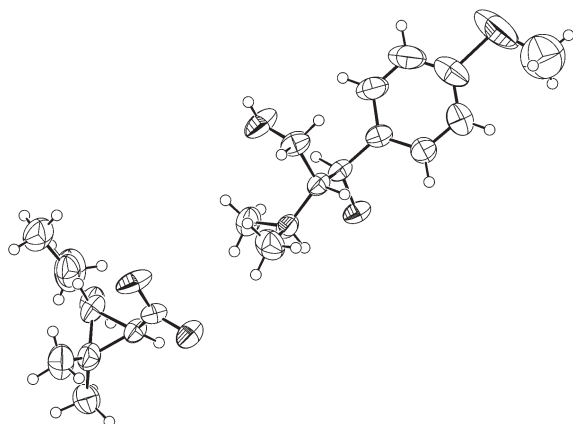


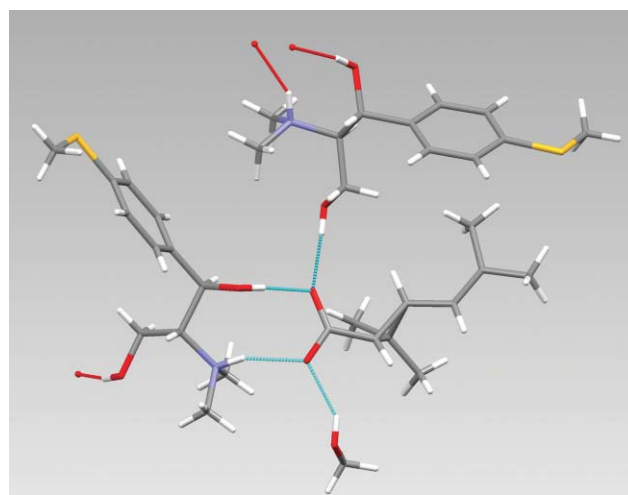
Fig. 9 ORTEP representation^{22,23} of the unsolvated salt.

In the methanol containing pseudopolymorph, the network of hydrogen bonds clearly shows that one molecule of base is involved twice with one lone pair for each oxygen of the carboxylate (Fig. 10a); one by the electrostatic interaction through its protonated nitrogen and one with its benzylic hydroxyl group. The other lone pair of the carboxylate oxygen participates to hydrogen bond with methanol while the last lone pair of the other oxygen establishes the same relationship with a second molecule of base through its primary hydroxyl group. Fig. 10a shows these features and points out the key role of the primary hydroxyl group in establishing intermolecular interactions needed to propagate the hydrogen bonded network. Therefore, each time the carboxylate oxygen atoms of ChA are involved in intermolecular relationships with two molecules of base and one molecule of methanol. This latter interaction could provide extra stability for the methanol containing pseudopolymorph.

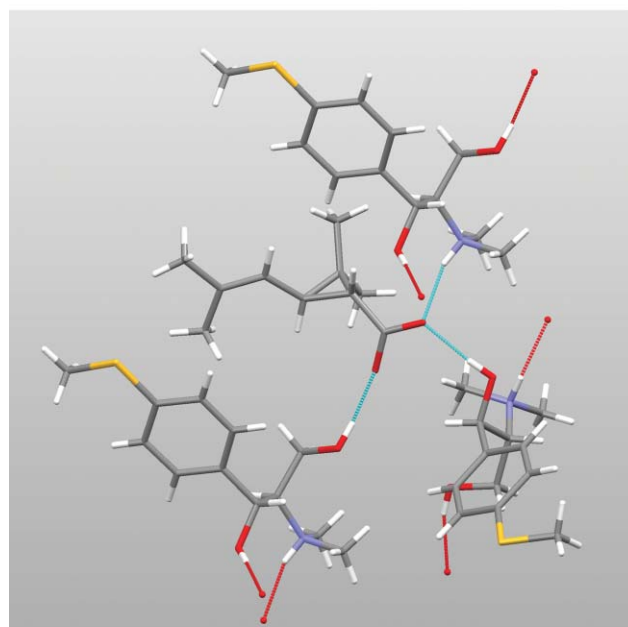
Only three of the four lone pairs of the carboxylate oxygen atoms are engaged in the network that builds up the unsolvated crystals (Fig. 10b). One of the oxygens forms an electrostatic bond with the protonated nitrogen and an intermolecular hydrogen bond with the benzylic hydroxyl group of another molecule of base. The second carboxylate oxygen is involved into a hydrogen bond with a third molecule of base through its primary hydroxyl group (Fig. 10b).

Thus, the crystal structures of *n* salts of *trans*-ChA with MTDP present a number of similarities with those reported by Fogassy using DMAD as the base: (a) both of them form two pseudopolymorphs, one unsolvated and one methanol solvated; (b) both share many similarities in the network of hydrogen bonds holding together these two crystals; and (c) the unsolvated crystal is monoclinic while the solvated one is orthorhombic. However, despite these similarities, methanol is a condition for a successful resolution when DMAD is used,¹⁵ while we have shown here that when MTDP is the resolving agent a clean and selective precipitation of the *n* salt is achieved in a single solvent, *i*-Pr₂O, without any other co-solvent.

Greater differences are observed for DMPP. The unsolvated *n* salt crystals are orthorhombic. Moreover, we have previously reported that DMPP enantiomers generate *p*₁,*n*₁ salts,¹⁶ an attitude never observed for MTDP and DMAD enantiomers.



(a)



(b)

Fig. 10 H-bonds (in cyan) of a single ChA unit in the two pseudopolymorphic *n* salts: (a) the methanol solvated structure (orthorhombic, four H-bonds), and (b) the unsolvated structure (monoclinic, three H-bonds). The network is propagated (red dotted lines) by three arms (a) against six (b).²⁴

The same and not the same, a further example of molecular mimicry like those lucidly delineated by Roald Hoffmann in his enlightening book.²⁵

Conclusions

Classical resolutions are based on the different solubility of diastereomers formed by interaction of the enantiomers with an enantiopure resolving agent. For an efficient and practical resolution the choice of a proper solvent is therefore as essential as the choice of the resolving agent.

(1*S*,2*S*)-(–) and (1*R*,2*R*)-(+)-MTDP are easily available and extremely efficient resolving agents for *trans*-ChA meeting

some of the requirements of green chemistry. In particular, this process compared with existing ones: (a) makes use of the chiral resolving agent just stoichiometrically to the enantiomer being resolved, and not with the whole racemic mixture;^{13c} (b) works in a single, easily available and safe solvent without any need for other co-solvents, thus making solvent recycling and reuse very easy; (c) can be used for the resolution of *trans*-ChA enantiomers directly from racemic *trans/cis* mixtures of industrial production, without prior separation of the *cis* stereoisomer.

All these remarks, coupled with the easy availability of *i*Pr₂O and the enantiomerically pure (1*S*,2*S*)-(–)- and (1*R*,2*R*)-(+)-MTDP, as well as their complete recovery and reuse for further utilizations,²⁶ induce us to point out this procedure as a valuable tool for industrial production also.

Experimental section

General experimental section

Enantiomeric composition of chrysanthemic acid samples was determined by CSP GC (capillary column Rt- β DEXsmTM-RESTEK Corp.; 30 m; 0.32 mmID; 0.25 μ m; injector 230 °C; FID detector 230 °C; 80 °C (2 min) then to 125 °C (1.5 °C min^{–1}); *t*_r (+)-*trans*-ChA = 29.63 min; *t*_r (–)-*trans*-ChA = 30.44 min. Melting points are uncorrected. NMR spectra were recorded in CDCl₃ at 20 °C and chemical shifts are expressed in ppm relative to Me₄Si. Where not otherwise stated, optical rotations were measured at 22 °C.

(1*R*,2*R*)-(–)-2-Dimethylamino-1-[4-(methylthio)phenyl]propane-1,3-diol, [(1*R*,2*R*)-(–)-MTDP]. A 250 mL, three-necked flask, fitted with a magnetic stirrer bar, a reflux condenser, and a thermometer, is charged with 42.6 g (200 mmol) of commercially available (1*R*,2*R*)-2-amino-1-[4-(methylthio)phenyl]propane-1,3-diol and, while cooling the flask with an ice bath, formic acid (32.0 g, 700 mmol) and 35% aq. formaldehyde (43.0 g, 500 mmol). After being heated for 24 h at 90 °C, the solution was cooled and 6 M aq. HCl (70 mL) was added. The resulting solution was washed with diethyl ether (3 \times 60 mL). The aqueous layer was made basic with 50% aq. NaOH and then extracted with toluene (3 \times 120 mL). The combined extracts were dried (MgSO₄) and the solvent was removed under reduced pressure to give 41.4 g (86%) of (1*R*,2*R*)-(–)-MTDP as a pale yellow solid: m.p. 89–91.5 °C (from ethyl acetate); [α]_D –24.0 (*c* 1.52, acetone), [α]_D –39.9 (*c* 1.36, chloroform); ν_{max} (KBr)/cm^{–1} 3437, 2942, 1598, 1457; δ_{H} (300 MHz) 2.42 (s, 9H), 2.56 (m, 1H), 3.35 (m, 2H), 4.25 (d, 1H, *J* 9.80), 7.18 (m, 4H); δ_{C} (75 MHz) 16.45, 41.96, 58.82, 71.50, 71.79, 127.26, 128.18, 138.71 and 139.35; *m/z* 241 (*M*[–]), 240 (*M*[–]–1), 195, 154, 137. Elemental analysis calculated for C₁₂H₁₉NO₂S: %C 59.72, %H 7.93, %N 5.80; found: %C 59.83, %H 7.88, %N 5.75.

(1*S*,2*S*)-(+)-2-Dimethylamino-1-[4-(methylthio)phenyl]propane-1,3-diol, [(1*S*,2*S*)-(+)-MTDP]. (1*S*,2*S*)-(+)-MTDP was prepared, starting from commercially available (1*S*,2*S*)-2-amino-1-[4-(methylthio)phenyl]propane-1,3-diol, *thiomica-mine*, according to the procedure described for the preparation of (1*R*,2*R*)-(–)-MTDP from: mp 89–91 °C; [α]_D + 23.7 (*c* 1.49,

acetone), [α]_D + 38.6 (*c* 1.30, chloroform). IR, ¹H NMR, ¹³C NMR and mass spectroscopic data proved to be identical to those found for (1*S*,2*S*)-(+)-MTDP. Elemental analysis calculated for C₁₂H₁₉NO₂S: %C 59.72, %H 7.93, %N 5.80; found: %C 59.85, %H 7.77, %N 5.72.

Resolution of racemic *trans*-ChA by the formation of *n* salts with the enantiomers (1*R*,2*R*)-(–)-MTDP and (1*S*,2*S*)-(+)-MTDP. *Recovery of (–)-trans-ChA* (Fig. 4). A three-necked 1 L flask, equipped with a mechanical stirring and a reflux condenser, is charged with 480 mL of isopropyl ether and 67.8 g (0.28 moles) of (1*S*,2*S*)-(+)-MTDP. The suspension is heated under reflux until completely dissolved, then a solution of 90.8 g (0.54 moles) of racemic *trans*-ChA dissolved in 220 mL of isopropyl ether is added. After a while, precipitation of the salt is observed. The mixture is kept under reflux and stirred for additional 30 min. It is cooled to ambient temperature and the precipitated salt is separated by filtration. The salt is then washed three times with 100 mL of isopropyl ether and dried at 25 °C/24 mbar to obtain 90.8 g of crude (+)-*n* salt, (1*S*,3*S*)-(–)-ChA·(1*S*,2*S*)-(+)-MTDP. GC analysis of a sample after the usual displacement of the base shows (–)-*trans*-ChA with an ee = 97%. Isopropyl ether (150 mL) is added to the salt thus obtained and the mixture is heated at reflux for 30 min while being stirred. The mixture is cooled to ambient temperature and the salt separated by filtration then dried under reduced pressure (24 mbar) at 30 °C to obtain 88.4 g of pure (+)-*n* salt: mp 138–140 °C; [α]_D + 10.7 (*c* 0.98, chloroform)

This salt is dissolved in a 1*N* aq. HCl solution and extracted with toluene to provide, after evaporation under reduced pressure, 36.3 g (total yield 80%) of (–)-*trans*-ChA (ee = 100%): bp 95–97 °C (0.5 mmHg), [α]_D –14.4 (*c* 5.02, EtOH), [lit.^{14b} (+)-*trans*-ChA: [α]_D + 14.52 (*c* 5.008, EtOH)]

The resolving agent, (1*S*,2*S*)-(+)-MTDP, precipitates from the mother liquors made alkaline with 10% aq. NaOH and it is recovered, without any detectable loss of optical purity, by filtration, washings with water and drying under vacuum (51.7 g, yield 76.2%). The remaining mother liquors can be extracted with toluene (2 \times 100 mL) to recover the remaining base (5.4 g).

Recovery of (+)-*trans*-ChA enriched mixture (Fig. 5). Combined mother and washing liquors from the previous step are treated with water acidified to pH 5.5 with 1*N* hydrochloric acid. The organic layer is washed with water, dried (MgSO₄), and evaporated under reduced pressure to provide 52.1 g of (+)-*trans*-ChA (ee = 73%). The aqueous layer is made basic to pH 10 with 10% aq. NaOH. A second crop of (1*S*,2*S*)-(+)-MTDP can be collected by filtration (10.22 g) for an overall recovery of 99%.

Recovery of *ep* (+)-*trans*-ChA from the 73% ee scalemic mixture (Fig. 6). The (+)-*trans*-ChA thus obtained (52.1 g, ee 73%, 0.31 moles) is dissolved in 420 mL of isopropyl ether, brought to boiling point, and 64.3 g (0.27 moles) of (1*R*,2*R*)-(–)-MTDP are added. The reaction mixture is kept boiling for half an hour then left to cool to room temperature. The precipitation of (–)-*n* salt (1*R*,3*R*)-(+)-ChA·(1*R*,2*R*)-(–)-MTDP

(102.0 g), the other enantiomer of the previous salt, is collected by filtration: mp 138–140 °C, $[\alpha]_{\text{D}} -10.7$ (c 0.986, chloroform) and, upon acidic treatment and extractions with toluene, provides 41.23 g (total yield 90.7%) of (+)-*trans*-ChA (ee = 98%). $[\alpha]_{\text{D}} +14.4$ (c 5.01, EtOH), [lit.:^{14b} $[\alpha]_{\text{D}} +14.52$ (c 5.008, EtOH)]. Alkalinization of the mother liquors with NaOH, as described above, enables precipitation of 59.12 g of the base (1*R*,2*R*)-(–)-MTDP used as resolving agent. Subsequent extraction of the mother liquors with toluene enables the total recovery of the base, enantiomerically intact. A residue remains in the mother liquors of salt precipitation, which, when suitably treated, provides 13.56 g of (+)-*trans*-ChA (ee = 47%).

Resolution of racemic *trans*-ChA directly from a 80 : 20 mixture of *trans*-ChA/*cis*-ChA through the formation of (–)-*n* salt with (1*R*,2*R*)-(–)-MTDP to obtain (+)-*trans*-ChA (Fig. 7). A three necked 2 L flask, equipped with a mechanical stirrer and a reflux condenser, is charged with 700 mL of isopropyl ether and 82.6 g (0.342 mol; 0.4 equiv) of (1*R*,2*R*)-(–)-MTDP. The suspension is heated under reflux until completely dissolved, then a solution of 144.0 g (0.857 mol) of a 4 : 1 mixture of racemic *trans*-ChA and *cis*-ChA of industrial origin dissolved in 300 mL of isopropyl ether is added. After a while, precipitation of the salt is observed. The mixture is kept under reflux and stirred for an additional 30 min. It is cooled to ambient temperature and the precipitated salt is filtered. The salt is then washed twice with 140 mL of isopropyl ether and dried at 25 °C/24 mbar to obtain 113.5 g of crude (–)-*n* salt, (1*R*,3*R*)-(+)–ChA·(1*R*,2*R*)-(–)-MTDP. Upon acidic displacement, a sample of this salt afforded (+)-*trans*-ChA with an ee = 94% by GC analysis (*trans*-ChA/*cis*-ChA = 97 : 3). This salt was added with *i*-Pr₂O (150 mL) and the suspension was refluxed for 30 min, cooled to room temperature and filtered. The product was dried under reduced pressure to obtain 109.3 g of almost pure (–)-*n* salt: mp 138–140 °C; $[\alpha]_{\text{D}} -10.7$ (c 0.98, CHCl₃).

When this second purification is performed by crystallization from methanol, a sovraturated solution forms which remains fluid and clear for a long time at room temperature. A subitaneous precipitation occurs only by scratching the walls of the flask with a glass rod or by seeding. The precipitate is collected by filtration, while methanol filtrate, when allowed to stand at room temperature for two days, gives very nice prismatic crystals, which were used for X-ray diffraction analysis.

This salt is dissolved in a 1 N aq. HCl solution and extracted with toluene to provide, after evaporation under reduced pressure, 46.5 g (overall yield 81%) of (+)-*trans*-ChA (ee = 98%).

The base (1*R*,2*R*)-(–)-MTDP, used as resolving agent, precipitates from the mother liquors made alkaline with NaOH. It is recovered (60.0 g), optically intact, by filtering, washings of the solids with water, and drying under vacuum. The remaining mother liquors can be extracted with isopropyl ether (2 × 100 mL) to recover the remaining base (7.0 g).

The filtered isopropyl ether mother liquor, to which the isopropyl ether used for washing the (–)-*n* salt is added, is evaporated under reduced pressure to give 108.84 g of a

residue that, after displacement with 1 N hydrochloric acid gives a 71 : 29 mixture of *trans*- and *cis*-ChA where *trans*-ChA is enriched in levorotating enantiomer (ee = 62%).

Acknowledgements

This research has been supported in part by Alma Mater Studiorum- Università di Bologna and MIUR, Italy (PRIN 2005-Metodologie innovative per la sintesi di reagenti e di prodotti enantiomericamente arricchiti)

References

- (a) S. Jeanmart, *Aust. J. Chem.*, 2003, **56**, 559 and references cited therein; (b) A. Fishman, D. Kellner, D. Ioffe and E. Shapiro, *Org. Process Res. Dev.*, 2000, **4**, 77 and references cited therein; (c) J. Crosby, *Pestic. Sci.*, 1996, **46**, 11; (d) J. Martel, in *Chirality in Industry*, ed. A. N. Collins, G. N. Sheldrake and J. Crosby, John Wiley & Sons, Chichester, UK, 1992, ch. 4 pp. 87–109; (e) K. Naumann, in *Chemistry of Plant Protection*, ed. W. S. Bowers, W. Ebing, D. Martin and R. Wegler, Springer Verlag, Berlin, Germany, 1990, vol. 5, ch.1, pp. 3–100; (f) J. Tessier, *Chem. Ind.*, 1984, 199; (g) *Pyrethrum—The Natural Insecticide*, ed. J. E. Casida, Academic Press, New York, USA, 1973; (h) D. Arlt, M. Jautelat and R. Lantzsch, *Angew. Chem., Int. Ed. Engl.*, 1981, **20**, 703; (i) M. Elliott and N. F. Janes, *Chem. Soc. Rev.*, 1978, **7**, 473.
- I. G. M. Campbell and S. H. Harper, *J. Chem. Soc.*, 1945, 283. A version for undergraduates has been published: L. F. Kelly, *J. Chem. Educ.*, 1987, **64**, 1061. For a fascinating report on the early industrial synthesis of chrysanthemic acid and then allethrin, see: H. J. Sanders and A. W. Taff, *Ind. Eng. Chem.*, 1954, **46**, 414.
- It is known that *trans*-ChA is the thermodynamically more stable isomer and the equilibrium, depending on the operative conditions, is on the order of 90% of *trans*-ChA and 10% *cis*-ChA. Mixtures with a lower content of *trans* isomer can be enriched in this component by epimerization.
- J. Martel and C. Huynh, *Bull. Soc. Chim. Fr.*, 1967, 985. For an undergraduate synthesis, see: P. F. Schatz, *J. Chem. Educ.*, 1978, **55**, 468. This approach has seen some variants involving the utilization of aliphatic nitro compounds: (a) J. H. Babler and K. P. Spina, *Tetrahedron Lett.*, 1985, **26**, 1923; (b) A. Krief, L. Hevesi, G. Chaboteaux, P. Mathy, M. Sevrin and M. J. De Vos, *J. Chem. Soc., Chem. Commun.*, 1985, 1693; (c) J.-M. Melot, F. Texier-Boullet and A. Foucaud, *Synthesis*, 1987, 364; (d) N. Ono, T. Yanai, I. Hamamoto, A. Kamimura and A. Kaji, *J. Org. Chem.*, 1985, **50**, 2807; (e) L. Lambs, N. P. Singh and J.-F. Biellmann, *J. Org. Chem.*, 1992, **57**, 6301.
- For an excellent review on stereoselective cyclopropanation reactions, see: H. Lebel, J.-F. Marcoux, C. Molinaro and A. B. Charette, *Chem. Rev.*, 2003, **103**, 977. For a comparison of different cyclopropanation catalysts, see: (a) M. P. Doyle, in *Catalytic Asymmetric Synthesis*, ed. I. Ojima, VCH, New York, 1993, ch. 3, pp 63–99; (b) M. P. Doyle, M. A. McKervey and T. Ye, *Modern Catalytic Methods for Organic Synthesis with Diazo Compounds—From Cyclopropanes to Ylides*, J. Wiley & Sons, New York, 1998.
- T. Aratani, *Pure Appl. Chem.*, 1985, **57**, 1839 and references cited therein.
- M. Breuer, K. Ditrach, T. Habicher, B. Hauer, M. Keßler, R. Stürmer and T. Zelinski, *Angew. Chem., Int. Ed.*, 2004, **43**, 788 and literature cited therein.
- Several hurdles hamper the use of enantioselective catalysis in production of enantiopure fine chemicals and agrochemicals. Among them catalyst availability, stability, efficiency, experience and costs, included costs associates with licensing industrial patents, all well oriented to the production of a defined target. A main hurdle is a need for specialised equipment to operate the enantioselective catalysis at production scale. Frequently, enantioselectivity is directly linked to very low reaction temperatures and needs the absence of any impurity to preserve the catalyst. If an asymmetric method will only work at cryogenic temperature, high purity of reagents and solvents, and high dilution for instance, then

- it might not be worth developing: H.-U. Blaser, *Chem. Commun.*, 2003, 293.
- 9 E. Fogassy, M. Nógrádi, D. Kozma, G. Egri, E. Pálovics and V. Kiss, *Org. Biomol. Chem.*, 2006, **4**, 3011.
 - 10 (a) For a comprehensive survey of studies on this method for obtaining enantiopure compounds, see: *CRC Handbook of Optical Resolutions via Diastereoisomeric Salt Formation*, ed. David Kozma, CRC Press, London, 2001; (b) For a book focused on theoretical explanations of the optical resolution of racemates by diastereoisomeric salt formation, see: J. Jacques, A. Collet, S. H. Wilen, *Enantiomers, Racemates, and Resolutions*, Wiley and Sons, New York, 1981.
 - 11 The letter *p* is used to designate the diastereoisomers resulting from reaction of two constituents having like sign of rotation and the letter *n* to designate the diastereoisomer formed from constituents of unlike sign. See ref. 10b, p. 251.
 - 12 A common definition of green chemistry is “the design, development, and implementation of chemical processes and products to reduce or eliminate substances hazardous to human health and the environment” (P. T. Anastas, J. Warner, *Green Chemistry Theory and Practice*, Oxford University Press, Oxford, 1998). A more recent article expands this definition to twelve principles (M. Poliakoff, J. M. Fitzpatrick, T. R. Farren and P. T. Anastas, *Science*, 2002, **297**, 807), reported also in National Research Council – Committee on Challenges for the Chemical Sciences in the 21st Century, *Beyond the Molecular Frontier-Challenges for Chemistry and Engineering Chemistry*, The National Academy Press, Washington, D.C., 2003, pp 150–153, www.nap.edu.
 - 13 (a) R. A. Sheldon, *Green Chem.*, 2005, **7**, 267; (b) J. S. Carey, D. Laffan, C. Thomson and M. T. Williams, *Org. Biomol. Chem.*, 2006, **4**, 2337; (c) D. J. C. Constable, A. D. Curzons and V. L. Cunningham, *Green Chem.*, 2002, **4**, 521.
 - 14 Inter alia: (a) quinine: (i) I. C. M. Campbell and S. H. Harper, *J. Sci. Food Agric.*, 1952, **3**, 189, (ii) L. Crombie, J. Crossley and D. A. Mitchard, *J. Chem. Soc.*, 1963, 4957; (b) L-lysine: M. Matsui and F. Horiuchi, *Agric. Biol. Chem.*, 1971, **35**, 1984; (c) L-2-benzylaminopropanol: F. Horiuchi and M. Matsui, *Agric. Biol. Chem.*, 1973, **37**, 1713; (d) (–)- α -(1-naphthyl)ethylamine: (i) F. Horiuchi, A. Higo and H. Yoshioka, Sumitomo Chemical Co. Ltd., *German Pat.* 2 300 325, 1975, (ii) K. Sasaki, Sumitomo Chem. Co. Ltd, *Japanese Pat.* 98–16789, 1999; (e) (S)-1-phenyl-2-(*p*-tolyl)ethylamine: (i) M. Itagaki, G. Suzukamo, K. Sasaki and K. Fujita, Sumitomo Chem. Co. Ltd, *Eur. Pat.* 933349 A1, 1999, (ii) G. Suzukamo and K. Sasaki, Sumitomo Chemical Co. Ltd., *Eur. Pat.* 1236708 A1, 2002; (f) (S)-1-phenyl-2-methylpropylamine: H. Hagiya, Sumitomo Chemical Co. Ltd., *Japanese Pat.* 2001114728 A2, 2001; (g) L- or D-N-methyl-ephedrine: C. Pavan, J. Bulidon, Roussel Uclaf, *US Pat* 4 257 976, 1981; (h) phenylglycinamide or 2-phenylglycinonitrile: F. Faigl, E. Fogassy, L. Nagy, L. Csiz, I. Czudor and E. Kovacsne Kozsda, CHINOIN-Budapest, *PCT WO* 90/08126, 1990.
 - 15 É. Kozsda-Kovács, G. M. Keserü, Z. Böcksei, I. Szilágyi, K. Simon, B. Bertók and E. Fogassy, *J. Chem. Soc., Perkin Trans. 2*, 2000, 149.
 - 16 G. Rosini, C. Ayoub, V. Borzatta, A. Mazzanti, E. Marotta and P. Righi, *Chem. Commun.*, 2006, 4294.
 - 17 p_1, n_1 Salts originate from a stable 1 : 1 combination of diastereoisomeric *p* and *n* salts. See ref. 10b, p. 295.
 - 18 MTDP is the dimethyl derivative of the corresponding primary amine, the (1*R*,2*R*)-enantiomer of which is a key precursor of thiamphenicol, a fully synthetic analogue of *chloramphenicol*. The (1*S*,2*S*)-enantiomer, the distomer, is called thiomcamine and considered as waste in the industrial production of thiamphenicol (approximately 100 tons per year). Two routes are available for the resolution of (±)-*threo*-2-amino-[4-(methylthio)phenyl]propane-1,3-diol: classical resolution using (+)-tartaric acid as resolving agent (R. A. Cutler, R. J. Stenger and C. M. Suter, *J. Am. Chem. Soc.*, 1952, **74**, 5475) and the resolution by preferential crystallization: (a) L. M. Long, Park, Davis & Co, *US Pat.* 2 767 213, 1956; (b) M. Portelli and G. Renzi, *Ann. Chim.*, 1969, **59**, 306; (c) M. Portelli, G. Renzi and B. Soranzo, *Ann. Chim.*, 1970, **60**, 160; (d) L. Coppi, C. Giordano, A. Longoni and S. Panossian, in *Chirality in Industry II*, ed. A. N. Collins, G. N. Sheldrake, J. Crosby, J. Wiley & Sons, Chichester, UK, 1997, pp 353. Both enantiomers of *threo*-2-amino-[4-(methylthio)phenyl]propane-1,3-diol have been prepared by asymmetric synthesis too: F. Davis, P. Zhou and G. Reddy, Drexel University, US, *PCT WO* 95/30672, 1995; P. Zhou and G. Reddy, *Tetrahedron Lett.*, 1994, **35**, 7525.
 - 19 The parameter *S* quantifies the resolving efficiency as the product of the chemical yield and the enantiomeric purity: E. Fogassy, A. Lopata, F. Faigl, F. Darvas, M. Ács and L. Töke, *Tetrahedron Lett.*, 1980, **21**, 647.
 - 20 (a) G. Suzukamo, Y. Sakito, M. Fukao and K. Hagiya, Sumitomo Chem. Co., Ltd, *U.S. Pat.* 4 898 655, 1990; (b) G. Suzukamo, M. Fukao and Y. Sakito, Sumitomo Chem. Co., Ltd, *Eur. Pat.* 289324, 1988; (c) G. Suzukamo, Y. Sakito, M. Fukao and K. Hagiya, Sumitomo Chem. Co., Ltd, *Eur. Pat.* 261824, 1988; (d) G. Suzukamo, Y. Sakito and M. Fukao, Sumitomo Chem. Co., Ltd, *Eur. Pat.* 282221, 1988; (e) G. Suzukamo and M. Fukao, Sumitomo Chem. Co., Ltd, *Eur. Pat.* 235940, 1987; *Eur. Pat.* 165070, 1985; (f) G. Suzukamo, M. Fukao and T. Nagase, *Chem. Lett.*, 1994, 1799; (g) K. Ueda and M. Matsui, *Tetrahedron*, 1971, **27**, 2771; K. Ueda and M. Matsui, *Agric. Biol. Chem.*, 1970, **34**, 1115.
 - 21 Principle of reciprocal resolution (Marckwald principle): “if both enantiomers of a resolving agent are available, they provide access to both enantiomers of a racemic substrate. The mother liquors of a first separation can be treated with the other enantiomer of the resolving agent.” (taken from: R. A. Sheldon, *Chirality*, Marcel Dekker, Inc., New York, 1993, p. 194); W. Marckwald, *Ber. Dtsch. Chem. Ges.*, 1896, **29**, 42–43.
 - 22 A. L. Spek, *Acta Crystallogr., Sect. A: Found. Crystallogr.*, 1990, **46**, C34; A. L. Spek, PLATON, A Multipurpose Crystallographic Tool, Utrecht University, Utrecht, The Netherlands, 2005.
 - 23 Displacement ellipsoid probability at 50%.
 - 24 Mercury 1.4.1 (<http://www.ccdc.cam.ac.uk/>).
 - 25 R. Hoffmann, *The same and not the same*, Columbia University Press, New York, 1995.
 - 26 During the course of this work, MTDP enantiomers were routinely recovered and reused without any loss of their optical purity, and, above all, without any detectable loss of optical purity of *trans*-ChA resolved by reused MTDP enantiomers.

The large scale synthesis of pure imidazolium and pyrrolidinium ionic liquids

Anthony K. Burrell,^{*a} Rico E. Del Sesto,^a Sheila N. Baker,^b T. Mark McCleskey^a and Gary A. Baker^b

Received 2nd November 2006, Accepted 18th January 2007

First published as an Advance Article on the web 16th February 2007

DOI: 10.1039/b615950h

Ionic liquids are being employed in almost all areas of chemistry and materials, yet there are inherent issues which arise if the utmost care is not taken in the preparation and purification of these materials. They are not easily synthesized and purified using the existing methods. We describe a reliable method for producing large quantities of high quality ionic liquids. Additionally, we show that imidazoliums are not 'special' due to their 'inherently fluorescent' nature, that spectroscopically clean imidazoliums are attainable, and most classes of ionic liquids do exhibit fluorescent backgrounds when extreme care is not taken during their synthesis and purification.

Introduction

Ionic liquids have become solvents of choice in many applications,¹ being used for purposes as diverse as electrochemiluminescence² and lubrication.³ The required purity of any solvent varies with its application. In many cases the purity of the ionic liquid is not important. However, in applications such as biology, electrochemistry, catalysis, electron transfer and spectroscopy, the highest purity materials are desirable and necessary. It is unfortunate that the ionic liquids that can currently be purchased and those prepared using the synthetic procedures found in the literature are not of particularly high quality. Here we report simple and reliable methods for producing high quality ionic liquids which can be carried out on large scales (>1 kg).

Few publications provide sufficient information that can be used to judge the purity of the ionic liquids being employed. We have been interested in the properties of ionic liquids and more importantly their use as solvents for electrochemistry and spectroscopy.⁴ Our initial samples were either prepared using the standard procedures or were purchased from commercial sources. However, these materials were almost always slightly yellow. More recent attempts to produce spectroscopic grade ionic liquids report that the materials can be cleaned, but limit their descriptions to only a few ionic liquids.⁵ In addition, the papers that describe synthetic routes to ionic liquids often do not describe any data related to the purity of the materials obtained. Even the recent synthesis of 1-butyl-3-methylimidazolium tetrafluoroborate described in *Organic Synthesis*, the gold standard for organic synthesis, describes the product as 'colourless to pale yellow'.⁶ The colour issue is shown in Fig. 1, where the sample on the left is a commercially purchased sample of 1-ethyl-3-methylimidazolium



Fig. 1 Commercial quality 1-ethyl-3-methylimidazolium bis(trifluoromethanesulfonyl)amide (left) and a sample made in our laboratory (right).

bis(trifluoromethanesulfonyl)amide and the right sample is prepared in our laboratory.

In general the commercial sources of ionic liquids are of dubious quality. Almost all commercial ionic liquids are coloured and often have strong odours. Merck currently describes most of their commercial ionic liquids as foul smelling coloured materials. However, ionic liquids are odourless and most are colourless!

The presence of colour in colourless materials is a clear indication of impurities. It is likely that the data obtained from employing impure ionic liquids may not be reliable and can lead to incorrect conclusions. For example, imidazolium-based ionic liquids have been described as possessing an inherent fluorescence.⁷ This is simply not true. When pure ionic liquids with imidazolium as the cation are prepared, they possess no inherent fluorescence.

Experimental

Commercial ionic liquids were purchased from Merck, Aldrich and Acros. All other reagents were purchased from Aldrich and used as received or purified as described.

UV-Vis measurements were carried out using an HP Model 8453. Fluorescent measurements were carried out using a PTI GL-3300 fluorimeter with an R955 photomultiplier. Nuclear Magnetic Resonance (NMR) spectra were measured at 400 MHz (¹H), on a Bruker Avance 400 Ultrashield spectrometer. All NMR spectra were recorded in deuteriochloroform unless otherwise stated, with reference to tetramethylsilane.

^aMaterials Chemistry, Materials Physics and Applications, Los Alamos National Laboratory, Los Alamos, NM 87545, USA.
E-mail: Burrell@LANL.GOV; Fax: +1-505-667-9905;
Tel: +1-505-667-9342

^bChemical Sciences Division, Oak Ridge National Laboratory, Oak Ridge, TN 37831-6110, USA

1-Ethyl-3-methylimidazolium chloride

Yellow 1-ethyl-3-methylimidazolium chloride (Aldrich) (50 g) was dissolved in deionized water (250 mL). Decolourizing charcoal (3 g) was added to the solution and the resulting mixture heated at 65 °C for 24 h. The solution was cooled to room temperature and filtered. At this point the solution should be completely colourless. However, in some cases colour remained and the decolourizing charcoal step was repeated. The water was then removed using a lyophilizer. The resulting solid was then heated under high vacuum for 48 h at 65 °C. The material was cooled and the pure white solid was obtained in essentially quantitative yield.

1-Ethyl-3-methylimidazolium bromide

1-Ethyl-3-methylimidazolium bromide (Aldrich) (50 g) was treated as for 1-ethyl-3-methylimidazolium chloride to yield the product as a white solid in quantitative yield.

1-Butyl-3-methylimidazolium chloride

n-Chlorobutane (600 g) was slowly added to freshly distilled methylimidazole (500 g) in a 2 L two-necked round-bottom flask fitted with a reflux condenser. This mixture was then stirred with a magnetic stirrer at 70 °C for one week. During the week a white solid formed, which slowly turned yellow. The solution was allowed to cool to room temperature and any remaining solution was separated by decanting. The yellow solid was then washed with diethyl ether (3 × 200 mL) and dried under vacuum for 24 h. The yellow solid was dissolved in water (1.5 L) and decolourizing charcoal (30 g) was added. This solution was heated to 70 °C for 24 h, cooled and filtered. At this point the solution should be completely colourless. However, in some cases colour remained and the decolourizing charcoal step was repeated. The water was then removed using a lyophilizer. The resulting solid was then heated under high vacuum for 48 h at 65 °C. The material was cooled and the pure white solid was obtained at 92% yield.

1-Butyl-3-methylimidazolium bromide

n-Bromobutane (860 g) was slowly added to freshly distilled methylimidazole (500 g) in a 2 L two-necked round-bottom flask fitted with a reflux condenser. *Caution: this reaction is exothermic and cooling is advisable for large scale reactions.* The addition was at such a rate that the temperature of the solution did not get above 40 °C. This mixture was then stirred with a magnetic stirrer at room temperature for one day. During this time a yellow solid formed. The yellow solid was then purified as for 1-butyl-3-methylimidazolium chloride to give the product in 94% yield.

1-Butyl-1-methylpyrrolidinium chloride

n-Chlorobutane (570 g) was slowly added to freshly distilled methylpyrrolidine (500 g) in a 2 L two-necked round-bottom flask fitted with a reflux condenser. This mixture was then stirred with a magnetic stirrer at 70 °C for one week. During the week a white solid formed, which slowly turned yellow. The solution was allowed to cool to room temperature and any

remaining solution was separated by decanting. The yellow solid was then purified as for 1-butyl-3-methylimidazolium chloride to give the product in 89% yield.

1-Butyl-1-methylpyrrolidinium bromide

n-Bromobutane (900 g) was slowly added to freshly distilled methylpyrrolidine (500 g) in a 2 L two-necked round-bottom flask fitted with a reflux condenser. *Caution: this reaction is exothermic and cooling is advisable for large scale reactions.* The addition was at such a rate that the temperature of the solution did not get above 40 °C. This mixture was then stirred with a magnetic stirrer for one day to give a yellow solid. The yellow solid was then purified as for 1-butyl-3-methylimidazolium chloride to give the product in 91% yield.

1-Butyl-2,3-dimethylimidazolium chloride

n-Chlorobutane (55 g) was slowly added to 1,2-dimethylimidazole (50 g) in a 200 mL two-necked round-bottom flask fitted with a reflux condenser. This mixture was then stirred with a magnetic stirrer at 70 °C for one week. During the week a white solid formed, which slowly turned yellow. The yellow solid was then purified as for 1-butyl-3-methylimidazolium chloride (adjusted for scale) to give the product in 85% yield.

1-Butyl-2,3-dimethylimidazolium bromide

n-Bromobutane (80 g) was slowly added to 1,2-dimethylimidazole (50 g) in a 200 mL two-necked round-bottom flask fitted with a reflux condenser. *Caution: this reaction is exothermic and cooling is advisable for large scale reactions.* The addition was at such a rate that the temperature of the solution did not get above 40 °C. This mixture was then stirred with a magnetic stirrer for one day to give a yellow solid. The yellow solid was then purified as for 1-butyl-3-methylimidazolium chloride (adjusted for scale) to give the product in 98% yield.

1-Butyl-3-methylimidazolium tetrafluoroborate

n-Bromobutane (600 g) was slowly added to freshly distilled methylimidazole (500 g) in a 2 L two-necked round-bottom flask fitted with a reflux condenser. *Caution: this reaction is exothermic and cooling is advisable for large scale reactions.* The addition was at such a rate that the temperature of the solution did not get above 40 °C. This mixture was then stirred with a magnetic stirrer at room temperature for one day. During this time a yellow solid formed. This solid was filtered and washed with diethyl ether (3 × 200 mL) then dried under vacuum. The yellow solid was then dissolved in deionized water (1.5 L). Decolourizing charcoal (30 g) was added to the solution and the resulting mixture heated at 65 °C for 24 h. The mixture was then cooled to room temperature and filtered. At this point the solution should be colourless. If any colour remained the decolourizing charcoal step was repeated. The clean 1-butyl-3-methylimidazolium bromide solution was then poured into a solution of sodium tetrafluoroborate (680 g) in 1 L of deionized water. The solution was then stirred at room temperature for 3 h. The solution was then transferred to a continuous liquid–liquid extractor and extracted with

dichloromethane for 48 h. The dichloromethane solution was filtered through a plug of silica (100 g), then the dichloromethane was removed under vacuum to give the neat 1-butyl-3-methylimidazolium tetrafluoroborate. This material was often contaminated with quantities of sodium bromide. A simple silver test was used to determine the presence of the bromide ion. If a positive test for bromide was obtained, the crude 1-butyl-3-methylimidazolium tetrafluoroborate was dissolved in deionized water (500 mL) and extracted in the liquid–liquid extractor with dichloromethane for 48 h. The dichloromethane solution was filtered through a plug of silica and the dichloromethane removed under vacuum. This process was repeated until a negative bromide test was obtained. The colourless, bromide-free 1-butyl-3-methylimidazolium tetrafluoroborate was obtained in >95% yield even with repeated liquid–liquid extractions.

1-Ethyl-3-methylimidazolium tetrafluoroborate

1-Ethyl-3-methylimidazolium bromide (50 g) was dissolved in deionized water (200 mL). Decolourizing charcoal (3 g) was added to the solution and the resulting mixture heated at 65 °C for 24 h. The mixture was then cooled to room temperature and filtered. At this point the solution should be colourless. If any colour remained the decolourizing charcoal step was repeated. The clean 1-ethyl-3-methylimidazolium bromide solution was then poured into a solution of sodium tetrafluoroborate (30 g) in 200 mL of deionized water. The solution was then stirred at room temperature for 3 h. The 1-ethyl-3-methylimidazolium tetrafluoroborate was then purified as for 1-butyl-3-methylimidazolium tetrafluoroborate. The colourless, bromide-free 1-ethyl-3-methylimidazolium tetrafluoroborate was obtained in >90% yield.

1-Ethyl-3-methylimidazolium triflate

1-Ethyl-3-methylimidazolium bromide (50 g) was dissolved in deionized water (200 mL). Decolourizing charcoal (3 g) was added to the solution and the resulting mixture heated at 65 °C for 24 h. The mixture was then cooled to room temperature and filtered. At this point the solution should be colourless. If any colour remained, the decolourizing charcoal step was repeated. The clean 1-ethyl-3-methylimidazolium bromide solution was then poured into a solution of sodium triflate (50 g) in 200 mL of deionized water. The solution was then stirred at room temperature for 3 h. The 1-ethyl-3-methylimidazolium triflate was then purified as for 1-butyl-3-methylimidazolium tetrafluoroborate. The colourless, bromide-free 1-ethyl-3-methylimidazolium triflate was obtained in >95% yield.

1-Butyl-3-methylimidazolium triflate

n-Bromobutane (60 g) was slowly added to freshly distilled methylimidazole (50 g) in a 2 L two-necked round-bottom flask fitted with a reflux condenser. *Caution: this reaction is exothermic and cooling is advisable for large scale reactions.* The addition was added at such a rate that the temperature of the solution did not get above 40 °C. This mixture was then stirred with a magnetic stirrer at room temperature for one

day. During this time a yellow solid formed. This solid was filtered and washed with diethyl ether (3 × 20 mL) then dried under vacuum. The yellow solid was then dissolved in deionized water 100 mL. Decolourizing charcoal (3 g) was added to the solution and the resulting mixture heated at 65 °C for 24 h. The mixture was then cooled to room temperature and filtered. At this point the solution should be colourless. If any colour remained the decolourizing charcoal step was repeated. The clean 1-butyl-3-methylimidazolium bromide solution was then poured into a solution of sodium triflate (110 g) in 200 mL of deionized water. The solution was then stirred at room temperature for 3 h. The 1-butyl-3-methylimidazolium triflate was then purified as for 1-butyl-3-methylimidazolium tetrafluoroborate. The colourless, bromide-free 1-butyl-3-methylimidazolium triflate was obtained in >95% yield.

1-Butyl-2,3-dimethylimidazolium triflate

Prepared as for 1-butyl-3-methylimidazolium tetrafluoroborate to give the product as a white solid in >90% yield.

1-Butyl-1-methylpyrrolidinium tetrafluoroborate

Prepared as for 1-butyl-3-methylimidazolium tetrafluoroborate to give the product as a white solid in >90% yield.

1-Butyl-1-methylpyrrolidinium triflate

Prepared as for 1-butyl-3-methylimidazolium tetrafluoroborate to give the product as a colourless liquid in >90% yield.

1-Ethyl-3-methylimidazolium bis(trifluoromethanesulfonyl)amide

Yellow 1-ethyl-3-methylimidazolium chloride (Aldrich) (50 g) was dissolved in deionized water (250 mL). Decolourizing charcoal (3 g) was added to the solution and the resulting mixture heated at 65 °C for 24 h. The solution was cooled to room temperature and filtered. At this point the solution should be completely colourless. However, in some cases colour remained and the decolourizing charcoal step was repeated. The clean 1-ethyl-3-methylimidazolium chloride solution was then poured into a solution of lithium bis(trifluoromethanesulfonyl)amide (115 g) in 200 mL of deionized water. The solution was then stirred at room temperature for 3 h after which two layers had formed. The bottom layer was separated and washed three times with deionized water (100 mL). The 1-ethyl-3-methylimidazolium bis(trifluoromethanesulfonyl)amide was then heated at 65 °C under vacuum for 48 h and then filtered through activated alumina to give colourless clean dry material in 89% yield.

1-Butyl-1-methylpyrrolidinium bis(trifluoromethanesulfonyl)amide

n-Bromobutane (900 g) was slowly added to freshly distilled methylpyrrolidine (500 g) in a 2 L two-necked round-bottom flask fitted with a reflux condenser. *Caution: this reaction is exothermic and cooling is advisable for large scale reactions.* The addition was added at such a rate that the temperature of

the solution did not get above 40 °C. This mixture was then stirred with a magnetic stirrer at room temperature for one day. During this time a yellow solid forms. This solid was filtered and washed with ether (3 × 200 mL) then dried under vacuum. The yellow solid was then dissolved deionized water (1 L). Decolourizing charcoal (30 g) was added to the solution and the resulting mixture heated at 65 °C for 24 h. The mixture was then cooled to room temperature and filtered. At this point the solution should be colourless. If any colour remains repeat the decolourizing charcoal step. The clean 1-butyl-1-methylpyrrolidinium bromide solution was then poured into a solution of lithium bis(trifluoromethanesulfonyl)amide (1800 g) in deionized water (2 L). The solution was then stirred at room temperature for 3 h after which two layers had formed. The bottom layer was separated and washed three times with deionized water (500 mL). The 1-butyl-1-methylpyrrolidinium bis(trifluoromethanesulfonyl)amide was then heated at 65 °C under vacuum (0.1 mbar) for 48 h and then filtered through activated alumina to give colourless clean dry material (89% yield).

1-Butyl-3-methylimidazolium bis(trifluoromethanesulfonyl)amide

n-Bromobutane (860 g) was slowly added to freshly distilled methylimidazole (500 g) in a 2 L two-necked round-bottom flask fitted with a reflux condenser. *Caution: this reaction is exothermic and cooling is advisable for large scale reactions.* The addition was added at such a rate that the temperature of the solution did not get above 40 °C. This mixture was then stirred with a magnetic stirrer at room temperature for one day. During this time a yellow solid forms. This solid was filtered and washed with diethyl ether (3 × 200 mL) then dried under vacuum. The yellow solid was then dissolved deionized water (1 L). Decolourizing charcoal (30 g) was added to the solution and the resulting mixture heated at 65 °C for 24 h. The mixture was then cooled to room temperature and filtered. At this point the solution should be colourless. If any colour remained the decolourizing charcoal step was repeated. The clean 1-butyl-3-methylimidazolium bromide solution was then poured into a solution of lithium bis(trifluoromethanesulfonyl)amide (1850 g) in 2 L of deionized water. The solution was then stirred at room temperature for 3 h after which two layers had formed. The bottom layer was separated and washed three times with deionized water (500 mL). The 1-butyl-3-methylimidazolium bis(trifluoromethanesulfonyl)amide was then heated at 65 °C under vacuum for 48 h and then filtered through activated alumina to give clean dry material in 89% yield.

Results and discussion

In our work on electrochromic and electrochemical applications of ionic liquids, we initially purchased our materials. Then we realised that the data we obtained from the commercial liquids were dependent on both supplier and the batch we used. The synthesis of ionic liquids using the standard literature methods always resulted in yellow materials. The most common organic ammonium cation-based

liquids, including the imidazolium and pyrrolidinium cations, should appear 'water-white' when pure.

A simple test is to place a vial of ionic liquid next to a vial of water. These should be indistinguishable by the naked eye.

Recently, it has been demonstrated that it is possible to distill ionic liquids.⁸ Unfortunately, this is a slow process and is not currently suitable for the purification of large volumes of material. The most commonly attempted method for purifying ionic liquids utilizes activated carbon or decolourizing charcoal.⁹ We examined these in the purification of synthesized and commercial ionic liquids and discovered that they did not significantly enhance the purity. Discussions with other research groups confirmed that this is a general finding. We therefore set about redesigning the synthesis of the ionic liquids. It is hard to think of a simpler synthesis than the preparation of salts by metathesis. Clearly there was little that could be done to improve this reaction. However, there is significant room for advancement in the purity of the precursors, and this is the crux of the purification of ionic liquids. It turns out that all of the reported preparations of ionic liquids almost never discuss the purification of the precursors. These precursors, when purchased commercially or prepared using the literature methods, are almost all coloured. However, it is clear that in the case of simple ammonium chlorides or bromides the colour is an indication of the presence of impurities.

We examined the synthesis of the ammonium chlorides and bromides and discovered that if the temperature was controlled very carefully the intensity of the yellow colour could be minimized, but not completely excluded. As we were interested in the large-volume synthesis of ionic liquids it was difficult to limit local heating and the formation of colour. Therefore we took the logical step and purified the ammonium chlorides and bromides after preparing them.

High quality ionic liquids can be obtained if the precursors are purified prior to the synthesis of the ionic liquid. This can be simply achieved using decolourizing charcoal in water. Either heating to reflux temperature for 3–5 min or heating at 65 °C for 24 h. We prefer the lower temperature with longer times, but both methods produce clean materials.

This is a general method for the production of ionic liquids based upon nitrogen cations and can be scaled to the limits of your glassware. There is a clear difference in the properties of the different classes of salts. The water-soluble materials can be effectively cleaned using decolourizing charcoal in water. If the salts are insoluble in water, we could find no solvent system that enabled decolourizing of the salts. Clearly, the ability to wet the decolourizing charcoal is a key issue and may explain why the ionic liquids are so difficult to clean-up once prepared.

The only other issue we had was the difficulty in obtaining useful yields in the synthesis of halide-free, water-miscible ionic liquids. Extraction using dichloromethane is tedious using simple extraction funnels. However, quantitative yields can be obtained using liquid–liquid continuous extractors. This straightforward modification to the extraction enables multiple rewashing of the ionic liquid and the systematic removal of the halide as determined by a silver halide test and mass spectrometry. We also filter the liquid through silica, and it is likely that the filtration through silica does more to remove the

salts than the water washing. We employ both due to the simple nature of the whole process.

We produce our own cations from alkylation using alkyl bromides and alkyl chlorides. This gives more control over the process. However, even commercial cation sources produce excellent ionic liquids when they are purified using this method. The purity of the ionic liquids can be judged using a variety of spectroscopic techniques.

UV-Vis spectroscopy is the simplest method to determine optical purity in the ionic liquids. Fig. 2 shows the UV-Vis spectrum for 1-butyl-1-methylpyrrolidinium bis(trifluoromethanesulfonyl)amide. This spectrum was performed using a neat sample (1 cm pathlength) and it is apparent that in the pure material there is no absorbance above 300 nm as shown in Fig. 2. This is the same for all of the ionic liquids described here. The solids can be examined using saturated aqueous solutions. If there is significant absorption above 350 nm the ionic liquid is impure.

Fluorescence spectroscopy is perhaps the most sensitive method for determining the purity of an ionic liquid. The fluorescence spectra of two commercial samples of 1-butyl-1-methylpyrrolidinium bis(trifluoromethanesulfonyl)amide (A and B), and a sample prepared using our synthesis (C) are shown in Fig. 3. We have observed that it is possible to reduce the fluorescence of the ionic liquids to effectively zero by systematic purification of the precursor salts. For the lowest fluorescence response it is necessary to take particular care with all aspects of the synthesis. For example, we initially filtered the aqueous solutions through Celite to remove the charcoal. However, we found that we obtained materials with lower fluorescence background when we do not use Celite – filter paper is sufficient. For convenience it is possible to judge the level of fluorescence impurity in the ionic liquid by exposing a sample to UV light from a hand scanner at 380 nm. If the ionic liquid has significant impurities it will fluoresce visibly.

The simple electrochemistry of ionic liquids provides a very quick indicator of the general purity. It is not necessary to even use an accurate reference electrode since a cyclic voltammogram scan provides the information required. We generally

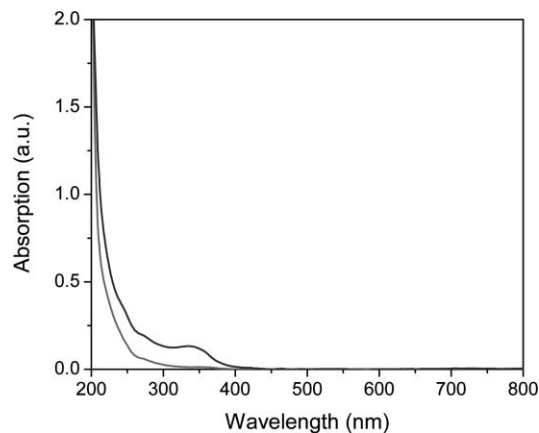


Fig. 2 UV-Vis spectrum of neat 1-butyl-1-methylpyrrolidinium bis(trifluoromethanesulfonyl)amide (the upper trace is commercial high purity grade, the lower trace is prepared in our laboratory).

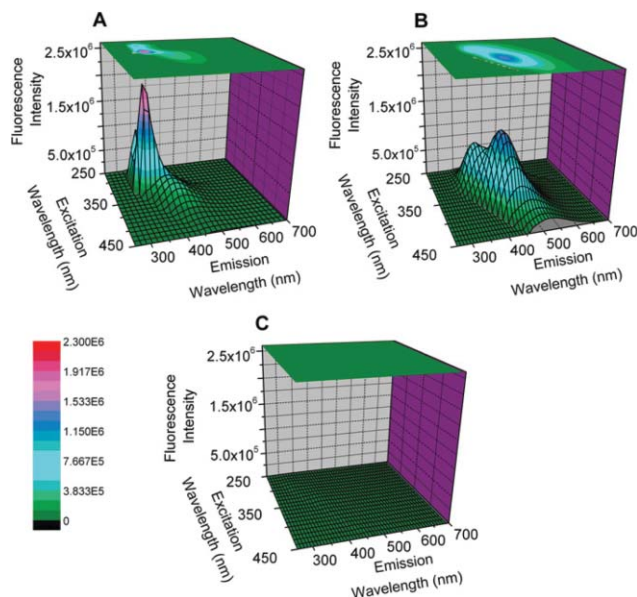


Fig. 3 Fluorescence spectra of 1-butyl-1-methylpyrrolidinium bis(trifluoromethanesulfonyl)amide, commercial samples (A and B) and a sample prepared in our laboratory (C).

employ a platinum working electrode, a platinum counter electrode and a silver wire as the reference electrode. All we are interested in is the electrochemical window and the current therein. Fig. 4 shows the cyclic voltammogram of clean 1-butyl-1-methylpyrrolidinium bis(trifluoromethanesulfonyl)amide.

Nuclear magnetic resonance spectroscopy is the most common method for characterizing ionic liquids. It is, however, the least useful for judging purity. Spectra of dark yellow ionic liquids generally look as clean as those which have no UV-Vis absorbance as seen in Fig. 5. It should be remembered that NMR cannot readily identify compounds present at less than 1%. So while NMR is a useful characterization tool, it is not an appropriate method for judging anything but gross purity.

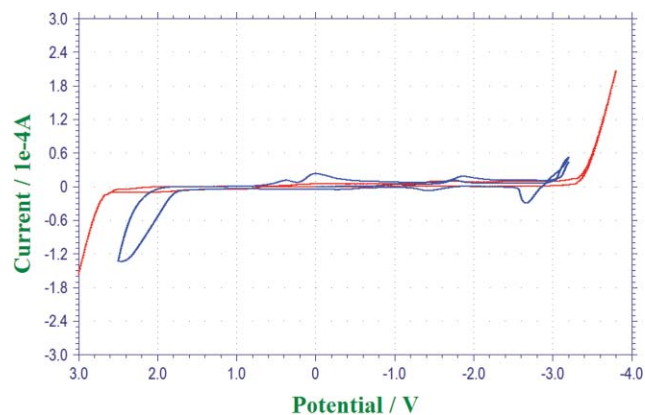


Fig. 4 Cyclic voltammogram of neat 1-butyl-1-methylpyrrolidinium bis(trifluoromethanesulfonyl)amide (blue is commercial, red is prepared in our laboratory), platinum working electrode, platinum counter electrode and a silver reference electrode scanned at 50 mV s⁻¹.

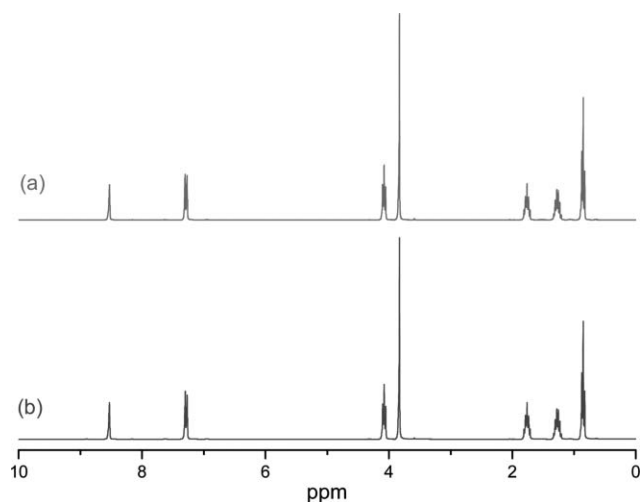


Fig. 5 ^1H NMR spectra of 1-butyl-3-methylimidazolium bis(trifluoromethanesulfonyl)amide, colourless sample (a) and yellow sample (b).

In the materials we have examined the issue of quantifying the levels of impurities is always problematic. Without a clear understanding of the nature of the impurity it is impossible to accurately determine the level of impurities in any given sample. In the material prepared in this report we have determined the levels of water to be less than 20 ppm. We estimate the levels of coloured impurities at less than 25 ppm, based upon a scenario of a highly coloured dye impurity with an $\epsilon = 50\,000\text{ L mol}^{-1}\text{ cm}^{-1}$. It is even more difficult to predict the levels of fluorescence impurities but we estimate that they will not be greater than the coloured impurities at 25 ppm. Halide impurities are generally present at less than 20 ppm.

Conclusions

The purity of ionic liquids has been the bane of many chemists and materials scientists almost since their discovery. In many cases the impurities present at the sub 1% level are not a cause

for concern. However, with more specialized applications, such as spectroscopy, electrochemistry, catalysts and where reaction kinetics are an issue, this is not the case. We have seen examples where incorrect assumptions have been derived from data collected from impure ionic liquids. How many other cases where negative data were obtained for reactions involving ionic liquids are due to the impurities? We would recommend that those who are doing research where the purity of ionic liquids may be important should at least examine the UV-Vis spectroscopy and quote those data in their publications.

Acknowledgements

This work was supported by the Department of Energy Buildings Technology Program. G. A. B. acknowledges generous support by a Frederick Reines Fellowship. R. E. D. S. wishes to acknowledge the LANL Director's Fellowship for support.

References

- 1 *Ionic Liquids, Industrial Applications for Green Chemistry*, ed. R. D. Rogers and K. R. Seddon, American Chemical Society, Washington DC, 2002; T. Welton, *Chem. Rev.*, 1999, **99**, 2071–2083.
- 2 B. M. Quinn, Z. Ding, R. Moulton and A. J. Bard, *Langmuir*, 2002, **18**, 1734–1742.
- 3 J. Qu, J. J. Truhan, S. Dai, H. Luo and P. J. Blau, *Tribology Lett.*, 2006, **22**, 207–214.
- 4 R. E. Del Sesto, G. A. Baker, S. N. Baker, B. L. Scott, T. S. Keizer, A. K. Burrell and T. M. McCleskey, *Chem. Commun.*, 2006, 272–274; B. P. Warner, T. M. McCleskey, A. Agrawal, J. P. Cronin, J. C. L. Tonazzi and A. K. Burrell, *US Pat.*, 2005, 6,853,472.
- 5 P. Nockemann, K. Binnemans and K. Driesen, *Chem. Phys. Lett.*, 2005, **415**, 131–136.
- 6 X. Creary and E. D. Willis, *Org. Synth.*, 2005, **82**, 166.
- 7 A. Paul, P. K. Mandal and A. Samanta, *Chem. Phys. Lett.*, 2005, **402**, 375–379.
- 8 M. J. Earle, J. M. S. S. Esperanca, M. A. Gilea, J. N. Canongia Lopes, L. P. N. Rebelo, J. W. Magee, K. R. Seddon, R. Kenneth and J. A. Widegren, *Nature*, 2006, **439**, 831–834.
- 9 V. Farmer and T. Welton, *Green Chem.*, 2002, **4**, 97.

Gaining pH-control in water/carbon dioxide biphasic systems

Christoph Roosen,^{ab} Marion Ansorge-Schumacher,^c Thomas Mang,^a Walter Leitner^b and Lasse Greiner^{*b}

Received 14th September 2006, Accepted 8th January 2007

First published as an Advance Article on the web 30th January 2007

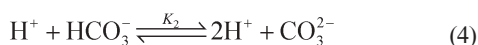
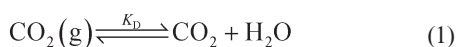
DOI: 10.1039/b613345b

Utilizing the biphasic system water/CO₂ as a reaction and extraction medium is of rising importance, because of its advantages as a green solvent combination. The problem of predictable pH control in the aqueous phase has to be addressed in view of optimized reaction conditions. The control is possible up to a pH of approximately 6 by means of buffer salts, and the resulting pH can be predicted by an algebraic equation.

1 Introduction

The application of supercritical fluids (scF) in chemical synthesis and processes¹ is finding increasing attention as media for extraction and separation,^{2–5} two-phase catalysis, homogeneous and enzymatic catalysis in multiphase approaches,^{6,7} and heterogeneous catalysis.^{8,9} In particular, the use of carbon dioxide is interesting because of its critical parameters at moderate temperature and pressure ($\theta_c = 304.2$ K and $p_c = 7.375$ MPa). Furthermore, CO₂ is intrinsically safe, non-toxic, economically attractive, environmentally benign, and can easily be removed.^{10,11} For these reasons it is particularly suitable for multiphase catalysis and continuous reactions.^{7,12,13}

It could be shown that CO₂ can efficiently be used for supercritical CO₂/aqueous biphasic reactions,^{14,15} inverted supercritical CO₂/aqueous biphasic reactions^{16,17} and enzymatic reactions under supercritical conditions.^{6,18} Intrinsically, the combination of CO₂ with water leads to the formation and dissociation of carbonic acid, resulting in low pH values of about 3.¹⁹



For acid promoted reactions this can be beneficial,^{20,21} but has also led to frustration for systems requiring neutral conditions.^{14,16} Control of pH is generally important for all aqueous reactions and especially for enzymes, as they mostly exhibit their highest catalytic activity and stability near neutrality. Thus, it is important not only to determine the aqueous pH, but also to be able to predictably shift the pH towards acceptable working points.²² Therefore we investigated the possibilities of measuring pH directly, its buffering and the prediction from starting conditions. We present a

simple means for buffering up to a pH of 6, and an algebraic equation for the prediction of pH from starting conditions.

2 Results and discussion

Eqn (1) to (4) show that the concentration of carbonic acid is dependent on the amount of dissolved CO₂, which is a function of temperature and partial pressure of CO₂ in the gas phase. Therefore, the carbonic acid concentration at a given temperature and pressure is constant. The dissociation of carbonic acid (eqn (3)) is the key step for pH in the system CO₂/water. The extent of dissociation, and thus the formation of protons can be influenced by bicarbonate concentration:^{19,23,24}

$$[\text{H}^+] = \frac{K_1 [\text{H}_2\text{CO}_3]}{a(\text{HCO}_3^-)} \quad (5)$$

Utilization of HCO₃[−]-salts should therefore be suitable as a buffer in the system water/scCO₂.

To confirm this, pH measurements were conducted in two different ways. A specifically designed autoclave equipped with a process pH-electrode was used for pressures up to 8 MPa and temperatures of 333 K (Fig. 1). The separation of compartments allowed for a slight overpressure, excluding CO₂ from the electrode room. By balancing the pressure between the two compartments within 0.1 MPa, safe handling of the glass electrode could be ensured. Measurements were carried out for two temperatures and a range of pressures (Table 1). For pressures up to 25 MPa semi-quantitative measurements of the

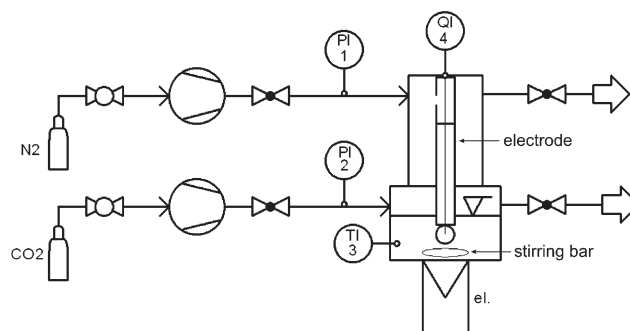


Fig. 1 Autoclave setup for pH-measurements with glass electrodes (PI: pressure, TI: temperature, QI: pH).

^aFH Aachen, IAP, Worringerweg 1, Aachen, 52074, Germany

^bRWTH Aachen University, ITMC, Worringerweg 1, Aachen, 52074, Germany. E-mail: greiner@itmc.rwth-aachen.de

^cTU Berlin, TC4/Enzyme Technology, Straße des 17. Juni 124, Berlin, 10623, Germany

Table 1 pH as a function of carbon dioxide partial pressure

p/MPa	pH 295 K	pH 333 K
0.1	3.94	—
0.2	3.86	—
0.3	3.78	—
0.7	3.65	—
1.0	3.53	3.64
2.0	3.34	3.50
3.0	3.27	3.39
4.0	3.23	3.33
5.0	3.19	3.29
6.0	—	3.26
7.0	—	3.24
8.0	—	3.20

pH have been carried out utilizing proton sensitive dyes in a window equipped autoclave (see Fig. 2). Such measurements can be quantified by UV/Vis-spectrometry.²⁵

Dependency of pH on pressure shows that the higher the CO₂ pressure is, the lower the pH-values are. By addition of bicarbonate, the saturation pH can be shifted towards pH values of approximately 6 (Fig. 3). Notably, even comparably low concentrations of HCO₃⁻ of 0.005 mol L⁻¹ stabilize the pH at 4. The pH obtained is dependent on the starting bicarbonate concentration, and slightly on pressure (Fig. 4). The apparent hyperbolic dependency of pH on pressure indicates the non-ideal behavior of CO₂, as solubility is not further increased with rising pressure, as would be expected from Henry's law. Nonetheless, the experimental data is in good agreement with the values predicted by eqn (9) (*vide infra*). The general trend and the buffer ability of bicarbonate is also demonstrated by the measurements with proton sensitive dyes at elevated pressures (Fig. 2).

The relevance of pH-control for reactive systems in water/CO₂ was shown by using the catalytic racemization of (*R*)-benzoin as a probe (Fig. 5).²⁶ For that we used the ruthenium based catalyst first proposed by Shvo and coworkers.²⁷ The reaction rate is dependent on pH, expressed by the time, t_{50} , to decrease the enantiomeric excess from >99% to 50%. Under

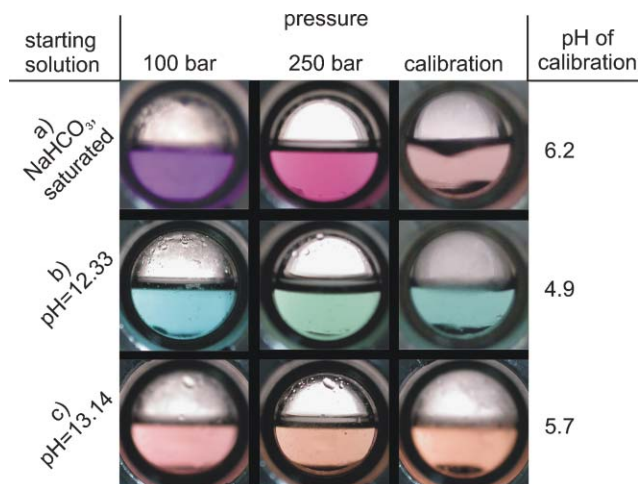


Fig. 2 pH-measurements with indicators; (a) Bromocresol Purple, (b) Bromocresol Green, (c) Bromocresol Purple.

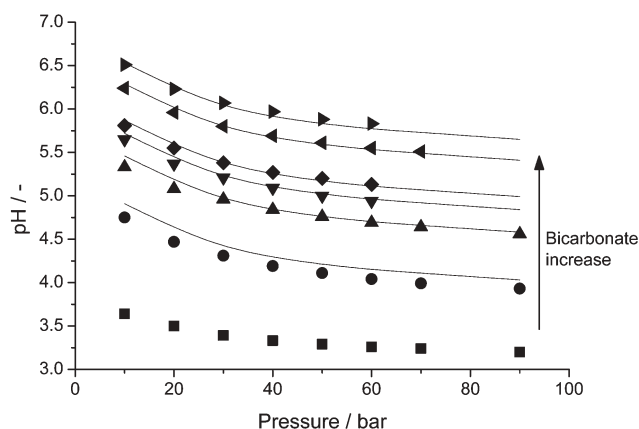


Fig. 3 Determination of pH with pressure at 333 K. Dots are the measured values, the solid lines represent pH calculated according to eqn (9); (concentrations: 0, 0.005, 0.02, 0.04, 0.06, 0.2, 0.4 mol L⁻¹).

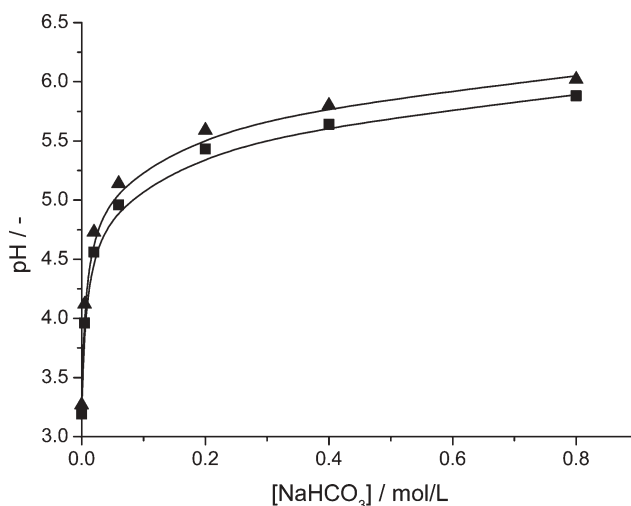


Fig. 4 Determination of pH with the concentration of NaHCO_3 at 295 K; points denote experimental values, the solid line represents pH calculated according to eqn (9) (triangle: 3.0 MPa, rectangle: 5.0 MPa).

unbuffered reaction conditions the t_{50} was 345 h at a temperature of 343 K and CO_2 -pressure of 22.0 MPa. The addition of $0.4 \text{ mol L}^{-1} \text{ NaHCO}_3$ increased the reaction rate, with $t_{50} = 142 \text{ h}$ at the same temperature and pressure.

The experimental results demonstrate that an increase in bicarbonate concentration leads to a decrease in H^+ -concentration, and therefore to an increase in pH. To predict the pH at a certain bicarbonate concentration, eqn (5) can be extended, taking into account that both K_1 and the HCO_3^- -concentration are dependent on the ionic strength I of the

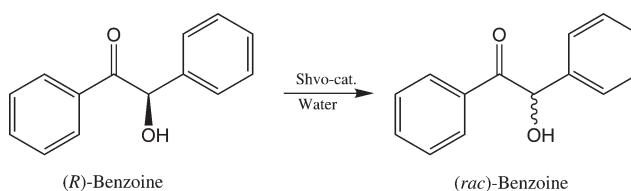


Fig. 5 Catalytic racemization of benzoin by Shvo's catalyst.

solution. K_1 is further dependent on the charge of the conjugate acid species z_a :²⁸

$$pK'_1 = pK_1 + (2z_a - 1) \left[\frac{A\sqrt{I}}{(1 + \sqrt{I})} - \frac{I}{10} \right] \quad (6)$$

and

$$K'_1 = 10^{(-pK'_1)} \quad (7)$$

with pK'_1 as the modified pK_1 value and A the Debye–Hückel parameter. The ionic strength can be calculated by:

$$I = \frac{1}{2} \sum_i c_i z_i^2 \quad (8)$$

where c_i is the concentration and z_i the charge of the ionic species. By using these equations to determine K_1 the pH can be predicted as a function of unbuffered pH, the amount of initial bicarbonate concentration $c(\text{HCO}_3^-)_{\text{added}}$, and I

$$\text{pH} = 2 \text{pH}_{\text{unbuffered}} + \log \left(c(\text{HCO}_3^-)_{\text{added}} \right) - \frac{\sqrt{I}}{1 + \sqrt{I}} \left(A + \frac{1}{2} \right) + \frac{I}{10} \quad (9)$$

for $c(\text{HCO}_3^-)_{\text{added}} \geq 0.005$ M. Lower additions are not of practical relevance for buffering purposes and are not covered by experimental values. Predicted and measured values are in good agreement considering the simple semi-empirical prediction of pH (Fig. 6).

Conclusion

Prediction and control of pH for the biphasic system of carbon dioxide and water was demonstrated for pressures up to 25.0 MPa. The simple semi-empirical prediction of pH derived here is in good accordance with experimental findings. The relevance for chemical synthesis was further demonstrated by the rate increase of a pH-dependent reaction. The results of this study allow the optimization of reactions with respect to

pH, and pave the way for the beneficial use of CO_2 in conjunction with aqueous systems.

3 Experimental

Safety warning: The use of highly compressed gases such as supercritical fluids must be conducted only with suitable high pressure equipment under appropriate safety conditions.

The indicators were obtained from Sigma–Aldrich GmbH and used as received. Gases were of at least 99.995% purity and used without further purification. Sodium bicarbonate was obtained from Merck. Calibration buffers were obtained from Riedel-de Haën. Deionized water was used in all experiments. The electrodes Polilyte Pro XP (Hamilton, Bonaduz/CH) and HA405-60-RB/130/3m (Mettler–Toledo GmbH, Giessen/D) were used for pH-measurements. The autoclave (mechanical workshop of the institute) was made of stainless steel and had a volume of 20 mL. The autoclave was heated to the desired temperature by placing it on a heating plate. The glass electrode was then calibrated with 15 mL calibration buffers (pH 4 and pH 7). The lower compartment was filled with 15 mL of the aqueous solution and closed. Under stirring, the lower and upper compartment were slowly pressurized with O_2 and nitrogen, respectively. The N_2 pressure was typically maintained at a differential pressure of 0.1 MPa. Readings were taken after 10 minutes equilibration time. Substituting carbon dioxide with nitrogen showed no dependency of measured values on pressure.

Shvo's catalyst (1-hydroxytetraphenylcyclopentadienyl-(tetraphenyl-2,4-cyclopentadien-1-one)- μ -hydrotetracarbonyl-diruthenium (II); CAS: 104439-77-2) was prepared according to the literature, as confirmed by ^1H - and ^{13}C -NMR spectroscopy (Bruker AMX-300).²⁹ A saturated (*R*)-Benzoin solution in water was prepared and Shvo's catalyst was added (0.9 mol L^{-1}). For buffering, sodium bicarbonate was added ($c(\text{NaHCO}_3) = 0.4 \text{ mol L}^{-1}$). The preheated autoclave ($T = 343 \text{ K}$) was filled with 5 mL of either solution and pressurized with carbon dioxide. Samples were analysed by HPLC as described elsewhere.²²

Acknowledgements

We thank M. Kaever and R. Thelen (both RWTH Aachen University) for technical support. This work was financially supported by Arbeitsgemeinschaft industrieller Forschungsvereinigungen "Otto von Guericke" e.V. (AiF) through "TRAFO", the Deutsche Forschungsgemeinschaft through SFB540 (www.sfb540.rwth-aachen.de) and Graduiertenkolleg 1166 (www.bionoco.org). We, furthermore, thank T. Hischer and A. van den Wittenboer (Biotechnology/RWTH Aachen University) for providing the (*R*)-Benzoin and Volker Donath (Mettler–Toledo GmbH) for discussion and technical support.

References

- 1 *Chemical Synthesis using supercritical fluids*, ed. P. G. Jessop and W. Leitner, Wiley-VCH, Weinheim, 1999.
- 2 K. Zosel, *Angew. Chem.*, 1978, **90**, 748–755.
- 3 M. A. McHugh and V. J. Krukonis, *Supercritical Fluid Extraction: Principles and Practice*, Butterworth, Stoneham, MA, USA, 1986.

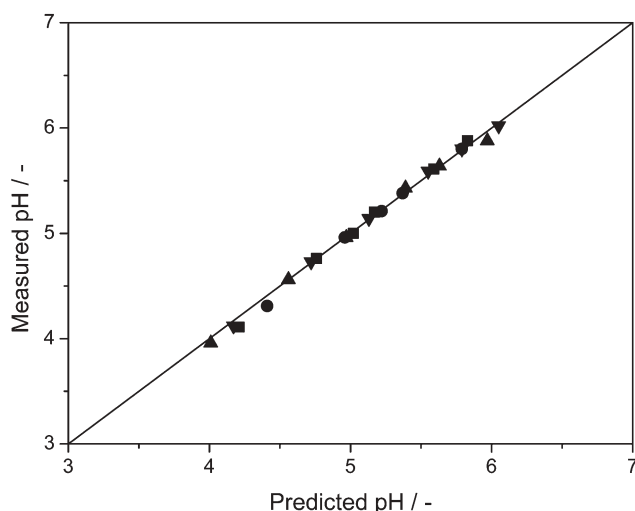


Fig. 6 Comparison of predicted and measured pH.

- 4 C. C. Tzschucke, C. Markert, W. Bannwarth, S. Roller, A. Hebel and R. Haag, *Angew. Chem., Int. Ed.*, 2002, **41**, 3964–4000.
- 5 J. da Cruz Francisco and E. S. Dey, *Acta Microbiol. Pol.*, 2003, **52**, 35–43.
- 6 A. Mesiano, J. E. J. Beckman and A. J. Russel, *Chem. Rev.*, 1999, **99**, 623–634.
- 7 *Multiphase homogeneous catalysis*, ed. B. Cornils, W. A. Herrmann, I. T. Horvath, W. Leitner, S. Mecking, H. Olivier-Bourbigou and D. Vogt, Wiley-VCH, Weinheim, 2005.
- 8 A. Baiker, *Chem. Rev.*, 1999, **99**, 453–473.
- 9 J. R. Hyde, P. Licence, D. Carter and M. Poliakoff, *Appl. Catal., A*, 2001, **222**, 119–131.
- 10 W. Leitner, *Acc. Chem. Res.*, 2002, **35**, 746.
- 11 N. Tanchoux and W. Leitner, in *Handbook of Green Chemistry and Technology*, ed. J. Clark and D. MacQuarrie, Blackwell Science, Oxford, UK, 2002, pp. 482–501.
- 12 W. Leitner, *Pure Appl. Chem.*, 2004, **76**, 635–644.
- 13 D. J. Cole-Hamilton, *Science*, 2003, **299**, 1702–1706.
- 14 D. A. Morgenstern, R. M. LeLacheur, D. K. Morita, S. L. Borkowsky, S. Feng, G. H. Brown, L. Luan, M. F. Gross, M. J. Burk and W. Tumas, in *Green Chemistry*, ed. P. T. Anastas and T. C. Williamson, ACS, New York, 1996, p. 132.
- 15 D. Hâncu and E. J. Beckman, *Green Chem.*, 2001, **3**, 80–86.
- 16 M. McCarthy, H. Stemmer and W. Leitner, *Green Chem.*, 2002, **4**, 501–504.
- 17 K. Burgemeister, G. Francio, V. H. Gego, L. Greiner, H. Hugl and W. Leitner, *Chem.–Eur. J.*, 2007, **13**, DOI: 10.1002/chem.200601717.
- 18 M. T. Reetz, W. Wiesenhöfer, G. Francio and W. Leitner, *Adv. Synth. Catal.*, 2003, **345**, 1221–1228.
- 19 J. D. Holmes, K. J. Ziegler, M. Audriani, C. T. J. Lee, P. A. Bhargava, D. C. Steytler and K. P. Johnston, *J. Chem. Phys.*, 1999, **103**, 5703–5711.
- 20 B. Ganchegui and W. Leitner, *Green Chem.*, 2007, **9**, 26–29.
- 21 Y. Liu, P. G. Jessop, M. Cunningham, C. A. Eckert and C. L. Liotta, *Science*, 2005, **313**, 958–960.
- 22 M. B. Ansorge-Schumacher, L. Greiner, F. Schroeper, S. Mirtschin and T. Hischer, *Biotechnol. J.*, 2006, **1**, 564–568.
- 23 J. D. Holmes, D. C. Steytler, G. D. Rees and B. H. Robinson, *Langmuir*, 1998, **14**, 6371–6376.
- 24 K. J. Ziegler, J. P. Hanrahan, J. D. Glennon and J. D. Holmes, *J. Supercrit. Fluids*, 2003, **27**, 109–117.
- 25 K. L. Toews, R. M. Shroll, N. G. Smart and C. M. Wai, *Anal. Chem.*, 1995, **67**, 4040–4043.
- 26 P. Hoyos, M. Fernández, J. V. Sinisterra and A. R. Alcántara, *J. Org. Chem.*, 2006.
- 27 Y. Blum, D. Czarkie, Y. Rahamim and Y. Shvo, *Organometallics*, 1985, **4**, 1459–1461.
- 28 R. J. Beynon, *Buffer Solutions: The Basics*, Oxford University Press, Oxford, UK, 1996.
- 29 M. J. Mays, M. J. Morris, P. R. Raithby, Y. Shvo and D. Czarkie, *Organometallics*, 1989, **8**, 1162–1167.

Baeyer–Villiger oxidation of substituted cyclohexanones *via* lipase-mediated perhydrolysis utilizing urea–hydrogen peroxide in ethyl acetate†

María Yolanda Ríos, Enrique Salazar and Horacio F. Olivo*

Received 18th December 2006, Accepted 8th February 2007

First published as an Advance Article on the web 23rd February 2007

DOI: 10.1039/b618175a

A green method for Baeyer–Villiger oxidation based on the chemo-enzymatic perhydrolysis of carboxylic acids and esters has been optimized using Novozyme-435, the immobilized form of *Candida antarctica* lipase B, and the complex urea–hydrogen peroxide (UHP) in ethyl acetate. This protocol previously employed for the chemo-enzymatic epoxidation of unfunctionalized olefins was shown to be effective for the Baeyer–Villiger oxidation of cyclohexanone and substituted cyclohexanones. The absence of water in the reaction media avoided any hydrolysis of the oxidized product. A minimum amount of enzyme was necessary to show the catalytic effect. The reaction yields of substituted ϵ -caprolactones varied depending on the nature of the substituent.

Introduction

The Baeyer–Villiger oxidation is a powerful tool for the preparation of lactones, which are important building blocks for the synthesis of natural products and many biologically significant molecules.¹ Currently, *m*-chloroperoxybenzoic acid (*m*-CPBA) is considered to be the work-horse for the Baeyer–Villiger oxidation.² However, *m*-CPBA is expensive, shock sensitive, and a potential explosive, which limits its commercial application.³ Several alternative methods have been developed for Baeyer–Villiger oxidations utilizing transition metal catalysts, organocatalysts, biocatalysts, *etc.*⁴ Considering atom-economy, efficiency factor, and sustainability, biocatalysis offers a green chemistry alternative to the Baeyer–Villiger oxidation.⁵

Various biocatalysts have been shown to catalyze Baeyer–Villiger oxidations, and monooxygenases have been the enzymes of choice.⁴ However, their dependence on a co-factor requires whole-cell biotransformation, where additional enzymes may be involved in unwanted side reactions, thereby increasing the complexity of the process.^{4c} An alternative and more practical method for Baeyer–Villiger oxidation is the *in situ* generation of peroxy acids through lipase-mediated perhydrolysis of carboxylic acids and esters.^{6,7} Several peroxycarboxylic acids were generated *via* a two-phase system of a medium-chain carboxylic acid in toluene or hexane and aqueous hydrogen peroxide in the presence of immobilized *Candida antarctica* lipase B on acrylic resin (Novozyme-435).⁸ Novozyme-435 is the most popular lipase for peroxidation owing to its stability in organic solvents and the ability to peroxidize various medium-chain carboxylic acids.⁹ The peroxycarboxylic acids generated *in situ* under mild conditions were able to oxidize alkenes,^{9–11} ketones,^{6,7} and sulfides.^{9b}

Roberts' group initially reported the Baeyer–Villiger oxidation of a range of cyclic ketones employing the lipase-mediated perhydrolysis in toluene, utilizing stoichiometric amounts of myristic acid and a four-fold excess of 30% aq. hydrogen peroxide.⁶ The reaction was slow (six days) and the yields were slightly lower than those obtained with *m*-CPBA. In addition, hydrogen peroxide was found to be toxic to the enzyme, and it had to be delivered slowly over a period of 10 h. Guibé-Jampel's group reported the autocatalytic Baeyer–Villiger oxidation of several 2-substituted cyclohexanones to investigate the enantioselective synthesis of lactones and hydroxycarboxylic acids.⁷ In this lipase-mediated oxidation, the non-toxic and anhydrous urea–hydrogen peroxide (UHP)^{12,13} was utilized as an oxidant, which could be added in one portion (compared to slow addition of aq. hydrogen peroxide) and was shown to give better conversions in a given time. In this method, Novozyme-435 was initially impregnated with ketone and then treated with a ten-fold excess of UHP, avoiding the use of a medium-chain carboxylic acid and solvent. Enantiomerically enriched lactones were obtained in 20–60 ee% and 20–50% isolated yields after approximately two days.

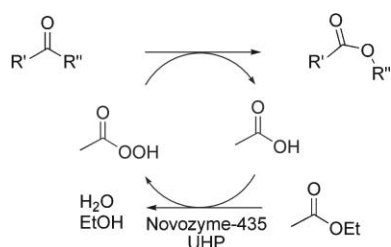
The lipase-mediated Baeyer–Villiger oxidation shows great promise for industrial applications, but higher conversions and optimization of reagents is required to compete with chemical and enzymatic mediated oxidations. The use of contaminant and toxic solvents must be replaced with more benign solvents and the use of toxic reagents such as peroxy acids has to be minimized to make the process green. As part of our program in environmentally beneficial catalysis,¹⁴ we report a new approach for lipase-mediated Baeyer–Villiger oxidations that minimizes its environmental footprint and cost.

Results and discussion

Baeyer–Villiger oxidations were performed using ethyl acetate, both as a reagent and as a solvent, by the chemo-enzymatic approach (Scheme 1).¹⁴ We selected ethyl acetate to be the solvent of choice because of its low boiling point, ability to

Medicinal and Natural Products Chemistry, The University of Iowa, Iowa City, Iowa, 52242, USA. E-mail: horacio-olivo@uiowa.edu; Fax: +1 (319) 335 8766; Tel: +1 (319) 335 8849

† Electronic supplementary information (ESI) available: Copies of ¹H- and ¹³C-NMR spectra for caprolactones 1–10. See DOI: 10.1039/b618175a



Scheme 1

dissolve many substrates, environmental friendliness, and non-toxicity. Novozyme-435 was used to generate peroxyacetic acid from ethyl acetate (or by recycling acetic acid formed in the reaction) using UHP as the oxidant. The peroxyacetic acid formed oxidizes cyclic ketones to the corresponding lactones forming acetic acid, which can be recycled. The amounts of reagents, enzyme, UHP and ethyl acetate, were optimized by studying their effect on the conversion of ketones to lactones. Novozyme-mediated resolution of substituted caprolactones was used to obtain enantiomerically enriched lactones *via* hydrolysis¹⁵ or butanolysis in a solvent-free system.¹⁶

Effect of the amount of enzyme

The amount of enzyme was varied from 0 to 50 mg to study its effect on the chemo-enzymatic Baeyer–Villiger oxidation of 0.5 mmol of 2-phenyl cyclohexanone in 1.5 cm³ of ethyl acetate (Fig. 1). The reactions were carried out with 0, 10, 20, 30, 40, and 50 mg of Novozyme-435. The conversion was measured after 24 h of stirring the mixture at room temperature. We observed that the conversion increases rapidly as the amount of enzyme was increased (up to 20 mg) and then the conversion slowed down. These results show that the enzyme-mediated formation of peroxyacetic acid could be the rate limiting step when a small amount of enzyme is available (less than 20 mg). However, when the amount of enzyme increases (more than 30 mg), the peroxyacetic acid chemical oxidation of the ketone becomes the rate limiting step. Therefore, we decided to use 20 mg of enzyme for further experiments. This amount of enzyme employed is much less compared to that used by

Roberts' group (125 mg)⁶ and Guibé-Jampel's group (250 mg) for 0.5 mmol of substrate.⁷

Effect of the amount of UHP

The amount of UHP was varied to study its effect on the chemo-enzymatic Baeyer–Villiger oxidation of 2-phenyl cyclohexanone. The reaction was run with one, two, and three equivalents of UHP (Fig. 1). We observed that at small amounts of enzyme (10 mg), the conversion was higher when only one equivalent of UHP was used. Interestingly, the conversion was higher when two or three equivalents of UHP and higher amounts of enzyme (>20 mg) were added. Conversions were consistently higher with two equivalents of UHP instead of three. To further study the effect, experiments were performed using the same amount of enzyme (25 mg) and 0 to 6 equivalents of UHP in two different volumes of ethyl acetate (Fig. 2). The conversion increases rapidly as the UHP equivalents increase from 0 to 2 and then it slightly decreases from 2 to 6 equivalents. Although only one equivalent of UHP is required in the reaction, the use of two equivalents was shown to improve the conversion. As expected, we observed that the reaction is slower at higher dilution (3 cm³ of ethyl acetate). A minimum amount of solvent (1.5 cm³) was used to ensure that the enzyme and the UHP were completely immersed in the solvent.

Baeyer–Villiger oxidations

The optimized amounts of the reagents were used to oxidize several substituted cyclohexanones, Table 1. We utilized two equivalents of UHP and 25 mg of Novozyme-435 in 1.5 cm³ of ethyl acetate to oxidize 0.5 mmol of cyclic ketones. Good to excellent yields were obtained utilizing this chemo-enzymatic approach. However, the chemo-enzymatic Baeyer–Villiger oxidation is considerably slower than the oxidation utilizing *m*-chloroperoxybenzoic acid in dichloromethane. Reactions are relatively fast when no substituent, a small substituent, an allyl, a phenyl or a benzyl group is found next to the carbonyl group (entries 1–3 and 6–8). Because the chemo-enzymatic epoxidation of terminal alkenes is very slow,¹⁴ no epoxidation was observed when the cyclohexanone was bearing an allyl group (entry 6). The reaction was slower when large groups are

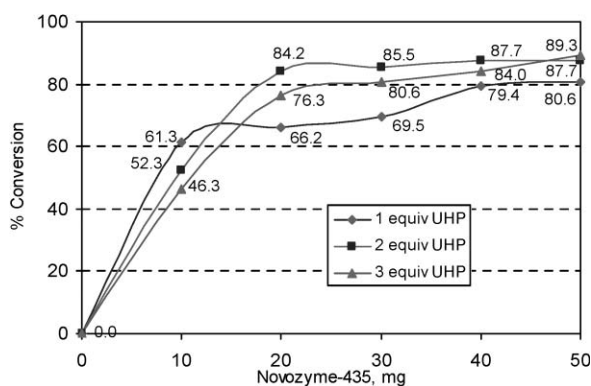


Fig. 1 Effect of the amount of Novozyme-435 and UHP on Baeyer–Villiger oxidation. Conditions: 0.5 mmol of 2-phenyl cyclohexanone, 1.5 cm³ of ethyl acetate, time = 24 h.

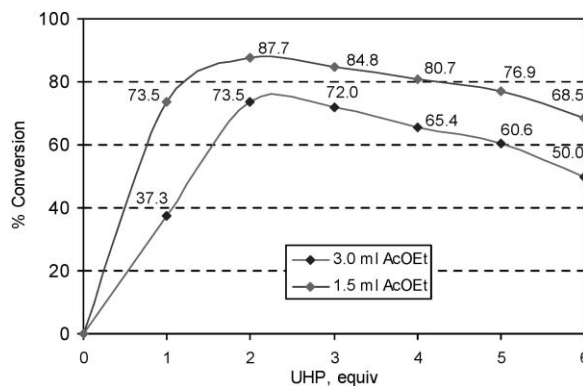
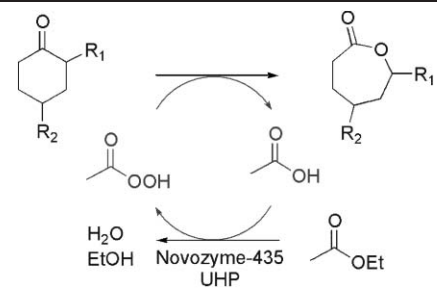


Fig. 2 Effect of the amount of UHP on Baeyer–Villiger oxidation. Conditions: 0.5 mmol 2-phenyl cyclohexanone, 25 mg Novozyme-435, time = 24 h.

Table 1 Baeyer–Villiger oxidation of cyclohexanone and substituted cyclohexanones


Entry	Ketone	Epoxide	Time/d	Yield (%)
1			6	80
2			8	75
3			3	95
4			12 19	68 78
5			26	8
6			3 6	85 92
7			5	93
8			1 3	88 94
9			9	96
10			15	28

substituted alpha to the ketone (entries 4 and 5). When tetralone was subjected to the chemo-enzymatic oxidation, only a small amount of lactone was observed after 15 days. We observed clean conversions of cyclohexanones to the corresponding caprolactones by ^1H - and ^{13}C -NMR spectroscopy.¹⁷ No ring opening polymerization of the caprolactones, hydrolysis, or alcoholysis was observed under the reaction conditions employed.

Conclusions

In summary, we presented an environmentally benign chemo-enzymatic Baeyer–Villiger oxidation of cyclohexanone and substituted cyclohexanones. The lipase-mediated perhydrolysis of ethyl acetate generates peracetic acid *in situ*, which oxidizes cyclohexanones to the corresponding lactones. The reaction is carried out in a non-chlorinated solvent utilizing mild conditions. The reaction times and yields of these oxidations were shown to depend on the nature of the substituent.

Experimental section

General method for chemo-enzymatic Baeyer–Villiger oxidation

To a solution of ketone (0.5 mmol) in ethyl acetate (1.5 cm³) in a test tube was added urea–hydrogen peroxide (1 mmol) and Novozyme-435 (25 mg). The test tube was closed tightly and placed in a shake-table at 27 °C and 250 rpm. The reactions were monitored by thin layer chromatography and ^1H -NMR. The reaction was stopped by diluting with diethyl ether and filtering through a plug of cotton. The organic solution was washed with water and 10% aq. sodium thiosulfate, dried over Na₂SO₄, filtered and the solvent evaporated under vacuum. The products were analyzed by ^1H - and ^{13}C -NMR.

ε-Caprolactone, 1

^1H -NMR (CDCl₃) δ 4.24 (2H, m), 2.65 (2H, m), 1.89–1.73 (6H, m); ^{13}C -NMR (CDCl₃) δ 176.7 (C, CO), 69.5 (CH₂, C-6), 34.6 (CH₂, C-2), 29.3 (CH₂), 29.0 (CH₂), 23.0 (CH₂).

4-Phenyl-ε-caprolactone, 2

^1H -NMR (CDCl₃) δ 7.26 (5H, m), 4.35 (2H, m), 2.81 (3H, m), 2.0–1.9 (3H, m), 1.9–1.7 (1H, m); ^{13}C -NMR (CDCl₃) δ 175.8 (C, CO), 145.1 (C), 128.9 (2CH), 127.0 (CH), 126.7 (2CH), 68.4 (CH₂), 47.3 (CH), 36.9 (CH₂), 33.8 (CH₂), 30.4 (CH₂);

6-Methyl-ε-caprolactone, 3

^1H -NMR (CDCl₃) δ 4.46 (1H, m), 2.72–2.57 (2H, m), 1.98–1.83 (3H), 1.72–1.55 (3H, m), 1.36 (3H, d, J = 6.4 Hz); ^{13}C -NMR (CDCl₃) δ 175.6 (CO), 76.8 (CH), 36.2 (CH₂), 35.0 (CH₂), 28.2 (CH₂), 22.9 (CH₂), 22.6 (CH₃).

6-sec-Butyl-ε-caprolactone (mixture of diastereomers), 4

^1H -NMR (CDCl₃) δ 4.23–4.10 (1H, m, H-6), 2.65 (2H, m, H-2), 2.06–1.78 (3H, m), 1.76–1.42 (5H, m), 1.35–1.13 (1H, m), 0.96 (3H, d, J = 7.0 Hz), 0.92 and 0.90 (3H, t, J = 7.2 Hz); ^{13}C -NMR (CDCl₃) δ 176.02, 175.95 (C, CO), 84.14, 83.32 (CH, C-6), 40.51, 39.88 (CH), 34.97, 34.93 (CH₂, C-2), 32.09, 30.60

(CH₂), 28.61, 28.51 (CH₂), 25.57, 24.84 (CH₂), 23.32 (CH₂), 14.65, 13.71 (CH₃), 11.82, 11.79 (CH₃).

6-*tert*-Butyl- ϵ -caprolactone, 5

¹H-NMR (CDCl₃) δ 3.76 (1H, d, J = 7.2 Hz, H-6), 2.64–2.47 (2H, m, H-2), 2.00–1.75 (3H, m), 1.60–1.27 (3H, m), 0.88 (9H, s); ¹³C-NMR (CDCl₃) δ 175.7 (C, CO), 88.0 (CH, C-6), 34.8 (C), 34.6, (CH₂, C-2) 29.3, (CH₂), 28.4 (CH₂), 25.7 (3CH₃), 23.3 (CH₂).

6-Allyl- ϵ -caprolactone, 6

¹H-NMR (CDCl₃) δ 5.9–5.7 (1H, m, H-b), 5.2–5.0 (2H, m, H-c), 4.27 (1H, dd, J = 6.4, 2.1 Hz, H-6), 2.72–2.55 (2H, m, H-2), 2.45 (1H, ddd, J = 13.0, 7.2, 6.6 Hz, H-a), 2.30 (1H, ddd, J = 13.0, 7.2, 6.6 Hz, H-a), 2.03–1.80 (3H, m) and 1.72–1.40 (3H, m) (H-3, H-4, H-5); ¹³C-NMR (CDCl₃) δ 175.5 (C, CO), 133.4 (CH, C-b), 118.1 (CH₂, C-c), 79.8 (CH, C-6), 40.6 (CH₂, C-a), 34.9 (CH₂, C-2), 33.8 (CH₂), 28.2 (CH₂), 22.9 (CH₂).

6-Benzyl- ϵ -caprolactone, 7

¹H-NMR (CDCl₃) δ 7.4–7.1 (2H, m, aromatic hydrogens), 4.44 (1H, dt, J = 8.7, 6.6 Hz, H-6), 3.06 (1H, dd, J = 13.9, 6.6 Hz, H-a), 2.80 (1H, dd, J = 13.9, 6.6 Hz, H-a), 2.60 (2H, m, H-2), 1.90 (3H, m), 1.55 (3H, m); ¹³C-NMR (CDCl₃) δ 175.4 (C, CO), 137.3 (C, C-1'), 129.6 (2CH, C-3', C-5'), 128.5 (2CH, C-2', C-6'), 126.7 (CH, C-4'), 81.2 (CH, C-6), 42.6 (CH₂, C-a), 34.9 (CH₂, C-2), 33.7 (CH₂), 28.2 (CH₂), 22.9 (CH₂).

6-Phenyl- ϵ -caprolactone, 8

¹H-NMR (CDCl₃) δ 7.3–7.1 (m, 5H, aromatic), 5.20 (1H, d, J = 9 Hz), 2.66 (2H, dd, J = 6.6, 4.0 Hz), 2.10–1.50 (6H, m); ¹³C-NMR (CDCl₃) δ 175.0 (C, CO), 140.9 (C), 128.6 (2CH), 128.1 (CH), 125.9 (2CH), 82.1 (CH, C-6), 37.5 (CH₂), 35.0 (CH₂), 28.6 (CH₂), 22.9 (CH₂).

6,6-Dimethyl- ϵ -caprolactone, 9

¹H-NMR (CDCl₃) δ 2.67–2.63 (2H, m, CH₂CO), 1.84–1.65 (6H, m, (CH₂)₃), 1.43 (6H, s, CH₃); ¹³C-NMR (CDCl₃) δ 175.0 (C, CO), 81.5 (C), 40.4 (CH₂), 37.3 (CH₂, C-2) 28.6 (2CH₃), 24.4 (CH₂), 23.5 (CH₂).

4,5-Dihydro-3H-benzo[*b*]oxepin-2-one, 10

¹H-NMR (CDCl₃) δ 7.28 (1H, m), 7.22–7.13 (2H, m), 7.08 (1H, d, J = 7.9 Hz), 2.83 (2H, t, J = 7.2 Hz), 2.48 (2H, t, J = 7.2 Hz), 2.19 (2H, q, J = 7.2 Hz); ¹³C-NMR (CDCl₃) δ 171.8 (CO), 152.0 (C), 130.2 (C), 129.8 (CH), 128.4 (CH), 126.0 (CH), 119.4 (CH), 31.2 (CH₂, C-2), 28.4 (CH₂), 26.7 (CH₂).

Acknowledgements

This research was supported with funds provided by the Center for Environmentally Beneficial Catalysis under the

National Science Foundation Engineering Research Grant (EEC-0310689). MYR is a Comexus Fulbright–Garcia Robles fellow and is thankful to Universidad Autónoma del Estado de Morelos for a sabbatical fellowship. We are also grateful to Novozymes for a gift of Novozyme-435.

References

- (a) G. R. Krow, *Org. React.*, 1993, **43**, 251–798; (b) C. H. Hassall, *Org. React.*, 1957, **9**, 73; (c) C. Bolm, in *Advances in Catalytic Processes*, Vol. 2, ed. M. P. Doyle, JAI Press, Greenwich, 1997, p 43; (d) M. Renz and B. Meunier, *Eur. J. Org. Chem.*, 1999, 737–750; (e) G. Strukul, *Angew. Chem., Int. Ed.*, 1998, **37**, 1198–1209.
- m*-Chloroperbenzoic acid in *Handbook of Reagents for Organic Synthesis*, ed. S. D. Burke and R. L. Danheiser, John Wiley and Sons, New York, 1999, p 84–89.
- (a) P. Brougham, M. S. Cooper, D. A. Cummmerson, H. Heaney and N. Thompson, *Synthesis*, 1987, 1015–1017; (b) G. J. ten Brink, I. W. C. E. Arends and R. A. Sheldon, *Chem. Rev.*, 2004, **104**, 4105–4123.
- (a) M. D. Mihovilovic, *Curr. Org. Chem.*, 2006, **10**, 1265–1287; (b) M. D. Mihovilovic, F. Rudroff and B. Grotzl, *Curr. Org. Chem.*, 2004, **8**, 1057–1069; (c) N. M. Kamerbeek, D. B. Janssen, W. J. H. Van Berkel and M. W. Fraaije, *Adv. Synth. Catal.*, 2003, **345**, 667–678; (d) M. D. Mihovolovic, B. Müller and P. Stanetty, *Eur. J. Org. Chem.*, 2002, 3711–3730; (e) S. M. Roberts and P. W. H. Wan, *J. Mol. Catal. B: Enzym.*, 1998, **4**, 111–136.
- (a) B. M. Trost, *Angew. Chem., Int. Ed. Engl.*, 1995, **34**, 259–281; (b) R. A. Sheldon, *Pure Appl. Chem.*, 2000, **72**, 1233–1246; (c) *Green Chemistry: Theory and Practice*, ed. P. T. Anastas and J. C. Warner, Oxford University Press, Oxford, UK, 1998.
- S. C. Lemoult, P. F. Richardson and S. M. Roberts, *J. Chem. Soc., Perkin Trans. 1*, 1995, 89–91.
- B. K. Pchelka, M. Gelo-Pujic and E. Guibé-Jampel, *J. Chem. Soc., Perkin Trans. 1*, 1998, 2625–2627.
- (a) E. M. Anderson, M. Karin and O. Kirk, *Biocatal. Biotransform.*, 1998, **16**, 181–204; (b) O. Kirk and M. W. Christensen, *Org. Process Res. Dev.*, 2002, **6**, 446–451; (c) C. Carboni-Oerlemans, P. D. de Maria, B. Tuin, G. Bargeman, A. van der Meer and R. van Gemert, *J. Biotechnol.*, 2006, **126**, 140–151.
- (a) F. Björkling, S. E. Godtfredsen and O. Kirk, *J. Chem. Soc., Chem. Commun.*, 1990, 1301–1303; (b) F. Björkling, H. Frykman, S. E. Godtfredsen and O. Kirk, *Tetrahedron*, 1992, **48**, 4587–4592; (c) O. Kirk, M. W. Christensen, T. Damhus and S. E. Godtfredsen, Enzyme Catalyzed Degradation and Formation of Peroxycarboxylic acids, *Biocatalysis*, 1994, **11**, 65–77; (d) U. T. Bornscheuer and R. J. Kazlauskas, *Angew. Chem., Int. Ed.*, 2004, **43**, 2–10.
- S. Warwel and M. R. gen. Klaas, *J. Mol. Catal. B: Enzym.*, 1995, **1**, 29–35.
- M. R. gen. Klaas and S. Warwel, *Org. Lett.*, 1999, **1**, 1025–1026.
- M. S. Cooper, H. Heaney, A. J. Newbold and W. R. Sanderson, *Synlett*, 1990, 533–535.
- S. Taliansky, *Synlett*, 2005, 1962–1963.
- E. G. Ankudey, H. F. Olivo and T. L. Peebles, *Green Chem.*, 2006, **8**, 923–926.
- K. Shioji, A. Matsuo, K. Okuma, K. Nakamura and A. Ohno, *Tetrahedron Lett.*, 2000, **41**, 8799–8802.
- L. Kondaveti, T. F. Al-Azemi and K. S. Bisht, *Tetrahedron: Asymmetry*, 2002, **13**, 129–135.
- Interestingly, studies of Baeyer–Villiger oxidation of cyclopentanones showed the formation of lactones and also *trans*-esterification products with ethanol. These results will be reported in due time.

Chemoselective reactions of dimethyl carbonate catalysed by alkali metal exchanged faujasites: the case of indolyl carboxylic acids and indolyl-substituted alkyl carboxylic acids

Maurizio Selva,* Pietro Tundo, Davide Brunelli and Alvise Perosa

Received 14th November 2006, Accepted 22nd January 2007

First published as an Advance Article on the web 14th February 2007

DOI: 10.1039/b616656c

At 160–180 °C, in the presence of alkali metal exchanged faujasites (MX or MY; M = Li, Na, K), the reaction of dimethyl carbonate with indolyl-3-acetic, -3-propionic, and -3-butyric acids proceeds towards the formation of the corresponding methyl esters or carbamate esters which can be isolated in 93–99% yields. The methylation of the indolyl-NH group is never observed. This high chemoselectivity is driven by the nature of the catalyst and the reaction temperature. In particular, among the six different zeolites used, the more basic MX faujasites show better performances in terms of both activity and selectivity than MY solids. A similar trend also holds for the reaction of dimethyl carbonate with indolyl-carboxylic acids, where MX compounds are still efficient catalysts for the formation of methyl esters. In this case, however, the overall reactivity/selectivity also reflects the relative positions of the NH and CO₂H groups which may account for significant decarboxylation reactions observed for indolyl acids substituted at positions 2 and 3. This process is totally absent for indolyl-6-carboxylic acid.

Introduction

In the past two decades, the non-toxic dimethyl carbonate (MeOCO₂Me, DMC) has emerged as a green candidate for the replacement of highly noxious compounds such as phosgene and methyl halides/sulfate, in both methylation and methoxycarbonylation reactions.¹ A number of homogeneous and heterogeneous catalysts have been reported for DMC-mediated processes:^{1,2} among them, we recently observed that alkali metal exchanged faujasites offered unique possibilities to catalyze methylation and esterification reactions. Most relevant examples were in the class of ambident nucleophiles. In the presence of NaY faujasite, the reaction of dimethyl carbonate with amino-phenols, -benzyl alcohols, -benzoic acids, and -benzamides not only showed a very high mono-*N*-methyl selectivity (up to 99%), but it proceeded with complete chemoselectivity towards the amino group [Scheme 1, path (a)].³ The other nucleophilic functionalities (OH, CO₂H, CH₂OH, CONH₂) were fully preserved from alkylation and/or transesterification reactions.

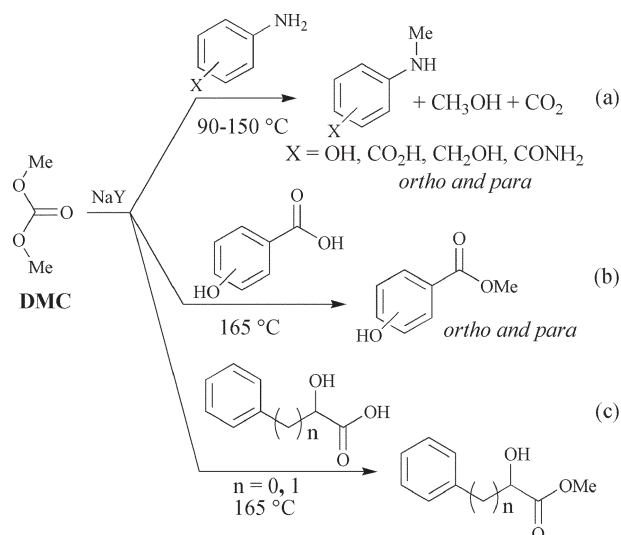
Likewise, at a higher temperature of 165 °C, the DMC/NaY system allowed the exclusive esterification of hydroxy-benzoic acids (*ortho*- and *para*-isomers), mandelic acid, and phenyllactic acid, without affecting aromatic and aliphatic OH-substituents [Scheme 1, paths (b) and (c)].⁴

All these processes were genuine green examples: they were truly catalytic, they did not require additional solvents (DMC served simultaneously as a reagent and solvent), and they released only MeOH and CO₂ as co-products. Moreover,

typical selectivities of reactions of Scheme 1 were in the range of 90–100%: in a single step, with no derivatization (protection/de-protection) sequences, the desired methylamines or methyl esters were isolated in 80–99% yields.

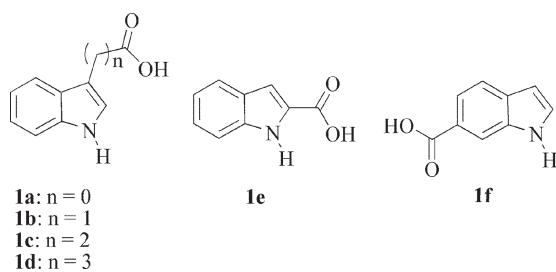
On the contrary, in the presence of basic catalysts (*i.e.* K₂CO₃), competitive reactions of *O*- and bis *N,N*-methylation, *N*- and *O*-methoxycarbonylation took place simultaneously.

These findings prompted us to face the problem of indolyl-substituted alkyl carboxylic acids and of indolyl carboxylic acids, which were both good models of ambident nucleophiles and examples of structural components of auxins and many pharmaceutical agents.⁵ In particular, we focused our

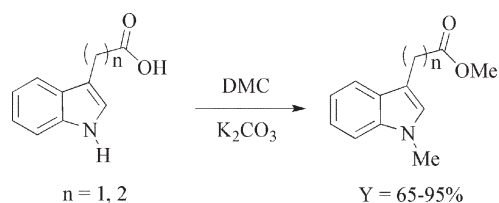


Scheme 1 Chemoselective reactions of DMC in the presence of NaY catalyst.

Dipartimento di Scienze Ambientali dell'Università Ca' Foscari, and Consorzio Interuniversitario "La Chimica per l'Ambiente" (INCA), UdR di Venezia, Calle Larga S. Marta 2137, Venezia, 30123, Italy. E-mail: selva@unive.it; Fax: +39 041 2348 620; Tel: +39 041 2348 687



Scheme 2



Scheme 3

attention on indolyl-3-carboxylic, -acetic, -propionic, and -butyric acids (compounds **1a–d**), and on indolyl-2-carboxylic, and -6-carboxylic acids (compounds **1e** and **1f**) (Scheme 2).

At 130 °C, Jiang *et al.* already reported that reactions of DMC with acids **1a–d** were efficiently catalyzed by K_2CO_3 ,⁶ however, chemoselectivity was elusive because competitive processes of esterification and *N*-methylation occurred to comparable extents (Scheme 3).

In the case of **1a**, it was observed that a decarboxylation process also took place to give *N*-methylindole in 45% yield.

We wish to report herein that at 150–180 °C, the same reactions of acids **1b–d** and **1f**, became highly selective when carried out over alkali metal exchanged faujasites, particularly of the X type: only methyl esters were obtained in substantially quantitative yields, without affecting the NH group. For longer reaction times, carbamate esters coming from simultaneous esterification and *N*-methoxycarbonylation of indolyl substrates were isolated in up to 99% yield. Under these conditions, acids **1a** and **1e** underwent both decarboxylation and esterification reactions, but the methylation of the indolyl-NH group was not appreciable. The outcome was primarily driven by the acido-basic properties of the zeolite catalysts.

Results

Six different faujasites, namely MY and MX ($M = Li, Na, K$) were used as catalysts: four of them ($M = Li$ and K), were prepared through conventional ionic exchange reactions, starting from two commercially available samples of zeolites (NaY and NaX, respectively) and LiCl or KCl as precursors.⁷ The main features of these catalysts are summarized in Table 1.

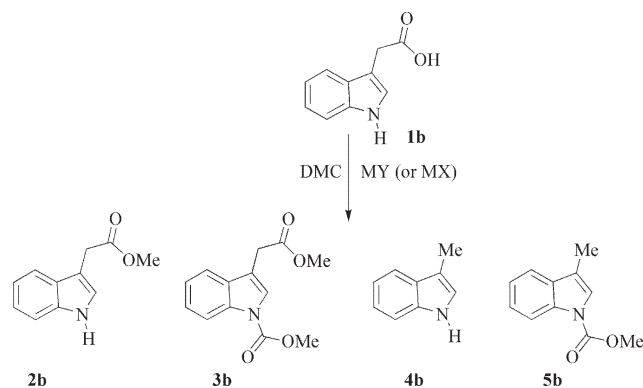
The reaction of DMC with indolyl-3-acetic acid **1b** was initially investigated. In the presence of MX or MY catalysts, a solution of **1b** in DMC (4.5×10^{-2} M, 30 mL) was set to react at 160 and 180 °C, in a stainless-steel autoclave (90 mL). Weight ratios (Q) MX : **1b** or MY : **1b** ranged from 1 to 0.05, and different reaction times of 4–15 h were considered.

Table 1 Faujasite catalysts used in the reaction of DMC with acids **1a–c**

Starting zeolite (Na, %) ^a	Product	Ionic exchange (%) ^b
NaX (7.5)	LiX	71
NaX (7.5)	KX	92
NaY (8)	LiY	67
NaY (8)	KY	86

^a The Na content was evaluated through atomic absorption (AA).

^b Percentage of ionic exchange (from NaX and NaY, respectively) was evaluated by AA (K) and emission (Li).



Scheme 4

After purification of reaction mixtures [flash-column chromatography (FCC): petroleum ether–diethyl ether, 2 : 3 v/v], four products were isolated and identified by GC/MS and by NMR (Scheme 4). The results are reported in Table 2.

In the absence of catalysts, the acid **2b** was recovered unreacted after 3 h at 180 °C (Table 2, entry 1). At the same temperature (180 °C, 4 h, $Q = 1$), reactions carried out over MY zeolites showed good conversions (68–75%) but modest selectivities (entries 2–4): the methyl ester **2b** was formed along with 3-methylindole (**4b**, 19–43%). The latter plausibly originated from the decarboxylation of indolyl-3-acetic acid.⁸

Table 2 The reaction of DMC with **1b** in the presence of different zeolites

Entry	Cat.	Cat. : substr. (Q) ^a	t/h	$T/^\circ C$	Conv. (%) ^b	Isolated product yield (%) ^c			
						2b	3b	4b	5b
1	None		3	180	<1				
2	LiY	1	4	180	68	25		43	
3	NaY	1	4	180	75	52		21	
4	KY	1	4	180	72	50		19	
5	NaY	0.1	15	180	75	56		16	
6	NaY	0.5	9	180	80	55		25	
7	NaY	0.5	15	180	100		61		35
8	LiX	1	4	180	95	87	10		
9	NaX	1	4	180	>99		97		
10	KX	1	4	180	>99		98		
11	NaX	1	3	160	>99	95			
12	NaX	0.1	9	160	>99	93			
13	NaX	0.05	9	160	46	44			
14	KX	0.1	8	160	>99	96			

^a Weight ratio zeolite : **1b**. ^b Based on the recovered starting reagent **1b**. ^c Yields of **2b–5b** were evaluated after purification by flash-column chromatography on silica gel (eluant: petroleum ether–diethyl ether, 2 : 3 v/v).

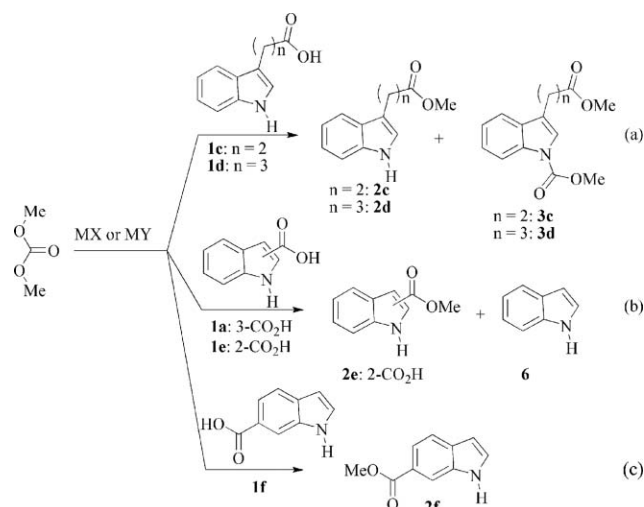
In the presence of NaY, a similar selectivity could be accomplished even by using lower Q ratios (NaY : **1b** = 0.1 and 0.5; **4b**: 16–25%, entries 5 and 6). If the reaction was continued for a longer time (15 h, Q = 0.5), a quantitative conversion was reached, and products **2b** and **4b** were transformed into the corresponding *N*-methoxycarbonyl derivatives, **3b** (61%) and **5b** (35%), respectively (entry 7).

MX faujasites were superior catalysts in terms of both efficiency and selectivity. At 180 °C (Q = 1, 4 h), the methyl ester **2b** was isolated in a 87% yield over LiX (entry 8), while compound **3b** [methyl(*N*-methoxycarbonyl)-3-indolyl acetate] was obtained in 97 and 98% yields, in reactions catalyzed by NaX and KX, respectively (entries 9 and 10). At a lower temperature (160 °C), the esterification of **1b** was the exclusive process observed with NaX and KX, even at Q ratios of 0.05–0.1. Isolated yields of **2b** were of 93–96% (entries 11, 12 and 14) and of 44% (entry 13). In all cases, side-products **4b** and **5b** were never detected.

Reactions of DMC with indolyl-3-propionic, -3-butyric acids, -3-carboxylic, -2-carboxylic, and -6-carboxylic acids (**1c**, **1d**, **1a**, **1e**, and **1f**, respectively) were investigated under the same conditions used for **1b**. Solutions of compounds **1** in DMC (4.5×10^{-2} M, 30 mL) were set to react at 160 and 180 °C, in the presence of NaY and MX (M = Na, Li) catalysts [weight ratios (Q) of catalyst : substrate were of 0.1 and 1]. In the case of substrates **1c,d**, products coming from the esterification of the acid function (compounds **2c,d**), and from the *N*-methoxycarbonylation of the indolyl NH group (compounds **3c,d**) were observed [Scheme 5, path (a)]. The reactions of DMC with acids **1a**, and **1e** and **1f** yielded methyl esters (**2e,f**) along with indole (**6**) originated by the decarboxylation of reagents [Scheme 5, paths (b) and (c)]. Products were isolated and identified by GC/MS and NMR. The results are reported in Table 3.

Acids **1c,d**

As in the case of indolyl-3-acetic acid (**1b**), MX faujasites were more active than NaY. At 180 °C (Q = 1), reactions of acids



Scheme 5

Table 3 The reaction of DMC with indolyl-3-propionic and indolyl-3-butyric acids (**1c** and **1d**) in the presence of different zeolites

Entry	Substrate	Cat.	Cat. : substr. (Q) ^a	t/h	T/°C	Conv. (%) ^b	Isolated product yield (%) ^c
1	1c	NaY	0.1	20	180	21	2c : 19
2	1c	NaY	1	6	180	100	2c : 99
3	1c	NaX	1	3	160	100	3c : 98
4	1c	LiX	1	2	180	100	3c : 96
5	1d	NaY	0.1	12	180	30	2d : 28
6	1d	NaY	1	3	180	100	2d : 99
7	1d	NaX	1	3	160	100	3d : 99
8	1a	None		3	160	7	6 : 5
9	1a	NaX	0.5	3	120	45	6 : 43
10	1a	NaX	1	3	160	100	6 : 99
11	1a	NaY	1	3	140	100	6 : 99
12	1e	NaX	1	3	160	100 ^d	2e : 55
13	1e	NaY	1	3	160	100	6 : 32
14	1f	NaX	0.1	5	160	22	2f : 19
15	1f	NaX	1	7	160	100	2f : 93
16	1f	NaY	1	3	180	40	2f : 36

^a Weight ratio zeolite : substrate. ^b Based on the recovered starting reagents **1a**, **1c**, **1d**, and **1f**. ^c Yields of **2c**, **2d**, **2f**, **3c**, **3d**, and **6** were evaluated after purification by flash-column chromatography on silica gel (eluant: petroleum ether–diethyl ether, 2 : 3 v/v). ^d Reaction mixture of entry 11 was not purified by FCC: yields of **2e** and **6** were by GC. Minor amounts of methyl (*N*-methyl)indolyl-2-carboxylate (<5%) were also observed.

1c,d catalyzed by NaY gave methyl esters **2c** and **2d** in substantially quantitative yields, after 6 and 3 h, respectively (Table 3, entries 2 and 6). Both processes were also possible with a lower Q ratio of 0.1 (entries 1 and 5).

Instead, in the presence of MX zeolites, simultaneous esterification and *N*-methoxycarbonylation reactions took place to yield compounds **3c** and **3d** as sole products (96–99%, entries 3, 4, and 7). These processes occurred at 160 and 180 °C, over NaX and LiX, respectively.

Crude esters **2c,d** and carbamate esters **3c,d** could be recovered in a very high purity (97–98%), by simple filtration of the zeolite and removal of DMC under vacuum.

It should be noted that, particularly for compounds **3**, very few synthetic methods are available in the literature, and they are always based on multistep sequences.⁹

Acids **1a**, **1e**, and **1f**

Indolyl-carboxylic acids (**1a**, **1e**, and **1f**) showed quite a different behaviour with respect to **1b–d**. Regardless of the reaction conditions (catalyst, temperature, and time), acid **1a**, substituted at position 3, gave only the decarboxylation reaction to produce indole **6** in a substantially quantitative yield (Table 3, entries 9–11). In this case, a sluggish formation of indole (5%, 3 h, 160 °C) was observed also without any catalyst (entry 8). In the presence of NaX, acid **1e**, substituted at position 2, yielded a mixture of the methyl ester **2e** (55%) and indole **6** (32%) (entry 12), whereas the decarboxylation of **1e** was the sole reaction observed over the NaY catalyst (entry 13). Only indolyl-6-carboxylic acid **1f** underwent a highly chemoselective esterification process: the reaction was catalyzed by both NaX and NaY, at 160 and 180 °C, respectively (entries 14–16). The methyl ester **2f** was isolated in up to 93% yield (entry 15).

In all cases, faujasite catalysts were easily recyclable: after reactions of acids **1a–f**, they could be separated by filtration and re-activated by a mild thermal treatment (90 °C/0.1 mm, overnight). Both catalytic activity and selectivity were fully restored. For instance, when a re-activated NaX was used under the conditions of entry 11 of Table 2, the reaction of indolyl-3-acetic acid (**1b**) with DMC yielded the corresponding methyl ester (**2b**) in 92% isolated yield.

Discussion

Acids **1b–d**

Acid–base properties of MY and MX faujasites affect the results of Tables 2 and 3. In particular, according to the scale proposed by Barthomeuf (Scheme 6),¹⁰ the more basic MX show better performances than MY. The latter, especially LiY, operates only at 180 °C: they promote either the competitive reactions of esterification and decarboxylation of **1b**, or the esterification of acids **1c,d**.¹¹

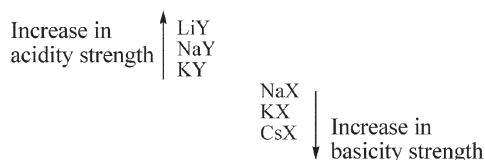
At 160 °C instead, NaX and KX faujasites selectively catalyze the formation of esters **2b** and carbamate esters **3c,d**. The same reactions require a higher temperature of 180 °C, with respect to the less basic LiX.

In the case of indolyl-3-acetic acid (**1b**), MX zeolites are further activated by the temperature: at 180 °C, NaX and KX allow a rapid and quantitative conversion of ester **2b** into **3b**. While, under the same conditions, a sluggish and not selective reaction is observed when NaY is the catalyst (Table 2, entry 6). Shieh *et al.* reported that the *N*-methoxycarbonylation of 5-bromoindole with DMC also takes place only in the presence of moderate-to-strong organic bases (DMAP and DBU).¹²

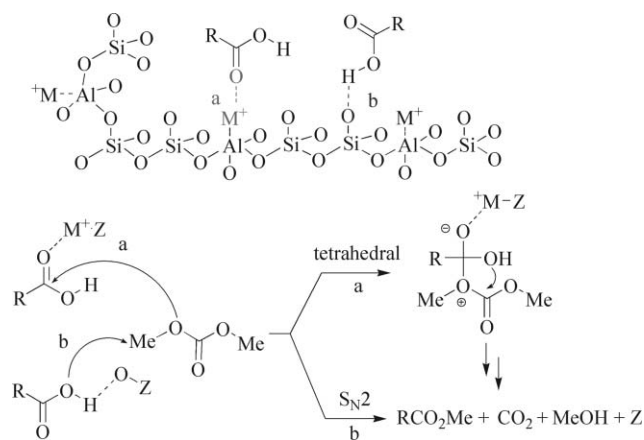
Acids **1a**, **1e,f**

For indolyl-carboxylic acids, the effect of the catalyst is evident for **1e** and, particularly, for **1f**: faster esterification reactions and better yields of products **2e** and **2f** are achieved over NaX faujasite with respect to NaY (entries 11–15, Table 3). However, the reactivity of compounds **1a**, and **1e** and **1f** also reflects the relative positions of the NH and CO₂H groups. The high electron density of positions 2 and, especially, 3 of the pyrrole ring of the indoles¹³ may account for the important, if not exclusive, decarboxylation reaction observed for reagents **1a** and **1e**. By contrast, this process is totally absent for indolyl-6-carboxylic acid. The lower reactivity of indolyl-3-acetic acid **1b** compared to its homologues **1c** and **1d** (Tables 2 and 3) can be explained accordingly.

Overall, the surface interactions between reagents and catalysts can be affected by the different acid–base features



Scheme 6



Scheme 7

of MY/MX solids. Scheme 7 describes two plausible modes of adsorption of carboxylic acids over alkali metal exchanged faujasites.¹⁴

The formation of methyl esters **2b,c** (Schemes 4 and 5) may proceed according to tetrahedral or S_N2-type or both mechanisms, which are possibly favored over more basic X zeolites.

Indole-NH groups of acids **1** are also expected to bind to the polar surface of MY/MX faujasites.¹⁵ Nevertheless, the reactivity of CO₂H and NH functionalities is highly discriminated. Not to mention that compounds **1** never undergo *N*-methylation reactions which are always observed over conventional basic catalysts (Scheme 3).^{16,17} This fine tuning of the selectivity suggests that the activation of acids **1** is a complex phenomenon where both the geometry of adsorption of reagents and the steric requisites of faujasites, can be involved.¹⁸

Conclusions

The combination of dimethyl carbonate and Y or X faujasites allows a straightforward and high-yield synthesis of methyl esters **2** or methyl carbamate esters **3** derived from indolyl acids **1**. In particular, alkali metal exchanged X zeolites are superior catalysts in terms of both efficiency and selectivity. Typical chemoselectivity is up to 99% at quantitative conversions, a result hitherto not possible with standard basic catalysts (*i.e.* K₂CO₃), where only products of simultaneous esterification and *N*-methylation of acids **1** are obtained. Under the explored conditions, the reaction outcome is affected by the acid–base nature of MX/MY zeolites which likely alters the surface interactions between reagents and catalysts.

Although the procedure is rather energy-intensive, multiple *green* features can be recognized: (i) the non-toxic DMC is used as a reagent/solvent which can be recycled;¹⁹ (ii) eco-safe solids (faujasites) are catalysts which can be easily separated and recycled; (iii) except for MeOH and CO₂, no organic/inorganic by-products are observed; and (iv) thanks to the high chemoselectivity, not only derivatization sequences can be avoided, but also purification steps are much simplified.

Experimental

Compounds **1** and DMC were ACS grade and were employed without further purification. Zeolites NaY and NaX were from Aldrich. Other MY and MX catalysts (M = Li, Na, K) were prepared according to a procedure previously reported by us.^{2h} Before each reaction, all the faujasites were dehydrated by being heated at 65 °C under vacuum (10 mm Hg) overnight.

MS (EI, 70 eV) analyses were run using HP5/MS capillary columns (30 m). ¹H and ¹³C NMR spectra were recorded on a 300 MHz spectrometer, using CDCl₃ as solvent.

Reactions carried out in autoclave. General procedure

A stainless-steel autoclave (90 mL of internal volume) was charged with a solution (4.5×10^{-2} M; 30 mL) of the chosen acid (**1**, 1.35 mmol), dimethyl carbonate (0.36 mol) and MY or NaX faujasites (catalyst : substrate in a 0.1–1 weight ratio, see Tables 2 and 3). At room temperature and before the reaction, air was removed by a purging valve with a N₂ stream. The autoclave was then heated by an oil-circulating jacket, while the mixture was kept under magnetic stirring throughout the reaction. A thermocouple fixed onto the autoclave head monitored the temperature (160–180 °C). After different time intervals (3–20 h), the autoclave was cooled to rt, purged from CO₂ and, finally, opened. The reaction mixture was analysed by GC/MS.

Crude esters **2b** and **2f**, and carbamate esters **3b–d** were isolated in 93–98% GC-purity by simple filtration of the NaX catalyst and removal of DMC under vacuum (35 °C/250 mm). Likewise, products **2c** and **2d** (98% GC) were obtained from reactions catalyzed by MY zeolites. Products **4b** and **5b** were obtained from the reaction of **1b** with DMC over MY faujasites (Table 2). Reaction mixtures were further purified by FCC on silica gel F60 (eluant: petroleum ether–diethyl ether in 2 : 3 v/v).

All compounds were characterized by GC/MS and ¹H NMR. Spectroscopic data of **2b–d**, **2f**, **3b**, **4b**, **5b**, and **6** were already reported in the literature.^{9,20–24} The structures of new compounds **3c** and **3d** were confirmed also by ¹³C NMR.

¹H NMR spectra were recorded at 300 MHz, ¹³C NMR at 75 MHz. Chemical shifts were reported in δ values downfield from TMS. CDCl₃ was used as the solvent.

The structures of esters **2b–d** and **2f**, and of indole **6** were confirmed also by comparison to authentic samples. Compound **2e** was not isolated: its structure was assigned by GC/MS.

Methyl indolyl-3-acetate **2b**

Mp 42–44 °C (pale yellow solid) [lit.^{20a} mp 47–48 °C]. ¹H NMR (300 MHz, CDCl₃) δ 3.74 (s, 3H), 3.82 (s, 2H), 7.12–7.29 (m, 3H), 7.34–7.39 (m, 1H), 7.62–7.68 (m, 1H), 8.18 (brs, 1H). MS (EI), m/z (relative int.): 189 (M⁺, 32%), 131 (11), 130 (M⁺ – CO₂Me, 100), 103 (7), 77 (8).

Methyl indolyl-3-propionate **2c**²¹

Mp 75–76 °C (white solid) [lit.^{20b} mp 79–80 °C]. ¹H NMR (300 MHz, CDCl₃) δ 2.75 (t, 2H, J = 8.1 Hz), 3.14 (t, 2H, J = 7.9 Hz), 3.7 (s, 3H), 7.03 (m, 1H), 7.10–7.26 (m, 2 H),

7.35–7.41 (m, 1H), 7.62–7.66 (m, 1H), 8.02 (brs, 1H). MS (EI), m/z (relative int.): 203 (M⁺, 18%), 131 (11), 130 (M⁺ – CH₂CO₂Me, 100), 103 (4), 77 (6).

Methyl indolyl-3-butyrate **2d**²²

Mp 70–71 °C (colorless solid) [lit.^{20c} mp 70–72 °C]. ¹H NMR (300 MHz, CDCl₃) δ 2.06 (qui, 2H, J = 7.35 Hz), 2.41 (t, 2H, J = 7.54 Hz), 2.82 (t, 2H, J = 7.54 Hz), 3.67 (s, 3H), 7.00 (m, 1H), 7.08–7.24 (m, 2 H), 7.33–7.39 (m, 1H), 7.57–7.65 (m, 1H), 7.98 (brs, 1H). MS (EI), m/z (relative int.): 217 (M⁺, 28%), 186 (M⁺ – OMe, 9), 143 (M⁺ – CH₂CO₂Me – H, 21), 130 (M⁺ – CH₂CH₂CO₂Me), 77 (7).

Methyl indolyl-2-carboxylate, **2e**²³

MS (EI), m/z (relative int.): 175 (M⁺, 65%), 144 (M⁺ – OMe, 21), 143 (100), 116 (M⁺ – CO₂Me, 12), 115 (53), 89 (28).

Methyl indolyl-6-carboxylate **2f**

Mp 74–76 °C (pale yellow solid) [lit.²⁴ mp 71–72 °C]. ¹H NMR (300 MHz, CDCl₃) δ 3.93 (s, 3H), 6.61 (m, 1H), 7.38 (m, 1H), 7.66 (d, 1H, J = 8.3 Hz), 7.82 (dd, 1H, J_1 = 8.5 Hz, J_2 = 1.5 Hz), 8.17 (m, 1H), 8.45 (brs, 1H). MS (EI), m/z (relative int.): 175 (M⁺, 73%), 145 (11), 144 (M⁺ – OMe, 100), 116 (M⁺ – CO₂Me, 50), 89 (18).

Methyl (*N*-methoxycarbonyl)indolyl-3 acetate **3b**

Mp 30–32 °C (white solid) [lit.⁹ mp 34–35 °C]. ¹H NMR (300 MHz, CDCl₃) δ 3.72 (s, 5H), 4.03 (s, 3H), 7.24–7.40 (m, 2H), 7.51–7.56 (m, 1H), 7.60 (s, 1H), 8.17 (d, 1H, J = 8.1 Hz). MS (EI), m/z (relative int.): 247 (M⁺, 56%), 189 (13), 188 (M⁺ – CO₂Me, 100), 143 (M⁺ – CH₂CO₂Me, 40), 129 [M⁺ – (CO₂Me)₂, 19], 128 (13), 102 (20), 76 (10).

3-Methylindole **4b**

Mp 96–98 °C (white solid) [lit.²⁵ mp 98–98.5 °C]. ¹H NMR (300 MHz, CDCl₃) δ 2.35 (d, 3H, J = 1.1 Hz), 6.97 (m, 1H), 7.09–7.24 (m, 2H), 7.32–7.38 (m, 1H), 7.57–7.63 (m, 1H), 7.87 (brs, 1H). MS (EI), m/z (relative int.): 131 (M⁺, 58%), 130 (M⁺ – H, 100), 102 (6), 77 (12).

(*N*-Methoxycarbonyl)-3-methylindole **5b**

Viscous oil [lit.²⁶ bp 101–102 °C/0.5 torr]. ¹H NMR (300 MHz, CDCl₃) δ 2.19 (d, 3H, J = 1.1 Hz), 3.93 (s, 3H), 7.15–7.32 (m, 3H), 7.40–7.45 (m, 1H), 8.00 (m, 1H). MS (EI), m/z (relative int.): 190 (12), 189 (M⁺, 100%), 144 (82), 130 (M⁺ – CO₂Me, 48), 103 (16), 77 (24).

Methyl (*N*-methoxycarbonyl)-3-indolyl propionate **3c**

Mp 40–43 °C (white solid); ¹H NMR (300 MHz, CDCl₃) δ 2.72 (t, 2H, J = 7.9 Hz), 3.01 (t, 2H, J = 8.0 Hz), 3.69 (s, 3H), 4.02 (s, 3H), 7.23–7.38 (m, 2H), 7.40 (s, 1H), 7.51–7.56 (m, 1H), 8.16 (d, 1H, J = 8.3 Hz); ¹³C NMR (75 MHz, CDCl₃) δ 20.18, 33.46, 51.62, 53.58, 115.12, 118.75, 120.18, 122.03, 122.70, 124.62, 130.12, 135.46, 151.30, 173.19. MS (EI), m/z (relative int.): 261 (M⁺, 44%), 201 (M⁺ – CO₂Me – H, 11), 188

($M^+ - CH_2CO_2Me$, 100), 144 (36), 143 [$M^+ - (CO_2Me)_2$, 20], 129 (13), 115 (22), 59 (14).

Methyl (*N*-methoxycarbonyl)-3-indolyl butyrate 3d

Mp 63–65 °C (white solid); 1H NMR (300 MHz, $CDCl_3$) δ 2.04 (qui, 2H, $J = 7.4$ Hz), 2.40 (t, 2H, $J = 7.3$ Hz), 2.73 (td, 2H, $J_1 = 7.5$ Hz, $J_2 = 1.1$ Hz), 3.67 (s, 3H), 4.02 (s, 3H), 7.22–7.37 (m, 2H), 7.39 (m, 1H), 7.51–7.56 (m, 1H), 8.16 (d, 1H, $J = 7.9$ Hz); ^{13}C NMR (75 MHz, $CDCl_3$) δ 24.17, 24.21, 33.45, 51.49, 53.59, 115.11, 118.98, 120.92, 122.11, 122.67, 124.55, 130.42, 135.59, 151.39, 173.78. MS (EI), m/z (relative int.): 276 (14), 275 (M^+ , 81%), 244 ($M^+ - OMe$, 16), 202 (17), 201 ($M^+ - CO_2Me - Me$, 78), 188 (100), 156 (15), 144 (43), 143 (18), 129 (20), 115 (15).

Indole 6

Mp 47–49 °C (yellow solid) [lit.²⁷ mp 52 °C].

Acknowledgements

MIUR (Italian Ministry of University and Research) and EU 6th-FP (solvsafe project: www.solvsafe.com) are gratefully acknowledged for financial support.

References

- (a) A.-A. G. Shaik and S. Sivaram, *Chem. Rev.*, 1996, **96**, 951–976; (b) P. Tundo and M. Selva, *Acc. Chem. Res.*, 2002, **35**, 706–716.
- (a) P. Tundo, *Continuous Flow Methods in Organic Synthesis*, Horwood, Chichester, UK, 1991; (b) M. Aresta and E. Quaranta, *Tetrahedron*, 1991, **47**, 9489–9502; (c) M. Selva, C. A. Marques and P. Tundo, *J. Chem. Soc., Perkin Trans. 1*, 1994, 1323–1328; (d) Z.-H. Fu and Y. Ono, *J. Catal.*, 1994, **145**, 166–170; (e) Y. Ono, *Appl. Catal.*, 1997, **155**, 136; (f) M. Selva, A. Bomben and P. Tundo, *J. Chem. Soc., Perkin Trans. 1*, 1997, 1041–1045; (g) M. Selva, P. Tundo and A. Perosa, *J. Org. Chem.*, 2001, **66**, 677–680; (h) D. Delledonne, F. Rivetti and U. Romano, *Appl. Catal., A*, 2001, **221**, 241–251; (i) M. Selva, P. Tundo and A. Perosa, *J. Org. Chem.*, 2002, **67**, 9238–9247; (j) M. Selva, P. Tundo, A. Perosa and S. Memoli, *J. Org. Chem.*, 2002, **67**, 1071–1077; (k) M. Selva, P. Tundo, A. Perosa and F. Dall'Acqua, *J. Org. Chem.*, 2005, **70**, 2771–2777.
- (a) M. Selva, P. Tundo and A. Perosa, *J. Org. Chem.*, 2003, **68**, 7374–7378; (b) M. Selva, P. Tundo and T. Foccardi, *J. Org. Chem.*, 2005, **70**, 2476–2485.
- M. Selva and P. Tundo, *J. Org. Chem.*, 2006, **71**, 1464–1470.
- (a) D. W. Armstrong, Y.-S. Liu, L. He and K. H. Ekborg-Ott, *J. Agric. Food Chem.*, 2002, **50**, 473–476; (b) G. R. Humphrey and J. T. Kuethe, *Chem. Rev.*, 2006, **106**, 2875–2911.
- X. Jiang, A. Tiwari, M. Thompson, Z. Chen, T. P. Cleary and T. B. K. Lee, *Org. Process Res. Dev.*, 2001, **5**, 604–608.
- M. Onaka, K. Ishikawa and Y. Izumi, *Chem. Lett.*, 1982, 1783.
- In ref. 6, a decarboxylation process was described for the reaction of indolyl-3-carboxylic acid (**1a**) with DMC, catalyzed by K_2CO_3 .
- M.-L. Bennasar, E. Zulaica, A. Ramirez and J. Bosch, *J. Org. Chem.*, 1996, **61**, 1239–1251.
- (a) D. Barthomeuf, *J. Phys. Chem.*, 1984, **88**, 42–45; (b) B. Su and D. Barthomeuf, *Stud. Surf. Sci. Catal.*, 1995, **94**, 598. The rationale of Scheme 6 is based on: (i) the charge-to-mass ratio of metal cations ($Li > Na > K > Cs$; acid sites); and (ii) the Si/Al ratio of the aluminosilicate framework (1–1.5 and 1.5–3, for MX and MY, respectively). This ratio directly affects the strength of basic sites identified with the oxygen atoms of the aluminosilicate framework.
- Likely, in the reactions of indolyl-3-acetic acid (Table 2), the second decarboxylated product (**5b**) comes from the *N*-methoxycarbonylation reaction of compound **3b** with DMC.
- W.-C. Shieh, S. Dell, A. Bach, O. Repic and T. J. Blacklock, *J. Org. Chem.*, 2003, **68**, 1954–1957.
- J. March, *Advanced Organic Chemistry, Reaction, Mechanisms, and Structure*, Wiley, New York, 4th edn, 1992, ch. 11, pp. 514–516.
- Spectroscopic investigations demonstrate that, upon adsorption over both MY and MX catalysts, both DMC and several nucleophiles (phenols, thiophenols, and amines) are activated *via* either interactions with acidic metal cations ($M^+ = Li, Na, K$), and H-bonds with basic oxygen atoms of the aluminosilicate structure of faujasites. See: (a) T. Beutel, *J. Chem. Soc., Faraday Trans.*, 1998, **94**, 985; (b) F. Bonino, A. Damin, S. Bordiga, M. Selva, P. Tundo and A. Zecchina, *Angew. Chem., Int. Ed.*, 2005, **44**, 4774–4777; (c) M. Czjzek, T. Vogt and H. Fuess, *Zeolites*, 1991, **11**, 832; (d) T. Beutel, M.-J. Peltre and B. L. Su, *Colloids Surf., A*, 2001, **187**, 319–325; (e) Z.-H. Fu and Y. Ono, *Catal. Lett.*, 1993, **21**, 43–47. To our knowledge, such data are not available for carboxylic acids, and particularly, for indolyl acids. Scheme 7 illustrates a reasonable hypothesis.
- Compounds **1** are also weak bases; see: B. Andonovski, I. Spirevska and A. Nikolovski, *Croat. Chim. Acta*, 1996, **69**, 1201–1213.
- Shieh *et al.* (see ref. 12) observed that also in the reaction of 5-bromoindole with DMC, the nature of the basic catalyst drives the overall selectivity: in particular, the increase of the basic strength ($DBU > DMAP > DABCO$), favors the *N*-methoxycarbonylation reaction *vs.* the competitive *N*-methylation process.
- In the presence of K_2CO_3 or TBAB (*n*-Bu₄NBr), also pyrrole and benzimidazole react with DMC to produce the corresponding *N*-methyl derivatives; see: M. Lissel, S. Schmidt and B. Neumann, *Synthesis*, 1986, 382–382; S. Ouk, S. Thiebaud, E. Borredon and B. Chabaud, *Synth. Commun.*, 2005, **35**, 3021–3026.
- In particular, supercages of the 3D-structure of MY and MX faujasites may induce a shape selectivity effect. See ref. 1b, 3, 4, 12, 13.
- DMC can be recovered quantitatively by distillation at atmospheric pressure (90 °C). However, both methylation and methoxycarbonylation reactions mediated by dimethyl carbonate produce MeOH (as a co-product) which forms a minimum boiling point azeotrope (70 : 30; 63 °C, 1 atm) with DMC itself. In the current practice, the azeotrope is separated by distillation under pressure (140 °C, 10 atm; see: (a) J. F. Knifton and R. G. Duranleau, *J. Mol. Catal.*, 1991, **67**, 389–399; (b) M. Fuming, P. Zhi and L. Guangxing, *Org. Process Res. Dev.*, 2004, **8**, 372–375).
- (a) Compound **2b**: J. A. Nieman, J. E. Coleman, D. J. Fallace, E. Piers, L. Y. Lim, M. Roberge and R. J. Andersen, *J. Nat. Prod.*, 2003, **66**, 183–199; (b) compound **2c**: Z. Iqbal, A. H. Jackson and K. R. Nagaraja Rao, *Tetrahedron Lett.*, 1988, **29**, 2577–2580; (c) compound **2d**: G. Dornyei, M. Incze, M. Kajtar-Peredy and C. Szantay, *Collect. Czech. Chem. Commun.*, 2002, **67**, 1669–1680.
- D. H. R. Barton, G. Bringmann and W. B. Motherwell, *Synthesis*, 1980, 68–70.
- J. Perregaard, E. K. Moltzen, E. Meier and C. Sanchez, *J. Med. Chem.*, 1995, **38**, 1998–2008.
- J. D. Freed, D. J. Hart and N. A. Magomedov, *J. Org. Chem.*, 2001, **66**, 839–852.
- F. J. Brown, L. A. Cronk, D. Aharony and D. W. Snyder, *J. Med. Chem.*, 1992, **35**, 2419–2439.
- Y. Tsuji, S. Kotachi, K.-T. Huh and Y. Watanabe, *J. Org. Chem.*, 1990, **55**, 580–584.
- E. Wenkert, M. E. Alonso, H. E. Gottlieb and E. L. Sanchez, *J. Org. Chem.*, 1977, **42**, 3945–3949.
- Dictionary of Organic Compounds*, ed. John Buckingham, Chapman and Hall, New York, 5th edn, 1982, vol. 3, p. 3305.

Oxidation, friction reducing, and low temperature properties of epoxy fatty acid methyl esters†‡

Brajendra K. Sharma,^{ab} Kenneth M. Doll*^a and Sevim Z. Erhan^a

Received 27th September 2006, Accepted 30th January 2007

First published as an Advance Article on the web 12th February 2007

DOI: 10.1039/b614100e

The use of oleochemicals as biobased lubricants is of significant interest. This article presents the oxidative stability of synthesized epoxidized methyl oleate (EMO), epoxidized methyl linoleate (EMLO), and epoxidized methyl linolenate (EMLN), as well as that of a commercial epoxidized soybean oil, and epoxidized 2-ethylhexyl soyate. The epoxides show increased stability over olefinic oleochemicals by both pressure differential scanning calorimetry (PDSC) and thin film micro oxidation (TFMO). Also reported are the viscosity indices, pour point, and cloud point of the compounds. All of the data indicate that some of these epoxides have significant potential to be used as a fuel additive or lubricating fluid, important areas in the replacement of petrochemicals with environmentally friendly biobased alternatives.

Introduction

There are several positive reasons for the use of vegetable oils, or vegetable oil derivatives, as lubricants and lubricant additives. Because as much as 40%^{1,2} of a lubricant can be lost to the environment, the inherent biodegradability of vegetable oils serves to reduce their environmental impact.

Vegetable oil, especially soybean oil, is also relatively inexpensive. The USA production of soybeans was a near record 3.09 billion bushels in 2005. There is also large and increasing production of soybeans in Brazil and South America (http://www.nass.usda.gov/Publications/Ag_Newsletter/nf1020106.pdf). At the same time, petroleum prices are high, and not likely to significantly decline in the near future.³

The use of oleochemicals as lubricants is well known. For example, the superior lubricity of biodiesel^{4,5} compared to petroleum based diesel, is often given as one of the major advantages of the biofuel. However, vegetable oil based lubricants have a lower oxidative stability^{6–9} and poor cold flow properties at low temperatures.^{10,11}

One potential way to change these properties is through chemical derivatization of the olefinic groups of the oleochemical. Hydrogenation,¹² transesterification, epoxidation,^{13–16} metathesis,^{17–19} and alkylation, or a combination of chemistries have all been used in order to synthesize an improved product.

Epoxidation of oleochemicals has been performed for more than 50 years,^{13,20} and has reached the point where epoxidized soybean oil (ESO) is available commercially at a reasonable cost.

One method we have previously studied is the epoxidation of the unsaturated methyl esters of soybean oil. These are methyl oleate, methyl linoleate, and methyl linolenate. The fully epoxidized compounds (Scheme 1): epoxidized methyl oleate (EMO; methyl-9,10-oxirane octadecanoate), epoxidized methyl linoleate (EMLO; methyl-9,10:12,13-dioxirane octadecanoate), and epoxidized methyl linolenate (EMLN; methyl-9,10:12,13:15,16-trioxirane octadecanoate), were studied as lubricant additives in hexadecane solution.²¹ Comparison of the performance of our compounds to the performance of their non-epoxidized counterparts was made using a ball and disk friction and wear test machine with steel specimen. The critical additive concentration, defined as the concentration sufficient to lower the coefficient to half of the value of hexadecane alone, of each additive was determined. The epoxidized materials showed effectiveness at the very low concentrations with critical concentrations of 11, 12, and 25 mM for EMO, EMLO, and EMLN respectively. In two of the three cases, the epoxidized samples outperformed their olefinic counterparts. Using the Langmuir model, absorption energies were calculated at $-11.3 \text{ kJ mol}^{-1}$ ($-2.7 \text{ kcal mol}^{-1}$). Additionally, thermogravimetric analysis of EMO and EMLO show an increased stability of 24 °C and 42 °C respectively,²² under nitrogen atmosphere.

Epoxide materials have also been patented for potential use as fuel and lubricant additives.²³ These promising results show that the epoxides merit additional study. Herein we report the viscosity, thermal stability and cold flow properties of the compounds EMO, EMLO, EMLN, as well as that of the commercial epoxidized products; ESO, and epoxidized 2-ethylhexyl soyate (VikoflexTM). We also report the stability in an oxygenated environment under conditions designed to simulate a lubrication environment, namely the thin film micro oxidation (TFMO) test. The results are

^aUSDA/NCAUR/ARS, Food and Industrial Oil Research, 1815 N, University Street, Peoria IL 61604, USA.

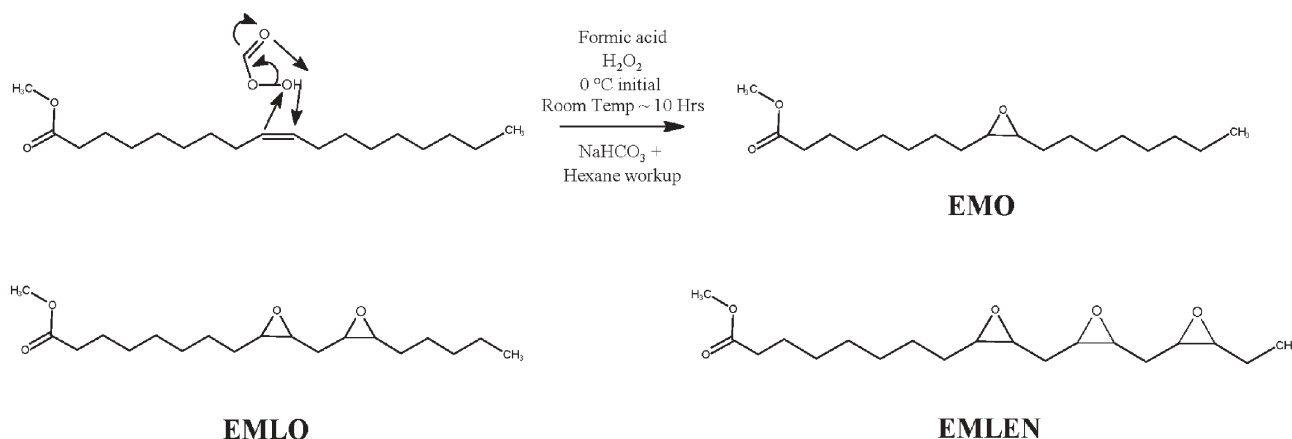
E-mail: dollkm@ncaur.usda.gov; Fax: +1 309 681 6340;

Tel: +1 309 681 6103

^bDepartment of Chemical Engineering, Pennsylvania State University, University Park, PA 16802, USA

† The use of trade, firm, or corporation names in this publication is for the information and convenience of the reader. Such use does not constitute an official endorsement or approval by the United States Department of Agriculture or the Agricultural Research Service of any product or service to the exclusion of others that may be suitable.

‡ Electronic supplementary information (ESI) available: A detailed synthesis of EMO, EMLO, and EMLN, including the ¹H and ¹³C NMR assignments of the compounds. See DOI: 10.1039/b614100e



Scheme 1 The epoxidation of methyl oleate to form EMO. The structures of EMLO and EMLN are also shown.

illustrative and may help in the development of biobased lubricants.

Experimental procedures

Materials

Epoxidized soybean oil (Atofina, VikoflexTM 7170, 4.2 oxirane moieties per triglyceride), methyl oleate (Sigma-Aldrich, St. Louis, MO, Tech 70%; Nu check Prep, Elsyian, MN, >99%); methyl linoleate (Nu check Prep, Elsyian, MN, >99%); 2-ethylhexyl epoxy soyate (Arkema, Philadelphia, PA, VikoflexTM 4050, 5.6% oxirane content); hydrogen peroxide (Sigma-Aldrich, St. Louis, MO, A.C.S. reagent, 30% solution); formic acid (Sigma-Aldrich, 96%, A.C.S. reagent); hexanes (Sigma-Aldrich, St. Louis, MO, >95%, HPLC grade); NaCl (Fisher, Fairlawn, NJ, A.C.S. reagent), NaHCO₃ (Fisher, Fairlawn, NJ, A.C.S. reagent), were all used as received.

Brookfield viscosities

The dynamic viscosity at 25 °C was measured on a Brookfield (Middleboro, MA), DV-III programmable Rheometer controlled by Rheocalc 2.4 software. It was equipped with a CP-40 spindle and programmed to vary the shear rate from 0.5–10 rpm. The viscosity was determined by the software using a Bingham model. In this model, the viscosity is found from the slope of a shear rate vs. shear stress relationship. An experiment was also performed varying the shear stress instead of the shear rate, and the results were identical. The temperature of the system was controlled by a Brookfield (Middleboro, MA) TC-602 water bath.

Kinematic viscosity using Cannon–Fenske viscometry

The kinematic viscosity was measured using Cannon–Fenske calibrated viscometers (Cannon Instrument Co., State College, PA) in a Cannon temperature bath (CT-1000) at 40 °C, according to ASTM standard method D445-95 (Annual Book of ASTM Standards, 2000). The viscosities obtained are average values of 2–3 determinations and the precision is within the limits of ASTM method specification.

Pour point and cloud point

Pour points and cloud points were measured by following the ASTM D-5949 and ASTM D-5773 method respectively using Phase Technology Analyzer, Model 70X (Phase technology, Hammersmith Gate, Richmond, B.C., Canada). The pour point is defined as the temperature in °C when the sample still pours when the jar is tilted. Statistically the method has shown quite good consistency for determining low temperature flow property of fluids.

Pressure differential scanning calorimetry (PDSC)

The experiments were carried out using a PC controlled DSC 2910 thermal analyzer from TA Instruments (New Castle, USA). The instrument has a maximum sensitivity of 5 mV cm⁻¹ and temperature sensitivity of 0.2 mV cm⁻¹. A 1.5–2.0 mg sample was placed in a hermetically sealed type aluminium pan with a pinhole lid for interaction of the sample with the reactant gas (dry air). The controlled diffusion of the gas through the hole greatly restricts the volatilization of the oil while still allowing for saturation of the liquid phase with air. A film thickness of less than 1 mm was required to ensure proper oil–air interaction and to eliminate any discrepancy in the result due to gas diffusion limitations. The module was first temperature calibrated using the melting point of indium metal (156.6 °C) at 10 °C min⁻¹ heating rate. Dry air was pressurized in the module at a constant pressure of 1378.95 kPa (200 psi) and a scanning rate of 10 °C min⁻¹ was used throughout the experiment. The onset temperature (OT) and signal maximum temperature (SM) of oxidation were calculated from the exotherm in each case.

Thin film micro oxidation (TFMO)

A small amount of oil (25 µl) was oxidized as a thin film on a freshly polished high carbon steel catalyst surface with a steady flow (20 cm³ min⁻¹) of dry air. Oxidation tests were done at various temperatures (150, 175, 200, and 225 °C) for 120 min inside a bottomless glass reactor. The temperature was maintained at ±1 °C with a heated aluminium slab placed on top of a hot plate. This arrangement eliminates temperature gradient across the aluminum surface and transferred heat to

Table 1 The physical properties of the oleochemical epoxides. The error bars on the dynamic viscosity are a standard deviation from multiple measurements

Sample	Viscosities				Low temperature properties		Friction reducing properties ^{a,b}	
	Dynamic, 25 °C/mPa s	Kinematic, 40 °C/mm ² s ⁻¹	Kinematic, 100 °C/mm ² s ⁻¹	Viscosity index	Pour point/°C	Cloud point/°C	CoF (0.04 M)	CoF (0.02 M)
EMO	12.1 ± 0.1	8.0	2.5	151	0	4.15	0.12	0.14
EMLO	24.8 ± 0.2	14.3	3.5	132	-1.5	2.55	0.13	0.17
EMLN	1488.5 ± 3.5	308.0	19.3	63	-7.5	-36.6	0.17	0.18
ESO	416.1 ± 1.3	174.9	21.0	142	3.0 ^a	ND	0.12	0.13
Vikoflex TM	27.5 ± 0.1	16.8	4.0	140	-4.5	-0.15	0.11	0.16

^a Determined in previous work.^{21,30} ^b The friction reduction coefficients are measured in hexadecane solution which displays a CoF of ~0.45 without additives. Load = 181.44 kg and speed = 6.22 mm min⁻¹ at 25 °C.

the catalysts placed on the slab. The constant airflow ensured removal of volatile oxidation products. The test was designed to eliminate any gas diffusion limitation.

After oxidation, the catalyst containing the oxidized oil sample was removed from the oxidation chamber and cooled rapidly under a steady flow of dry N₂ and transferred to a desiccator for temperature equilibration. After approximately 2 h, the catalyst containing the oxidized oil was weighed to determine the volatile loss (or gain) due to oxidation and then soaked (30 min) with tetrahydrofuran (THF) to dissolve the soluble portion of the oxidized oil. After dissolving the soluble portion of the oxidized oil, the catalyst was dried and weighed to determine the remaining insoluble deposit.

Friction measurement by ball-on-disk method

Boundary lubrication properties of epoxy samples were studied using a multi-specimen friction measurement apparatus of FALEX (Sugar Grove, IL). Ball-on-disk experiments (1018 steel disk, hardness of 15–25 as measured on the Rockwell C scale) were carried out under low speed 6.22 mm sec⁻¹ (5 rpm) and high load 181.44 kg at 25 °C using 0.02 M and 0.04 M concentrations of epoxy samples in hexadecane. Measurements of coefficient of friction (CoF) and torque were made in each case. The CoF values reported are averages of two or three independent experiments and the standard deviation observed was ±0.02.

Epoxidations

EMO has been synthesized in our lab^{21,22,24} as well as in the labs of others.²⁵ Epoxidation reactions of oleochemicals was first performed by Swern *et al.*¹³ and Schmits and Wallace²⁰ and methods have been refined and improved considerably over the years.^{14,26,27}

Using ~200 g of the olefinic starting material, an epoxidation reaction was performed using hydrogen peroxide, and a formic acid catalyst (Scheme 1). The reaction was followed directly by GC, in order to ensure complete conversion, yet limit the productions of various poly hydroxy compounds. Purification was achieved using a separatory funnel. Extraction of the material with hexanes was also possible in the EMO and EMLO syntheses which improved yields to 97% and 95% respectively. The yield in the EMLN case was 85%. Details on these syntheses are available in the ESI.†

Results and discussion

The dynamic viscosity of the products was measured at 25 °C by a Brookfield rheometer and by standard Cannon–Fenske methods at 40 and 100 °C. The results (Table 1) show two things. First, with the exception of EMLN, the viscosities are fairly low even at room temperature, a favourable additive property. Second, among compounds with the methyl head group; EMO, EMLO, and EMLN, as the amount of epoxidation increases from 1 to 3 oxirane per molecule, the viscosity increases, dramatically in the case of EMLN. This can be rationalized by an increase in the interaction of the lone electron pairs on the extra oxygen groups in the epoxy compounds. There is also a strong possibility that there is some viscosity increasing polymer in the EMLN sample. This is also supported by the oxidation data discussed later in this section. Because the VikoflexTM 4550 (VikoflexTM) has a larger headgroup (2-ethyl hexyl) it displays a slightly higher viscosity than its oxirane content of ~1.43 per molecule would suggest. ESO, with its glyceride backbone and nearly 3-fold larger molecular weight, is more viscous than all except for EMLN.

Pour point and cloud point measurements show the opposite trend. That is, EMLN displays a much lower cloud point followed by VikoflexTM, EMLO, then EMO. This can be rationalized by looking at the molecular structure, where the larger number of epoxide groups will cause considerable kinking in the chain, inhibiting crystallization. Another possible effect may be caused by the residual saturated oleochemicals, which are at slightly higher levels in the VikoflexTM and EMO samples. These compounds may have increased the observed cloud points and pour points.

Table 2 The PDSC data for the samples showing the temperatures of the onset of oxidation and the temperature of the maximum rate of oxidation

Sample	Onset temp./°C	Signal maxima/°C
EMO	189.75	213.65
EMLO	180.3	214
EMLN	131.2	NA
ESBO	199	233.6
MO	177.15	200.45
MLO	138.95	177.3
MLEN	117.2	160.05
SBO	155.05	189.35
Vikoflex TM	192.75	219.2

One of the most important properties of lubricants is their ability to maintain a stable lubricating film at the metal contact zone. Fatty acid esters are known to provide excellent lubricity due to their ester functionality. The polar heads of the fatty acid esters attach to metal surfaces and allow a monolayer film formation with the non-polar end of fatty acids sticking away from the metal surface. The fatty acid alkyl chain offers a sliding surface that prevents the metal-to-metal direct contact. When a film is not formed, metal-to-metal contact may result in rising temperature at the contact zones of moving parts causing adhesion, scuffing or even welding. The epoxy group offers active oxygen sites that trigger binding on the metal surface forming a protective film. This protective film builds further with time to reduce friction.

The friction reducing properties of the compounds as additives in hexadecane solution, is reported (Table 1). Higher concentrations result in lower CoF of the corresponding sample. This is because a higher proportion of additive will increase its rate of diffusion to the metal surface. Even at low concentration, the epoxy compounds are reducing the CoF to a great extent, thereby acting as additives. The low values for the coefficient of friction (CoF) of <0.2 at either 0.04 M or 0.02 M are a considerable improvement over hexadecane solution alone, ~ 0.45 . They are also lower than the values using methyl oleate, 0.18 and 0.19, as an additive at the same concentrations.²¹ A possible explanation for our results is that the extra oxygen moieties on the epoxide groups help the compounds adhere to the metal surface and reduce friction, especially under load. The active functional groups of these compounds start acting during the metal rubbing process. During this time, these molecules undergo chemical transformation at the metal contact zone and develop a stable tribochemical film to protect further wear of the metal. These compounds show excellent friction reducing properties as additives compared to methyl oleate and linoleate using a ball-on-disk test geometry.

PDSC has been shown to be an effective tool in the measurement of oxidative stability in oleochemicals.^{7,28,29} The OT is the temperature at which a rapid increase in the rate of oxidation is observed and obtained by extrapolating the tangent drawn on the steepest slope of reaction exotherm to the baseline. A high OT would suggest a high oxidation stability of the oil. We compared the stabilities of the olefinic and the epoxy compounds (Table 2). In general the methyl olefins compounds displayed a range of onset oxidation temperatures from 117 to 177 °C. This is in agreement with the general rule that doubly allylic positions on the molecule increase oxidation susceptibility. The data also shows that OT increases with a decrease in percentage of olefin carbons and bis-allylic-CH₂ moieties. In other words, decreasing unsaturation number in oil samples increases oxidation stability. The data further shows that oxidation instabilities are due to a high content of linoleic and linolenic fatty acids that are characterized by two and three double bonds respectively. Therefore oleic-acid ester distribution in a naturally occurring ester basestock plays a major role in fluid performance. More double bonds make a material more prone to rapid oxidation and also lead to an increase in viscosity, total acid number and metal corrosion. However, some unsaturation is required to

maintain low temperature fluidity. One of the ways to reduce the viscosity increase after oxidation is epoxidation of double bonds. The epoxidation of MO, MLO and MLEN improves their thermo-oxidative stability due to removal of multiple unsaturations in fatty acid chains as shown by their higher OT. In the epoxide cases, the range is narrow, owing to a lack of allylic hydrogen atoms. Using the signal maxima temperatures as a measured value, the same trend is displayed. The olefinic ranges from 160 to 200 °C whereas both the measured epoxide values are around 214 °C. In other words, the PDSC data confirms our earlier thermogravimetric result²¹ and shows that epoxidation gives a 12–52 °C more stable compound. The VikoflexTM compound was slightly more stable than the methyl, probably owing to larger molecular weight.

We also wanted to test our samples by TFMO. In most applications, lubricants act as thin film, so TFMO test best simulates industrial conditions where oxygen diffusion is not limiting. The TFMO is a test of choice for quantitative evaluation of lubricants thermal and oxidative stability, because it is reasonably rapid and has a strong correlation with the PDSC method and the time consuming rotary bomb oxidation test. During the oxidation process, several primary oxidation products are formed. Some of these products are small fragments of the molecules and are lost as volatiles. Others in presence of excess oxygen, undergo further oxy-polymerization reactions to form oil insoluble deposits. The tendency to form such deposits is the main detrimental factor associated with unsaturated oleochemicals in their use as high-temperature lubricants. The volatile loss obtained from TFMO tests may be used to predict the useful life of lubricants, as it provides information about the amount of base fluid left for lubrication in the form of un-oxidized oil, polar oxidation products and polymerized products.

In order to generate information regarding the repeatability of the TFMO test, the oxidation test at 150 °C was performed in quadruplicate for 2 h on oleochemical samples and a standard deviation of 0.08 was obtained. The coefficient of variation is 4.5% and the % weight loss values vary within ± 0.1 of the average. This shows that the data generated in this study is accurate and reliable.

Fig. 1 shows that the volatile loss increases rapidly as the temperature is raised from 150 to 200 °C and then it is constant from 200 to 225 °C. This indicates that breakdown of molecules as a result of oxidative degradation is maximized at 200 °C. The volatile loss decreases with increasing epoxy rings in the molecules, possibly due to increasing molecular weights and viscosity. At 200 °C, it can be seen that the volatile loss of EMLN, is $< \frac{1}{2}$ of that of the closest competitor. TFMO deposit results (Fig. 2), show no significant oxidative degradation occurs up to 175 °C for all epoxy samples. This onset temperature for deposit formation corroborates the PDSC onset temperatures. The percent insoluble deposit for EMO, EMLO and VikoflexTM becomes stable after 200 °C with EMO remaining lower compared with other oils. The following sharp increase in the deposit formation of EMLN after 175 °C suggests a rapid breakdown of the epoxy group leading to oxidative polymerization through oxygen bonding. For EMO and EMLO, there is no appreciable change in deposit formation even after 175 °C. EMO and EMLO are

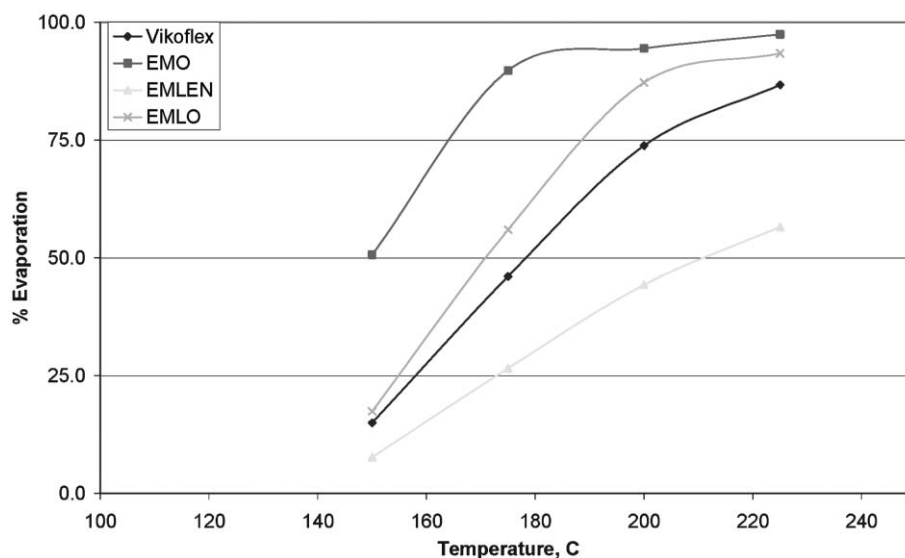


Fig. 1 TFMO data showing the % evaporation of samples at different reaction temperature. The weight loss is from both evaporation and chemical breakdown to more volatile products.

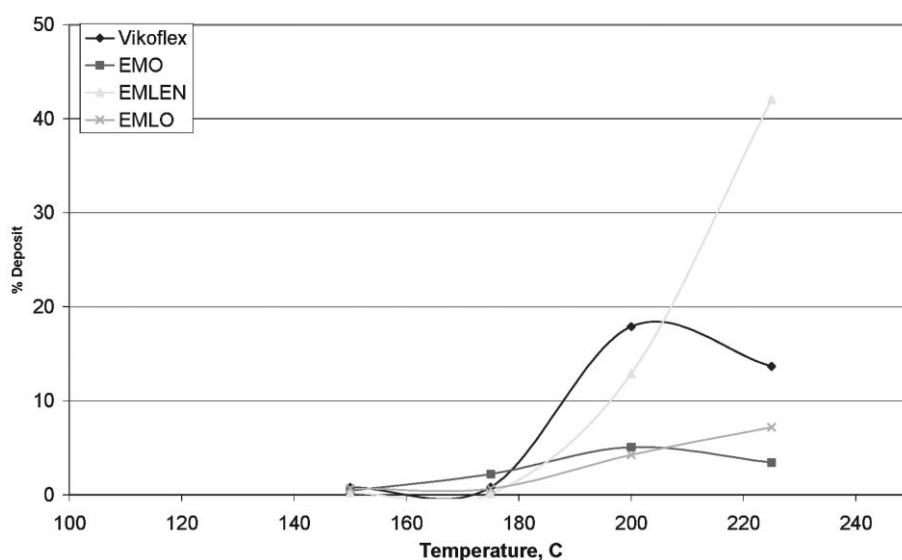


Fig. 2 TFMO data showing the % deposit of samples at different reaction temperature.

stable to deposit formation tendency up to 225 °C. The deposit forming tendency of VikoflexTM is two times higher than EMO and EMLO at 200 and 225 °C. Larger insoluble deposits observed in EMLN compared with other samples are mainly due to higher epoxy content. The presence of more epoxy rings in the EMLN are attractive sites for reaction with primary oxidation products, which results in more polymerization (leading to more insoluble deposits) and less volatile product formation. This indicates that some decomposition occurs, but to a non-volatile material. The TFMO thermo-oxidative study should correlate more readily with various high temperature bearing tests. Oxidation in the TFMO test occurs on a metal surface in an open atmosphere where evaporation can occur. Therefore, TFMO may be used as a lubricant development

and specification tool for applications in specific operating conditions and component metallurgy.

Conclusions

Lubrication is a complicated process, and one lubrication fluid or additive will not necessarily work for all situations. Our results show that under some conditions, epoxy fatty methyl esters have stability and friction reducing properties which enable them to outperform their methyl ester analogues. The epoxy moieties increase oxidative stability, probably *via* elimination of the doubly allylic hydrogen positions in the compound. Additionally, they maintain the advantages inherent from their biobased nature. Potential issues, such as

susceptibility to ring opening under acidic conditions remain. However, epoxy fatty ester compounds remain a viable option for application in the lubricant industry.

References

- 1 I. Gawrilow, *Inform*, 2004, **15**, 702.
- 2 B. K. Sharma, A. Adhvaryu, Z. Liu and S. Z. Erhan, *J. Am. Oil Chem. Soc.*, 2006, **83**, 129.
- 3 D. de Guzman, *Chem. Mark. Rep.*, 2005, **267**, 15.
- 4 G. Knothe, in *The history of vegetable oil-based diesel fuels*, ed. G. Knothe, Champaign, 2005.
- 5 A. K. Bhatnagar, S. Kaul, V. K. Chhibber and A. K. Gupta, *Energy Fuels*, 2006, **20**, 1341.
- 6 A. R. Coscione and W. E. Artz, *J. Agric. Food Chem.*, 2005, **53**, 2088.
- 7 R. O. Dunn, *Fuel Process. Technol.*, 2005, **86**, 1071.
- 8 J. Polavka, J. Paligová, J. Cvengros and P. Simon, *J. Am. Oil Chem. Soc.*, 2005, **82**, 519.
- 9 S. Z. Erhan, B. K. Sharma and J. M. Perez, *Ind. Crops Prod.*, 2006, **24**, 292.
- 10 H.-S. Hwang and S. Z. Erhan, *J. Am. Oil Chem. Soc.*, 2001, **78**, 1179.
- 11 S. Li, J. Blackmon, A. Demange and T.-C. Jao, *Lubr. Sci.*, 2004, **16**, 127.
- 12 J. W. King, R. L. Holliday, G. R. List and J. M. Snyder, *J. Am. Oil Chem. Soc.*, 2001, **78**, 107.
- 13 T. W. Findley, D. Swern and J. T. Scanlan, *J. Am. Chem. Soc.*, 1945, **67**, 412.
- 14 G. L. Crocco, W. F. Shum, J. G. Zajacek and H. S. J. Kesling, Epoxidation Process, 5166372, Nov. 24, 1992.
- 15 K. D. Carlson, R. Kleiman and M. O. Bagby, *J. Am. Oil Chem. Soc.*, 1994, **71**, 175.
- 16 A. Campanella, M. A. Baltanás, M. C. Capel-Sánchez, J. M. Campos-Martín and J. L. G. Fierro, *Green Chem.*, 2004, **6**, 330.
- 17 S. Z. Erhan, M. O. Bagby and T. C. Nelsen, *J. Am. Oil Chem. Soc.*, 1997, **74**, 703.
- 18 R. A. Holser, K. M. Doll and S. Z. Erhan, *Fuel*, 2006, **85**, 393.
- 19 E. Verkuijlen, F. Kapteijn, J. Mol and C. Boelhouwer, *Chem. Commun.*, 1977, 198.
- 20 W. R. Schmits and J. G. Wallace, *J. Am. Oil Chem. Soc.*, 1954, **31**, 363.
- 21 T. L. Kurth, B. K. Sharma, K. M. Doll and S. Z. Erhan, *Chem. Eng. Commun.*, 2006, in press.
- 22 K. M. Doll and S. Z. Erhan, *J. Agric. Food Chem.*, 2005, **53**, 9608.
- 23 R. J. Muir, *Detergent anti-oxidant additives for fuels and lubricants*, 20050172543, Aug. 11, 2005.
- 24 K. M. Doll and S. Z. Erhan, *J. Surfactants Deterg.*, 2006, **9**, 377.
- 25 S. P. Bunker and R. P. Wool, *J. Polym. Sci., Part A: Polym. Chem.*, 2002, **40**, 451.
- 26 J. A. Nowak, T. A. Zillner and I. Mullin, Leslie Patrick; *Thin-film Epoxidation of an Unsaturated Oil or Alkyl Fatty Acid Ester*, US 6734315, May 11, 2004.
- 27 J. La Scala and R. P. Wool, *J. Am. Oil Chem. Soc.*, 2002, **79**, 373.
- 28 Y. Y. Zhang, T. H. Ren, H. D. Wang and M. R. Yi, *Lubr. Sci.*, 2004, **16**, 385.
- 29 A. Adhvaryu, G. Biresaw, B. K. Sharma and S. Z. Erhan, *Ind. Eng. Chem. Res.*, 2006, **45**, 3735.
- 30 A. Adhvaryu, B. K. Sharma, H. S. Hwang, S. Z. Erhan and J. M. Perez, *Ind. Eng. Chem. Res.*, 2006, **45**, 928.

One-pot synthesis of 1,4-naphthoquinones and related structures with laccase

Suteera Witayakran and Arthur J. Ragauskas*

Received 15th June 2006, Accepted 18th January 2007

First published as an Advance Article on the web 5th February 2007

DOI: 10.1039/b606686k

The one-pot synthesis of 1,4-naphthoquinones by the Diels–Alder reaction of dienes with *para*-quinones generated *in situ* with laccase (EC 1.10.3.2, *p*-diphenol:dioxygen oxidoreductase) in an aqueous medium was developed in this study. The *para*-quinones were generated *in situ* by the laccase oxidation of the corresponding 1,4-hydroquinones and subsequently underwent the Diels–Alder reaction with dienes, and further oxidation to finally generate 1,4-naphthoquinones, in good yields. This reaction methodology provides unique green chemistry synthesis for isolation of the naphthoquinones, and without relying on organic solvents or hazardous heavy metal reagents. In this paper, the effects of laccase dose, temperature, and substrate sensitivity on the overall reaction were investigated.

Introduction

The most abundant and available resource on the planet, one in which biochemical processes take place, is the aqueous medium, water. Recently, water has begun to be regarded as an environmentally friendly solvent in organic chemistry. In addition to its environmental benefits, the use of water as a solvent is both inexpensive and safe. In recent decades, the study of the organic reactions in aqueous solvent has accelerated and many, often surprising, discoveries have been made.^{1,2} Breslow and Rideout³ were the first to show the beneficial effects of water on the reactivity and selectivity of the Diels–Alder reaction. This discovery stimulated further research in this area. Shortly after, several studies showed that many chemical reactions (such as pericyclic,^{1,4} condensation,¹ oxidation,^{1,5} and reduction^{1,6} reactions) could be conducted efficiently in the aqueous medium.

Among the organic reactions investigated in the aqueous medium, the most widely studied reaction is the Diels–Alder reaction,⁷ a powerful tool frequently employed to synthesize six-membered ring systems, and one of the most useful reactions for introducing structural complexity in (total) synthesis.⁸ The Diels–Alder reaction has many useful variations, one of which is its use in the synthesis of anthraquinones and naphthoquinones.⁹ Naphthoquinones have attracted considerable attention in total synthesis because of their wide spectrum of biological activities, such as antitumor,¹⁰ wound healing,¹¹ anti-inflammatory,¹¹ and antimicrobial¹² and antiparasitic activities.¹³ Another useful application of the Diels–Alder reaction is the quinone Diels–Alder (QDA) reaction¹⁴ (Fig. 1). In this reaction, quinones are employed as dienophiles, which normally possess electron-withdrawing groups. This class of quinones are usually unstable and difficult to isolate. To overcome these difficulties, many studies have focused on the Diels–Alder reaction of *in situ*-generated quinones.¹⁵ Herein, we report the use of the enzyme, laccase, used in the *in situ* generation of quinones.

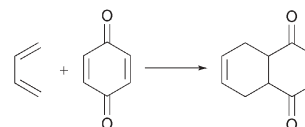


Fig. 1 The quinone Diels–Alder (QDA) reaction.

Laccases (benzenediol:oxygen oxidoreductase, EC 1.10.3.2) are multi-copper-containing oxidoreductase enzymes widely distributed in plants and fungi. They are able to catalyze the oxidation of various low-molecular weight compounds, specifically, phenols and anilines; while concomitantly, reducing molecular oxygen to water.^{16,17} Moreover, due to their high stability, selectivity for phenolic substructures, and mild reaction conditions used in laccase-catalyzed reactions, laccases are attractive for fine chemical synthesis. Therefore, interest in the potential use of these enzymes in organic synthesis has recently increased.¹⁸

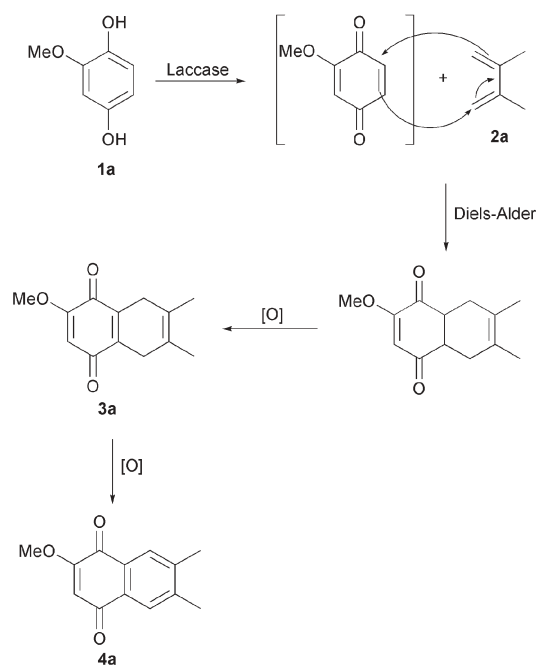
This study presents work on the synthesis of 1,4-naphthoquinones and related structures in an aqueous medium. In this procedure, *para*-quinone, generated *in situ* from the oxidation of *para*-hydroquinone by laccase, underwent the quinone Diels–Alder reaction with a diene, and then the Diels–Alder adduct was converted directly into dihydro-1,4-naphthoquinone. Upon extended treatment, this initial product was further oxidized to naphthoquinone as summarized in Scheme 1. The effects of laccase dosage and temperature on these reactions, with the reaction of 2-methoxyhydroquinone (**1a**) and 2,3-dimethyl-1,3-butadiene (**2a**) as a model system, are reported here. This study also investigated the sensitivity of this reaction system to a variety of *para*-hydroquinones and dienes.

Results and discussion

Preliminary study of the reaction system

The reaction procedure was initially investigated by using **1a** and **2a** as the model reagents and laccase as an oxidizing agent.

School of Chemistry and Biochemistry, Georgia Institute of Technology, Atlanta, GA, USA. E-mail: arthur.ragauskas@chemistry.gatech.edu; Fax: +1 404 894 4778; Tel: +1 404 894 9701



Scheme 1 The proposed reaction pathway.

The role of laccase for this reaction was to convert **1a** to 2-methoxy-1,4-benzoquinone, and then 2-methoxy-1,4-benzoquinone reacted with diene **2a** by the Diels–Alder reaction. The Diels–Alder adducts then underwent further oxidation to generate 5,8-dihydro-2-methoxy-6,7-dimethyl-1,4-naphthoquinone (**3a**) and 2-methoxy-6,7-dimethyl-1,4-naphthoquinone (**4a**).

In this preliminary study, the total amount of laccase used in the reaction was 1000 U per 1 g of substrate, and the equivalence ratio of 2-methoxyhydroquinone and 2,3-dimethyl-1,3-butadiene was 1 : 2, to ensure that no *in situ*-generated 2-methoxy benzoquinone remained to further oxidize the Diels–Alder adducts. The reaction was conducted in 0.10 M acetate buffer pH 4.5, in the presence of oxygen at 50 °C, for 24 hours (Fig. 2). A pH of 4.5 was chosen for this reaction system because many studies have shown that pH 4.5 is the optimum pH for laccase activity in the formation of quinone, as in the work of Ishihara, Leonowicz *et al.*, and Raguaskas.¹⁹ In this reaction system, vigorous stirring was

required to disperse **2a**, which is slightly dissolved in water, in an emulsion to increase the reaction rate between the *in situ*-generated quinone and **2a**. Moreover, the hydrophobic interactions between relatively apolar quinone and **2a** forced them into close proximity and favour the Diels–Alder reaction products.

In the preliminary study, we examined the effect of oxygen on the formation of the products. We found that the quantity of oxygen affected the reaction. When an excessive amount of oxygen, such as bubbling oxygen through the end of reaction and pressurizing oxygen at 145 psi, was used, the main product was 2-methoxy-1,4-benzoquinone (26%) and very small amounts of **3a** and **4a** were generated. In contrast, stirring the reaction under air generated **3a** (13%) and **4a** (45%). However, we also found that bubbling oxygen for 30 minutes into a laccase/buffer solution before adding all the reagents and gradually adding ¼ of the laccase (250 U per 1 g of substrate) at the beginning of each of the first four hours of the 24 hour reaction improved the yield of **3a** and **4a** to 15% and 50%, respectively. After this reaction procedure was examined, the control reaction adding no laccase was studied. The result showed that when no laccase was added to the system, no desired products were obtained. Therefore, the oxidizing agent, laccase, must be added to generate 2-methoxy-1,4-benzoquinone *in situ*. This quinone then underwent further reaction with diene to generate **3a** and **4a**.

The effect of laccase dose

After the preliminary study, the next approach was to optimize the reaction conditions. The optimization was studied by investigating the effects of laccase dose and temperature. The laccase doses used in these experiments were 500, 1000, 2000, and 4000 U per 1 g of **1a**. The reaction was conducted at 50 °C. The method for this study is described in the Experimental. The quantitative study of **3a** and **4a** was measured by ¹H-NMR spectroscopy using tetrafluorobenzaldehyde as an internal standard. Fig. 3 shows the results of the study.

According to Fig. 3, the amount of laccase in the reaction affected the formation of **3a** and **4a**. When the amount of laccase used in the reaction was increased from 500 to 4000 U per 1 g of substrate, the percent yield of **3a** and **4a** at the end of the reaction (24 hours) also increased from 15% to 34% and from 47% to 60%, respectively. In addition, the formation of **3a** sharply increased in the first three hours, and then decreased gradually throughout the reaction. In contrast, the formation of **4a** increased slightly in the first two hours, and then gradually increased after the third hour of the reaction. The explanation of this result is that the formation of **3a** was predominant at the beginning of the reaction, and upon further treatment, some of **3a** was gradually oxidized to generate **4a**, leading to the continual increase in the yield of **4a** at the longer reaction time. The proposed reaction pathway is summarized in Scheme 1. Laccase first converted **1a** to 2-methoxy-1,4-benzoquinone and then the quinone reacted with diene **2a** by the Diels–Alder reaction to generate the Diels–Alder adduct. The Diels–Alder adduct was then oxidized by either laccase or quinone in the reaction solution to generate **3a**, and upon further treatment, **3a** was oxidized to

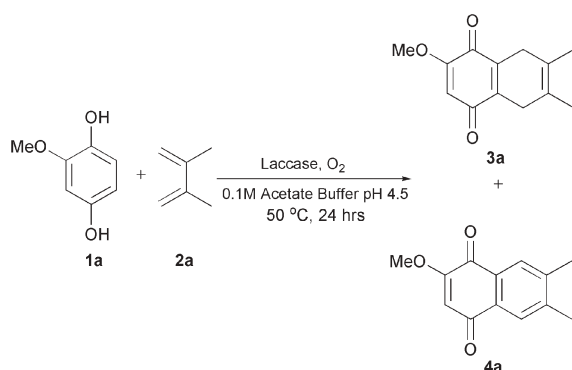


Fig. 2 The preliminary reaction system.

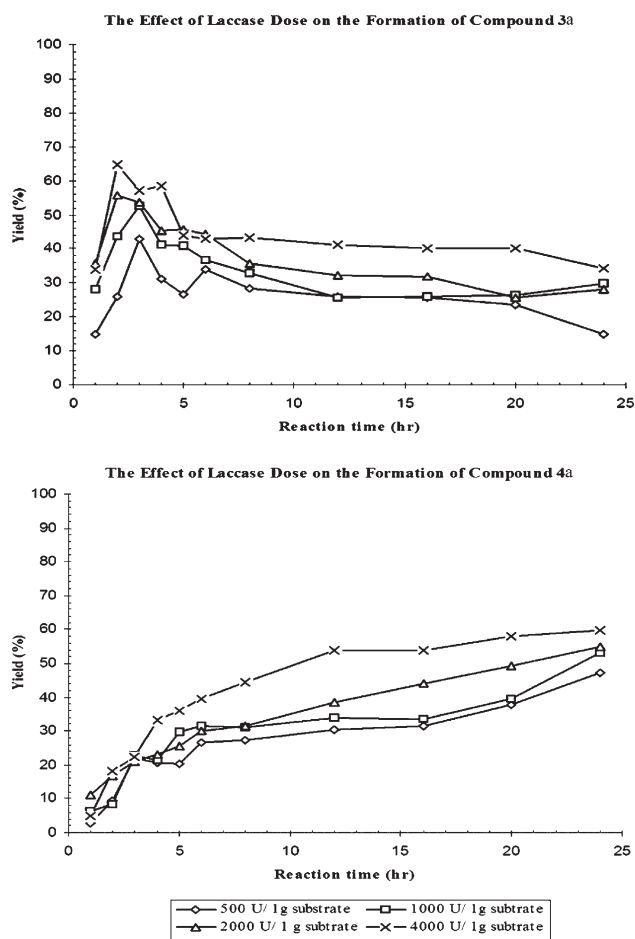


Fig. 3 The effect of laccase dose on the formation of compound **3a** and **4a**. The percent yield of **3a** and **4a** was measured by $^1\text{H-NMR}$ spectroscopy.

4a. To confirm the proposed reaction pathway, we stirred **3a** in 0.10 M acetate buffer, pH 4.5 at 70 °C for 24 hours, with either laccase (4000 U per 1 g of **3a**) or with 2-methoxybenzoquinone (model quinone) (1 equiv.). The results show that the percent conversion of **3a** to **4a** was 35% and 16% with laccase and 2-methoxybenzoquinone respectively. Therefore, these results show that both laccase and quinone in the reaction solution can oxidize **3a** to generate **4a**. However, laccase appears to be a better oxidizing agent than the quinone in this reaction system.

The effect of temperature

As demonstrated in the previous section, laccase dose has an influence on the formation of compounds **3a** and **4a**. The more laccase we used, the more products we obtained. Another factor that should affect the reaction is temperature. Thus, the experiment was conducted at different temperatures, including 25 °C, 50 °C, 70 °C, and 100 °C. The reaction procedure was the same as that used before except 4000 U per 1 g of **1a** was used. Fig. 4 illustrates the effect of temperature on the reaction.

It is obvious that when **4a** was formed, its yield increased when the temperature of the reaction increased. For example, at the end of the reaction, the percent yield of **4a** was 17%,

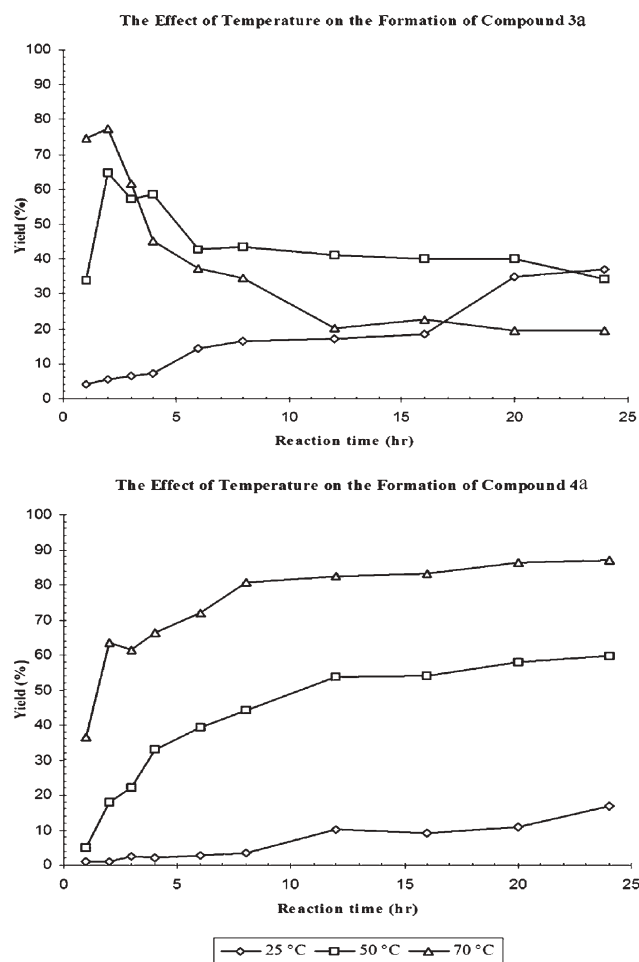


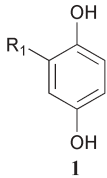
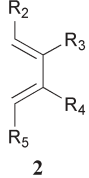
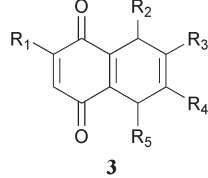
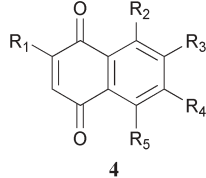
Fig. 4 The effect of temperature on the formation of compound **3a** and **4a**. The percent yield of **3a** and **4a** was measured by $^1\text{H-NMR}$ spectroscopy. (No products were obtained at 100 °C.)

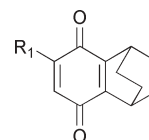
60%, and 87% for the reaction at 25 °C, 50 °C, and 70 °C, respectively. In contrast, the formation of **3a** exhibited a different response to temperatures. For the reaction at 50 °C and 70 °C, the amount of **3a** sharply increased in the first two hours, and then decreased after the second hour. However, the decrease at 70 °C was faster than that at 50 °C because a higher temperature can more easily accelerate the conversion of **3a** to **4a**. For the reaction at 25 °C, the formation of **3a** gradually increased throughout the reaction. Moreover, we found that 2-methoxy-6,7-dimethyl-4a,5,8,8a-tetrahydro-1,4-naphthoquinone, the Diels–Alder adduct, was the main product of the reaction at 25 °C, instead of **3a** and **4a**. Therefore, this reaction best underwent the quinone Diels–Alder reaction to generate the Diels–Alder adduct at a low temperature, and upon further treatment, the Diels–Alder adduct was slowly converted to **3a**, and only a small amount of **4a** was obtained. For the reaction at 100 °C, no products were obtained because, at this high temperature, laccase was denatured.

The reaction of *p*-hydroquinones and dienes

From the optimization experiments, we chose to conduct the reaction with 4000 U of laccase per 1 g of substrate at 70 °C for

Table 1 The reaction of *p*-hydroquinones and dienes^a

<i>p</i> -Hydroquinone	Diene	Products(% yield) ^b	
			
1	2	3	4
1a: R ₁ = OMe	2a: R ₂ = R ₅ = H, R ₃ = R ₄ = Me	3a (10%)	4a (60%)
1a	2b: R ₂ = R ₄ = H, R ₃ = R ₅ = Me	3b (9%)	4b (55%)
1a	2c: R ₃ = R ₄ = H, R ₂ = R ₅ = Me	3c (46%)	no product formed
1a	2d: R ₂ = R ₅ = H, R ₃ = R ₄ = OMe	no product formed	4c (12%)
1a	2e: R ₃ = R ₄ = R ₅ = H, R ₂ = OMe	no product formed	4d (79%) R ₂ = H
1b: R ₁ = Me	2a	3d (20%)	4e (22%)
1b	2c	3e (19%)	no product formed
1b	2d	no product formed	4f (4.28%) ^c
1b	2e	no product formed	4g (40%), R ₂ = H
1c: R ₁ = Br	2a	no product formed	4h (21%)
1a	2f	3f (64%)	
1b	2f	3g (49%)	
1c	2f	3h (51%)	



^a Reaction conditions: the reaction of *p*-hydroquinone (1 equiv.) and diene (2 equiv.) was stirred with laccase (4000 U per 1 g substrate) in 0.10 M acetate buffer pH 4.5 at 70 °C for 24 hours. ^b Isolated yield. ^c Found 26% of methylbenzoquinone as another product.

24 hours to investigate the reaction of various *para*-hydroquinones and dienes as shown in Table 1.

In this experiment, three different *p*-hydroquinones, in which R₁ represented the OMe, Me, and Br groups, were used, and the reaction conducted with a variety of dienes. The data in Table 1 shows that, in most cases, 1,4-naphthoquinone products (**4**) were obtained as major products, and only small amounts or none of the dihydro-1,4-naphthoquinone products (**3**) were obtained. However, when dienes have alkyl groups at R₂ and R₅ (e.g., **2c** and **2f**), only **3**-type products were formed. In addition, when R₁ is the OMe group, the yield of products was higher than when R₁ is the Me or Br groups. Although quinones with a Br substituent, a strong electron-withdrawing group, have been proven to be very reactive dienophiles for the Diels–Alder reaction, it produced a lower yield of the products than quinones with an OMe substituent, an electron-donating group. This result can be explained by the substrate affinity of laccase, which varies depending on the substituents and their reciprocal positions on the aromatic ring. Therefore, *p*-hydroquinones that have higher affinity to laccase are more easily oxidized, and generate higher amounts of the starting quinone that react with diene in the first step of the reaction. In this case, *p*-hydroquinones with the Br substituent have lower affinity to laccase than *p*-hydroquinones with OMe. This result agrees with a previous study that reported the high affinity of phenolic compounds bearing methoxyl groups to laccase.²⁰ In addition, substituents also have an effect on the redox potential of the hydroquinone starting material. Xu²¹ showed that the electron-withdrawing substituents reduce the electron density at the phenoxy group and increase the redox potential of the molecule, thus making it more difficult to be oxidized and less reactive in surrendering electrons to the substrate pocket in laccase. In contrast, the presence of the

electron-donating substituents results in a reduction in redox potential. These trends are consistent with our results, since the *p*-hydroquinone with an OMe group is more easily oxidized than that with the Br group.

Conclusions

Here, we reported a new green chemistry synthesis of 1,4-naphthoquinones and related structures by using both a non-hazardous oxidizing agent, laccase, and the environmentally benign solvent, water. This study also shows another potential use of laccase as an oxidizing agent in organic synthesis. Moreover, the reaction system we used in this study produced the 1,4-naphthoquinone products in high yield. However, the reactivity of the reaction depends on the substrate specificity of laccase and the reactivity of both generated quinones and dienes.

Experimental

Materials

2-Methoxyhydroquinone was obtained from TCI America. Other hydroquinones, dienes, and reagents were obtained from Aldrich. All chemicals were used as received. Laccase (EC 1.10.3.2) from *Trametes villosa* was donated by Novo Nordisk Biochem, North Carolina.

Enzyme assay

Laccase activity was determined by oxidation of 2,2'-azinobis-(3-ethylbenzylthiozoline-6-sulfonate) (ABTS).²² The assay mixture contained 25 μM ABTS, 0.1 M sodium acetate (pH 5.0), and a suitable amount of enzyme. The oxidation of

ABTS was followed by an absorbance increase at 420 nm ($\epsilon_{420} = 3.6 \times 10^4 \text{ M}^{-1} \text{ cm}^{-1}$). Enzyme activity was expressed in units (U = μmol of ABTS oxidized per minute).

General procedure for the study of the effect of laccase dose and temperature

Oxygen was bubbled through a stirred solution of 30 ml of 0.1 M acetate buffer (pH 4.5) and laccase ($\frac{1}{4}$ of the total amount of laccase used in this reaction) at a desired temperature for 30 minutes. Next, 2-methoxyhydroquinone (0.1 g, 0.714 mmol) and diene (2 equiv., 1.428 mmol) were added to the reaction mixture, and stirred under air. In the first three hours of the reaction, $\frac{1}{4}$ of the total amount of laccase was added each hour. After the reaction reached the desired reaction time, the reaction mixture was extracted by EtOAc ($3 \times 30 \text{ ml}$). The organic phase was combined, dried over MgSO_4 , and evaporated. Then, the quantitative analyses of **3a** and **4a** were determined by ^1H -NMR spectroscopy of the crude mixture using tetrafluorobenzaldehyde as an internal standard.

General procedure for the reaction of *p*-hydroquinones and dienes (Table 1)

Oxygen was bubbled through a stirred solution of 30 ml of 0.1 M acetate buffer (pH 4.5) and laccase (100 U) at 70 °C for 30 minutes. Next, *p*-hydroquinone (0.1 g, 1 equiv.) and diene (2 equiv.) were simultaneously added into the reaction mixture, and stirred under air, at 70 °C. In the first three hours of the reaction, 100 U of laccase was added each hour. After 24 hours of the reaction, the reaction mixture was extracted by EtOAc ($3 \times 30 \text{ ml}$). The organic phase was combined, dried over MgSO_4 , and evaporated. The resulting crude products were purified by silica column chromatography, using ethyl acetate and hexane as an eluent to obtain the products. Products **3a**, **3b**, **3c**, **3d**, **4a**, **4b**, **4c**, **4d**, **4e**, **4g**, and **4h** have been previously reported and characterized. Compounds **3e**, **3g**, and **4f** have also been previously reported but without complete spectral characterization. Structures **3f** and **3h** are, to the best of our knowledge, new compounds. All known products provided satisfactory analytical and spectroscopic data corresponding to the reported literature values.

5,8-Dihydro-2,5,8-trimethyl-1,4-naphthoquinone (3e)

Yellow liquid; ^1H NMR (400 MHz; CDCl_3): δ 1.25 (d, $J = 2.2 \text{ Hz}$, 3H), 1.26 (d, $J = 2.2 \text{ Hz}$, 3H), 2.10 (s, 3H), 3.43 (m, 2H), 5.83 (d, $J = 2.7 \text{ Hz}$, 2H), 6.61 (s, 1H); ^{13}C NMR (100 MHz, CDCl_3): δ 15.7, 22.8, 22.9, 29.3, 29.5, 128.8, 128.9, 133.2, 144.0, 144.1, 145.4, 186.9, 187.3; m/z (EI) 202 (M^+ , 100%), 187 (79), 159 (41), 119 (56), 91 (26), 39 (7); m/z (EI) 202.09985 ($\text{C}_{13}\text{H}_{14}\text{O}_2$ requires 202.09938).

1,4-Dihydro-6-methoxy-1,4-Ethanonaphthalene-5,8-dione (3f)

Yellow needles; mp 123–124 °C (from EtOH); ^1H NMR (400 MHz; CDCl_3): δ 1.35 (d, $J = 6.8 \text{ Hz}$, 2H), 1.49 (d, $J = 8 \text{ Hz}$, 2H), 3.80 (s, 3H), 4.34 (br s, 1H), 4.37 (br s, 1H), 5.76 (s, 1H), 6.39 (br s, 2H); ^{13}C NMR (100 MHz, CDCl_3): δ 24.4, 24.4, 33.4, 33.7, 56.2, 105.9, 133.5, 133.7, 146.0, 149.2, 158.5,

178.1, 183.7; $\nu_{\text{max}}/\text{cm}^{-1}$ 3055, 2938, 2869, 1668, 1642, 1624, 1598, 1582, 1452, 1380, 1224, 1135, 1013, 868, 818; m/z 216 (M^+ , 21%), 188 (100, $\text{M} - \text{CH}_2\text{CH}_2$), 173 (39), 158 (52), 130 (14), 102 (28), 89 (33), 69 (14), 51 (8); m/z (EI) 216.08073 ($\text{C}_{13}\text{H}_{12}\text{O}_3$ requires 216.07864).

1,4-Dihydro-6-methyl-1,4-Ethanonaphthalene-5,8-dione (3g)

Yellow needles; mp 81–82 °C (from EtOH); ^1H NMR (400 MHz; CDCl_3): δ 1.34 (m, 2H), 1.47 (m, 2H), 2.03 (d, $J = 1.6 \text{ Hz}$, 3H), 4.31 (br m, 1H), 4.35 (br m, 1H), 6.38 (dd, $J = 2.7 \text{ Hz}$, 3.8 Hz, 2H), 6.44 (q, $J = 1.6 \text{ Hz}$, 1H); ^{13}C NMR (100 MHz, CDCl_3): δ 15.7, 24.5, 24.5, 33.5, 33.7, 132.1, 133.6, 133.7, 144.8, 148.1, 148.1, 183.8, 184.1; m/z (EI) 200 (M^+ , 14%), 172 (100, $\text{M} - \text{CH}_2\text{CH}_2$), 144 (27), 116 (14), 104 (18), 76 (10), 39 (3); m/z (EI) 200.08399 ($\text{C}_{13}\text{H}_{12}\text{O}_2$ requires 200.08373).

1,4-Dihydro-6-bromo-1,4-Ethanonaphthalene-5,8-dione (3h)

Orange crystals; mp 104–106 °C (from EtOH); ^1H NMR (400 MHz; CDCl_3): δ 1.39 (d, $J = 8.5 \text{ Hz}$, 2H), 1.53 (d, $J = 8 \text{ Hz}$, 2H), 4.35 (br m, 1H), 4.44 (br m, 1H), 6.42 (t, $J = 3.4 \text{ Hz}$, 2H), 7.15 (s, 1H); ^{13}C NMR (100 MHz, CDCl_3): δ 24.5, 24.6, 33.9, 34.8, 133.5, 133.7, 136.7, 137.0, 147.9, 148.9, 175.8, 181.1; $\nu_{\text{max}}/\text{cm}^{-1}$ 3043, 2998, 2935, 2869, 1660, 1645, 1627, 1571, 1445, 1331, 1302, 1263, 1233, 1051, 892, 777; m/z (EI) 266 ($\text{M} + 2$, 9%), 264 (M^+ , 9%), 238 (82, ($\text{M} + 2) - \text{CH}_2\text{CH}_2$), 236 (80, $\text{M} - \text{CH}_2\text{CH}_2$), 185 (10), 157 (100), 129 (41), 101 (21), 76 (11), 51 (7); m/z (EI) 263.97755 ($\text{C}_{12}\text{H}_9\text{O}_2\text{Br}$ requires 263.97859).

2-Methyl-6,7-dimethoxy-1,4-naphthoquinone (4f)

Orange-yellow solid; ^1H NMR (400 MHz; CDCl_3): δ 2.16 (s, 3H), 4.01 (s, 6H), 6.73 (s, 1H), 7.47 (s, 1H), 7.51 (s, 1H); ^{13}C NMR (100 MHz, CDCl_3): δ 16.5, 56.5, 56.5, 107.5, 108.0, 111.4, 126.9, 127.1, 135.2, 147.7, 153.2, 184.6, 185.1; m/z (EI) 232 (M^+ , 100%), 202 (31), 189 (19), 136 (12), 93 (7), 39 (8); m/z (EI) 232.08528 ($\text{C}_{13}\text{H}_{12}\text{O}_4$ requires 232.07356).

CAS Registry No. **3a**, 91910-25-7; **3b**, 174769-02-9; **3c**, 174768-72-0; **3d**, 55699-87-1; **3e**, 55922-70-8; **3g**, 91902-54-4; **4a**, 52280-68-9; **4b**, 174769-29-0; **4c**, 62345-15-7; **4d**, 2348-82-5; **4e**, 59832-90-5; **4f**, 91903-58-1; **4g**, 58-27-5; **4h**, 18690-93-2.

Acknowledgements

The authors acknowledge financial support from the IPST@GT student fellowship and the Royal Thai Government Scholarship. We also would like to thank R. A. Braga for IR measurements.

References

- 1 *Organic Synthesis in Water*, ed. P. A. Grieco, Blackie Academic and Professional, London, 1998.
- 2 C.-J. Li, *Chem. Rev.*, 1993, **93**, 2023–2035; U. M. Lindstrom, *Chem. Rev.*, 2002, **102**, 2751–2772; S. Narayan, J. Muldoon, M. G. Finn, V. V. Fokin, H. C. Kolb and K. B. Sharpless, *Angew. Chem., Int. Ed.*, 2005, **44**, 3275–3279; C.-J. Li, *Chem. Rev.*, 2005, **105**, 3095–3165.
- 3 D. C. Rideout and R. Breslow, *J. Am. Chem. Soc.*, 1980, **102**, 7816–7817.

- 4 F. Fringuelli, O. Piermatti and F. Pizzo, *Targets in Heterocyclic Systems*, ed. A. O. Attanasi and D. Spinelli, Società Chimica Italiana, Rome, 1997, vol. 1, 57.
- 5 K. Surendra, N. S. Krishnaveni, V. P. Kumar, R. Sridhar and K. R. Rao, *Tetrahedron Lett.*, 2005, **46**, 4581–4583; K.-H. Tong, K.-Y. Wong and T. H. Chan, *Tetrahedron*, 2005, **61**, 6009–6014; R. Liu, C. Dong, X. Liang, X. Wang and X. Hu, *J. Org. Chem.*, 2005, **70**, 729–731.
- 6 X. Wu, X. Li, F. King and J. Xiao, *Angew. Chem., Int. Ed. Engl.*, 2005, **44**, 3407–3411; R. Nakao, H. Rhee and Y. Uozumi, *Org. Lett.*, 2005, **7**, 163–165.
- 7 F. Fringuelli and A. Taticchi, *The Diels–Alder Reaction: Selected Practical Method*, John Wiley & Sons, Ltd, West Sussex, 2002, pp. 251–267; F. Fringuelli, O. Piermatti, F. Pizzo and L. Vaccaro, *Eur. J. Org. Chem.*, 2001, 439–455.
- 8 W. Carruthers, *Some Modern Methods of Organic Synthesis*, Cambridge University Press, Cambridge, 3rd edn, 1986, ch. 3; W. Carruthers, *Cycloaddition Reactions in Organic Synthesis*, Pergamon Press, Oxford, 1990, pp. 124–129; E. Marsault, A. Toró, P. Nowak and P. Deslongchamps, *Tetrahedron*, 2001, **57**, 4243–4260; K. C. Nicolaou, S. A. Synder, T. Momtagnon and G. Vassilikogiannakis, *Angew. Chem., Int. Ed.*, 2002, **41**, 1668–1698.
- 9 R. H. Thomson, in *The Total Synthesis of Natural Products*, ed. J. ApSimon, John Wiley, New York, 1992, vol.8, pp. 325–404; R. H. Thomson, *The Chemistry of the Quinonoid Compounds Part I*, ed. S. Patai, John Wiley & Sons, Bristol, 1974, pp. 149–152.
- 10 S. Subramanian, M. M. C. Ferreira and M. Trsic, *Struct. Chem.*, 1998, **9**, 47–57; G. Powis, *Free Radical Biol. Med.*, 1989, **6**, 63–101.
- 11 V. P. Papageorgiou, A. N. Assimopoulou, E. A. Couladouros, D. Hepworth and K. C. Nicolaou, *Angew. Chem., Int. Ed.*, 1999, **38**, 270–300.
- 12 T. B. Machado, A. V. Pinto, M. C. F. R. Pinto, I. C. R. Leal, M. G. Silva, A. C. F. Amaral, R. M. Kuster and K. R. Netto-dosSantos, *Int. J. Antimicrob. Agents*, 2003, **21**, 279–284.
- 13 A. F. dos Santos, P. A. L. Ferraz, A. V. Pinto, M. C. F. R. Pinto, M. O. F. Goulart and A. E. G. Sant'Ana, *Int. J. Parasitol.*, 2000, **30**, 1199–1202; M. O. F. Goulart, C. L. Zani, J. Tonholo, L. R. Freitas, F. G. Abreu, A. B. Oliveira, D. S. Raslan, S. Starling and E. Chiari, *Bioorg. Med. Chem. Lett.*, 1997, **7**, 2043–2048.
- 14 J. B. Hendrickson and V. Singh, *J. Chem. Soc., Chem. Commun.*, 1983, **15**, 837–838; J. I. Levin, *Tetrahedron Lett.*, 1996, **37**, 3079–3082; J. D. White and Y. Choi, *Helv. Chim. Acta*, 2002, **85**, 4306–4327; D. A. Evans and J. Wu, *J. Am. Chem. Soc.*, 2003, **125**, 10162–10163; A. A. Boezio, E. R. Jarvo, B. M. Lawrence and E. N. Jacobsen, *Angew. Chem., Int. Ed.*, 2005, **44**, 6046–6050.
- 15 K. Chiba and M. Tada, *J. Chem. Soc., Chem. Commun.*, 1994, **21**, 2485–2486; K. Chiba, M. Jinno, A. Nozaki and M. Tada, *Chem. Commun.*, 1997, **15**, 1403–1404; K. Chiba, M. Jinno, R. Kuramoto and M. Tada, *Tetrahedron Lett.*, 1998, **39**, 5527–5530.
- 16 C. Thurston, *Microbiology*, 1994, **140**, 19–26; A. Yaropolov, O. Skorobogatko, S. Vartanov and S. Varfolomeyev, *Appl. Biochem. Biotechnol.*, 1994, **49**, 257–280.
- 17 S. G. Burton, *Curr. Org. Chem.*, 2003, **7**, 1317–1331; H. Claus, *Micron*, 2004, **35**, 93–96; S. Nicotra, A. Intra, G. Ottolina, S. Riva and B. Danieli, *Tetrahedron: Asymmetry*, 2004, **15**, 2927–2931; S. Nicotra, R. M. Cramarossa, A. Mucci, M. U. Pagnoni, S. Riva and L. Forti, *Tetrahedron*, 2004, **60**, 595–600; X. Zhang, G. Eigendorf, W. D. Stebbing, D. S. Mansfield and N. J. Saddler, *Arch. Biochem. Biophys.*, 2002, **405**, 44–54.
- 18 T. H. J. Niedermeyer, A. Mikolasch and M. Lalk, *J. Org. Chem.*, 2005, **70**, 2002–2008; S. Ciecholewski, E. Hammer, K. Manda, G. Bose, A. T. H. Nguyen, P. Langer and F. Schauer, *Tetrahedron*, 2005, **61**, 4615–4619.
- 19 T. Ishihara, *Mokuzai Gakkaishi*, 1983, **29**, 801–805; A. Leonowicz, R. U. Edgehill and J.-M. Bollag, *Arch. Microbiol.*, 1984, **137**, 89–96; F. S. Chakar and A. J. Ragauskas, ACS Series Fundamentals and Catalysis of Oxidative Delignification Processes, in *Oxidative Delignification Chemistry, Fundamentals and Catalysis*, ed. D.A. Argyropoulos, ACS Symposium Series, Oxford University Press, Washington, 2001, vol. 785, 444–455.
- 20 A. D'Annibale, D. Celletti, M. Felici, E. DiMattia and G. Giovannozzi-Sermanni, *Acta Biotechnol.*, 1996, **16**, 257–270.
- 21 F. Xu, *Biochemistry*, 1996, **35**, 7608–7614.
- 22 R. Bourbonnais, D. Leech and G. M. Paice, *Biochem. Biophys. Acta*, 1998, **1379**, 381–390.

Self-aggregation of ionic liquids: micelle formation in aqueous solution†

Marijana Blesic,^a Maria Helena Marques,^a Natalia V. Plechkova,^b Kenneth R. Seddon,^{ab} Luís Paulo N. Rebelo^{*a} and António Lopes^{*a}

Received 23rd October 2006, Accepted 12th January 2007

First published as an Advance Article on the web 15th February 2007

DOI: 10.1039/b615406a

Interfacial tension (using a drop-shape analysis technique), fluorescence (of a widely used spectroscopic molecular probe, pyrene), and ¹H NMR measurements were used to monitor the adsorption at the aqueous solution–air interface and self-aggregation behaviour (critical micelle concentration, CMC) of room-temperature ionic liquids (ionic liquids) of the 1-alkyl-3-methylimidazolium family of cations, [C_nmim]⁺, with different linear alkyl chain lengths, C_nH_{2n+1} (¹/₂*n* = 1–7), and different counter-ions, namely [C_nmim]Cl (*n* = 2–14), [C_nmim][PF₆] (*n* = 4 or 10), and [C₁₀mim][NTf₂]. Only [C_nmim]Cl with *n* > 8 unambiguously form aggregates in solution and the nature of this self-aggregation is discussed in terms of the electrostatic vs. hydrophobic contributions of the isolated cation. In contrast, the shortest chains behave, as anticipated, as simple salts. In turn, the transitional ionic liquid, [C₆mim]Cl is able to develop a monolayer at the aqueous solution–air interface but shows no noticeable self-aggregation in the bulk fluid. Moreover, the micellar characteristics of the well-studied sodium dodecyl sulfate (SDS) aqueous solutions as a function of the total concentration of [C_nmim]Cl (¹/₂*n* = 1–7) showed a clear change in the behaviour of the mixtures [C_nmim]Cl + SDS for *n* ≈ 6–8, with a characteristic mixed-micelle formation for the longer and a pure salt effect for the shorter chain lengths of [C_nmim]Cl.

1. Introduction

Stable room-temperature liquid salts, *viz.* ionic liquids, in general, usually exhibit unique properties such as negligible vapour pressure,^{1–3} non-flammability, broad liquid temperature range and extended, specific, solvent abilities.^{4,5} These are key features that grant some of them ‘green’ credentials. Those ionic liquids exhibiting in addition low toxicity and low bioaccumulation would be elected as environmentally suitable, ‘green’ solvents. Hence, they are highly attractive as alternatives to hazardous volatile organic compounds.^{4,5} Besides the significant academic interest they have recently received, ionic liquids have been recognised as a novel class of solvents with a variety of significant contributions to novel technological processes.⁶ Some examples of potential applications include processes that cover extraction and separation,⁷ biphasic catalysis and organic synthesis,⁸ electrochemistry,⁹ photochemistry,¹⁰ and liquid crystals.¹¹

From a fundamental perspective, ionic liquid solutions present extraordinary features. The liquid–liquid (L–L) and solid–liquid (S–L) phase diagrams have demonstrated unusual richness in the phase behaviour including unexpected and novel L–L^{12,13} and S–L¹⁴ phase transitions, uncommonly large

co-solvent effects,¹⁵ and useful combinations with kosmotropic inorganic salts¹⁶ and polymers.¹⁷

On the other hand, the impressive solvation ability of ionic liquids facilitates their interaction with classical surfactants.^{18,19} It was shown that solvatophobic interactions are present between ionic liquids and the hydrocarbon portion of the surfactant, thus leading to the formation of surfactant micelles in ionic liquids and enhancing the solvation characteristics of the (ionic liquid + surfactant) system.¹⁹ Obvious analogies exist between commonly used, traditional ionic surfactants (most of them are solid salts), phase-transfer catalysts, and ionic liquids (liquid salts). The latter present low melting temperature points, usually a consequence of the presence of bulky, asymmetric cations, whilst the first are typically less entropic – *e.g.* sodium dodecyl sulfate (SDS), Na[C₁₂SO₄], with a melting point close to 200 °C. It should not thus be *a priori* surprising if many of the most popular ionic liquids would also exhibit surfactant-like behaviour.²⁰

Therefore, the inherent amphiphilic nature of some cations, *e.g.* [C_nmim]⁺, leads us to anticipate that, in aqueous solution, interfacial and aggregation phenomena should become an important issue that ultimately can drive micelle formation with specific structure, shape and properties.¹⁸ With the possibility of fine-tuning the hydrophobicity of ionic liquids by changing the alkyl chain length, the type of head group, and/or the nature and size of the counter-ion, one can affect both the structure and delicate dynamics of these micellar aggregates. This can lead to the modification of their major characteristics such as the critical micelle concentration, CMC, and the aggregation number.¹⁸ This particular aspect allows us to consider ionic liquids (when dispersed in aqueous solutions), in fact, as a new class of surfactants with unique abilities. In

^aInstituto de Tecnologia Química e Biológica, ITQB 2, Universidade Nova de Lisboa, Apartado 127, 2780-901 Oeiras, Portugal.

E-mail: luis.rebelo@itqb.unl.pt; alopes@itqb.unl.pt

^bThe QUILL Centre, The Queen's University of Belfast, Stranmillis Road, Belfast, UK BT9 5AG

† Electronic supplementary information (ESI) available: ¹H NMR spectrum of [C₁₂mim]Cl, salt-type effect on CMC of [C₁₂mim]Cl, [C₁₂mim]Cl effect on SDS aggregation, and concentration effect of [C₁₂mim]Cl. See DOI: 10.1039/b615406a

this regard, along with the catalytic effect that ionic liquids can possess by themselves, the appearance of aggregated ionic liquids dispersed in the solvent provides the possibility of combining, to some extent, two reactants completely different in nature (hydrophilic and hydrophobic) into a macroscopically homogeneous solution. This highly advantageous characteristic of these 'green systems' makes them desirable compounds to act as 'micellar catalysts'.¹¹

Thus, in a ternary mixture [water + common surfactant (or co-surfactant) + water-soluble long-chain ionic liquid], mixed micelles are expected to occur. This extends the intrinsic micellar characteristics of the ionic liquids to very low concentration *régimes* (especially when oppositely charged surfactants are used), where they can act as co-surfactants^{21,22} and consequently be easily applied to 'micellar catalysis'. However, previous studies from other groups^{18,21} report contradictory conclusions, and do not conform with an easy differentiation between electrostatic and hydrophobic contributions for the self-aggregation of this family. Fortunately, the formation of aggregates, particularly micelles, can be detected using several different instrumental methods.²³ Hence, it is generally possible, though sometimes difficult, to obtain comparative results.

The aim of the present paper is to offer a systematic study and establish the *rôle* of the alkyl chain length of the cation, concentration, and the nature of the anion on both the surface properties and the aggregation behaviour of compounds of the $[C_n\text{mim}]X$ family in aqueous solutions, as well as to elucidate those hydrophobic and electrostatic contributions for the building up of the micellar aggregates. Finally, with the future goal of building up mixed micelles where the ionic liquids can act as co-surfactants for micellar catalysis, we want to ascertain the effects that these compounds produce on the aggregation behaviour of commonly studied and characterised surfactants such as SDS in aqueous solutions.

2. Experimental

Chemicals

The 1-alkyl-3-methylimidazolium chlorides, $[C_n\text{mim}]\text{Cl}$ ($n = 1-7$), $[C_n\text{mim}][\text{PF}_6]$ ($n = 4$ or 10), and $[C_{10}\text{mim}][\text{NTf}_2]$, were all synthesised and initially purified at QUILL (The Queen's University Ionic Liquid Laboratories, Belfast) according to recipes found elsewhere.^{11,24} ^1H and ^{13}C NMR analyses showed no major impurities in the untreated, original samples, except for the presence of adventitious water. All samples were then further thoroughly degassed, dried, and freed from any small traces of volatile compounds by applying a vacuum (0.1 Pa) at moderate temperatures (60–80 °C) for typically 72 h. After this treatment, the purity of longer chain ionic liquids ($n > 6$) was checked with interfacial tension (IFT) measurements and no minimum²⁵ was observed for the concentration range used in this work. Na_2SO_4 (Aldrich, Germany, 99%), tetrabutylammonium bromide, $[\text{N}_{444}]\text{Br}$, (Aldrich, Germany, 99%), and NaCl (Merck, Germany, 99.5%) were used without purification and pyrene (Fluka, Germany, 99%) was recrystallised from benzene. SDS (Bethesda Research Laboratories, USA, 99.5%) and alkylammonium bromide and chloride and alkyltrimethylammonium bromide and chloride salts (TCI,

Japan, 99%) were also used without purification, but their purity was checked with IFT measurements and no minimum²⁵ was observed for the concentration range used in this work. Sodium hexafluorophosphate was obtained from hexafluorophosphoric acid (Aldrich, Germany, 60 wt% in water) adjusting the pH to *ca.* 7. The solution was stirred overnight and then the pH readjusted. The solution was filtered and evaporated to dryness, and the solid recrystallised from ethanol and dried under vacuum before use. Doubly-distilled deionised water was obtained from a Millipore Milli-Q water purification system (Millipore, USA). SDS, inorganic salt and $[C_n\text{mim}]X$ stock solutions were prepared in a 1.74×10^{-6} M pyrene aqueous solution and all work solutions were prepared from the stock solutions diluting with the same pyrene aqueous solution. All the mixtures were left under mild shaking at 25 °C for 24 h to equilibrate. For NMR experiments, D_2O (Cambridge Isotope Lab., USA, D, 99.9%) was used and, apart from pyrene, all other procedures were the same as for solution preparation.

Interfacial tension (IFT) measurements

Interfacial tension (IFT) was measured using a Drop Shape Analysis Tensiometer Kruss DSA1 v 1.80 working in the pendant drop mode at a constant temperature of (23 ± 0.5) °C. The needle diameter was chosen as a function of the maximisation of the scale of measurement. Brightness (contrast) was changed in order to minimise noise in the image acquisition and digitisation. IFT is derived from the fit of the pendant drop profile, and care was taken to ensure that the apparatus was calibrated with several solvents of known IFT in the range of interest. The drops were left to equilibrate close to the rupture point and at least three consistent measurements per solution were recorded. For highly viscous solutions, care was taken to ensure equilibration. Before each measurement, the syringe was abundantly rinsed with deionised water and left to dry out in a clean environment. Special care was taken in the handling of all material prior to, and during, the IFT measurements in order to avoid any error due to possible contamination.

Fluorescence spectroscopy

Steady-state fluorescence spectra of the pyrene-containing solutions were recorded with a Cary Varian Eclipse Fluorescence Spectrometer and collected from a 1 cm² quartz cuvette at 25 °C. Excitation was set to a wavelength of 337 nm and all emission spectra measured were corrected for emission monochromator response and were background-subtracted using appropriate blanks. Slits and rate of acquisition were chosen for a convenient signal/noise ratio. Intensities of first (I1) and third (I3) vibronic bands in the pyrene emission spectra located at 373 and 384 nm, respectively, were measured and used to determine the ratio I3/I1, a well-known 'solvent' polarity scale.²⁶ Band I1 corresponds to an $S_0(v=0) \leftarrow S_1(v=0)$ transition and band I3 is a $S_0(v=1) \leftarrow S_1(v=0)$ transition, and as the I3/I1 ratio increases with decreasing solvent polarity; this ratio makes it possible to ascertain the concentration for the start of the self-aggregation of hydrophobic material in aqueous solution.

¹H NMR spectroscopy

Proton NMR spectra were recorded on a BRUKER AMX300 spectrometer, operating at 300.13 MHz and equipped with a 5 mm diameter inverse detection broadband probe head, with the following acquisition parameters: spectral width, 6 kHz; pulse width, 4 μ s (70° flip angle); data points, 16k; repetition delay, 5 s; number of transients, 48; temperature, 298 K. The water resonance was suppressed with a pre-saturation pulse.

The assignments of the ¹H NMR spectra of these ionic liquids in aqueous solution follow those well established in the literature.²⁷ The assignment of the peaks in D₂O at 25 °C and concentrations lower than the CMC was as the following: ¹H NMR (300 MHz; D₂O), δ_{H} : 0.74 (t, CH₃), 1.14 (m, CH₃CH₂), 1.74 (m, CH₂), 3.77 (s, N-CH₃), 4.07 (t, N-CH₂), 7.31 [s, H(4)], 7.35 [s, H(5)], 8.60 [s, H(2)] – cf. ESI (Fig. S4).†

3. Results and discussion

Binary mixtures (ionic liquid + water)

Since 1-alkyl-3-methylimidazolium chlorides, [C_{*n*}mim]Cl, are completely miscible with water at all compositions of interest, the first group of experiments examined the behaviour of the aqueous solution–air interface for this series of compounds (*n* = 2, 4, 6, 8, 10, 12 or 14). The results of the IFT for the aqueous solutions as a function of the total concentration of [C_{*n*}mim]Cl are presented in Fig. 1(a). It is well known that a sharp decrease of the IFT followed by a plateau reveals the aforementioned amphiphilic characteristic of the cation, which is the cause for the possible micelle formation.²³ The break point of each concentration–surface tension curve determines the saturation of the outer monolayer of the surface of the drop, and the consequent onset of aggregation in the bulk, the critical micelle concentration, CMC, when dissolution permits.

Fig. 1(a) clearly shows that the plateaux are present only in the case of alkyl chains with a hydrocarbon ‘tail’ equal or greater than *n* = 8, suggesting that micelle formation is only present for these cases. [C₄mim]Cl does not achieve any plateau, even in the limit of tending to the pure compound (higher concentration point). For pure and highly concentrated solutions of [C₆mim]Cl, it was not possible to determine IFT due to the extremely high viscosity of the solutions (which does not allow the drop to develop the correct shape, and, then, collapses). Nevertheless, if we assume that the start of the plateau regions are similar for all compounds, *i.e.* 42–43 mN m^{−1}, it is possible to estimate a hypothetical break point at about 900 mM. This possible occurrence of a similar value of IFT for the beginning of the plateaux for the whole family indicates that a monolayer of the compounds is essentially equal in terms of its compactness. The occurrence of a similar value of IFT for the beginning of the plateaux for the whole family is conceivable. It indicates that at the monolayer the projected surface of the cation is alkyl chain length-independent. This agrees with the fact that all of them possess the same head (with a large cross-section and volume) contacting the aqueous solution and the hydrocarbon tail (with a small cross-section compared to the head) pointing toward the air has some freedom regardless of the chain length (up to *n* = 14). Naturally, as the concentration increases (after

the break), the larger hydrocarbon chains allow a higher compactness and consequently the IFT keeps lowering slightly. The experimental values for the break points in IFT are presented in Table 1 (along with other CMC results from different techniques). To the best of our knowledge, other experimental CMC data for these systems exist only for aqueous solution of [C₈mim]Cl.¹⁸ Even so, the comparison is interesting, as it points to the question of purity of ionic liquids, and strengthens the necessity for comparative and systematic studies. The CMC value obtained by Bowers *et al.*¹⁸ is roughly half the value reported here, and shows a minimum in the curve – which is characteristic of mixtures or contaminated surfactants.^{23,28} It is clear that the data from Bowers *et al.*¹⁸ are unreliable due to sample contamination, which was stressed by the authors themselves.¹⁸

In order to corroborate the above-mentioned results for self-aggregation, two spectroscopic techniques were also utilised: (i) fluorescence measurements that involve a pyrene solvatochromic probe, and (ii) ¹H NMR spectroscopy of the [C_{*n*}mim]⁺ salts themselves. It is well known that plots of the pyrene I3/I1 ratio as a function of the total surfactant (in our case the ionic liquid) concentration show a specific sigmoidal-type curve, the increase of which is attributed to the formation of micelles with a well-defined hydrophobic core into which pyrene partitions preferentially.²⁹ Fig. 1(b) shows the pyrene response for aqueous [C_{*n*}mim]Cl solutions (for the sake of clarity, data for *n* = 2 are not included but they also show constant I3/I1 similar to *n* = 4) as a function of [C_{*n*}mim]Cl concentration. In agreement with the surface tension measurements above, Fig. 1(b) clearly provides evidence that no hydrophobic environment is formed in solutions for *n* < 6.

Although the I3/I1 ratio shows the typical increase indicating the presence of a hydrophobic environment for tails equal to or greater than six carbons, we can only be certain that a plateau is reached for *n* = 10, 12, and 14. Consequently, the intersection point between that plateau and the descending part is used for the CMC determination only for these three [C_{*n*}mim]⁺ salts. The reason for the absence of a plateau at higher concentrations of ionic liquids in the case of the other three systems (*n* = 4, 6, and 8) may be attributed to the progressive dense packing of the individual cation that constitutes a micelle-like structure. This produces a steady increase in the hydrophobicity sensed by pyrene that reflects the continuous increase in the probe response. These observations are, however, yet speculative as tentative measurements with light scattering did not clarify this point. Even in the case of [C₁₂mim]Cl, a breakpoint in the total intensity light scattering *vs.* [C₁₂mim]Cl concentration is revealed close to 12–15 mM, but the trials to get a Zimm plot^{23,28} were unfruitful, which is likely to occur if there is a progressive growing of the aggregates in the narrow range of concentrations for the tentative plot (10–30 mM).

¹H NMR resonances for the protons of [C_{*n*}mim]Cl undergo reasonable shifts as a function of the [C_{*n*}mim]Cl concentration. Fig. 1(c) shows the evolution of the largest shifts ($\Delta\delta$ /ppm) in the ¹H NMR for the H(2) ring protons as a function of the [C_{*n*}mim]Cl concentration. Once again, although the chemical shift shows a distinctive increase for all *n* > 6, indicating the change in the environment for these molecules as a function of

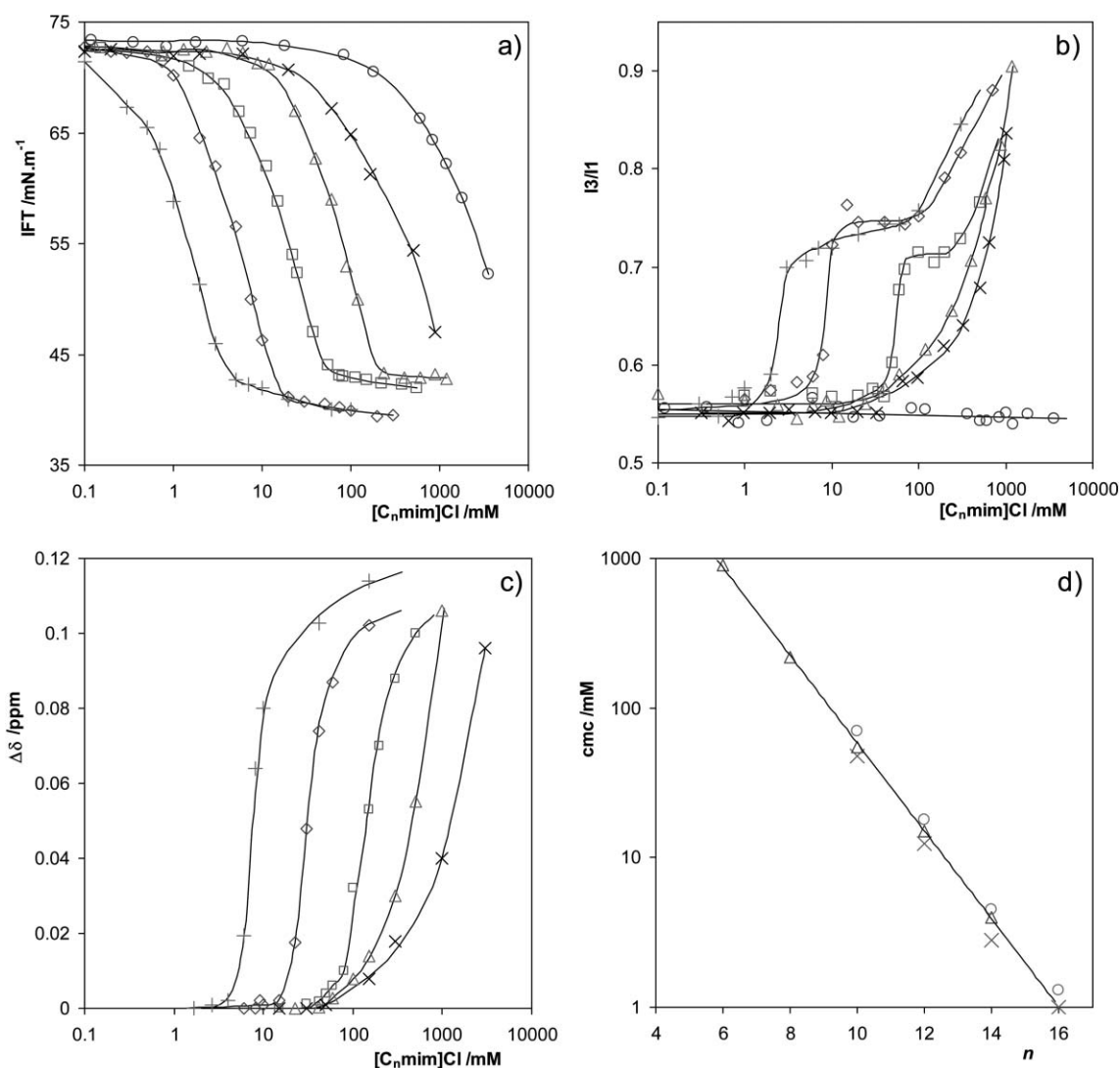


Fig. 1 Monitoring the self-aggregation of $[C_n\text{mim}]\text{Cl}$ using different techniques: (a) IFT, (b) fluorescence, (c) ^1H NMR spectroscopy; results for $\text{H}(2)$ for different chain lengths: $n = \circ$ (4), \times (6), Δ (8), \square (10), \diamond (12), $+$ (14); (d) summary of results for \circ ($[\text{N}_{111n}]\text{Cl}$), \times ($[\text{H}_3\text{N}_n]\text{Cl}$), Δ ($[C_n\text{mim}]\text{Cl}$).

Table 1 Critical micelle concentration, CMC (mM), of $[C_n\text{mim}]\text{Cl}$ obtained by IFT, fluorescence (Fluor) and ^1H NMR spectroscopy as a function of chain length, n . For comparison purposes, values obtained for the alkyltrimethylammonium chlorides ($[\text{N}_{111n}]\text{Cl}$) and alkylammonium chlorides ($[\text{H}_3\text{N}_n]\text{Cl}$) are depicted (only IFT)

n	$[C_n\text{mim}]\text{Cl}$			$[\text{N}_{111n}]\text{Cl}$	$[\text{H}_3\text{N}_n]\text{Cl}$
	IFT	Fluor	NMR	IFT	IFT
6	900	—	—		
8	220	—	200		
10	55	45	55	70	48
12	15	7	13	18	12.5
14	4	3	4	4.5	2.8
16				1.3	1

their concentration, only for $n = 10, 12$ and 14 is there a change followed by a plateau region (for figure clarity not all data are shown) related to the self-aggregation in small micellar-type aggregates.

Fig. 1(d) summarises the CMC values obtained with the IFT methodology plotted as a function of the number of

carbons for $n = 6$ – 14 . For comparison purposes, data obtained by the same method for cationic surfactants of the alkyltrimethylammonium and alkylammonium chloride families, $[\text{N}_{111n}]\text{Cl}$ and $[\text{H}_3\text{N}_n]\text{Cl}$, with similar hydrocarbon chain lengths are depicted. As one can perceive, there is a good free energy correlation for all the $[C_n\text{mim}]\text{Cl}$ family and the results show the same dependence for micellisation as a function of n as observed for the other two families (which have smaller head groups). It is even possible to notice that the CMC values for $[C_n\text{mim}]\text{Cl}$ are located somehow between those of $[\text{H}_3\text{N}_n]\text{Cl}$ and $[\text{N}_{111n}]\text{Cl}$, possibly reflecting the interaction with the chloride counter-ion with the delocalised charge density of the imidazolium ring (aromatic) as something in between the other alkyltrimethylammonium (3 carbons, 1 nitrogen) and alkylammonium (1 carbon, 1 nitrogen) head groups. Moreover, as perceived from Fig. 1(a), the plateau after the break in IFT measurements reflects a slightly higher degree of compactness (lower IFT) for the monolayer of $[C_n\text{mim}]\text{Cl}$, suggesting the more dense

packing of the planar heads in the monolayer when compared to $[N_{111n}]Cl$ – see also Fig. 2.

Fig. 2 shows the effect of the anion of the ionic liquid on the surface tension of aqueous solutions of $[C_{10}mim]X$ (where X is Cl^- , $[NTf_2]^-$ or $[PF_6]^-$). The concentration of ionic liquid at which the surface tension starts to lower decreases as the hydrophobicity and bulkiness of the anion increases. This is believed to result from decreased electrostatic repulsion between head groups in the monolayer due to the relatively strong binding of the hydrophobic counter-ion to the IL cations and the hydrophobicity of the anions themselves. Generally, this may lead to lower CMC values, thus promoting micelle formation.²⁸ However, in the cases of the $[NTf_2]^-$ and $[PF_6]^-$ anions, no micelle formation was detected, as the low solubility of the corresponding ionic liquids induced phase separation before any bulk aggregation occurred. At this point, we can only speculate that the $[NTf_2]^-$ and $[PF_6]^-$ anions are too big to fit the micelle surface region, the so-called Stern layer, and the system breaks down into two phases. Although this fact obstructs a comparison of the IFT plateau for the different counter-ions, it is possible to guess that those values are not too different, as the last point in the series for the double phase systems are within 2 mN m^{-1} (Fig. 2). This is consistent with a monolayer build up of the same monolayer of cations. Experiments with similar counter-ions for the $[N_{111n}]X$ systems were only possible for $X = Cl^-$, along with some tentative data for $X = [PF_6]^-$. The results agree with a lower solubility for $[PF_6]^-$ salts and a higher IFT for $[N_{11110}]X$ compared with $[C_{10}mim]X$ (see Fig. 2).

Salt effects on micelle formation in aqueous solutions of $[C_{10}mim]Cl$ and $[C_{12}mim]Cl$ are presented in Table 2, along with some data for $[N_{11112}]Cl$ for comparison purposes. Fluorescence experiments yield a slightly lower CMC than IFT experiments but the difference is consistent for all cases regardless of the type of salt or ionic strength. The addition of salts decreases the CMC and facilitates micelle formation – a

Table 2 Critical micellar concentration, CMC (mM), of $[C_nmim]Cl$ ($n = 10$ or 12) obtained by IFT and fluorescence (Fluor) as a function of salt concentration for NaCl, $Na_2[SO_4]$, $[N_{4444}]Br$ and $[C_4mim]Cl$. Values obtained for dodecyltrimethylammonium chloride ($[N_{11112}]Cl$) are listed for comparison purposes

salt	Ionic strength/mM	$[C_{10}mim]Cl$		$[C_{12}mim]Cl$		$[N_{11112}]Cl$	
		Fluor	IFT	Fluor	IFT	Fluor	IFT
NaCl	0	45	55	7	15	12	20
	50	37	40	2.5	7	7	12
	150	18	25	2	4	4	6
$Na_2[SO_4]$	0	—	55	—	15	—	20
	50	—	40	—	8	—	11
	15	—	22	—	3.5	—	6
$[C_4mim]Cl$	0	45	55	7	15	12	20
	50	37	50	2.1	8	6.5	12
	150	28	35	1.4	5	3.5	6
$[N_{4444}]Br$	0	45	55	7	15	12	20
	50	25	35	1.5	4	5	7
	150	17	20	0.9	2	2.5	3.5

phenomenon that can be attributed to the fact that the increase of the counter-ion concentration diminishes the repulsion between the head groups, and, thus, lowers the opposition factor to micelle formation.^{23,28} In this regard, three salts were chosen of quite different natures – NaCl, $Na_2[SO_4]$, and tetrabutylammonium bromide ($[N_{4444}]Br$) – allowing comparison of the overall effect with $[C_nmim]Cl$ ($n = 2$ and 4). These possess small hydrocarbon chains, thus providing neither sufficient hydrophobicity to the cation to form any micellar aggregates by itself, nor to diminish the IFT in any noticeable way when dissolved in water (up to 150 mM), as observed in Fig. 1. Both mono-negative and di-negative ions decrease the $[C_{12}mim]Cl$ and $[N_{11112}]Cl$ CMC in the same manner, but what it is quite remarkable is that also the small hydrocarbon chain $[C_nmim]Cl$ decreases the CMC of both surfactants by the same amount as the other salts (values for $n = 2$ were omitted from the table, but are similar to those for $n = 4$). This corroborates the previous statement about the self-aggregation impediment of these small hydrocarbon chain $[C_nmim]Cl$ in aqueous solution, *i.e.* roughly they behave as common non-hydrophobic salts for micelle formation, interacting only with the micelle surface region (Stern layer) and screening the ionic charges around that surface. Nevertheless, while there is no noticeable change in the IFT plateau region as a function of the NaCl concentration, this is not the case for the $[C_nmim]Cl$, in which we observe a progressive decrease in the IFT [data not shown, *cf.* ESI (Fig. S4)†] consistent with a stronger compactness of the outside monolayer of the drop, and, consequently, of the compactness of the micellar interface.

For $[N_{4444}]Br$, a larger change in the surfactant's CMC was observed, which can be attributed to the extra hydrophobicity of these cations. The overall effect can be seen in Fig. 3, where only surfactants with $n = 12$ are compared and the lines are best fits for NaCl. As one can see, the difference between the two surfactants is roughly maintained regardless of the salt concentration. The comparison for IFT profiles as a function of $[N_{4444}]Br$ concentration is displayed in the inset to this figure – there is progressive decrease on both the initial and plateau (after break) IFT regions with the $[N_{4444}]Br$ concentrations, showing evidence for the extra hydrophobicity

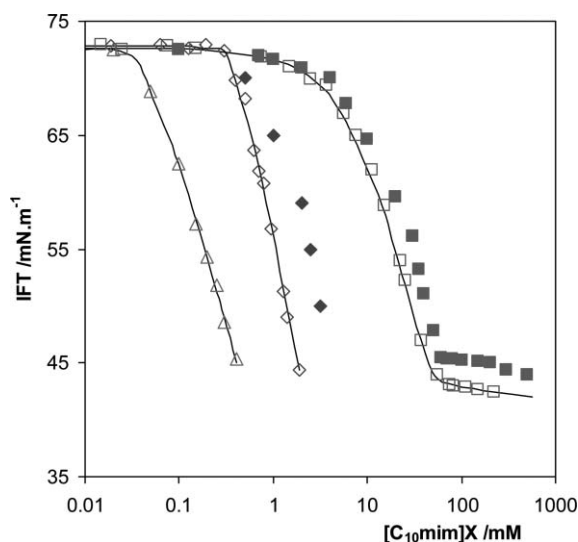


Fig. 2 Counter-ion effect on $[C_{10}mim]X$ aggregation from IFT measurements: $X = \Delta$ ($[NTf_2]^-$), \diamond ($[PF_6]^-$), \square (Cl^-). Note: \blacksquare ($[N_{11110}]Cl$) and \blacklozenge ($[N_{11112}]Cl$) are included for comparison purposes.

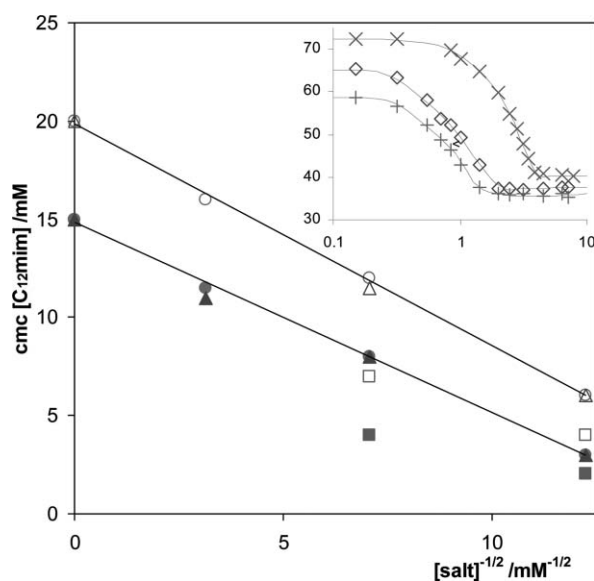


Fig. 3 Salt-type effect on the CMC of $[C_{12}mim]Cl$ by IFT: ● (NaCl), ▲ ($[C_4mim]Cl$), ■ ($[N_{4444}]Br$), and comparison with $[N_{11112}]Cl$: ○ (NaCl), △ ($[C_4mim]Cl$), □ ($[N_{4444}]Br$). Inset: $[N_{4444}]Br$ concentration effect (mM) on $[C_{12}mim]Cl$ aggregation: × (0), ◇ (50), + (150).

(and consequently a more tightly packed surface in the micelle) of this salt compared with the others, which allows rationalisation of the different behaviour of this salt toward the surfactant's CMC previously described.

Ternary mixtures (ionic liquid + SDS + water)

In this section, the self-aggregation of a well-characterised surfactant, sodium dodecyl sulfate (SDS), in the presence of $[C_nmim]Cl$ solutions is compared with the self-aggregation of SDS in pure water.

The observed effects can be systematised in different ways. If the total $[C_nmim]Cl$ concentration is maintained below its CMC, the longer the hydrocarbon chain length, then the more favourable will be the self-aggregation of the mixed aggregates. This effect is depicted in Fig. 4 for $[C_nmim]Cl = 10$ mM based on (a) fluorescence measurements, and (c) IFT (NB: the $n = 12$ and 14 cases are excluded from these graphs in order to avoid any influence of its self-aggregation even at 0 mM SDS). Similar graphs were obtained [data not shown, cf. ESI (Fig. S3)†] for other different ionic liquid concentration, but in some cases we have additional problems in their interpretation due to either the self-aggregation of the ionic liquid, or its precipitation close to the neutrality point. That is the case for $[C_nmim]Cl$ (ca. 5 mM). The plots are similar to those of Fig. 4(a) and 4(c), but present a rather complex pattern due to the precipitation occurring close to the CMC of SDS. In contrast, for $[C_nmim]Cl \gg 10$ mM, most of ionic liquids lower appreciably the IFT and addition of SDS (although micellised) does not present any noticeable difference in IFT curves, and because the ionic liquid is self-aggregated even without SDS, the baseline in I3/I1 moves upward, making the change in the fluorescence graphs also less and less sensitive.

Fig. 4(a) shows clearly that 10 mM $[C_2mim]Cl$ already decreases the CMC by a factor of 2, but a deep analysis on the

I3/I1 ratio shows a decrease from 0.83 to 0.75. This fact constitutes evidence that the $[C_2mim]^+$ cation causes significant derangement in the packing of SDS monomers and the Stern layer of the SDS micelles expose more pyrene to water (when compared with pure SDS micelles). Nevertheless, no significant change in the IFT plateau is observed, meaning that the monolayer at the surface of the drop is not appreciably affected by the presence of 10 mM $[C_2mim]Cl$; actually, even for 100 mM $[C_2mim]Cl$, that plateau changes less than 2 mN m^{-1} [data not shown, cf. ESI (Fig. S3)†].

Besides the progression in CMC lowering (quite visible in all Fig. 4 graphs) with 10 mM $[C_nmim]Cl$ for $n > 4$, the I3/I1 ratio approaches the usual compactness of SDS micelles [I3/I1 ca. 0.82 after micellisation in Fig. 4(a)]. Nevertheless, Fig. 4(c) clearly shows that the IFT plateau (after the break) is lowered down to 24 (for $n = 10$) – evidence that the compactness of the monolayer properties are changing progressively with the presence of a longer alkyl chain. It is also worth noticing that, besides the change in CMC (mostly due to electrostatic forces), the plateau after the break drops from ca. 42 mN m^{-1} to ca. 24 mN m^{-1} with $[C_{10}mim]Cl$ when SDS is added (for $n = 12$, the plateau after the break is also around 24 mN m^{-1}). This is a combined effect of attractive electrostatic forces (surfactant monomers can come closer), salt effect (screening of charges by counter-ions at the Stern layer), and a geometric factor – the 'void' left by the tail of the ionic liquids (as discussed previously, there is a significant difference between cross-sections of the head and tail in ionic liquids) can be filled by the SDS tail rendering a much more compact monolayer. This is not accompanied by a change in the I3/I1 plateau because of the significant curvature of the micelle, exposing pyrene roughly to the same environment in mixed micelles for $n > 4$.

Noticeably in Fig. 4(c), the effect of the competition between electrostatic and hydrophobic forces is clear [we obtained similar plots showing the same pattern for other concentrations of ionic liquids – data not shown, cf. ESI (Fig. S2)†]. While for $n < 6$, the aggregation as seen from the monolayer is lowering progressively, for greater chain lengths one observes a turnover and a 'recovering' of larger break points for monolayer saturation ($n = 12, 14$ not shown for the sake of graph clarity, but the break point concentrations are close to pure SDS, i.e. ca. 8 mM). There is clear evidence of the turning point from a pure salt effect (electrostatic) to a mixed micelle formation effect (hydrophobic)³⁰ between $n = 6$ and 8.

A plot for IFT or I3/I1 as a function of the SDS concentration for different $[C_6mim]Cl$ concentrations (Fig. 5) shows a peculiar behaviour. As can be seen (more evident in the IFT graph), all solutions behave roughly in the same way, regardless of the ionic liquid concentration (at least for IL concentrations larger than 5 mM). One possible explanation is that the electrostatic and hydrophobic forces in aggregation are so well balanced for $[C_6mim]Cl$ that any addition of the monomers (up to 100 mM) does not change significantly the outer monolayer, but a very small amount of SDS (almost two orders of magnitude smaller than its own CMC in water) starts to interact at the surface, possibly forming a kind of 1 : 1 complex,³¹ and in that form lowering the IFT [Fig. 5(a)]. However, if a 1 : 1 complex forms at the surface, the IFT curves

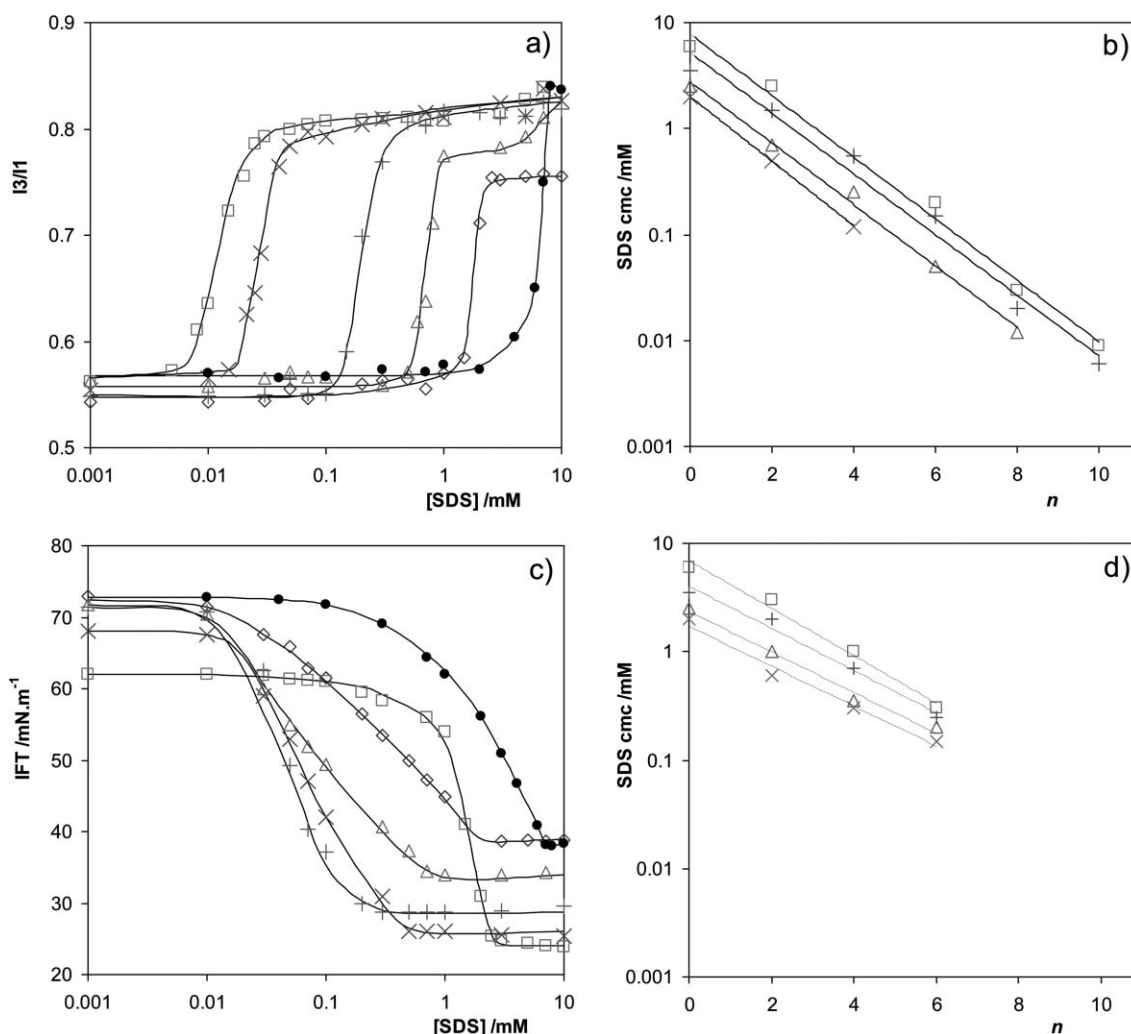


Fig. 4 $[C_n \text{mim}]Cl$ effect on the SDS aggregation using different techniques: (a) fluorescence, (c) IFT, results in the presence of $[C_n \text{mim}]Cl = 10$ mM as a function of chain lengths: $n = \diamond$ (2), Δ (4), $+$ (6), \times (8), \square (10); note: \bullet (without ionic liquid, pure SDS). SDS CMC obtained with: (b) fluorescence, (d) IFT, as a function of $[C_n \text{mim}]Cl$ concentration (mM): \square (5), $+$ (10), Δ (30), \times (100), for different chain lengths, n .

look the same regardless of the $[C_6 \text{mim}]Cl$ concentration, because the SDS can displace extra $[C_6 \text{mim}]Cl$ from the surface, and only when the surface is covered with this 1 : 1 complex self-aggregation starts in bulk (micelles). Actually, this build up of micelles by the growing concentration of SDS in bulk at a constant $[C_6 \text{mim}]Cl$ concentration raises the proportion of SDS monomers in the mixed micelle, thus explaining what is observed with fluorescence – a nett gradual effect on SDS CMC (although very small when compared with other hydrocarbon chain lengths in $[C_n \text{mim}]Cl$). Of course, this deserves a deeper investigation of the type of thermodynamic interaction parameters (β) for the mixed micelle formation in this system.³¹

When the overall effect of SDS CMC as a function of the $[C_n \text{mim}]Cl$ concentration (for different chain lengths) is compared [Fig. 4(b) and 4(d)], there is a good free energy correlation for the entire $[C_n \text{mim}]Cl$ family presented by both techniques (and data agree) even though, as stated above, an appreciable amount of the longer hydrocarbon chain $[C_n \text{mim}]Cl$ obstructs the detection of the ‘true’ SDS CMC by IFT. Nevertheless, the CMC values obtained by both methods

and for any $[C_n \text{mim}]Cl$ concentration coincide as far as it is possible, *i.e.* up to $n = 6$.

The only paper of which we are aware that allows us to compare similar situations is that of Beyaz *et al.*²² While a progressive decrease in the CMC as a function of the chain length (similar to Fig. 4) was reported, the values stated for the CMC of the smaller $[C_n \text{mim}]Cl$ ($n = 2$ and 4) must be incorrect because the CMC of SDS in the presence of an ionic additive (with a hydrophobic chain or not) cannot be larger than that of the SDS alone. Even for $n = 6$ and 8 systems, where the order is correct, the values they state are much higher than those reported here.

Fig. 6 shows SDS CMC as a function of $[C_n \text{mim}]Cl$ for all hydrophobic chain lengths ($n = 14$ is excluded for the sake of clarity). In order to evaluate the electrostatic *versus* hydrophobic competition for the SDS micellisation in the presence of salts, NaCl (a non-hydrophobic salt) is included. As we can see from Fig. 6(a), even with $[C_2 \text{mim}]Cl$ there is a nett effect in the CMC decrease as compared to NaCl, *i.e.* the SDS feels already the slight hydrophobicity of this cation. As the chain length increases, the effect in lowering the CMC is more

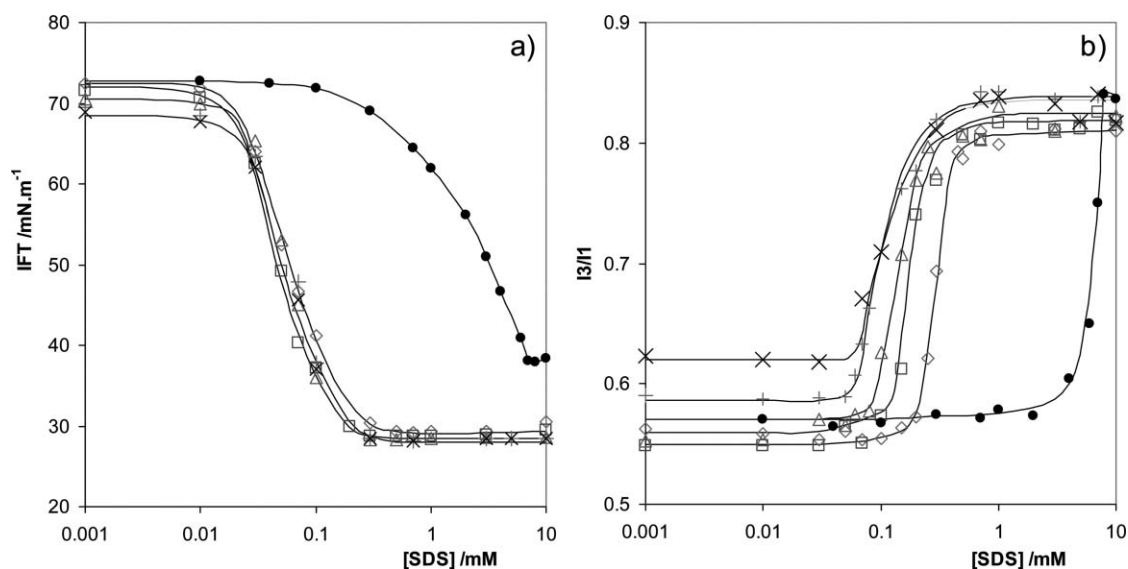


Fig. 5 $[\text{C}_6\text{mim}]\text{Cl}$ effect on the SDS aggregation obtained with: (a) IFT, and (b) fluorescence, for different $[\text{C}_6\text{mim}]\text{Cl}$ concentrations (mM): \diamond (5), \square (10), Δ (20), $+$ (30), \times (100); note: \bullet (without ionic liquid, pure SDS).

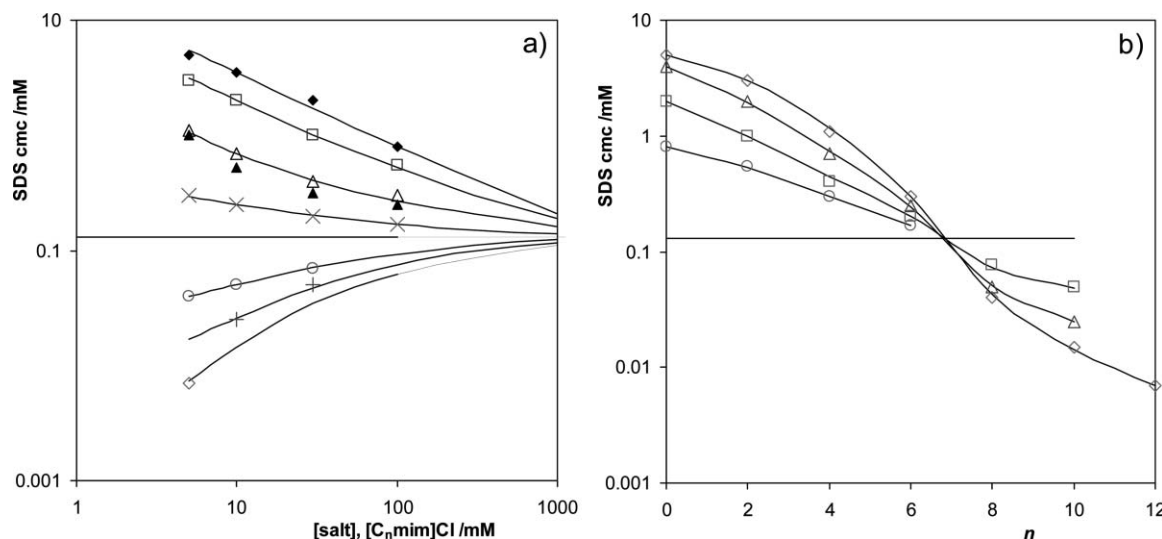


Fig. 6 (a) Effect of chain length of $[\text{C}_n\text{mim}]\text{Cl}$ on the CMC of SDS as a function of the ionic liquid concentration (mM): $n = \square$ (2), Δ (4), \times (6), \circ (8), $+$ (10), \diamond (12); note: \blacklozenge (NaCl) and \blacktriangle $[\text{C}_4\text{mim}][\text{PF}_6]$ are included for comparison purposes. (b) Effect of ionic liquid concentration (mM) on the CMC of SDS as a function of the chain length: \diamond (5), Δ (10), \square (30), \circ (100).

pronounced, and up to $n = 6$, Fig. 6 undoubtedly reveals a 'salt' effect of the ionic liquids for SDS micelles, *i.e.* the greater the amount of ionic liquid, the smaller the CMC. In other words, ionic liquids are interfering with the external Stern layer of the 'pure' SDS micelles. Nevertheless, as the length of the hydrocarbon chain is increased, although the CMC keeps lowering in a more or less proportional way (for a constant 'salt' concentration), a sudden inversion in the trend for the total 'salt' concentration is observed. Although the lines in Fig. 6(a) are not fitted (just visual guides), there is an asymptotic convergence of all of them for high 'salt' concentration to a value of SDS CMC close to the one observed for very high NaCl concentration.²³ Furthermore, the comparison between $[\text{C}_n\text{mim}]\text{X}$, for $\text{X} = \text{Cl}^-$ and $[\text{PF}_6]^-$, reveals that although both counter-ions put into effect quite

different behaviour when one considers pure ionic liquids (as seen in Fig. 2), the difference becomes negligible when one refers to the mixture (ionic liquid + SDS) [Fig. 6(a)].

In contrast, if the SDS CMC decrease is plotted as a function of the hydrocarbon chain length for the different ionic liquid concentrations [Fig. 6(b)], a very peculiar trend is perceived. While for very high 'salt' concentrations, there is almost no hydrophobic differentiation amid the different hydrocarbon tail lengths (meaning that the salt effect is near 'saturation'), for small amounts of 'salt' there is a profound dependence of this hydrophobic effect. Moreover, all lines for different 'salt' concentration crossover at a distinctive point whose coordinates coincide with the previously presented line of asymptotic convergence (*ca* 0.13 mM SDS) and a number of carbons in the hydrocarbon chain length between 6 and 8.

Once again, the lines are only guides (not fitted), but the overall effect seems to point out a 'well balanced' $[C_n\text{mim}]\text{Cl}$ for $n = 6-8$ in terms of electrostatic *versus* hydrophobic competition.

4. Conclusions

Aqueous solutions of ionic liquids of the 1-alkyl-3-methylimidazolium chloride family, $[C_n\text{mim}]\text{Cl}$, with n ranging from 8 to 14, when scrutinised using interfacial tension, fluorescence, and ^1H NMR measurements, present evidence for the self-aggregation of the $[C_n\text{mim}]^+$ cations into micellar aggregates. This is also supported by the observed ability of $[C_n\text{mim}]\text{Cl}$ to template MCM-41 syntheses in the place of $[\text{N}_{11116}]\text{Cl}$; for $n = 2$ or 4, no MCM-41 was formed; for $n > 8$, mesoporous MCM-41 was formed (the larger n , the larger the mesopores); for $n = 6$, the results were poor, giving a marginally crystalline material.³²

Moreover, the observed critical micelle concentration, CMC, shows a good free energy correlation as a function of n and the dependence for the micellisation is similar to alkyltrimethylammonium and alkylammonium chloride families, $[\text{N}_{111n}]\text{Cl}$ and $[\text{H}_3\text{N}_n]\text{Cl}$. Although interfacial tension results show a decrease in IFT even for $n < 8$, these compounds do not show an IFT plateau at higher $[C_n\text{mim}]\text{Cl}$ concentration, which indicates that the hydrophobicity is not enough to build up micelles in these cases. This is corroborated by fluorescence and NMR data, where no noticeable spectral variation indicates that self-aggregation is not present.

The addition of salt to the micelle-forming systems due to screening of micellar surface charge diminishes the repulsion between the head groups, and, thus, decreases its CMC. Also in this case, the general behaviour of this family agrees with what is observed in alkyltrimethylammonium and alkylammonium chloride families, $[\text{N}_{111n}]\text{Cl}$ and $[\text{H}_3\text{N}_n]\text{Cl}$. Moreover, the exchange of chloride anion for a more hydrophobic counter-ion such as $[\text{NTf}_2]^-$ or $[\text{PF}_6]^-$, besides CMC diminution, brings the system to a non-micellar state and the system breaks down into two phases.

Acting as oppositely charged counter-ions, the $[C_n\text{mim}]^+$ cations favour the micellisation of SDS in aqueous solution. Nevertheless, a clear change is observed in the behaviour of the mixtures ($[C_n\text{mim}]\text{Cl} + \text{SDS}$) for $n \approx 6-8$, with a characteristic mixed micelle formation for the longer, and an almost pure salt effect for the shorter, chain lengths of the $[C_n\text{mim}]^+$ cations.

The ionic liquids studied here, when dispersed in aqueous solutions, act as a new class of surfactants with unique abilities because along with the highly advantageous characteristic of these 'green fluids' as bulk solvents, they can be nano-dispersed in water. Here, one can combine two reagents of completely different natures (hydrophilic and hydrophobic) into a macroscopically homogeneous solution. Some very recent preliminary results suggest that in equimolar mixtures of SDS and long hydrocarbon chain ionic liquids, both mixed micelle behaviour and possible catalytic effects are present. These phenomena are currently under deeper investigation.³¹

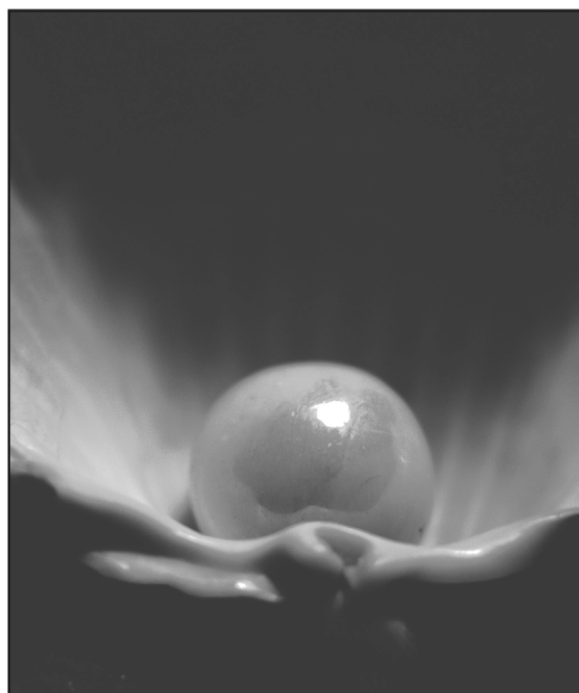
Acknowledgements

This work was supported by the Fundação para a Ciência e Tecnologia (FCT), Portugal (Projects POCTI/QUI/35413/2000 and POCI/QUI/57716/2004. M. B. thanks FCT for a Ph.D. grant SFRH/BD/13763/2003, and K. R. S. thanks the EPSRC (Portfolio Partnership Scheme, grant no. EP/D029538/1) for funding. Helena Pereira (ITQB) is acknowledged for providing ^1H NMR data.

References

- 1 M. J. Earle, J. M. S. S. Esperança, M. A. Gilea, J. N. Canongia Lopes, L. P. N. Rebelo, J. W. Magee, K. R. Seddon and J. A. Widegren, *Nature*, 2006, **439**, 831–834.
- 2 Y. U. Paulechka, Dz. H. Zaitsau, G. J. Kabo and A. A. Strechan, *Thermochim. Acta*, 2005, **439**, 158–160.
- 3 L. P. N. Rebelo, J. N. Canongia Lopes, J. M. S. S. Esperança and E. Filipe, *J. Phys. Chem. B*, 2005, **109**, 6040–6043.
- 4 J. D. Holbrey and K. R. Seddon, *Clean Prod. Process.*, 1999, **1**, 223–236.
- 5 *Ionic Liquids in Synthesis*, ed. P. Wasserscheid and T. Welton, Wiley-VCH, Weinheim, 2003.
- 6 K. R. Seddon, *Nat. Mater.*, 2003, **2**, 363–365; R. D. Rogers and K. R. Seddon, *Science*, 2003, **302**, 792–793; M. Deetlefs and K. R. Seddon, *Chim. Oggi*, 2006, **24**, 16–23.
- 7 A. E. Visser, R. P. Swatloski and R. D. Rogers, *Green Chem.*, 2000, **2**, 1–4.
- 8 J. G. Huddleston, H. D. Willauer, R. P. Swatloski, A. E. Visser and R. D. Rogers, *Chem. Commun.*, 1998, 1765–1766.
- 9 C. L. Hussey, in *Chemistry of Nonaqueous Solutions*, ed. G. Mamantov and A. I. Popov, VCH, Weinheim, 1994, pp. 227–276; F. Endres and S. Z. El Abedin, *Phys. Chem. Chem. Phys.*, 2006, **8**, 2101–2116.
- 10 C. M. Gordon and A. J. Mclean, *Chem. Commun.*, 2000, 1395; M. Grätzel, *J. Photochem. Photobiol., C*, 2003, **4**, 145–153.
- 11 C. M. Gordon, J. D. Holbrey, A. R. Kennedy and K. R. Seddon, *J. Mater. Chem.*, 1998, **8**, 2627; C. J. Bowles, D. W. Bruce and K. R. Seddon, *Chem. Commun.*, 1996, 1625–1626.
- 12 J. Łachwa, J. Szydłowski, V. Najdanovic-Visak, L. P. N. Rebelo, K. R. Seddon, M. Nunes da Ponte, J. M. S. S. Esperança and H. J. R. Guedes, *J. Am. Chem. Soc.*, 2005, **127**, 6542–6543.
- 13 J. Łachwa, J. Szydłowski, A. Makowska, K. R. Seddon, J. M. S. S. Esperança, H. J. R. Guedes and L. P. N. Rebelo, *Green Chem.*, 2006, **8**, 262–267.
- 14 J. Łachwa, I. Bento, M. T. Duarte, J. N. Canongia Lopes and L. P. N. Rebelo, *Chem. Commun.*, 2006, 2445.
- 15 V. Najdanovic-Visak, J. M. S. S. Esperança, L. P. N. Rebelo, M. Nunes da Ponte, H. J. R. Guedes, K. R. Seddon and J. Szydłowski, *Phys. Chem. Chem. Phys.*, 2002, **4**, 1701–1703.
- 16 K. E. Gutowski, G. A. Broker, H. D. Willauer, J. G. Huddleston, R. P. Swatloski, J. D. Holbrey and R. D. Rogers, *J. Am. Chem. Soc.*, 2003, **125**, 6632–6633.
- 17 A. Triolo, O. Russina, U. Keiderling and J. Kohlbrecher, *J. Phys. Chem. B*, 2006, **110**, 1513–1515; Y. He, Z. Li, P. Simone and T. P. Lodge, *J. Am. Chem. Soc.*, 2006, **128**, 2745–2750.
- 18 J. Bowers, C. P. Butts, P. J. Martin and M. C. Vergara-Gutierrez, *Langmuir*, 2004, **20**, 2191–2198.
- 19 J. L. Anderson, V. Pino, E. C. Hagberg, V. V. Sheares and D. W. Armstrong, *Chem. Commun.*, 2003, 2444–2445.
- 20 S. E. Friberg, Q. Yin, F. Pavel, R. A. Mackay, J. D. Holbrey, K. R. Seddon and P. A. Aikens, *J. Dispersion Sci. Technol.*, 2000, **21**, 185–197.
- 21 Z. Miskolczy, K. Sebök-Nagy, Biczók and S. Göktürk, *Chem. Phys. Lett.*, 2004, **400**, 296–300.
- 22 A. Beyaz, W. S. Oh and V. P. Reddy, *Colloids Surf., B*, 2004, **35**, 119–124; A. Beyaz, W. S. Oh and V. P. Reddy, *Colloids Surf., B*, 2004, **36**, 71–74.
- 23 Y. Moroi, *Micelles: Theoretical and Applied Aspects*, Kluwer Academic/Plenum Publishers, New York, 1992.
- 24 P. Bonhôte, A.-P. Dias, M. Armand, N. Papageorgiou, K. Kalyanasundaram and M. Grätzel, *Inorg. Chem.*, 1996, **35**, 1168–1178.

- 25 K. Mittal, *Micellization, Solubilization and Microemulsions*, Plenum Press, New York, 1977.
- 26 J. Lakowicz, *Principles of Fluorescence Spectroscopy*, Kluwer Academic/Plenum Publishers, New York, 2nd edn, 1999.
- 27 A. G. Avent, P. A. Chaloner, M. P. Day, K. R. Seddon and T. Welton, *J. Chem. Soc., Dalton Trans.*, 1994, 3405–3413; A. G. Avent, P. A. Chaloner, M. P. Day, K. R. Seddon and T. Welton, in *Proceedings of the Seventh International Symposium on Molten Salts, Vol. PV 90–17*, ed. C. L. Hussey, J. S. Wilkes, S. N. Flengas and Y. Ito, The Electrochemical Society Inc., Pennington, New Jersey, 1990, pp. 98–133.
- 28 D. F. Evans and H. Wennerstrom, *The Colloidal Domain: Where Physics, Chemistry, Biology and Technology Meet*, VCH, New York, 1994.
- 29 R. Zana, *Surfactant Solutions: New Methods of Investigation*, Marcel Dekker, New York, 1986.
- 30 C. Tanford, *The Hydrophobic Effect: Formation of Micelles and Biological Membranes*, Wiley-Interscience, New York, 1980.
- 31 This hypothesis is investigated in a following paper of the series dealing with mixed micelle thermodynamics; to be submitted.
- 32 C. J. Adams, A. E. Bradley and K. R. Seddon, *Aust. J. Chem.*, 2001, **54**, 679–681.



Looking for that **special** chemical biology research paper?

TRY this free news service:

Chemical Biology

- highlights of newsworthy and significant advances in chemical biology from across RSC journals
- free online access
- updated daily
- free access to the original research paper from every online article
- also available as a free print supplement in selected RSC journals.*

*A separately issued print subscription is also available.

Registered Charity Number: 207890

RSC Publishing

www.rsc.org/chembiology

22030681

Thermophysical and bionotox properties of solvo-surfactants based on ethylene oxide, propylene oxide and glycerol

Sébastien Queste,^a Youlia Michina,^c Anny Dewilde,^b Roland Neueder,^c Werner Kunz^c and Jean-Marie Aubry^{*a}

Received 6th December 2006, Accepted 30th January 2007

First published as an Advance Article on the web 22nd February 2007

DOI: 10.1039/b617852a

Thermophysical and bionotox properties of a new class of natural solvo-surfactants, glycerol 1-monoethers, were investigated in comparison with widespread but harmful glycol ethers. Vapour pressures and heats of vaporization were measured between 25 °C and 50 °C, and calculated thanks to two group contribution methods. Evaporation rates and Hansen parameters, evaluated from TGA measurements and group contributions respectively, were compared as well. Bionotox properties, *i.e.* cytotoxicity, irritating power and biodegradability, were evaluated experimentally. Glycerol 1-monoethers turned out to be less volatile than glycol derivatives, but contrary to the latter they will not be considered as VOCs. Toxicities and irritating powers are equivalent and increase with increasing alkyl chain length, *i.e.* with increasing amphiphilicity. Glycerol ethers are degradable at lower concentrations compared to glycol compounds, which is related to their higher interfacial activity.

Introduction

Among the huge number of available organic solvents some, such as glycol ethers, have the advantage of possessing an amphiphilic structure and exhibit some affinity for both hydrophilic and lipophilic compounds. These solvents are particularly appropriate for hard surface cleaning where volatility and interfacial activity are both required. By comparison, the degreasing power of aqueous solutions of polar solvents (MeOH, DMSO, DMF...) is generally poor, whereas “true” surfactants, though efficient, leave smears on the surface after evaporation of water.

Amphiphilic solvents may be considered as hydrotropes.¹ They are nicknamed solvo-surfactants² because they are volatile, unlike ionic hydrotropes. Their potential industrial interest is wide since they may be used in every application requiring a controlled evaporation (windows, floor, or kitchen cleaning, coatings...). Their performance results directly from their physico-chemical properties a knowledge of which is thus very important.

Glycol monoethers (C_iE_j) are the main solvo-surfactants on the market (Fig. 1). Historically, C₁E₁ was the first introduced under the denomination methylcellosolve in 1930, as a solvent of cellulose polymers. Their use became widespread in the 1970s with the development of polyurethane based epoxydic and aqueous (acrylic, vinylic) paints.^{3–5} Until 1980 their propylene glycol counterparts (C_iP_j) (Fig. 1), were totally ignored, but in 1985 the genotoxicity of C₁E₁ and C₂E₁ was

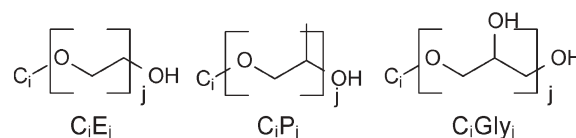


Fig. 1 Molecular structures of the solvo-surfactants studied in this work. Glycerol 1-monoethers (C_iGly_j) are potential green substitutes of the controversial ethylene glycol ethers (C_iE_j) and the moderately efficient propylene glycol ethers (C_iP_j).

put forward^{6–9} and they became of major importance. They will soon become more widespread than C_iE_j.

Even if four glycol ethers are today forbidden in Europe in medicines, cosmetics and household products, others are still very common in many applications. However, the whole family is tarnished in consumers' minds and manufacturers try to replace them in their formulations. C_iP_j, which are at present their main substitutes, exhibit satisfying properties¹⁰ but also derive from petrochemistry and suffer from the label “glycol ethers” as well. The growing green tendency encourages the development of molecules based on renewable resources. Among them, glycerol is more and more abundant as a major by-product of the biodiesel industry. We described recently in this journal¹¹ the synthesis and the aqueous behaviour of a new family of solvo-surfactants, glycerol 1-monoethers (C_iGly_j), in comparison with glycol ethers C_iE_j and C_iP_j. Their main characteristics are higher water solubility and amphiphilicity and a strong sensitivity to salt effects but not to temperature. Their excellent efficiency in the field of hard surface cleaning was also described recently.¹² In the present paper we report on our investigations concerning their so-called thermophysical and bionotox properties, which are of utmost relevance for many applications of these new green solvents. Results will systematically be discussed in comparison with C_iE_j and C_iP_j. The first part of this work will

^aLCOM, Equipe Oxydation et Formulation, ENSCL BP 90108, F-59652 Villeneuve d'Ascq Cedex, France.

E-mail: jean-marie.aubry@univ-lille1.fr; Fax: +33 3 20 33 63 65; Tel: +33 3 20 33 63 65

^bLaboratoire de Virologie, UPRESEA 3610, CHRU de Lille, Faculté de Médecine, Université de Lille 2, F-59037 Lille Cedex, France

^cInstitut für Physikalische und Theoretische Chemie, Universität Regensburg, D-93040 Regensburg, Germany

be dedicated to boiling points, vapour pressures and heats of vaporization that were determined experimentally. Results will be compared with theoretical estimates, calculated from molecular structures thanks to a group contribution method (Joback method—calculation of critical parameters P_c and T_c) and two analytical methods (Lee–Kesler and Kirschhoff–Reducted methods—estimation of vapour pressures). The second part of the paper will report on the comparison of evaporation rates, deduced from simple thermogravimetric analysis (TGA) measurements. In the third part, we will focus on solubility parameters. Hansen and Hildebrand parameters were calculated thanks to group contributions, and Hildebrand's parameter was also deduced from experimental heats of vaporization. Finally, we will describe in the last part of this work the bionotox properties of the molecules, *i.e.* their cytotoxicity, their irritant effects to skin and eyes, and their biodegradability.

Materials and methods

Materials

Ethylene glycol and propylene glycol derivatives were all purchased from Sigma–Aldrich at the highest grades available (C_4E_1 99+%, C_4E_2 99+%, C_3P_1 98.5% and C_4P_1 99%) and used without further purification. Glycerol 1-monoethers were synthesized according to a procedure described elsewhere.¹¹ Their purity was checked by GC/FID on an Agilent 6890N apparatus and by 1H and ^{13}C NMR on a Bruker AC200 spectrometer. *n*-Butyl acetate (99.5%) for TGA experiments was also purchased from Sigma–Aldrich.

Vapour pressure measurements

Measurements of vapour pressure were performed at the University of Regensburg with a precise vapour pressure apparatus that was designed especially for vapour pressure measurements of pure fluids and of electrolyte solutions over a wide temperature range (278.15 to 473.15 K) with an overall uncertainty in temperature of 0.01 K and a reproducibility of 0.1% in pressure. Owing to uncertainties of the zero point pressure of the manometer, volatile impurities, incomplete degassing of the samples, and leakage, an overall uncertainty of about 5 Pa can be estimated. The temperature is based on the international temperature scale ITS-90. The apparatus and the measuring method, as well as the degassing procedure, are described in detail elsewhere.¹³ For each compound and at each temperature, between 2 and 5 measurements were performed and the mean value was taken as the final result. The building of $\ln P_{\text{vap}} = f(1/T)$ curves allowed us to evaluate ΔH_{vap} .

TGA experiments

Measurements were performed at the University of Lille on a TA Instruments TGA Q50 apparatus. The atmosphere was composed of a nitrogen–oxygen mixture with a ratio of 60:40 (V/V). Two drops (about 20 mg) of product were poured into a Pt crucible and a temperature ramp of $5\text{ }^\circ\text{C min}^{-1}$ was applied from $20\text{ }^\circ\text{C}$. The decrease of the mass was followed as a function of time and temperature.

Cytotoxicity

Cytotoxicity was assessed in the human embryonic fibroblast cell line MRC5 using the MTT assay.¹⁴ This test is based on the reduction of the yellow MTT salt (dimethylthiazoldiphenyltetrazolium bromide) to a blue formazan dye by mitochondrial dehydrogenase in viable cells. It is notably used to express the irritating power towards skin of pharmaceutical or cosmetic products.^{15–18} Its ability to describe irritancy towards eyes is lower.¹⁹ Cells were grown in 96-well tissue culture plate in a 5% CO_2 atmosphere and exposed to serially diluted solutions of the different solvo-surfactants ranging from 0.001 to 1% over 24 h. After washing with PBS to remove test materials MTT was added, and after an extra incubation time of 3 h, the percentage of living cells was evaluated. The concentration of surfactant that induced a 50% loss of viability (IC_{50}) relative to untreated control cells was determined. Detailed procedures to perform this assay are available elsewhere.^{15–19}

Eye-irritancy

MTT assay being inaccurate in the case of eye-irritancy, another test called RBC (red blood cell test) was performed. This *in vitro* assay has been assessed by COLIPA (European Cosmetic and Fragrance Association) and is associated with models to estimate equivalent *in vivo* results that would be obtained with the reference Draize test. The detailed procedure to carry it out is available in reference publications. Rabbit red blood cells are mixed with the studied molecules, and spectrophotometric measurements allow the determination of the concentration H50 where a 50% hemolysis is obtained and the denaturation level obtained with a 1% solution, relative to sodium dodecyl sulfate. Estimates of corresponding *in vivo* results allow the irritancy of the molecules to be evaluated.

Biodegradability

Biodegradability was studied in accordance with the OCDE 301F norm. Sludges from a local wastewater treatment plant were used to provide the required amount of bacteria. An IBUK respirometer allowed the detection of oxygen consumption during the degradation process. Experiments were performed at $20\text{ }^\circ\text{C}$ for 28 d. A reference solution, sodium acetate, was used to check the validity of the measurements.

Results and discussion

Estimation and measurement of thermophysical parameters

The evolution of the vapour pressure of any organic compound as a function of temperature can be described by the well known Clausius–Clapeyron equation (eqn 1):

$$\frac{d\ln P_{\text{vap}}}{dT} = \frac{\Delta H_{\text{vap}}}{RT^2} \quad (1)$$

ΔH_{vap} being the molar heat of vaporization in J mol^{-1} .

ΔH_{vap} , directly linked to the cohesive energy within the liquid, can be deduced from vapour pressure measurements or calculated from different equations containing more or less serious approximations.²⁰

The integrated form of the Clausius–Clapeyron equation is given by eqn 2:

$$\ln P_{\text{vap}} = \frac{-\Delta H_{\text{vap}}}{R} \times \frac{1}{T} + \text{cste} \quad (2)$$

According to this relationship, plotting P_{vap} as a function of $1/T$ gives a straight line whose slope is proportional to ΔH_{vap} . Solving for ΔH_{vap} is thus possible if at least two (P_{vap} , T) couples are known, with the assumption that it remains constant within the considered temperature range. This assumption is valid as long as the temperature is far from the critical point.

To estimate new P_{vap} values, it is possible to get rid of ΔH_{vap} with the use of Trouton's rule (eqn 3) which presupposes that the vaporization entropy ΔS_{vap} is constant and links ΔH_{vap} to the boiling point T_b :

$$\Delta S_{\text{vap}} = \frac{\Delta H_{\text{vap}}}{T_b} \approx 85 \text{ J mol}^{-1} \text{ K}^{-1} \quad (3)$$

According to this rule, P_{vap} can be calculated with temperature as sole variable if T_b is known. This assumption led to the building of so-called temperature–pressure nomographs, very handy but often inaccurate since Trouton's rule is valid only for very simple organic compounds and not for molecules bearing hydroxyl groups.

More efficient predictive methods exist. They can be divided into 2 main families. The first one gathers all quantitative structure properties relationships. These equations are built from several molecular descriptors which make the link between the structure of the compound and its properties. Such relationships have already been settled for many different parameters (melting and boiling temperatures,²¹ solvent polarities,²² critical micellar concentration of surfactants²³...) and give excellent results. However, their use requires the knowledge of the value taken by each of the molecular descriptors, which is difficult for new and original compounds.

The second main family of predictive methods gathers those which have been developed from a huge number of experimental measurements. In the case of vapour pressure, the best example is the well known Antoine's equation (eqn 4) whose expression is the following:

$$\log P_{\text{vap}} = A - \frac{B}{T + C} \quad (4)$$

where A , B , and C are experimental coefficients available for many compounds in specialized databanks.²⁴

Apart from this equation, more general methods exist, among which some are based on group contributions. These methods are handy because thermodynamic properties can be determined even if only the molecular structure is known. The different structural elements considered can be atoms, links, atom groups or chemical functions.²⁵ In the case of liquid–vapour equilibria, all relationships rely on reduced temperature and pressure T_r and P_r . This is interesting because only one single equation is required for all compounds, but in return critical parameters T_c and P_c have to be known (because $P_r = P/P_c$ and $T_r = T/T_c$). The critical point is the limit of the

liquid–gas equilibrium curve above which one single phase, called the supercritical phase, is present.

Critical parameters have been determined experimentally only for very common molecules and have to be calculated to be used for the determination of P_{vap} and ΔH_{vap} . For this purpose the best method is Joback's,²⁶ which is also based on group contributions. This method, introduced in 1984, is used to calculate not only P_c and T_c , but also T_b using the following equations (eqns 5–7):

$$T_b = 198 + \Sigma(\Delta T_b) \quad (5)$$

$$\frac{T_b}{T_c} = \theta = 0.584 + 0.965 \times \Sigma(\Delta T_c) - \Sigma(\Delta T_c)^2 \quad (6)$$

$$P_c = (0.113 + 0.0032 \times \text{na} - \Sigma(\Delta P_c))^2 \quad (7)$$

na being the global number of atoms of the molecule, T_b and T_c being expressed in K and P_c in bars. ΔT_b , ΔT_c and ΔP_c are the group contributions.

When T_c and P_c are known, two main methods are available to calculate P_{vap} : Kirchhoff (the reduced form below was used)²⁷ and Lee–Kesler²⁸

The Kirschhoff–Reduced method (eqn 8):

$$\ln P_{\text{vap},r} = h \times \left(1 - \frac{1}{T_r}\right) \text{ with } h = \frac{\theta}{1-\theta} \times \ln(P_c/\text{atm}) \quad (8)$$

$$\text{and } \theta = \frac{T_b}{T_c}$$

The Lee–Kesler method (eqn 9):

$$\ln P_{\text{vap},r} = f^0(T_r) + \omega \times f^1(T_r) \quad (9)$$

f^0 , f^1 and ω being expressed as follows (eqns 10–12):

$$f^0(T_r) = 5.92714 - \frac{6.09648}{T_r} - 1.28862 \ln(T_r) + 0.169347 T_r^6 \quad (10)$$

$$f^1(T_r) = 15.2518 - \frac{15.6875}{T_r} - 13.4721 \ln(T_r) + 0.43577 T_r^6 \quad (11)$$

$\omega =$

$$\frac{-\ln(P_c/\text{atm}) - 5.92714 + 6.09648/T_r + 1.28862 \ln(T_r) - 0.169347 T_r^6}{15.2518 - 15.6875/T_r - 13.4721 \ln(T_r) + 0.43577 T_r^6} \quad (12)$$

The volatility of C_iE_j , C_iP_j and C_iGly_1 was studied experimentally, but also with the methods presented above. Vapour pressures measured at different temperatures are reported in Table 1.

Table 1 Experimental vapour pressures of some C_iE_j , C_iP_j and C_iGly_1

Compound	P_{vap}/Pa					
	25 °C	30 °C	35 °C	40 °C	45 °C	50 °C
C_4E_1	160.1	224.6	318.6	454.0	619.5	833.9
C_4E_2	30.1	40.8	54.4	72.7	96.8	124.7
C_3P_1	355.2	501.3	703.3	964.5	1306.7	1755.9
C_4P_1	132.3	195.4	277.7	392.0	545.9	746.6
C_4Gly_1	15.4	17.4	23.8	34.5	46.9	54.5
iC_5Gly_1	8.3	15.2	23.6	34.4	47.6	64.1
C_5Gly_1	13.4	21.3	29.7	44.5	57.0	76.8

The experimental values are compared with those obtained from L–K and K–R equations in Fig. 2 and 3 where $P_{\text{vap}} = f(T)$ curves were drawn for C_4E_1 and C_4Gly_1 respectively. Experimental values obtained between 25 and 50 °C were extrapolated to higher temperatures by using the Clausius–Clapeyron equation.

Generally speaking, calculated values match experimental ones quite well for each compound. The best method for prediction varies according to the solvo-surfactant. In the case of C_4E_1 , the L–K equation is better at higher temperatures, whereas the K–R one is more appropriate at lower ones. In the case of C_4Gly_1 the K–R equation is on the contrary better at high temperatures and both predictions are equivalent at lower ones. Globally, both methods are quite reliable for predicting the behaviour of any unknown compound. One has, however, to take into account the fact that experimental values were extrapolated at high temperatures assuming that ΔH_{vap} is constant, which is only a very crude approximation. The experimental curves shown in Fig. 2 and 3 are consequently not exactly representative of the results that would have been obtained if measurements had been carried out above 50 °C.

From these values the heats of vaporization ΔH_{vap} were in each case evaluated by plotting $\ln P_{\text{vap}}$ as a function of $1/T$ according to the Clausius–Clapeyron equation. Table 2

Table 2 Comparison of ΔH_{vap} of different solvo-surfactants

	C_4E_1	C_4E_2	C_3P_1	C_4P_1	C_4Gly_1	iC_5Gly_1	C_5Gly_1
ΔH_{vap} exp/ kJ mol^{-1}	53.3	45.7	51.2	55.3	44.2	64.3	55.4
ΔH_{vap} L–K/ kJ mol^{-1}	91.0	75.2	60.2	63.8	97.4	105.1	104.0
ΔH_{vap} K–R/ kJ mol^{-1}	45.9	54.1	46.5	48.6	69.4	75.6	71.6

gathers the resulting values at 25 °C. The heats of vaporization determined from experimental P_{vap} are well correlated by K–R calculations, whereas the L–K equation gives less accurate results.

The volatility of C_7Gly_1 is clearly lower compared to other solvo-surfactants. C_5Gly_1 and C_4E_2 have equivalent molecular weights but P_{vap} is two times lower for C_5Gly_1 . Differences are less important for heats of vaporization. This hints at equivalent interactions within the liquid phase. The influence of hydrogen bonding is important. The $\Delta H_{\text{vap}}/T_b$ ratio reaches values up to 109 for iC_5Gly_1 , whereas Trouton's rule yields only 85 $\text{J mol}^{-1}\text{K}^{-1}$. The 109 value is similar to those of water and ethanol. It is however interesting to notice that the heats of vaporization of 1,2-diols obtained by replacing the oxygen atom of the ether function by a carbon atom are much higher with values up to 90 kJ mol^{-1} at 25 °C.²⁹ The ether function provides, as expected, some volatility, unlike the alcohol functions.

Regulations³⁰ concerning solvents specify that every organic compound exhibiting a vapour pressure of 0.01 kPa (10 Pa) or more at 20 °C or in particular conditions of use is considered as a volatile organic compound (VOC). According to our data every C_iE_j and C_iP_j has to be considered as a VOC, whereas C_iGly_j are not VOCs, except C_4Gly_1 . This is interesting because C_iGly_j remains relatively volatile but will not, as a non-VOC, be subject to the same restrictions as competing solvents.

Evaporation rates

The volatility of an organic compound is often evaluated by the determination of its evaporation rate relative to a reference compound which is in general in Europe *n*-butyl acetate. There is no direct relationship between the evaporation rate and the boiling point. Within a homogeneous family of solvents volatility decreases as the boiling point rises,³¹ but hydrogen bonded solvents (alcohols, amines...) are in general less volatile than others with similar boiling points.

Globally, the evaporation rate of a liquid depends on its vapour pressure, but also on its heat of vaporization, its surface tension or its hygroscopic nature. Moreover, these factors are inter-dependent so that it is almost impossible to predict theoretically an evaporation rate.³² From experiments it can be inferred by calculating the ratio between the time required by a known quantity of the solvent to evaporate and the time required by the same quantity of the reference solvent to evaporate under the same experimental conditions. Evaporation rates have already been determined for a great number of organic compounds, among which are some glycol ethers.

To compare the rates of evaporation of C_iGly_j and some C_iE_j and C_iP_j , TGA measurements were carried out. This

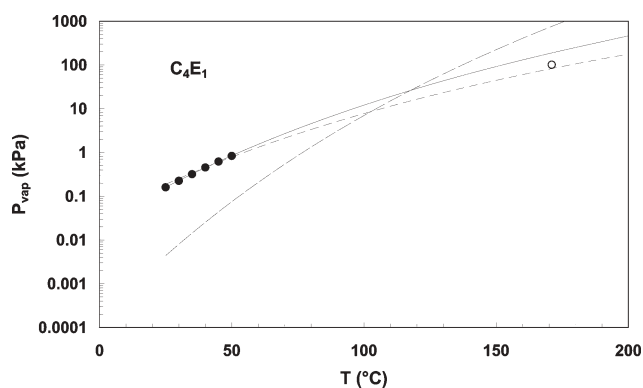


Fig. 2 comparison of experimental vapour pressures (—) of C_4E_1 with values calculated using the Lee–Kesler equation (— —) and Kirschhoff–Reducted equation (— —). The experimental boiling point is also included (○).

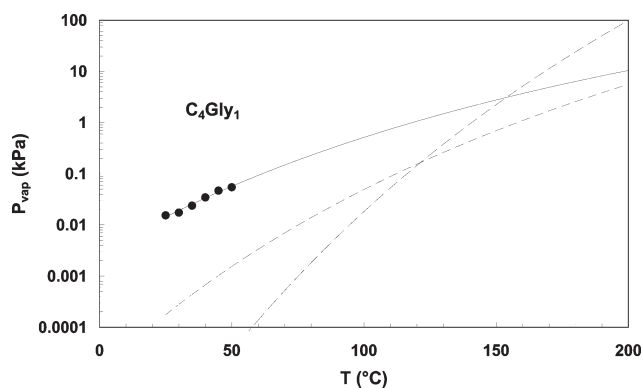
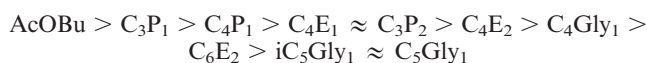


Fig. 3 comparison of experimental vapour pressures (—) of C_4Gly_1 with values calculated using the Lee–Kesler equation (— —) and Kirschhoff–Reducted equation (— —).

technique has already been used to investigate the thermal stability of C_7Gly_1 which turned out to be stable up to quite high temperatures.³³ Moreover, the comparison between experiments carried out under an air and a helium stream showed that these compounds are not subject to thermal oxidation. The temperatures used here were much lower than temperatures of the thermal degradations so that only evaporation was observed. Similar conditions were used for every molecule, with an atmosphere containing 60% v/v of nitrogen and 40% of oxygen. A temperature ramp of $5\text{ }^{\circ}\text{C min}^{-1}$ was applied in each case from $20\text{ }^{\circ}\text{C}$. Two drops of liquid, *i.e.* around 20 mg, were used for each product. Evaporation curves are collected in Fig. 4.

The shape of the curves are all similar, the evolution being slow at first and then very fast above a threshold temperature. We calculated in each case the time corresponding to a loss of 90% of the weight and deduced evaporation rates relative to *n*-butyl acetate C_4Ac (Table 3).

Taking the rate of the reference compound to be 1, compounds with the highest rates are the most volatile. From our results, the following classification can be established, from the most to the least volatile compound:



The rates deduced here from TGA measurements can obviously only be compared with other rates calculated under the same conditions. Classical evaporation rates are generally determined by the “transpiration” method,^{34–36} where a small quantity of vapour is carried by a nitrogen stream and then condensed and weighed. The comparison with literature data is consequently reliable only if a correlation is shown between TGA rates and evaporation rates. Whereas our TGA rates are not clearly linked to boiling points or heats of vaporization, a linear tendency ($R^2 = 0.96$) is observed with experimental

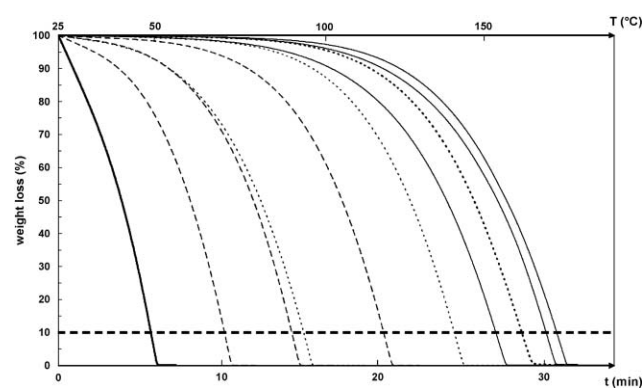


Fig. 4 TGA evaporation curves of a series of C_iE_j , C_jP_i and C_jGly_i . By increasing evaporation time: *n*-butyl acetate $AcOBu$ (ref.), C_3P_1 , C_4P_1 , C_4E_1 , C_3P_2 , C_4E_2 , C_4Gly_1 , C_6E_2 , iC_5Gly_1 , C_5Gly_1 .

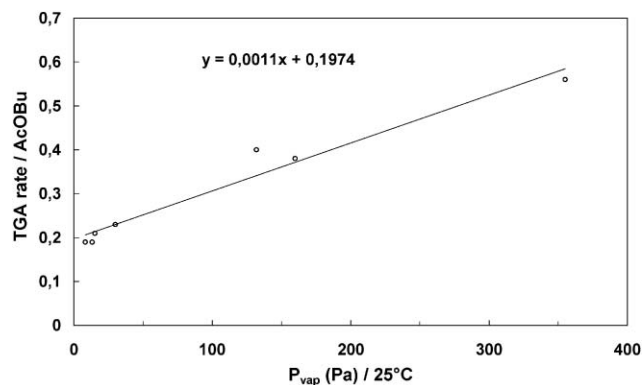


Fig. 5 Evolution of the TGA evaporation rate of glycol and glycerol ethers as a function of vapour pressure measured at $25\text{ }^{\circ}\text{C}$.

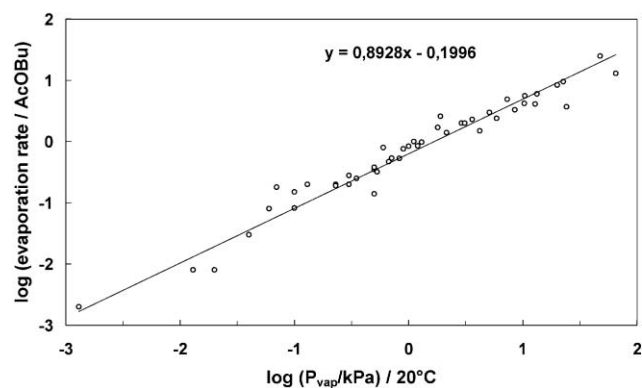


Fig. 6 Evolution on a log-log scale of the evaporation rate (literature data³⁷) as a function of vapour pressure at $20\text{ }^{\circ}\text{C}$.

vapour pressures at $25\text{ }^{\circ}\text{C}$, see Fig. 5. If literature evaporation rates³⁷ are correlated with vapour pressures, a linear log-log relation ($R^2 = 0.94$) is found, see Fig. 6. It is thus possible to predict evaporation rates not only from experimental vapour pressures but also from TGA measurements. The values collected in Table 4 were calculated and compared to literature data.

C_4E_1 and C_4E_2 were used to check the validity of our method since their evaporation rates are available in the literature. In the case of C_4E_1 , the correlation is excellent: almost the same value is found. It is much worse for C_4E_2 for which literature data of 0.004 was found. However our value seems more in agreement with all our observations and reflects better the behaviour of C_4E_2 , which is intermediate between those of C_3P_2 and C_4Gly_1 . Our method appears to be appropriate for the prediction of evaporation rates and has the advantage of supplying an evaluation of P_{vap} at $20\text{ }^{\circ}\text{C}$ from a simple and rapid experiment only, carried out with a common apparatus.

Table 3 Evaporation rates deduced from TGA measurements, relatively to *n*-butyl acetate, after correlation with vapour pressures at $20\text{ }^{\circ}\text{C}$

Compound	C_4Ac	C_3P_1	C_4P_1	C_3P_2	C_4E_1	C_4E_2	C_6E_2	C_4Gly_1	iC_5Gly_1	C_5Gly_1
Rate	1	0.56	0.40	0.28	0.38	0.23	0.20	0.21	0.19	0.19

Table 4 Evaporation rates calculated from experimental vapour pressures and from TGA (*italic*) in comparison with literature (**bold**)

Compound	C ₃ P ₁	C ₄ P ₁	C ₃ P ₂	C ₄ E ₁	C ₄ E ₂	C ₆ E ₂	C ₄ Gly ₁	iC ₅ Gly ₁	C ₅ Gly ₁
<i>P</i> _{vap} 20 °C	253.6	92.6	<i>160.5</i>	111.65	22.2	<i>1.586</i>	10.6	6.1	10.4
Evaporation rate/AcOBu	0.188	0.058	<i>0.123</i>	0.089/ 0.082	0.021/ 0.004	<i>0.002</i>	0.011	0.007	0.011

The evaporation rates of C_iGly₁ are among the lowest for liquid compounds, reflecting a volatility which is lower than that of most common organic solvents (NMP, DMF, acetone, cyclohexanone, hexane, octane, cyclohexane...) and also slightly lower than those of C_iP_j and some C_iE_j. The behaviour of C₄Gly₁ is similar to the one of C₄E₂ whose molecular weight is slightly higher (148 g mol⁻¹ compared to 162 g mol⁻¹). In terms of applications the use of these compounds is favourable when a slow evaporation is required but they must be heated to evaporate quickly.

Hansen solubility parameters

Solubility parameters are used to predict the behaviour of various substances and give some information about the miscibility of two or several solvents or the solubility of a compound.³⁸ They are very useful from a qualitative point of view and can be used for quantitative calculations, even if they are not systematically very accurate.

When the parameters of a substance are not known, they may be calculated with group contribution methods. The contributions of different common groups were published by Fedors³⁹ and collected later by Barton⁴⁰ in the handbook of solubility parameters. Hansen's parameters are expressed by the following equations (eqn 13–15):

$$\delta_d = \frac{\Sigma F_D}{\Sigma V_i} \quad \delta_p = \frac{\sqrt{\Sigma F_p^2}}{\Sigma V_i} \quad \delta_h = \frac{\sqrt{\Sigma E_h}}{\Sigma V_i} \quad (13)$$

where *F_d*, *F_p* and *E_h* are the dispersive, polar and cohesive contributions respectively, and *V_i* are the group contributions to the molar volumes of the molecules. Calculations of the different solvo-surfactants gave the results collected in Table 5.

Table 5 Hansen solubility parameters of some C_iE_j, C_iP_j and C_iGly_j were calculated by group contributions. Values originally proposed by Hansen are given *in italic*. δ_{exp} values were calculated from experimental heats of vaporization. $\delta_{\text{exp}} = [(\Delta H_{\text{vap}} - RT)/V_m]^{1/2}$, *V_m* being the molar volume estimated from group contributions

	MPa ^{1/2}								
Compound	δ_d	δ_p	δ_h	δ	δ_{exp}				
C ₄ Gly ₁	16.0	5.5	17.0	24.0		16.8			
iC ₅ Gly ₁	15.6	4.9	16.0	22.9		19.2			
C ₅ Gly ₁	15.8	4.9	16.1	23.1		17.8			
C ₆ Gly ₁	16.0	4.5	15.4	22.7					
iC ₈ Gly ₁	16.8	3.8	14.15	22.3					
C ₈ Gly ₁	16.4	3.8	14.3	22.1					
C ₄ E ₁	15.8	16.0	4.9	5.1	13.2	21.2	20.8	19.7	
C ₄ E ₂	15.9	16.0	4.4	7.0	12.3	10.6	20.6	20.4	15.9
C ₆ E ₂	16.0	16.0	3.7	6.0	11.3	10.0	20.0	19.8	
C ₃ P ₁	15.2	15.8	4.8	7.0	13.1	9.2	20.6	19.6	19.0
C ₄ P ₁	15.2	15.3	4.2	4.5	12.3	9.2	20.0	18.4	18.6
C ₃ P ₂	15.05		3.9		11.65		19.4		

C_iGly₁ have higher parameters than their E_j or P_j counterparts and theoretically show a better solubilizing power. Differences come mostly from δ_h and partly from δ_p . The dispersive part is not dependent on the nature of the polar head and is only a function of the length of the alkyl chain. The global number of carbon atoms in this chain is important, but branching has almost no effect. The glycerol head brings a higher polarity and above all a strong ability to create hydrogen bonds, and its derivatives have a better affinity with polar and protic solvents.

Hildebrand's parameter can also be obtained from experimental ΔH_{vap} values and molar volumes. It is interesting to notice that if δ is calculated from these values (Table 5), the results do not match group contribution values. δ is for example 16.8 against 24.0 for C₄Gly₁, 19.2 against 22.9 for iC₅Gly₁ and 17.8 against 23.1 for C₅Gly₁. Hansen had already noticed these differences many years ago but was unable to explain them. They show that these values have to be used with care, and that only δ determined by the same method can be compared.

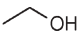
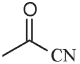
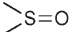
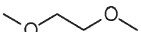
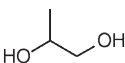
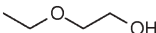
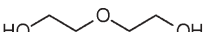
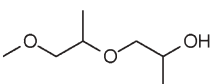
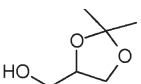
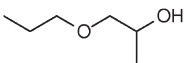
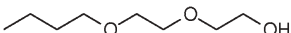
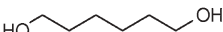
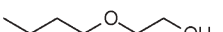
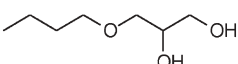
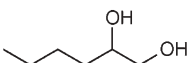
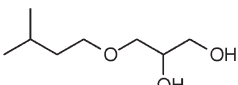
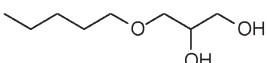
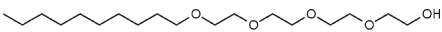
Cytotoxicity

Cytotoxicity was evaluated for some C_iGly₁, C_iE_j, C_iP_j, and a series of reference solvents. The same kind of cells was used in each case since IC₅₀ values can vary from one cell family to another.⁴¹ Results are collected in Table 6 and ordered according to increasing toxicity.

Among our reference solvents, many have already been tested previously and can be used as references. Ethanol or propylene glycol exhibit for instance a very low toxicity, whereas Solketal is considered moderately toxic.⁴¹ In comparison C₃P₁ is also moderately toxic whereas C_iGly₁ are more harmful. Globally cytotoxicity increases with amphiphilicity and, more precisely, it seems that the alkyl chain length has a major influence. This hypothesis was already proposed when, recently, we evaluated the IC₅₀ of some carboxylated surfactants and correlated them with their CMC.⁴² Here the "true" surfactant C₁₀E₄ has the lowest IC₅₀, followed by C_iGly₁ which are the most amphiphilic solvo-surfactants. In the same way, it was observed that 1,2-hexanediol has a much lower IC₅₀ than its symmetrical isomer 1,6-hexanediol.

The fact that the most amphiphilic compounds exhibit the highest cytotoxicity is not surprising since the killing of cells is linked to the ability of the molecules to penetrate the membranes and thus make them less resistant. Cytotoxicity has already been correlated with log*P*_{octane/water} for a large number of molecules.⁴³ Glycerol ethers are particularly oil soluble and excellent solubilizers. Numerous studies in the literature refer to their ability to deliver medicines by helping them to cross cellular membranes.^{44–48} Consequently their relatively high cytotoxicity is not surprising. However, the validity of the *in vitro* tests carried out here can be discussed

Table 6 IC₅₀ measured by the MTT method

Compound	Formula	IC ₅₀ (%)	IC ₅₀ /mmol L ⁻¹
Ethanol		7.1	1540
Acetonitrile		7.2	1040
Dimethylsulfoxide		5.3	680
C ₁ E ₁ C ₁		6.1	675
Propylene glycol		5.0	660
C ₂ E ₁		2.1	230
Diethylene glycol		1.9	180
C ₁ P ₂		2.5	170
Solketal		2.0	150
C ₃ P ₁		1.2	101
C ₄ E ₂		1.3	80
1,6-Hexanediol		0.9	76
C ₄ E ₁		0.7	59
C ₄ Gly ₁		0.5	33
1,2-Hexanediol		0.3	25
iC ₅ Gly ₁		0.25	15
C ₅ Gly ₁		0.2	12
C ₁₀ E ₄		0.02	0.0006

for amphiphilic compounds which are highly oil soluble. According to this observed tendency, iC₈Gly₁ for instance may be expected to be harmful whereas it is commercially available as a skin-friendly cosmetic additive (Schulke & Mayr). Another example is C₄E₁ which is less toxic than C₇Gly₁ but which is labelled as irritating to skin and eyes. The results proposed here have consequently to be used with great care, the main conclusion being that C₇Gly₁ seem to be more cytotoxic than glycol ethers.

Eye-irritancy

The RBC test carried out in this work was assessed in 1999 by the European Cosmetic and Fragrance Association to estimate *in vivo* results obtained by the reference Draize test. Three

products were studied: C₄E₁, C₃P₁ and C₄Gly₁. Their H50 and %D were calculated and are reported in Table 7.

In order to discuss these results two classifications were used: Lewis's classification which links the H50 in mmol L⁻¹ to the *in vivo* result and Pape's which correlates the H50/%D ratio also with the *in vivo* values. Tables 8 and 9 show these classifications

Table 7 Results of the RBC test performed with C₄E₁, C₃P₁ and C₄Gly₁

Compound	H50 (ppm/mmol L ⁻¹)	%D	H50 (ppm)/%D
C ₄ E ₁	129 440/1095	15.1	8572
C ₃ P ₁	52 823/447	10.2	5179
C ₄ Gly ₁	52 570/355	10.2	5154

Table 8 Lewis's classification for RBC test (MMTS: maximum mean total Draize score)

Classification	<i>In vitro</i> result: H50 in mmol L ⁻¹	<i>In vivo</i> result: MMTS
Non irritating	>10	0–5
Very slightly irritating	1–10	>5–15
Slightly irritating	0.1–1	>15–25
Moderately irritating	<0.1	>25–50
Highly irritating	<<0.1	>50–80

Table 9 Pape's classification for RBC test (MIOI: mean index ocular irritation)

Classification	<i>In vitro</i> result: H50/%D ratio	<i>In vivo</i> result: MIOI
Non irritating	>100	<5
Slightly irritating	>10	<15
Moderately irritating	>1	<25
Irritating	>0.1	<40
Highly irritating	<0.1	>40

The three compounds have similar H50 and %D, C₃P₁ and C₄Gly₁ being nevertheless slightly more irritating than C₄E₁. According to both classifications, all compounds are non irritating since the values are far higher than the limits fixed by Lewis and Pape. However, these results have once more to be used with great care, since C₄E₁ is labelled as irritating. This makes it difficult to correlate forward, *in vitro* and *in vivo* results. In our case, the nature of the molecules may be problematic, since the RBC test is advised for amphiphilic molecules but not for solvents, whereas solvo-surfactants possess by definition similarities with solvents. It is thus wise to conclude that C₄Gly₁ has a similar effect compared to competing molecules, without drawing further conclusions.

Biodegradability

The evaluation of the biodegradability of organic compounds is important since it expresses their long term effect on the environment. The ultimate degradation in H₂O and CO₂ was studied according to the OCDE 301F standard that requires the measurement of the BOC (biological oxygen consumption) and the calculation of the TOC (theoretical oxygen consumption). The BOC is determined with a respirometer for 28 d in a medium containing diverse mineral substances (sodium and potassium phosphates, ammonium, calcium and iron chlorides, magnesium sulfate) and bacteria collected from the local wastewater treatment plant. The TOC (in mg of oxygen per mg of product) is calculated from the molecular structure of the molecule, according to eqn 14. It corresponds to the amount of oxygen required to oxidize totally the product.

TOC =

$$16 \times \frac{(2 \times C + 0.5 \times (H - Cl - 3 \times N) + 3 \times S + 2.5 \times P + 0.5 \times Na - O)}{PM} \quad (14)$$

The biodegradability is thus calculated using eqn 15:

$$\% \text{ biodeg} = \frac{BOC}{TOC} \times 100 \quad (15)$$

Four substances were tested in addition to a reference compound (sodium acetate): C₄E₁, C₃P₁, C₄Gly₁ and iC₅Gly₁.

Each of them was studied at several concentrations in order to detect a possible harmful effect on bacteria. Several parameters were checked to assess the validity of the experiment. (1) The degradation of sodium acetate had to be higher than 60% after 14 d. Here it reached 80%. (2) The oxygen consumption of the mineral medium had to be lower than 60 mg L⁻¹ after 28 d. In this work it was only 6 mg L⁻¹. (3) The pH had to be between 6 and 8.5 after 28 d, which we obtained in each case.

According to the OCDE standard, the biodegradation has to reach 60% 10 d after the attainment of the 10% level and globally at least 60% after 28 d in order to consider a molecule as biodegradable. In the case of surfactants, the European norm CE2004/648 requires only the attainment of at least 60% after 28 d. Fig. 7 shows the evolution of the biodegradation of the compounds after 28 d, as a function of their concentrations. A threshold concentration is observed in each case, around 70 and 55 mg L⁻¹ for C₄E₁ and C₃P₁ respectively, and around 20 mg L⁻¹ for C₄Gly₁. It could not be determined for iC₅Gly₁. This threshold expresses a harmful effect of the solvo-surfactants on the bacteria which are supposed to degrade them. It seems that it is linked to the cytotoxicity of the compounds, certainly through their ability to dissolve hydrophobic cellular membranes. Similar to the cytotoxic effect, it increases with the hydrophobicity and the alkyl chain length, iC₅Gly₁ being the most harmful. According to these results, amphiphilicity, cytotoxicity, irritancy and biodegradability are all linked and similar phenomena are certainly involved in each process.

According to the OCDE, products have to be tested at 100 mg L⁻¹ and the concentration can be decreased afterwards if necessary. Our results show that none of the products is degradable at 100 mg L⁻¹, the threshold concentration being 50 mg L⁻¹ for glycol ethers and lower for glycerol ethers (20 mg L⁻¹ max.)

Conclusion

The volatility of short chain glycerol 1-monoethers was investigated in comparison with two others families of solvo-surfactants, namely ethylene glycol and propylene glycol monoethers. Calculated and experimental boiling points and vapour pressures as well as deduced heats of vaporization were

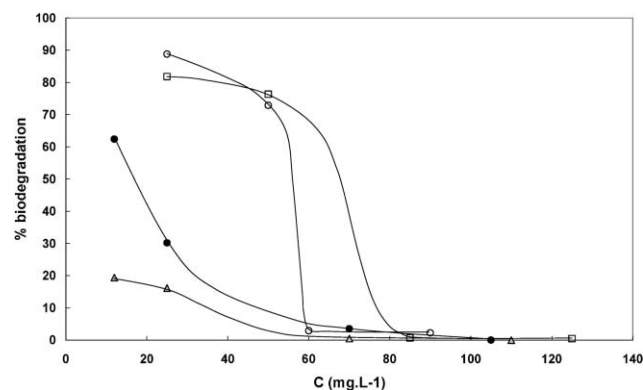


Fig. 7 Evolution of the biodegradability after 28 d as a function of the concentration for C₄E₁ (□), C₃P₁ (○), C₄Gly₁ (●) and iC₅Gly₁ (Δ).

compared and discussed, and evaporation rates were calculated from simple TGA experiments. Glycerol derivatives turned out to be less volatile than their glycol counterparts. Because of their great tendency to form hydrogen bonds, they have lower vapour pressures and higher boiling points even if their heats of vaporization are similar. Their evaporation rates also are lower, the rate of a given monoglycerol ether being similar to one of a diethylene glycol equivalent. These molecules are thus appropriate for applications where low evaporation is required at ambient temperature. Their low volatility can be seen as a drawback from a practical point of view, but the advantage is that contrary to glycol ethers, they will not be considered as VOCs because their vapour pressures at 20 °C are lower than 10 Pa.

Bionotox properties were also studied and compared with those of glycol ethers. Even if the validity of the cytotoxicity and irritancy tests can be in our particular case a matter of debate, they show that C_6Gly_1 are not as interesting as C_iE_j and C_iP_j in terms of irritating power towards skin and eyes. Their biodegradability is also lower, more precisely they are degradable at lower concentrations. All solvo-surfactants have, above a threshold concentration, a harmful effect on the bacteria supposed to degrade them. This effect is detected at lower concentrations in the case of C_6Gly_1 .

In spite of their poor volatility, glycerol 1-monoethers exhibit a theoretically high solubilizing power according to their Hildebrand and Hansen parameters. Their solubility in many organic solvents was assessed experimentally. Their high affinity for water has already been reported elsewhere. This results in their excellent ability to put initially insoluble compounds into solution in water and to co-solubilize water and organic solvents, with a consequently improved degreasing power, as we observed in a previous study.¹³ Taking into account the fact that most of them will not be considered as VOCs, they show an interesting potential as substitutes for genotoxic glycol ethers.

Acknowledgements

The authors wish to thank Prof. S. Pietrzyk for his help in the calculation of thermodynamic data and Dr. F. Cazaux for ATG measurements. The company ARD (Agroindustrie Recherche et Développement), based in Reims (France), is also gratefully acknowledged for irritating power and biodegradability assays.

References

- 1 S. E. Friberg, *Hydrotropy*, in *Surfactant Science Series*, Marcel Dekker, New York, 1997, vol. **129**, p. 21.
- 2 K. Lunkenheimer, S. Schroedle and W. Kunz, *Prog. Colloid Polym. Sci.*, 2004, **126**, 14.
- 3 M. Charretton, *Cah. Notes Doc.*, 1987, **128**, 417.
- 4 M. Charretton, *Chim. Inf.*, 1987, **3**, 33.
- 5 M. Leleu, *Cah. Notes Doc.*, 1980, **98**, 53.
- 6 A. Cicolella, *Cah. Notes Doc.*, 1992, **148**, 359.
- 7 J. Etienne, Les éthers de glycol. Une toxicité variable selon les composés, *l'Actualité chimique*, 2003, (Nov–Dec), 145.
- 8 www.inrs.fr.
- 9 www.ETHERS-de-glycol.com.
- 10 P. Bauduin, L. Wattebled, S. Schrödle, D. Touraud and W. Kunz, *J. Mol. Liq.*, 2004, **115**, 23.

- 11 S. Queste, P. Bauduin, D. Touraud, W. Kunz and J. M. Aubry, *Green Chem.*, 2006, **8**, 822.
- 12 S. Queste, P. Sabre and J. M. Aubry, in *Proceedings of the Spanish Committee of Detergents, Surfactants and Related Industries (CED) Annual Meeting*, Barcelona, 2006.
- 13 K. Nasirzadeh, D. Zimin, R. Neueder and W. Kunz, *J. Chem. Eng. Data*, 2004, **49**, 607.
- 14 T. Mosmann, *J. Immunol. Methods*, 1983, **65**, 55.
- 15 L. Sanchez, M. Mitjans, M. R. Infante and M. P. Vinardell, *Pharm. Res.*, 2004, **21**(9), 1637.
- 16 W. Warisnoicharoen, A. B. Lansley and M. J. Lawrence, *J. Pharm. Sci.*, 2003, **92**(4), 859.
- 17 J. K. Lee, D. B. Kim, J. I. Kim and P. Y. Kim, *Toxicol. in Vitro*, 1999, **14**, 345.
- 18 M. A. Perkins, R. Osborne, F. R. Rana, A. Ghassemi and M. K. Robinson, *Toxicol. Sci.*, 1999, **48**, 218.
- 19 J. F. Sina, G. J. Ward, M. A. Laszek and P. D. Gautheron, *Fundam. Appl. Toxicol.*, 1992, **18**, 515.
- 20 M. Gaune-Escard and J. P. Bros, *Calcul des constantes thermodynamiques*, in *Techniques de l'ingénieur*, dossier K-540.
- 21 A. R. Katritzky, L. Mu, V. S. Lobanov and M. Karelson, *J. Phys. Chem.*, 1996, **100**, 10400.
- 22 A. R. Katritzky and L. Mu, *J. Chem. Inf. Comput. Sci.*, 1997, **37**, 756.
- 23 P. D. T. Huilbers, V. S. Lobanov, A. R. Katritzky, D. O. Shah and M. Kabelson, *J. Colloid Interface Sci.*, 1997, **187**, 113.
- 24 C. L. Yaws and H. C. Yang, *Hydrocarbon Process.*, 1989, 65.
- 25 B. E. Poling, J. M. Prausnitz, and J. P. O'Connell, in *The Properties of Gases and Liquids*, Mc Graw-Hill, New York, 5 edn, 2000.
- 26 K. G. Joback and R. C. Reid, *Chem. Eng. Commun.*, 1987, **57**, 233.
- 27 A. H. Manji and J. Lielmezs, *Thermochim. Acta*, 1984, **75**(1–2), 207.
- 28 J. M. Prausnitz, R. N. Lichenthaler, E. G. de Azavedo, in *Molecular Thermodynamics of Fluid Phase Equilibria*, Prentice Hall, Englewood Cliffs, NJ, 2nd edn, 1986.
- 29 S. P. Verevkin, *Fluid Phase Equilib.*, 2004, **224**, 23.
- 30 *European Council Directive n° 1999/13/CE*, 1999, March, 11.
- 31 C. H. Fischer, *J. Coat. Technol.*, 1991, **63**(799), 79.
- 32 A. L. Rocklin, *J. Coat. Technol.*, 1976, **48**(622), 45.
- 33 S. Mateo, Propriétés physico-chimiques et réactivité du carbonate de glycéril – faisabilité de l'obtention des α -monoéthers de glycéril et propriétés solvantes, *PhD. Thesis—Institut National Polytechnique de Toulouse*, 2001.
- 34 S. P. Verevkin, *J. Chem. Eng. Data*, 2000, **45**, 946.
- 35 J. S. Chickos, D. G. Hesse, S. Hosseini, J. F. Liebman, G. D. Mendenhall, S. P. Verevkin, K. Rakus, H. D. Beckhaus and C. Rüchardt, *J. Chem. Thermodyn.*, 1995, **27**, 693.
- 36 J. D. Cox, G. Pilcher, in *Thermochemistry of Organic and Organometallic Compounds*, Academic Press, London, 1970.
- 37 *Ullmann's Encyclopedia of Industrial Chemistry, Solvents*, Wiley-VCH GmbH & Co.KgaA, Weinheim, Berlin, 2002.
- 38 J. H. Hildebrand, R. L. Scott, in *The Solubility of Nonelectrolytes*, Dover Publications Inc., Mineola, NY, 3rd edn, 1964.
- 39 R. F. Fedors, *Polym. Eng. Sci.*, 1974, **14**, 472.
- 40 A. F. M. Barton, in *CRC Handbook of Solubility Parameters and Other Cohesion Parameters*, CRC Press, Boca Raton, FL, 1983.
- 41 H. C. Korting, S. Schindler, A. Hartinger, M. Kerscher, T. Angerpointner and H. I. Maibach, *Life Sci.*, 1994, **55**(7), 533.
- 42 N. Chailloux, Synthèse et propriétés amphiphiles des carboxylates de sodium des monoesters d'acides α , ω -dicarboxyliques, *PhD. Thesis, Université de Lille 1*, 2004.
- 43 H. Tani, S. Saito and K. Hashimoto, *Arch. Toxicol.*, 1992, **66**(5), 368.
- 44 B. Erdlenbruch, V. Jendrosseck, W. Kugler, H. Eibl and M. Lakomek, *Cancer Chemother. Pharmacol.*, 2002, **50**(4), 299.
- 45 B. Erdlenbruch, V. Jendrosseck, H. Eibl and M. Lakomek, *Exp. Brain Res.*, 2000, **135**(3), 417.
- 46 C. Unger and H. Eibl, *Drugs Today*, 1994, **30**, 53.
- 47 K. Mahendra, D. Jahagirdar, M. Van Linde, B. Roelofsen and H. Eibl, *Biochim. Biophys. Acta*, 1985, **818**(3), 356.
- 48 C. Unger, H. Eibl, H. W. Von Heyden, B. Krisch and G. A. Nagel, *Klin. Wochenschr.*, 1985, **63**(12), 565.

Water-medium isomerization of homoallylic alcohol over a Ru(II) organometallic complex immobilized on FDU-12 support

Hexing Li,^{*a} Fang Zhang,^a Hong Yin,^a Ying Wan^a and Yunfeng Lu^b

Received 21st December 2006, Accepted 7th February 2007

First published as an Advance Article on the web 2nd March 2007

DOI: 10.1039/b618681e

A novel Ru(II) organometallic catalyst with highly ordered cage-like mesoporous structure was prepared by coordinating the Ru(II) with the PPh₂-ligand incorporated into the FDU-12 support (Ru–PPh₂-FDU-12). During water-medium isomerization of 1-phenyl-3-buten-1-ol, the Ru–PPh₂-FDU-12 exhibited almost the same activity and selectivity as the corresponding RuCl₂(PPh₃)₃ homogenous catalyst and could be used for at least 5 repetitions, showing good potential for industrial application. The excellent performance of the Ru–PPh₂-FDU-12 could be attributed to the high and uniform dispersion of the Ru(II) active sites on the FDU-12 support, the large size of both the pore entrance and pore cages, which facilitated the diffusion, the adsorption and the transformation of organic substrates on the catalyst surface. The decrease in the activity of the Ru–PPh₂-FDU-12 after being used for 5 times could be mainly attributed to the decrease in the pore entrance size and the pore cage size rather than the leaching of the Ru(II) active species from the FDU-12 support.

Introduction

The use of water instead of organic solvents as an environmentally friendly medium for organic syntheses has become an important branch of green chemistry.¹ Up to now, most studies have been focused on homogeneous organometallic catalysts due to the solubility limit of organic substrates in water.² However, homogeneous catalysts are difficult to separate from products, which may eventually increase the cost and also cause environmental pollution by heavy metallic ions. Immobilized homogeneous catalysts could be easily separated and used repetitively.^{3–6} To achieve high activity, both the dispersion of the active sites on the support and the diffusion of the organic substrate molecules should be considered, especially in the case where water is used as the reaction medium.⁷ Ordered mesoporous structure supports (MCM-41, SBA-15 *etc.*)^{8–10} are superior to the traditional inorganic supports (SiO₂, active carbon *etc.*) owing to their high surface area and relatively large pore diameter. In our previous papers,^{11–14} we reported that metallic Pd and Ru(II) organometallic complexes deposited on the MCM-41 and SBA-15 exhibited high activity and selectivity. However, when bulky organic molecules are involved in the organic synthesis, these supports still exhibit a diffusion limit due to their one-dimensional structure. For example, the isomerization of homoallylic alcohols which has been widely used in organic synthesis for the manufacturing of biologically active molecules.^{15–17} Li's group found that the RuCl₂(PPh₃)₃ homogeneous catalyst exhibited excellent activity and selectivity in water-medium isomerization of homoallylic alcohols.¹⁸ To

design immobilized Ru(II) catalysts for such reactions, supports with larger pore size in a three-dimensional structure should be considered. In addition, the size of the pore entrance is also important for the diffusion of organic molecules from bulk solution to the porous channel. In this paper, we report a novel immobilized Ru(II) catalyst by coordinating the Ru(II) with the PPh₂-ligand originally incorporated in the FDU-12 support (Ru–PPh₂-FDU-12). The FDU-12 possessed a cage-like mesoporous structure with both large porous channels and large pore entrances, which was favorable for achieving high activity and selectivity.

Experimental

Catalyst preparation

The FDU-12 functionalized with pendant diphenylphosphine group, denoted as PPh₂-FDU-12, was prepared *via* co-condensation of tetraethoxysilane (TEOS) and 2-(diphenylphosphino)ethyltriethoxysilane (DPPES). In a typical synthesis, 1.0 g triblock copolymers EO₁₀₆PO₇₀EO₁₀₆ (F127), 1.0 g 1,3,5-trimethylbenzene (TMB) and 2.5 g KCl were dissolved in 60 ml of 2 M HCl and stirred for 24 h. Then, 3.94 g TEOS and 0.357 g DPPES were added dropwise into the above solution. After being stirred at 313 K for 24 h, the solution was transferred to an autoclave and kept at 373 K for 24 h. The as-received white solid was dissolved in 2 M HCl and the obtained slurry mixture was transferred into a Teflon autoclave for hydrothermal treatment at 393 K for 72 h. The resulted solid was collected by filtration and dried in vacuum at 353 K for 24 h, followed by extraction in ethanol at 353 K for 24 h to remove surfactants and other organic residues.

The Ru–PPh₂-FDU-12 catalyst was prepared through covalent tethering techniques according to the following procedure: 1.0 g PPh₂-FDU-12 was added into 30 ml toluene

^aDepartment of Chemistry, Shanghai Normal University, Shanghai, 200234, China. E-mail: HeXing-Li@shnu.edu.cn; Fax: 86-21-64322272; Tel: 86-21-64322272

^bChemical & Biomolecular Engineering Department, University of California, Los Angeles, California, USA. E-mail: hucla@ucla.edu

solution containing 96 mg $\text{RuCl}_2(\text{PPh}_3)_3$ and stirred for 24 h at 303 K under argon atmosphere. The resulting yellow solid was washed thoroughly with toluene, followed by Soxhlet-extraction with toluene to remove all impurities including the Ru species uncoordinated with the PPh_2 -ligand in the PPh_2 -FDU-12. Finally, the Ru-PPh_2 -FDU-12 catalyst was dried under vacuum at 373 K for 24 h. ICP analysis revealed that the Ru loading in the Ru-PPh_2 -FDU-12 catalyst was around 0.70 wt%.

Characterization

The content of Ru element in the Ru-PPh_2 -FDU-X catalysts was analyzed by an inductively coupled plasma optical emission spectrometer (ICP, Varian VISTA-MPX). The X-ray powder diffraction (XRD) was carried out on a Rigaku D/Max-RB diffractometer with $\text{CuK}\alpha$ radiation. Transmission electron microscopy (TEM) was performed on a JEOL JEM2010 electron microscope at an acceleration voltage of 200 kV. Fourier transform infrared (FTIR) spectra were collected with a Nicolet Magna 550 spectrometer by using the KBr method. N_2 adsorption-desorption isotherms were measured at 77 K using a Quantachrome Nova 4000e analyzer. The samples were measured after being degassed at 423 K overnight. The Brumauer-Emmett-Teller (BET) method was utilized to calculate the specific surface area (S_{BET}). Based on the NLDFT sphere and cylindrical models, both the size of the pore entrance (D_{entrance}) and the size of the pore channel (D_{p}) as well as the pore volume (V_{p}) were calculated from the adsorption and desorption branches, respectively. Solid-state ^{29}Si MAS NMR, ^{13}C CP MAS NMR and ^{31}P CP MAS NMR spectra were recorded at 79.5, 100.6 and 169.3 MHz on a Bruker AV-400 NMR spectrometer.

Activity test

The water-medium isomerization of 1-phenyl-3-buten-1-ol was chosen as a probe to evaluate the performance of the as-prepared catalysts. The reaction was conducted at 373 K under vigorous stirring in a glassy reactor containing 0.2 g Ru-PPh_2 -FDU-12 (equivalent to 1.4 mg Ru), 0.025 ml 1-phenyl-3-buten-1-ol and 5.0 ml H_2O . Each reaction run was refluxed for 8 h, with care not to allow solvent loss due to evaporation. The reaction mixture was extracted by ether and dried by MgSO_4 . The products were identified by ^1H NMR spectroscopy. Quantitative analysis was performed on a high-performance liquid chromatograph (Shimadzu SPD-10AVP) equipped with a UV-Vis detector and a KR100-5C18 liquid column, from which both the reaction conversion and selectivity were calculated. For comparison, isomerization of 1-phenyl-3-buten-1-ol with homogenous $\text{RuCl}_2(\text{PPh}_3)_3$ catalyst containing 1.4 mg Ru was also carried under the same conditions. The reproducibility of all results was checked by repeating the results at least three times and was found to be within acceptable limits ($\pm 5\%$).

In order to determine the catalyst durability, the Ru-PPh_2 -FDU-12 catalyst was allowed to settle after each run of reactions and the catalyst was collected, which was re-used under the same reaction conditions. The content of Ru species

leached off from the Ru-PPh_2 -FDU-12 catalyst in each run was determined by ICP analysis.

Results and discussion

The FTIR spectra (Fig. 1) revealed that, besides the peaks observed in the pure FDU-12, the PPh_2 -FDU-12 sample displayed several new peaks. A weak peak in the range from 2983 to 2890 cm^{-1} could be attributed to the asymmetric and symmetric stretching modes of C-H bonds.¹⁹ The peaks at 691 cm^{-1} and 1435 cm^{-1} could be assigned to the -H out-of-plane deformation of the monosubstituted benzene ring and the vibrations of P-CH₂, respectively. These results confirmed the successful incorporation of the PPh_2 -CH₂-CH₂-group into the network of the FDU-12.²⁰ Replacement of FDU-12 surface OH groups by PPh_2 -CH₂-CH₂-groups resulted in a decrease of the absorbance peak at 3450 cm^{-1} indicative of the Si-OH. The PPh_2 vibration normally appears in the range from 1130 to 1090 cm^{-1} , which could not be resolved clearly due to the overlap by the intense absorbance at 1100 cm^{-1} owing to the Si-O vibration.²⁰

As shown in Fig. 2, the ^{29}Si MAS NMR spectra of the PPh_2 -FDU-12 sample displayed three resonance peaks up-field corresponding to Q^4 ($\delta = -110$ ppm), Q^3 ($\delta = -102$ ppm), and Q^2 ($\delta = -92$ ppm), and two peaks down-field corresponding to T^3 ($\delta = -65$ ppm) and T^2 ($\delta = -57$ ppm), where $Q^n = \text{Si}(\text{OSi})_n(\text{OH})_{4-n}$, $n = 2-4$ and $T^m = \text{RSi}(\text{OSi})_m(\text{OH})_{3-m}$, $m = 1-3$. The presence of T^m peaks also confirmed the incorporation of the PPh_2 -CH₂-CH₂-group as a part of the silica wall structure.^{21,22} The $T^m/(T^m + Q^n)$ ratio in the PPh_2 -FDU-12 sample was determined as 10.1%, almost the same as the DPPTS/(DPPTS + TEOS) molar ratios in the initial mixture, suggesting that nearly all the DPPTS incorporated with the TEOS, *i.e.*, the loss of DPPTS during the co-condensation could be neglected.²³ In addition, the ^{13}C CPMAS NMR spectra clearly displayed two peaks around 10 and 58 ppm, corresponding to two C atoms in the -CH₂-CH₂- group connected with the PPh_2 group and one peak around 138 ppm

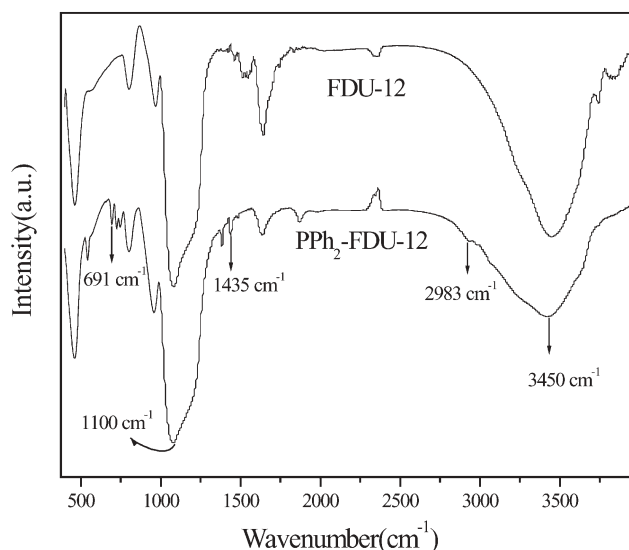


Fig. 1 FTIR spectra of FDU-12 and the PPh_2 -FDU-12 samples

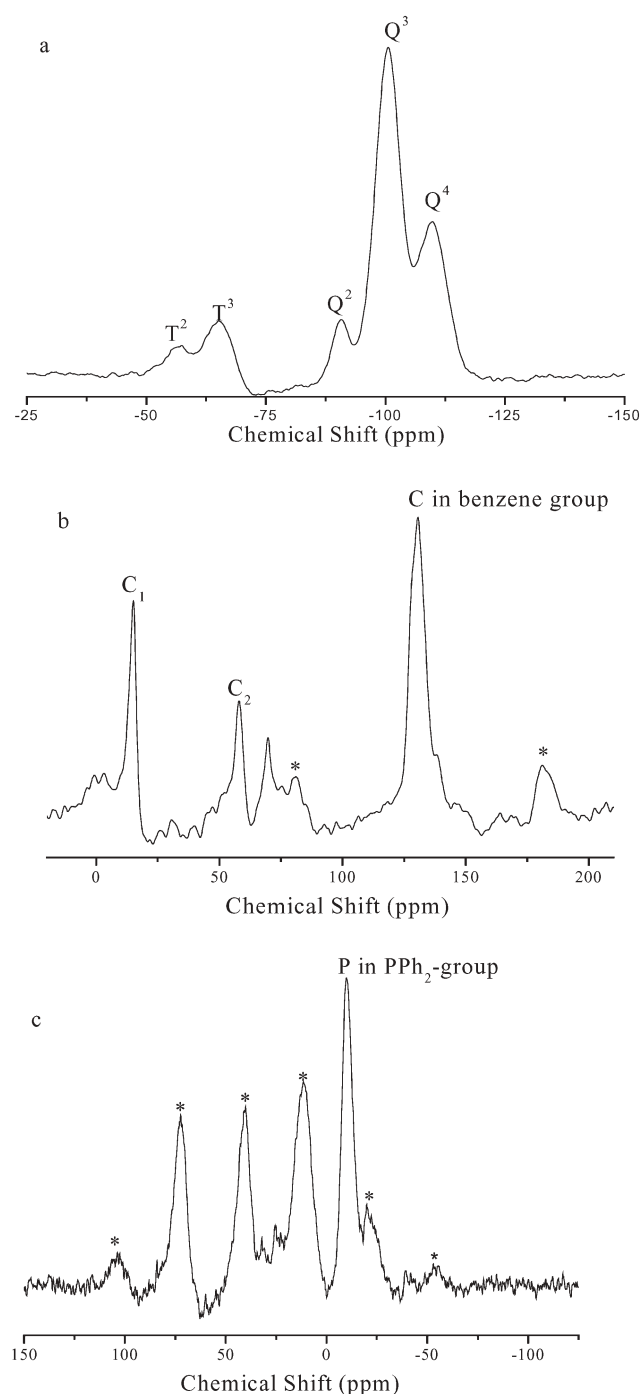


Fig. 2 NMR spectra of the PPh₂-FDU-12 samples (a) ²⁹Si MAS NMR, (b) ¹³C CP/MAS NMR, and (c) ³¹P CP/MAS NMR

indicative of the C atoms in the benzene ring in the PPh₂ group.²⁴ The small resonance peaks observed in the range of 67–77 ppm could be attributed to trace P123 surfactant in the PPh₂-FDU-12.²⁵ Other peaks marked with asterisks were rotational sidebands, which often appeared in the CP/MAS process.²⁶ Furthermore, from the ³¹P MAS NMR spectrum, one could see a strong peak at $\delta = -10.2$ ppm, indicative of the P atom in the PPh₂ group.²⁷ All of these results demonstrated that the PPh₂-CH₂-CH₂-group successfully incorporated into the network of the FDU-12 without significant decomposition.

Fig. 3 shows the small-angle XRD patterns of both the PPh₂-FDU-12 and the Ru-PPh₂-FDU-12 samples. The PPh₂-FDU-12 displayed four well-resolved peaks around $2\theta = 0.72^\circ$, 1.0° , 1.2° and 1.5° with the d -spacing ratios of $\sqrt{3} : \sqrt{8} : \sqrt{11} : \sqrt{24}$, indicative of the (111), (220), (311) and (422) reflections similar to those found in pure FDU-12.^{28,29} Thus, the incorporation of the PPh₂-CH₂-CH₂-group with the FDU-12 caused no significant damage to the highly ordered mesoporous structure in the FDU-12. These four reflection peaks could still be observed clearly in the Ru-PPh₂-FDU-12 sample, though the peak intensities decreased. Thus, one could conclude that the immobilization of the Ru(II) complex onto the PPh₂-FDU-12 support did not destroy the mesoporous structure, but only caused a decrease in the ordering degree of the mesopores.

TEM images along the [110] and [111] directions (Fig. 4) revealed that both the PPh₂-FDU-12 and the Ru-PPh₂-FDU-12 displayed a highly ordered lattice array over large domains, indicating a uniform, well-defined cubic mesostructure (Fm-3m).²⁹ No significant damage to the mesoporous structure of the FDU-12 was observed, which could be attributed to the high dispersion of the PPh₂-CH₂-CH₂-groups and even the Ru(II) complexes on the porous surface of the PPh₂-FDU-12.

As shown in Fig. 5, both the PPh₂-FDU-12 and the Ru-PPh₂-FDU-12 samples exhibited typical type-IV nitrogen adsorption-desorption isotherms with an H₂ hysteresis loop indicative of mesoporous structure.³⁰ The initial step of adsorption isotherms represented the adsorption in mesopores to form multilayers of adsorbed nitrogen on the pore surface. Based on the nitrogen adsorption-desorption isotherms, some textural parameters were calculated. As shown in Table 1, the PPh₂-FDU-12 sample exhibited high surface area (S_{BET}), high pore volume (V_p), large size of the pore channel (cage-size, D_p), and large pore size at the entrance (D_{entrance}). The immobilization of the Ru(II) complex onto the PPh₂-FDU-12 caused a slight decrease in these textural parameters, which could be easily understood by considering the occupation of the Ru(II) species in the pore channels, making the pore narrower.

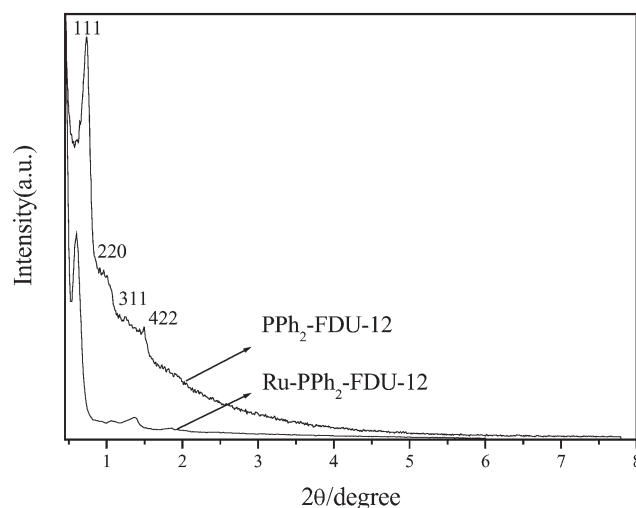


Fig. 3 Small-angle XRD patterns of the PPh₂-FDU-12 and Ru-PPh₂-FDU-12 samples.

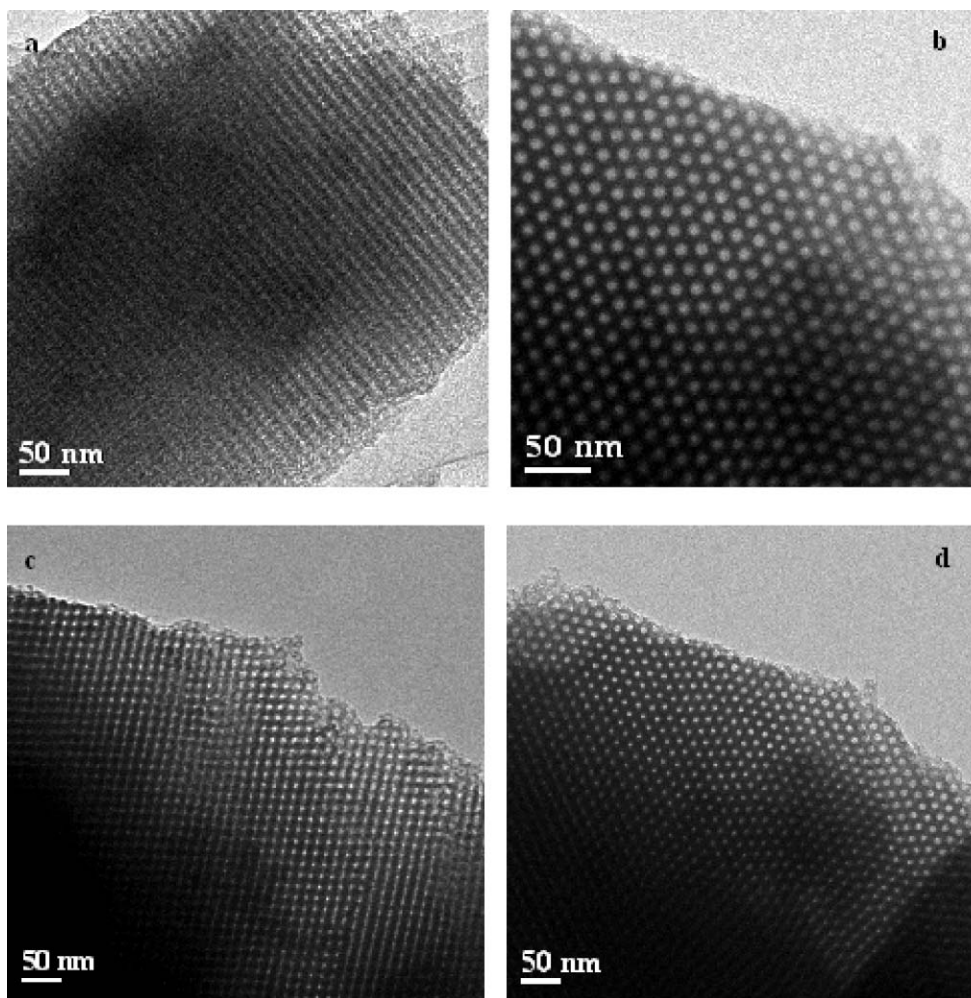


Fig. 4 TEM images of the PPh₂-FDU-12 (a, b) and the Ru-PPh₂-FDU-12 (c, d) samples along with (110) and (111) directions.

Water-medium isomerization of 1-phenyl-3-buten-1-ol as the substrate was employed to evaluate the catalytic behavior of the as-prepared Ru-PPh₂-FDU-12. The ¹H NMR analysis revealed that, besides the main product, 4-phenyl-3-buten-2-ol, only one byproduct, 1-phenyl-butanone-1, was identified

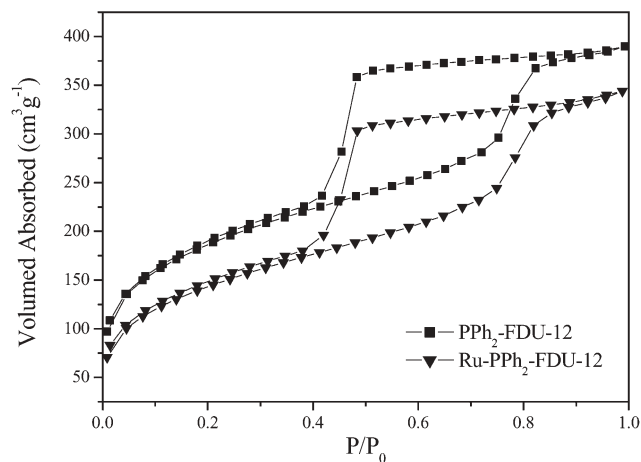


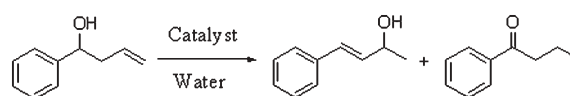
Fig. 5 N₂ adsorption-desorption isotherms of the PPh₂-FDU-12 and the Ru-PPh₂-FDU-12 samples.

under the present reaction conditions, and thus the reaction route could be simply expressed in Scheme 1. As shown in Table 2, the Ru-PPh₂-FDU-12 exhibited nearly the same activity and selectivity, as well as 4-phenyl-3-buten-2-ol yield, as the corresponding RuCl₂(PPh₃)₃ homogenous catalyst. To make sure that the reaction carried out on the Ru-PPh₂-FDU-12 was truly heterogeneous,³¹ the reactions were allowed to occur until 30% of conversion. Then, the solid was filtered out and the mother solution was allowed to react for another 8 h.

Table 1 Physical properties of PPh₂-FDU-12 materials and Ru-PPh₂-FDU-12 catalysts

Sample	$S_{\text{BET}}/\text{m}^2 \text{ g}^{-1}$	D_p/nm	$V_p/\text{cm}^3 \text{ g}^{-1}$	$D_{\text{entrance}}/\text{nm}$
PPh ₂ -FDU-12	532	10.2	0.98	3.8
Ru-PPh ₂ -FDU-12	425	9.4	0.84	2.7
Ru-PPh ₂ -FDU-12 ^a	330.	7.6	0.55	1.9

^a The catalyst after being used repeatedly for 5 times.



Scheme 1

Table 2 Water-medium isomerization of 1-phenyl-3-buten-1-ol to 4-phenyl-3-buten-2-ol over the homogenous $\text{RuCl}_2(\text{PPh}_3)_3$ and the heterogeneous Ru-PPh₂-FDU-12 catalysts^a

Catalyst	Recycling times	Conversion (%)	Selectivity (%)	Yield (%)
$\text{RuCl}_2(\text{PPh}_3)_3$	1	79	95	75
Ru-PPh ₂ -FDU-12	1	71	96	68
Ru-PPh ₂ -FDU-12	2	71	96	68
Ru-PPh ₂ -FDU-12	3	69	95	66
Ru-PPh ₂ -FDU-12	4	65	95	62
Ru-PPh ₂ -FDU-12	5	60	94	57

^a Reaction conditions: 0.025 ml 1-phenyl-3-buten-1-ol, 5.0 ml water, 14 mg $\text{RuCl}_2(\text{PPh}_3)_3$ or 0.2 g heterogeneous Ru-PPh₂-FDU-12 catalyst (each containing 1.4 mg Ru), reaction temperature = 373 K, reaction time = 8 h.

No significant change in either the conversion or the selectivity was observed, which confirmed that the reaction really proceeded on the heterogenous Ru-PPh₂-FDU-12 catalyst, since catalysis by Ru(II) active species dissolved in the aqueous solution could be ruled out. The superiority of the Ru-PPh₂-FDU-12 over the corresponding $\text{RuCl}_2(\text{PPh}_3)_3$ homogeneous catalyst was that it could be used repetitively, which might reduce the cost and diminish the environmental pollution by heavy metallic ions. From Table 2, one could also see that the selectivity remained almost unchanged while the conversion decreased only by less than 15% after the Ru-PPh₂-FDU-12 was used for 5 repetitions.

The high reactivity and selectivity of the Ru-PPh₂-FDU-12 could be mainly attributed to the high dispersion of Ru(II) active sites on the FDU-12 support owing to its high surface area. Meanwhile, the modification of the FDU-12 with the PPh₂-CH₂-CH₂-groups could enhance the surface hydrophobicity, and thus could facilitate the adsorption of the organic molecules on the active sites. Furthermore, the Ru-PPh₂-FDU-12 catalyst displayed a highly ordered three-dimensional mesoporous structure with both large entrance and large channel sizes, which was also favorable for achieving high activity, since the organic molecules could easily enter the porous channels and also diffuse freely in such channels. This could be further confirmed by comparing the activity of the Ru-PPh₂-FDU-12 with that of the Ru-PPh₂-SBA-15. As reported previously,¹¹ the maximum 4-phenyl-3-buten-2-ol yield could be obtained after reaction for 10 h under the Ru-PPh₂-SBA-15 containing 1.4 mg Ru. However, only 8 h was needed to achieve maximum 4-phenyl-3-buten-2-ol yield under the same reaction conditions when Ru-PPh₂-FDU-12 containing 1.4 mg Ru was used instead of Ru-PPh₂-SBA-15 as the catalyst. The Ru-PPh₂-FDU-12 exhibited higher activity than the Ru-PPh₂-SBA-15 obviously owing to the larger size of both the pore entrance and the pore channels.

The ICP analysis demonstrated that, after being used for 5 repetitions, the content of Ru(II) species in the solution leached off from the Ru-PPh₂-FDU-12 was less than 10 ppm, showing that the loss of the active Ru(II) sites could be neglected. Meanwhile, the nitrogen adsorption-desorption isotherm in Fig. 5 demonstrated that the used Ru-PPh₂-FDU-12 still retained a mesoporous structure. However, remarkable decreases in S_{BET} , V_{P} , D_{P} and D_{entrance} were observed after the Ru-PPh₂-FDU-12 was used for

5 repetitions, which might limit the diffusion and the adsorption of the organic substrate on the active sites, making the activity decrease.

Conclusions

In summary, a new way of conducting the isomerization of homoallylic alcohol in water as an environmentally friendly medium was developed by using the immobilized Ru(II) organometallic complex (Ru-PPh₂-FDU-12) as a heterogeneous catalyst, which exhibited nearly the same activity and selectivity as the corresponding Ru(II) homogeneous catalyst but could be used for at least 5 repetitions. The excellent performance of the Ru-PPh₂-FDU-12 could be attributed to the high and uniform dispersion of the Ru(II) active sites on the support owing to the high surface area of the FDU-12. The strong immobilization of the Ru(II) onto the FDU-12 support through coordination with the PPh₂-ligand could effectively protect the active species from leaching. The higher activity of the Ru-PPh₂-FDU-12 than that of the Ru-PPh₂-SBA-15 suggested that the large size of both the pore entrance and the pore channel was also an important factor for improving the performance of the heterogeneous catalyst by diminishing the diffusion limit.

Acknowledgements

This work was supported by the National Natural Science Foundation of China (20377031 and 20407014), Ministry of Science and Technology in China (2005CCA01100), and Shanghai Municipal Scientific Commission (06JC14060 and 03QF14037).

References

- (a) C. J. Li and T. H. Chan, *Organic Reactions in Aqueous Media*, Wiley, New York, 1997; (b) P. A. Grieco, *Organic Synthesis in Water*, Thomson Science, Glasgow, Scotland, 1998; (c) C. J. Li, *Chem. Rev.*, 2005, **105**, 3095.
- U. M. Lindstrom, *Chem. Rev.*, 2002, **102**, 2751.
- S. Narayan, J. Muldoon, M. G. Finn, V. V. Fokin, H. C. Kolb and K. B. Sharpless, *Angew. Chem., Int. Ed.*, 2005, **44**, 3275.
- (a) R. A. Sheldon, *Green Chem.*, 2005, **7**, 267; (b) P. Metivier, *Fine Chemicals through Heterogeneous Catalysis*, Wiley, Weinheim, 2001.
- (a) D. E. De Vos, I. F. J. Vankelecom and P. A. Jacobs, *Chiral Catalyst Immobilization and Recycling*, Wiley-VCH: Weinheim, 2000; (b) Y. Iwasawa, *In Tailored Metal Catalysts*, D. Reidel Publishing Company, Dordrecht, Holland, 1986.
- (a) C. E. Song, *Annu. Rep. Prog. Chem., Sect. C: Phys. Chem.*, 2005, **101**, 143; (b) C. Li, *Catal. Rev. Sci. Eng.*, 2004, **46**, 419.
- D. E. De Vos, M. Dams, B. F. Sels and P. A. Jacobs, *Chem. Rev.*, 2002, **102**, 3615.
- C. T. Kresge, M. E. Leonowicz, W. J. Roth, J. C. Vartuli and J. S. Beck, *Nature*, 1992, **359**, 710.
- D. Zhao, Q. Huo, J. Feng, B. F. Chmelka and G. D. Stucky, *J. Am. Chem. Soc.*, 1998, **120**, 6024.
- (a) M. E. Davis, *Nature*, 2002, **417**, 813; (b) A. Corma, *Chem. Rev.*, 1997, **97**, 2373.
- H. X. Li, F. Zhang, Y. Wan and Y. F. Lu, *J. Phys. Chem. B*, 2006, **110**, 22942.
- Y. Wan, J. Chen, D. Q. Zhang and H. X. Li, *J. Mol. Catal.*, 2006, **258**, 89.
- H. X. Li, J. Chen, Y. Wan, W. Cai, F. Zhang and Y. F. Lu, *Green Chem.*, 2007, DOI: 10.1039/b612370h.

- 14 Y. Wan, F. Zhang, Y. F. Lu and H. X. Li, *J. Mol. Catal.*, 2006, DOI: 10.1016/j.molcata.2006.11.029.
- 15 D. V. McGrath and R. H. Grubbs, *Organometallics*, 1994, **13**, 224.
- 16 L. E. Overman, C. B. Campbell and F. Knoll, *J. Am. Chem. Soc.*, 1978, **100**, 4822.
- 17 J. Cymerman, I. M. Heibron and E. R. Jones, *J. Chem. Soc.*, 1945, 90.
- 18 C. J. Li, D. Wang and D. Chen, *J. Am. Chem. Soc.*, 1995, **117**, 12867.
- 19 A. S. Chong and X. S. Zhao, *J. Phys. Chem. B*, 2003, **107**, 12650.
- 20 Q. Y. Hu, J. E. Hampsey, N. Jiang, C. J. Li and Y. F. Lu, *Chem. Mater.*, 2005, **17**, 1561.
- 21 S. L. Burkett, S. D. Sims and S. Mann, *Chem. Commun.*, 1996, 1367.
- 22 S. Huh, J. W. Wiench, J. C. Yoo, M. Pruski and V. S. Y. Lin, *Chem. Mater.*, 2003, **15**, 4247.
- 23 C. E. Fowler, S. L. Burkett and S. Mann, *Chem. Commun.*, 1997, 1769.
- 24 R. K. Zeidan, V. Dufaud and M. E. Davis, *J. Catal.*, 2006, **239**, 299.
- 25 J. A. Margolese, S. C. Melero, B. F. Christiansen and G. D. Stucky, *Chem. Mater.*, 2000, **12**, 2448.
- 26 T. Posset, F. Rominger and J. Blumel, *Chem. Mater.*, 2005, **17**, 586.
- 27 R. J. P. Corriu, C. Hoarau, A. Mehdi and C. Rey  , *Chem. Commun.*, 2000, 71–72.
- 28 T. Yu, H. Zhang, X. W. Yan, Z. X. Chen, X. D. Zou, P. Oleynikov and D. Y. Zhao, *J. Phys. Chem. B*, 2006, **110**, 21467.
- 29 J. Fan, C. Z. Yu, F. Gao, J. Lei, B. Z. Tian, L. M. Wang, Q. Luo, B. Tu, W. Z. Zhou and D. Y. Zhao, *Angew. Chem., Int. Ed.*, 2003, **42**, 3146.
- 30 J. R. Matos, M. Kruk, L. P. Mercuri, M. Jaroniec, L. Zhao, T. Kamiyama, O. Terasaki, T. J. Pinnavaia and Y. Liu, *J. Am. Chem. Soc.*, 2003, **125**, 821.
- 31 R. A. Sheldon, M. I. Wallau, W. C. E. Arends and U. Schuchardt, *Acc. Chem. Res.*, 1998, **31**, 485.

Find a SOLUTION

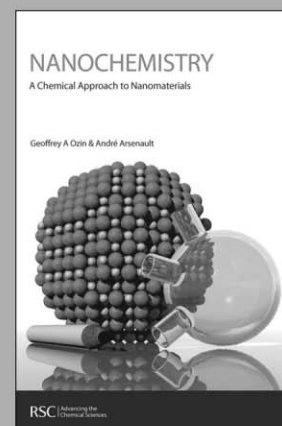
... with books from the RSC

Choose from exciting textbooks, research level books or reference books in a wide range of subject areas, including:

- Biological science
- Food and nutrition
- Materials and nanoscience
- Analytical and environmental sciences
- Organic, inorganic and physical chemistry

Look out for 3 new series coming soon ...

- RSC Nanoscience & Nanotechnology Series
- Issues in Toxicology
- RSC Biomolecular Sciences Series



RSC Publishing

www.rsc.org/books



Impact factor
now
13.747!

No time to keep up with your reading?

Let *Chem Soc Rev* do the hard work for you. Our mission is to provide authoritative, accessible, succinct and reader-friendly reviews on carefully selected topics of broad and specialist interest in the chemical sciences. Highly cited and engaging to read, *Chem Soc Rev* articles are designed to highlight important primary research papers, provide concise updates of technological progress and give insight into emerging industry trends. Don't waste time scouring the literature – pick up a copy of *Chem Soc Rev* and regain back some of your precious time.

RSC Publishing

www.rsc.org/chemsocrev

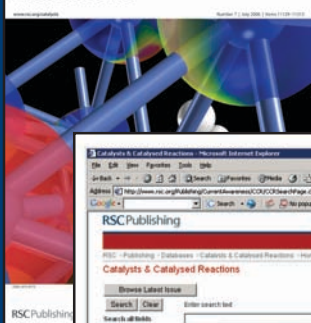
Specialised searching



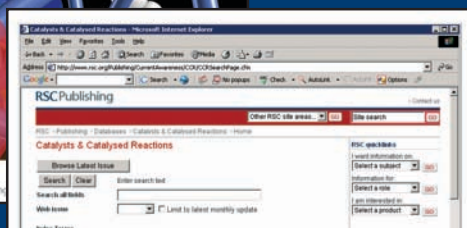
The graphical abstracting services at the RSC are an indispensable tool to help you search the literature. Focussing on specific areas of research they review key primary journals for novel and interesting chemistry.

requires specialised tools

Catalysts & Catalysed Reactions

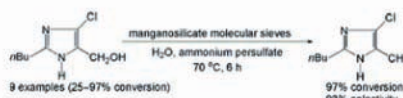


Catalysts and Catalysed Reactions covers all areas of catalysis research, with particular emphasis on chiral catalysts, polymerisation catalysts, enzymatic catalysts and clean catalytic methods.



The online database has excellent functionality. Search by: authors, products, reactants and catalysts, catalyst type and reaction type.

11086 The green catalytic oxidation of alcohols in water by using highly efficient manganosilicate molecular sieves
H. G. Manyar, G. S. Chaure, A. Kumar*
Green Chem., 2006, 8(4), 344-348



With Catalysts and Catalysed Reactions you can find exactly what you need. Search results include diagrams of reaction schemes. Also available as a print bulletin.

Registered charity Number 207890

For more information visit

RSC Publishing

www.rsc.org/databases

Listen up Speak out



chemistryworld

Your favourite monthly magazine invites you to go interactive



The free monthly podcast from *Chemistry World* includes interviews and discussions on the latest topics in science: all in one bite sized chunk. Subscribe now at iTunes or download past and present podcasts directly from the *Chemistry World* website.

**Chemistry
World Blog**

News, opinion & discussion

Got something to say? Then why not speak out on our new *Chemistry World* Blog: an interactive forum, updated daily, for the latest news, opinions and discussion about the chemical sciences. Why not post a question or comment on the science hitting the headlines.

RSC | Advancing the
Chemical Sciences

www.chemistryworld.org

Registered Charity Number 207890